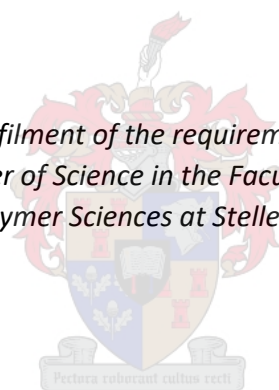


Synthesis of Small Molecule Bioactive Compounds with Potential Anti–Cancer Activity

by
Moscos Avgenikos

*Thesis presented in fulfilment of the requirements for the degree of
Master of Science in the Faculty of
Chemistry and Polymer Sciences at Stellenbosch University*



Supervisor: Prof. W.A.L van Otterlo
Co-supervisor: Dr C.H. Kaschula

March 2020

Declaration

By submitting this thesis electronically, I declare that the entirety of the work contained therein is my own, original work, that I am the sole author thereof (save to the extent explicitly otherwise stated), that reproduction and publication thereof by Stellenbosch University will not infringe any third party rights and that I have not previously in its entirety or in part submitted it for obtaining any qualification.

March 2020

Copyright © 2020 Stellenbosch University

All rights reserved

ACKNOWLEDGEMENTS

“As the bonfires of knowledge grow brighter, we illuminate the surface of ignorance
greater”

– Terrence Mckenna

A special thanks to

The ever-patient Prof. W. Van Otterlo & Dr. C. Kaschula

Dr. G. Schäfer and the NRF

Khaya & Kim

Mom, Dad and Evi

Support Staff

and denizens of the De Beers building

ABSTRACT

Cancer is a major burden on human health and infrastructure as a leading cause of death worldwide. A collective name for a group of diseases characterised by uncontrolled cellular growth; cancer can be caused by a variety of factors including genetic factors and lifestyle choices. The approach to managing these diseases can be summarised into two broad categories, prevention and treatment. The pool of natural products (broadly chemicals derived from natural sources) has long been drawn upon for healing effect and a starting point for the development of pharmaceuticals. Humans have passed down knowledge of the healing properties of certain species plants, for example, for many generations.

The paths to maximise the positive effect natural products have to offer against cancer, within the context of the studies herein, are twofold. Achieving a biological understanding of how these products gain their effect paving the way for new treatments and preventions to be developed; and improving access to, and quality of, the active compounds we have at our disposal already. This study is composed of three parts.

Firstly, an investigation into the nutraceutical compounds of Flavokawain A and Fisetin, naturally occurring in the Kava plant of Fijian origin and strawberries respectively. These agents display prophylactic properties, and are proposed to reduce the occurrence of certain cancers in the populations that consume the plants these compounds occur in. The mechanism by which these compounds achieve their properties is not well understood. Fluorescent analogues of these compounds were achieved synthetically and imaged via confocal microscopy. Both compounds were found to collect in the endoplasmic reticulum of A549 lung cancer cells as well as displaying low micromolar toxicities to these cells.

The second study arose as a short-term collaboration with researchers from Leipzig University, Germany. The researchers have developed synthetic strategies useful for forming 1-4 dihydroquinoline-3 carboxylate derivatives enantioselectively. This scaffold is similar to those of 4-aza-podophyllotoxins, a synthetic analogue to the natural product podophyllotoxin. Previous research reveals that a single enantiomer is responsible for the low nanomolar efficiencies this compound class displays. Thus, our study attempted to achieve an enantioselective synthesis of 4-aza-podophyllotoxin and succeeded in achieving enantioenriched samples using binaphthol phosphoric acid catalysts.

Lastly, an investigation into the synthesis of a modified lung cancer drug combatting resistant, mutant epidermal growth factor receptor (EGFR) lung cancer was attempted. Within the investigation a synthetic scaffold was achieved based on WZ 4002 – an irreversible inhibitor currently undergoing clinical trials for resistant lung cancers. EGFR mediated resistance rejects the covalent modifiers currently in use; within this study sulfonyl fluorides have been proposed as replacements. Demonstrated within the study is a viable copper mediated triazole formation strategy which tolerates the sulfonyl fluoride electrophile. The scaffold is primed to achieve a variety of triazole linked probes containing sulfonyl fluorides which we

proposed to investigate the chemical space around the EGFR binding site to combat resistance.

ABSTRAK:

Kanker is een van die hooforsake van sterftes wêreldwyd en plaas 'n groot las op menslike gesondheid en infrastruktuur. Kanker is 'n versamelnaam vir 'n groep siektes wat deur onbeheerde sellulêre groei gekenmerk word. Die siekte kan deur 'n verskeidenheid faktore veroorsaak word, insluitend genetiese faktore en slegte leefstyl keuses. Die benadering en bestuur van die siekte kan in twee breë kategorieë vervat word: voorkoming en behandeling. Die versameling natuurlike produkte (chemikalieë van natuurlike bronne) is al lank vir genesende effek gebruik en as 'n beginpunt vir die ontwikkeling van farmaseutiese produkte.

Hierdie studie ondersoek die moontlikhede waaronder die positiewe effek van natuurlike produkte die grootste uitwerking op die behandeling van kanker het. Die studie is tweeledige en vestig 'n begrip van die werking van hierdie natuurlike produkte wat kan lei tot nuwe behandelinge en voorkoming, asook die verbetering van kwaliteit en toeganklikheid tot die natuurlike verbindings wat ons reeds tot ons beskikking het. Hierdie studie bestaan uit drie afdelings. (This part does not make sense as the word tweeledig means in two parts and now they are saying it comprises of three parts.) Hierdie studie bestaan uit drie dele.

Die eerste studie ondersoek die voedingsverbindinge van Flavokawain A en Fisetin wat natuurlik in die Kava-plant, van Fidjiaanse oorsprong, en aarbeie voorkom. Hierdie middels het profilaktiese eienskappe en word voorgestel om die voorkoms van sekere kanker in die bevolkingsgroepe wat hierdie plante verteer, te verminder. Die meganisme waardeur hierdie verbindings hul eienskappe voortbring, word nie volkome verstaan nie. Fluoreserende analoë van hierdie verbindings is sinteties bewerkstellig en deur middel van konfokale mikroskopie ondersoek. Daar is gevind dat albei verbindings in die endoplasmiese retikulum van A549 longkankerselle versamel en lae mikromolêre toksisiteit vir die selle vertoon.

Die tweede studie het ontstaan as 'n korttermyn samewerking met navorsers van die Leipzig Universiteit in Duitsland. Die navorsers het sintetiese strategieë ontwikkel wat nuttig is vir die vorming van 1-4 dihidrokinolien-3 karboksilaatderivate enantioselektief. Hierdie steierwerk is soortgelyk aan dié van 4-aza-podofilotoksiene, 'n sintetiese analoog aan die natuurlike produk podofilotoksien. Vorige navorsing toon aan dat 'n enkele enantiomeer verantwoordelik is vir die lae nanomolêre doeltreffendheid wat hierdie saamgestelde klas vertoon. Dus het ons studie gepoog om 'n enantioselektiewe sintese van 4-aza-podofilotoksien te bewerkstellig en het daarin geslaag om enantioen-verrykte monsters met behulp van binaftol-fosforsuurkatalisators te verkry.

Laastens is 'n ondersoek na die sintese van 'n gemodifiseerde longkankermiddel gebruik om weerstandige, mutante epidermale groeifaktorreseptor (EGFR) longkanker te bestry. Binne die ondersoek is 'n sintetiese steierwerk op grond van WZ 4002 bewerkstellig - 'n onomkeerbare inhibeerder wat tans kliniese ondersoeke ondergaan vir die gebruik teen weerstandbiedende longkanker. EGFR-gemedieerde weerstand verwerp die kovalente wysigers wat tans in gebruik is; binne hierdie studie word sulfoniëlfuoriede as vervanging

voorgestel. Die studie demonstreer die lewensvatbaarheid van koperbemiddelde triasoolvormingstrategie wat die sulfonielfluoried-elektrofiel verdra. Die steier word voorberei om 'n verskeidenheid triasoolgekoppelde probe wat sulfonielfluoriede bevat te bewerkstellig, wat ons voorgestel het om die chemiese ruimte rondom die EGFR-bindingsplek te ondersoek om weerstandigheid teen te staan.

TABLE OF CONTENTS

| | |
|--|----|
| Acknowledgements..... | 3 |
| Abstract..... | 4 |
| Abstrak:..... | 6 |
| Chapter 1 Synthesis and Imaging of Fluorescent Dietary Compound Analogues | 10 |
| Introduction | 10 |
| Nutraceuticals | 10 |
| Flavokawain and Fisetin | 11 |
| Mechanism Elucidation techniques..... | 11 |
| Aim | 12 |
| Design of the Fluorescent Probes..... | 12 |
| Discussion..... | 13 |
| Synthesis | 13 |
| Fluorescent fragment..... | 13 |
| Synthesis of Flavokawain A Fragment | 14 |
| Synthesis of Fisetin derivative fragment | 15 |
| Target Compounds | 16 |
| Biological Evaluation | 19 |
| Summary of Methods..... | 19 |
| Results..... | 20 |
| Validity of the probes | 27 |
| Control Compound | 27 |
| Control Colocalization Studies..... | 27 |
| Conclusions | 29 |
| References | 29 |
| Experimental | 30 |
| Chapter 2 Towards a Bronsted Acid Catalysed Enantioselective Synthesis of 4-aza-podophyllotoxin..... | 40 |
| Introduction | 40 |
| Podophyllotoxin | 40 |
| Mechanism of Action | 40 |
| Aza-analogues | 41 |

| | |
|--|----|
| <i>Ortho</i> -Quinone Methides and their Aza Analogues..... | 41 |
| Chiral control over <i>N</i> -heterocycles demonstrated by Schneider and coworkers | 42 |
| Aim | 44 |
| Retrosynthesis..... | 44 |
| Results and Discussion | 45 |
| Model Substrate synthesis | 45 |
| Proof of concept..... | 47 |
| Initial chiral catalyst screening | 48 |
| Synthesis of Enamine Tetronic Acid Analogue..... | 50 |
| Further Screening..... | 50 |
| Conclusion..... | 52 |
| Future work..... | 52 |
| References | 53 |
| Experimental | 54 |
| Chapter 3 Sulfonyl Fluorides as Kinase Inhibitors..... | 60 |
| Introduction | 60 |
| Aims | 62 |
| Discussion..... | 63 |
| Synthesis | 63 |
| AZD alkyne core..... | 63 |
| WZ 4002 alkyne core synthesis | 69 |
| Warhead synthesis | 72 |
| Model Click study | 74 |
| Conclusions | 76 |
| Further studies | 76 |
| References | 76 |
| Chapter 4 General practices..... | 91 |
| Solvents and Reagents Chemicals | 91 |
| Chromatography and Purification | 91 |
| Sprectroscopy..... | 91 |
| Glassware and Inert Conditions..... | 92 |
| Cell Cytotoxicity Assay..... | 92 |
| Confocal Microscopy | 92 |

SYNTHESIS AND IMAGING OF FLUORESCENT DIETARY COMPOUND ANALOGUES

INTRODUCTION

This work was presented in part as a poster presentation at the International Symposium on Tumor Microenvironment and Cancer Prevention & Therapeutics, February 08-09 2019 at the School of Life Sciences, Jawaharlal Nehru University, New Delhi. The work relates to an ongoing collaboration between the working groups of Dr C.H. Kaschula, University of Stellenbosch and Prof. R. Singh, Jawaharlal Nehru University, New Delhi.

NUTRACEUTICALS

Nutraceuticals is portmanteau of 'nutrition' and 'pharmaceuticals' and describes those components of foods and dietary intake which have medicinal effect.¹ These may be in the form of functional foods and specific dietary choices, concentrates, extracts and dietary supplements.¹ However, the common factor between all these examples is the fact that they are sourced from some form of food product, usually a plant source.² Phytochemicals, such as polyphenols, are likely to play a role in human longevity.¹ Natural products have long been a starting point for medicinal development.¹ In this light, nutraceuticals provide a springboard for novel treatments and prophylactic medicine.² Nutraceuticals as foods and extracts are at times poorly described in terms of the compounds, concentrations and composition; however, the positive effects of these mixtures on human health can be detected.³ Approaching nutraceuticals in this manner can be beneficial; nutraceuticals can be incorporated into daily dietary intake as prophylactics or as therapeutics for certain conditions despite the active components being ill defined.¹ Special care or controlled intake is less necessary to acquire benefits, rather being controlled as a foodstuff than a therapeutic. Adding garlic or broccoli, containing the pro-apoptotic compounds ajoene and sulforaphane respectively,⁴ to one's diet has been shown to reduce the risk of certain cancers in population wide studies. These factors are limited by sensible intake of these foods, which can be seen as both positive and negative. Dosages of these active compounds may be higher than what is feasible to acquire from foods may be required in certain individuals. As such, researchers have isolated and characterised certain components of active plant extracts that have been described to have medicinal effect. These molecules provide a better understanding of the effects of consuming the foodstuffs and provide a platform for further improved medicines. Several commercial drugs have started out as natural products which were then derived synthetically to produce more active or potent drugs. To complete these kinds of studies the

Chapter 1 Synthesis and Imaging of Fluorescent Dietary Compound Analogues

biological mechanism of the drug or natural product can be described which may then lead to further innovation.

FLAVOKAWAIN AND Fisetin

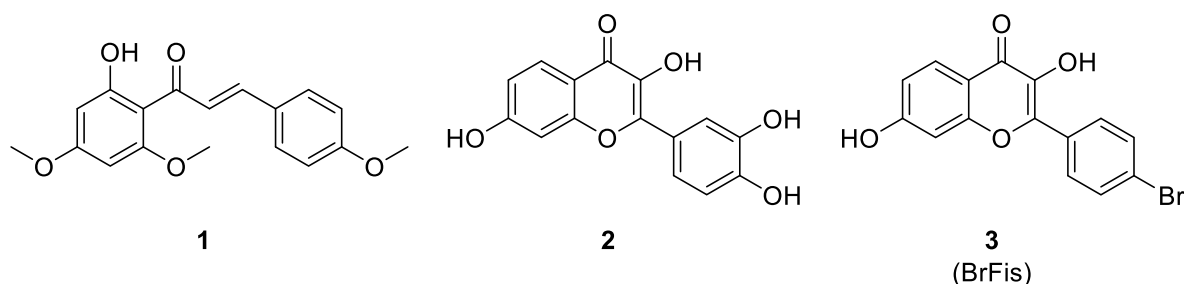


Figure 1 Flavokawain A **1**, Fisetin **2** and a brominated derivative of Fisetin (BrFis) **3**.

Flavokawain A (FKA) **1**, described in **figure 1**, was isolated from the Kava plant, *Piper methysticum*.³ This is a medicinal plant found on the islands of the south pacific including Fiji.³ The indigenous populations use this plant as a tea and display a 30% decreased occurrence of bladder cancer.³ Flavokawain A (FKA) which has been shown to exhibit both pro-apoptotic and anti-proliferative effects against bladder cancer cells and it is proposed that the presence of the polyphenol FKA in Kawa tea may contribute to the effects observed. FKA is member of a family of bioactive compounds known as the chalcones.⁵ However, the exact mechanism by which FKA achieves its biological properties is unknown.

Fisetin **2** is a natural polyphenol which is found in common dietary components such as strawberries and displays anti-cancer activity at micromolar concentrations (**Fig 1**).⁶ It is part of a class of compounds known as the flavonols, which commonly show antioxidant effects in biological systems.⁷ The working group of Dr. C Kaschula has developed a brominated analogue **3** of fisetin **2**. Fisetin **2** itself displays pro-apoptotic effects on certain cancer cell lines, however the working group noticed the brominated derivative **3**, among others synthesized, displays a marked increase in activity compared to the natural product as part of an ongoing investigation yet to be published. Naturally occurring fisetin **2** has been shown, among other properties, to induce apoptosis or programmed cell death in human gastric cancer cells.⁶

MECHANISM ELUCIDATION TECHNIQUES

As stated, pharmaceutically active compounds interact with specific cellular components to achieve their effect. Understanding the cellular location of the phytochemical of interest assists greatly in elucidating a specific target and biological mechanism. There are several established methods of tracking compounds as they journey through the cellular environment. These techniques include methods such as tracking isotopically enriched analogues of studied compounds via radioactive decay or biotin labelling; making use of the

Chapter 1 Synthesis and Imaging of Fluorescent Dietary Compound Analogues

biotin-streptavidin binding strength to identify targets. Another method, most relevant to this discussion is fluorescent labelling.⁴ Fluorescent labelling involves the covalent attachment of a fluorescent moiety, such as fluorescein and dansyl sulphonamide derivatives, via a suitable linker to a molecule of interest.⁴ The labelled molecule is then incubated in cell cultures, possibly concentrating at certain target sites. The fluorescent moiety should, by the same token, concentrate at this target site, insulated from the pharmacophore and its action via the covalent linker. This allows for indirect visualisation of the compound of interest via fluorescence microscopy. Other well-established dyes fluorescing with wavelengths sufficiently different to that of the investigative tag can then be used to confirm which organelles or cellular structures the target molecule are binding to. This yields information about the mechanism and possible targets of the compound of interest. Known as a colocalization study, exploiting fluorescence in this way is a cost effective and reasonable synthetic challenge to acquire biological information about a compound. For example, the action of cisplatin, a chemotherapeutic agent, has been demonstrated via fluorescent techniques by Rodríguez-Fernández *et. al.*⁸ to bind to DNA. It does not require the specialised conditions and working environments associated with radiolabelling and easily interpretable visual information using lower cost confocal microscopy as the elucidation method is an advantage.

AIM

This project aims to synthesise and evaluate fluorescent synthetic analogues of flavokawain **A 1** and a brominated derivative of fisetin, BrFis **3**, previously developed in our laboratories (**Fig 2**). These labelled derivatives are then to be evaluated for their toxicity against lung and breast cancer cell lines and imaged via confocal fluorescence microscopy. The focus is to gather intracellular localisation information of these compounds via colocalization mapping with known organelle stains, in order to draw conclusions about their mechanisms of action.

DESIGN OF THE FLUORESCENT PROBES

Dansyl sulphonamides absorb in the UV range (λ_{abs} 340 nm) and fluoresce in the visible light region (λ_{em} 520 nm; ϵ 4.2 L.mmol⁻¹.cm⁻¹) with high quantum efficiencies. These properties make it an excellent candidate for fluorescence labelling, where the fluorescence can be observed at low concentrations of the tag. The dansyl tag's "blue" emission spectrum is substantially divorced from the emission wavelengths of commercial fluorescent organelle stains for it to be useful for colocalization studies using these dyes.

Dansyl sulphonamide was the chosen fluorescent moiety for this study, building on the successful labelling of ajoene by Kaschula and coworkers.⁴ Colocalization of ajoene with commercial "red" organelle stains allowed for the elucidation of the compound's biological

Chapter 1 Synthesis and Imaging of Fluorescent Dietary Compound Analogues

mechanism of action. Our study is modelled after this method of tagging and proposes the dansyl-tagged analogues of the compounds Flavokawain A (DFKA) **4** and BrFis (DBrFis) **5**.

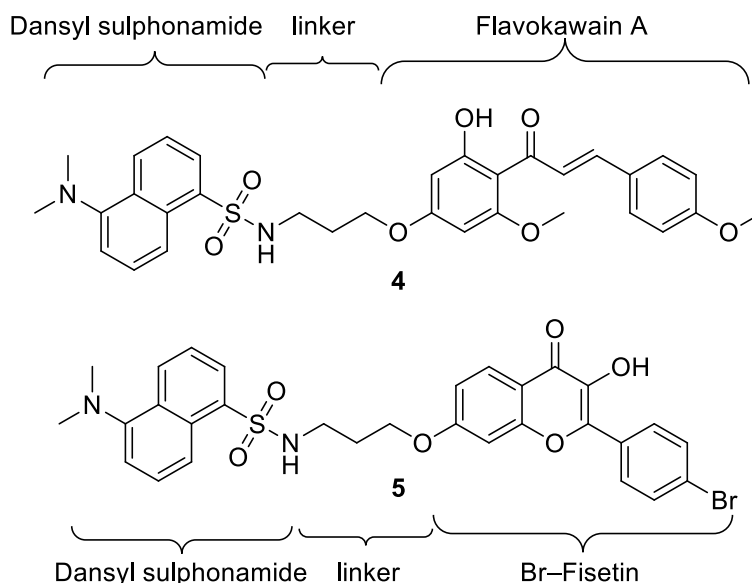


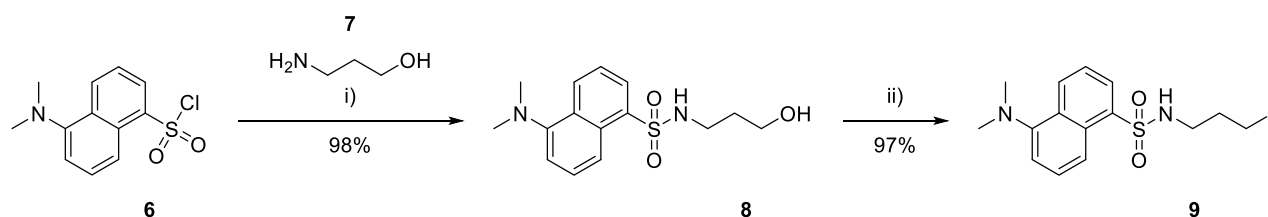
Figure 2 The study aims to synthesise and image the dansyl sulphonamide containing analogues of Flavokawain A **4** and Br-Fis **5**.

DISCUSSION

SYNTHESIS

FLUORESCENT FRAGMENT

A dansyl sulphonamide and linker assembly intermediate has been developed previously and was synthesized according to these previously established methods:⁴



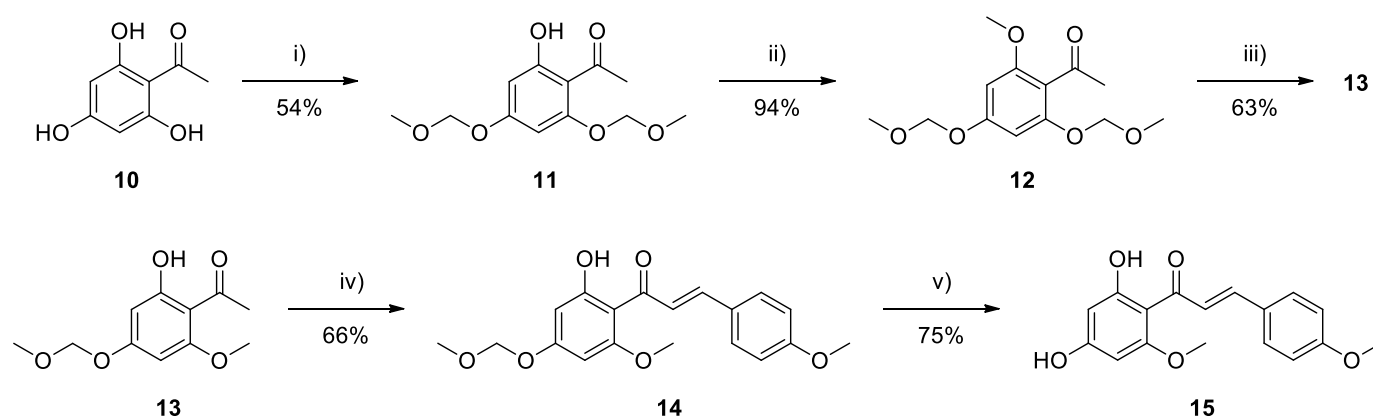
Scheme 1 Synthesis of fluorophore. Conditions: i) **7** (1.5 eq), Et₃N (2.0 eq), DCM, 0 °C – rt, 6 h; ii) I₂ (1.5 eq), Imidiazole (1.5 eq), PPh₃ (1.5 eq), DCM, 0 °C – rt, 6 h.

Commercially available dansyl chloride **6** was reacted with 1,3-aminopropanol **7** in DCM under basic conditions overnight at room temperature to afford sulphonamide **8** in near quantitative yield. This alcohol was then transformed to the corresponding iodide **9** via Appel conditions in excellent yield to afford the desired alkyl iodide as a yellow fluorescent oil. The synthesis for this fragment was well established and spectral data for these compounds compared well with literature values.⁴

Chapter 1 Synthesis and Imaging of Fluorescent Dietary Compound Analogues

SYNTHESIS OF FLAVOKAWAIN A FRAGMENT*

The desired phenolic FKA fragment **15** was synthesised as described in **scheme 2** as per literature procedure.⁵ Starting with commercially available 1,3,5-trihydroxyacetophenone **10** which was dialkylated with methoxymethyl chloride at reflux in acetone, using K_2CO_3 as a base yielding **11** in reasonable yield. The product was confirmed via 1H NMR, with the distinct singlets of the introduced protecting groups appearing slightly shifted from each other due to the asymmetry introduced by the acetal group. Additional signals present in the ^{13}C NMR spectrum describing the methoxymethylene moiety assisted in the confirmation of this product alongside the literature.⁵ The resulting clear oil was then subjected to methylation in acetone using dimethyl sulphate as methylating agent and K_2CO_3 as base and allowed to stir at room temperature for 24 h. Column chromatography of the quenched and filtered mixture afforded the desired product **12** as colorless oil in 94% yield. Both 1H , ^{13}C NMR and mass spectral data confirm the addition of the methyl group. This product was then selectively monodeprotected of a methoxymethyl ether protecting group using a catalytic amount of iodine in methanol over 2 h at room temperature to afford compound **13**. The appearance of a sharp peak at 13.8 ppm in the 1H spectrum of this compound was deemed characteristic of a hydrogen bonded phenolic proton and was further supported by an OH stretch at 2952 cm^{-1} in the IR spectrum confirming the formation of a phenol and the removal of a single protecting group. This hydrogen bonded phenolic proton is consistent with literature⁵ and characteristic of o-hydroxyacetophenones. This is due to the favourable six membered ring formed by the H-bonding between



Scheme 2 Synthesis of Flavokawain A phenolic fragment. Conditions: i) MOMCl (2.1 eq), K_2CO_3 (2.8 eq), Acetone, refl., 2 h; ii) Me_2SO_4 (2.4 eq), K_2CO_3 (12 eq), Acetone, refl., 24 h; iii) I_2 (0.05 eq), Methanol, rt, 2 h; iv) p-Anisaldehyde (1.0 eq), aq KOH 50% w/w / Ethanol (1:1), rt, 24 h; v) 3 M aq. HCl / Methanol (3:5), refl., 2 h.

*The synthesis for this compound was adapted from efforts previously described by M. Avgenikos, C. H. Kaschula, Synthesis and Imaging of a Novel Fluorescently Labelled Analogue of Flavokawain A, Stellenbosch University Honours program paper (Unpublished) 2017

Chapter 1 Synthesis and Imaging of Fluorescent Dietary Compound Analogues

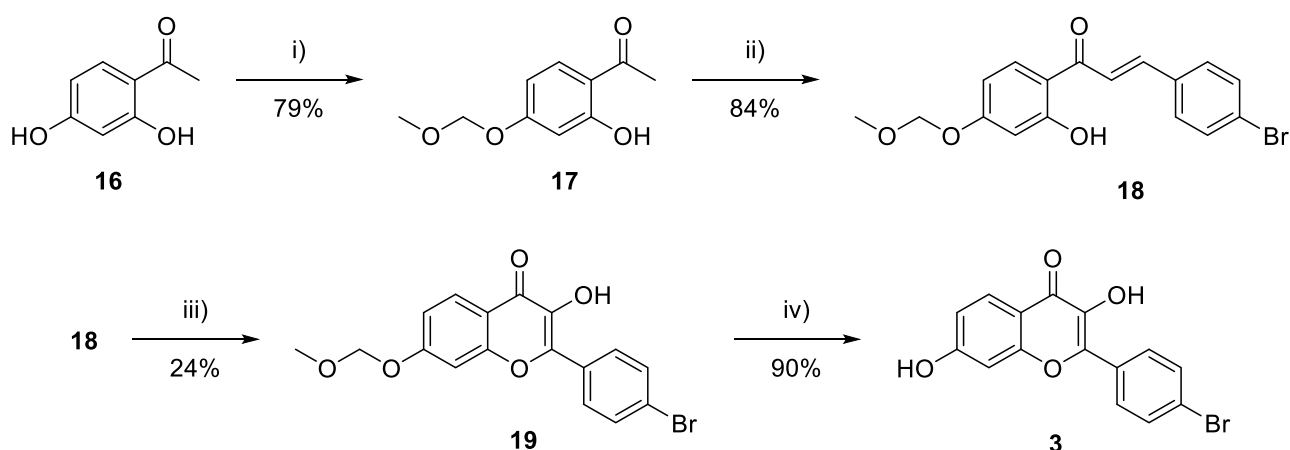
the phenol and carbonyl oxygen and can be detected spectroscopically in compounds **10** – **15**, excluding compound **12**. The resulting oil of compound **13** then underwent an aldol condensation with *p*-anisaldehyde in a mixture of ethanol and 50 % w/w KOH aqueous solution. After being subjected to an acidic workup the mixture was purified by column chromatography resulting in a yellow solid in 66% yield. ^1H NMR spectroscopy of this product displayed a set of doublets at 6.08 and 6.27 ppm respectively both with coupling constants of 2.5 Hz. This is uncharacteristic of α,β -unsaturated carbonyl compounds, however spectroscopic data matched literature reports.⁵ Additionally, two doublets (integration = 2H) and a singlet (integration = 3H) corresponding to the *p*-methoxy substituted aromatic ring of compound **14** were observed at 7.56, 6.93 and 3.93 ppm respectively. These structures were also supported by ^{13}C NMR spectroscopy evidence corresponding to each of the mentioned structural features. With the bulk of the structure of the natural product now formed, compound **14**, the final protecting group was then removed by heating **14** under reflux in a solution of methanol and 3 M aqueous HCl. Column chromatography afforded the deprotected product **15** in a reasonable yield of 75%. The molecular weight was then confirmed by HRMS and signals corresponding to the removed moiety were no longer present in the ^1H or ^{13}C NMR spectra. A broad band at 3140 cm^{-1} appeared in the IR spectrum of this compound confirming the formation of the desired phenolic derivative of Flavokawain A.

SYNTHESIS OF Fisetin DERIVATIVE FRAGMENT

The phenolic BrFis **3** fragment was achieved as described in **scheme 3** from commercially available 2,4-dihydroxyacetophenone, which was monoprotected with methoxymethyl chloride in a similar fashion to the previous synthesis. Column chromatography was performed and afforded a clear oil in 79% which was characterised and confirmed as **16**, displaying the methoxymethylene signals similar to those described previously for compound **11**. Using the same conditions as the synthesis of **14** previously described, an aldol condensation between **17** and *p*-bromobenzaldehyde was carried out. After extraction the resulting compound was purified by crystallization in ethanol to yield 84% of the desired chalcone product **18**. Characteristic enone doublets were noted for the chalcone intermediate **18** as well as the appropriate aromatic signals in the ^1H NMR spectrum for this compound as a key indicator for the molecule was in hand. Mass spectral for **18** data confirmed the molecular ion and additional peaks corresponding to the relative isotopic distribution of bromine. Continuing with the synthesis, the protected chalcone **18** was then subjected to an Algar-Flynn-Omayada oxidative ring closure. This afforded the corresponding brominated flavanol **19** in low yields, possibly due to degradation of the peroxide. Several spectroscopic techniques were employed to confirm the formation of the desired product however most notable change to the spectral data was noticed via ^{13}C NMR spectroscopy. The shifting of two peaks in the ^{13}C NMR spectrum relative to that of **19**, corresponding to the

Chapter 1 Synthesis and Imaging of Fluorescent Dietary Compound Analogues

newly formed quaternary carbons of **19** were assigned to the enol component of the formed pyranone ring. HRMS confirmed the molecular ion, ensuring that the additional alcohol relative to the precursor **18** was present. The final phenolic compound **3** was achieved by acidic deprotection of the flavanol by acid mediated elimination of the methoxymethyl protecting group. ^1H NMR spectroscopy revealed two downfield, broad singlets corresponding to the phenol and enol moieties, the former not being present in the spectrum of the starting material **19**. Additionally, the two singlets in the ^1H NMR spectrum of **19** which describe the protecting group were not present in the spectrum of **3**. HRMS confirmed the molecular ion supporting the structure proposed for **3**.

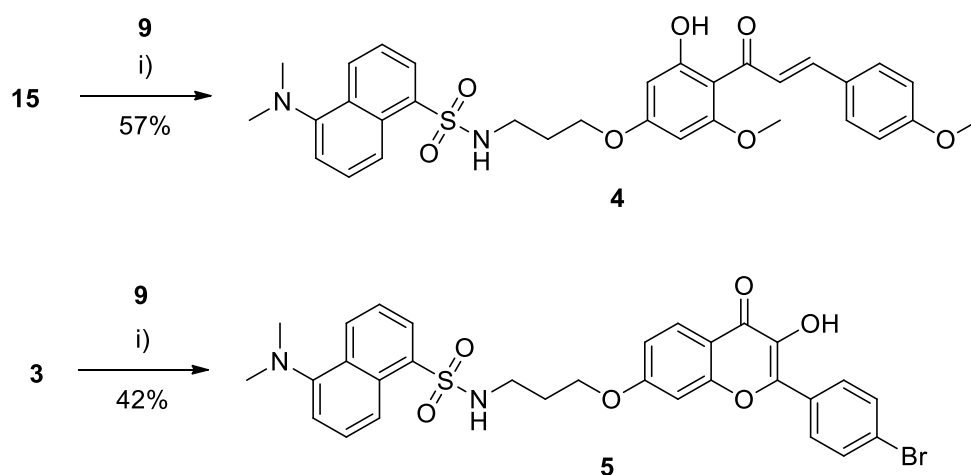


Scheme 3 Synthesis of BrFis. MOMCl (1.5 eq), K_2CO_3 (3 eq), Acetone, refl., 2 h; ii) p-bromobenzaldehyde (1.0 eq), aq KOH 50% w/w / Ethanol (3:20), rt, 24 h; iii) aq. 3 M KOH / methanol / H_2O_2 (2:2:1), rt, 18 h; iv) 3 M aq. HCl / Methanol (3:5), refl., 2 h

TARGET COMPOUNDS

The final targets, **4** and **5**, were achieved via a Cs_2CO_3 mediated alkylation of the prepared phenolics. Both **3** and **15** were fairly insoluble in common reaction solvents outside of DMF, which was selected as the reaction solvent to solve this problem. Also soluble in DMF, Cs_2CO_3 was chosen as an appropriate base for the alkylation of the phenols **3** and **15**. The pK_a of the sulphonamide **9** should be considered – where a stronger base may lead to unwanted side products. The solubility of Cs_2CO_3 also allows for more control over the number of equivalents of base added. Traditional alkylation conditions for phenols such as those employed in this study to achieve compounds **11**, **12** and **17**, require large excesses of carbonate base due to the salts insolubility in common lab solvents. The dansyl tag **9**, and the phenols **15** and **3** were stirred overnight at room temperature in DMF to afford the final targets. The isolated products were then characterized by NMR and HRMS to confirm the desired alkylated products. The structures of **4** and **5** and their respective ^1H NMR spectra have been colour coded in **figures 3 and 4**.

Chapter 1 Synthesis and Imaging of Fluorescent Dietary Compound Analogues



Scheme 4 Alkylation of the fragments **3** and **15** with the dansyl containing fluorescent marker. Conditions: i) **9** (1 eq), Cs_2CO_3 (1.2 eq), DMF, rt, 18 hr.

^1H NMR spectra of the final targets **4** and **5**, presented in **figures 3** and **4**, were key analyses confirming the success of the synthesis. Common to both probes **4** and **5** are the dansyl sulphonamide and linker moieties. In both **figures 3** and **4** these signals are highlighted by blue and green respectively. The dansyl sulphonamide signals tend to collapse at lower field strengths which is made most clear when observing the pair of doublets near 8.5 ppm in **figures 3** and **4**, where the two pairs are distinct in **figure 3** but convoluted in **figure 4**. Despite this factor the signals were assigned in both cases. The alkyl linker portion (**figure 2**) provided three signals, marked in green for both probes **4** and **5**. Each signal integrating for two protons and the accompanying splitting patterns describe the propyl chain well. The quartet present in both cases describes the methylene adjacent to the sulphonamide, due to coupling to the sulphonamide proton. Again in both spectra, the methylene of the linker assembly adjacent to the ether linkage can be described in both cases as the most downfield triplet marked in green in **figures 3** and **4** as a result of the deshielding nature of the ethereal oxygen. The most shielded signal marked in green in **figures 3** and **4**, a pentet, describes the remaining middling methylene of the propyl chain. In **figure 3** the two protons of the phenolic ring of **4** were assigned as the singlet seen at 7.79 ppm and described as a collapsed AB spin pair. The substitutions of this tetra substituted ring system were deemed such that the electronic properties of this electron rich ring may make the environments of these two protons equivalent at this field strength. The anisole structure was assigned two apparent doublets at 7.75 and 6.94 ppm in the aromatic region. The enone moiety was described by an apparent doublet of doublets at 5.84 ppm a major coupling constant of 8.4 Hz, again a collapsed pair of signals due to electronic effects of the now alkylated ring. The coupling constant, while not fully representative of the enone, does assist in describing an *E*-substituted double bond, which was also seen in the spectra of the precursors **14** and **15**. HRMS confirmed the molecular ion for **4**, assisting in the elucidation of this compound. As previously described the

Chapter 1 Synthesis and Imaging of Fluorescent Dietary Compound Analogues

phenolic group adjacent to the acetophenone is hydrogen bonded to the carbonyl oxygen of the acetophenone which eliminates this phenol as a candidate for alkylation. Under the conditions used, this phenol would be far less reactive and as such the alkylation product **4** was proposed.

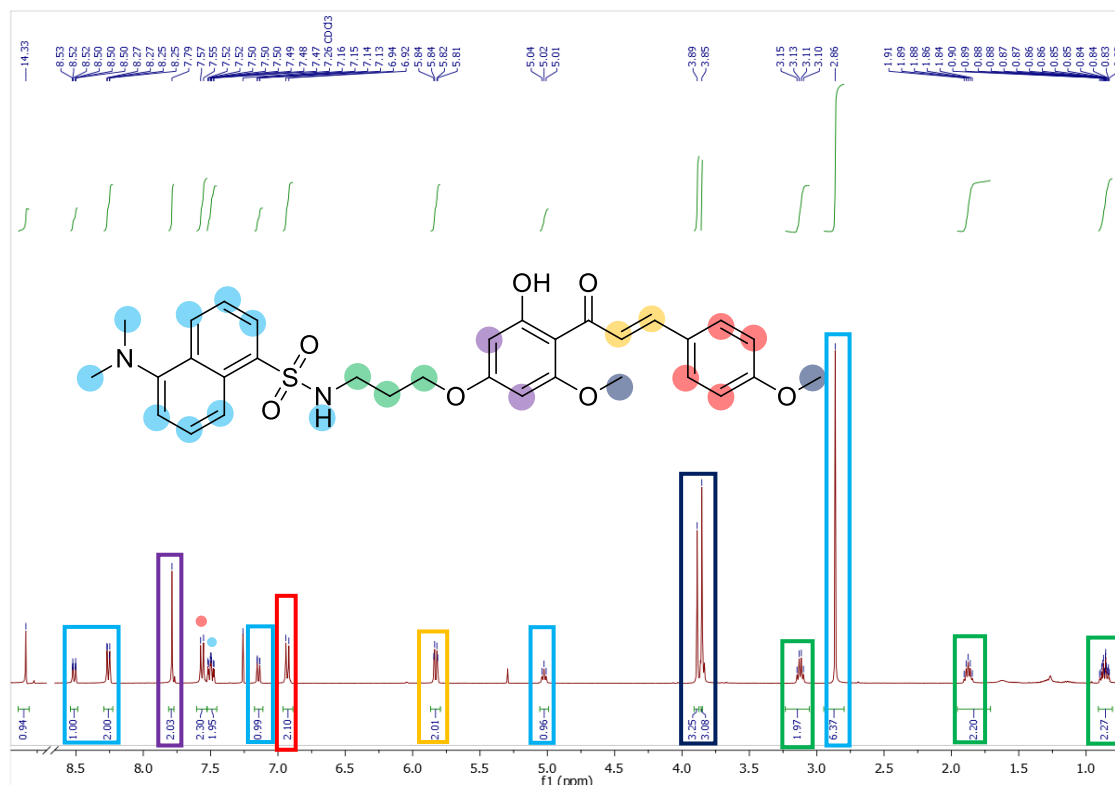


Figure 3 ^1H NMR spectrum of the target FKA analogue **4** in Chloroform- d at 300 MHz.

The BrFis probe, **5**, also relied heavily on the ^1H NMR spectrum (**figure 4**) to confirm its successful synthesis. Aside from the signals assigned to the dansyl and linker portions of the molecule which were discussed earlier, several other signals in this spectrum were key to identifying compound **5**. Highlighted in red in **figure 4** at 7.78 and 7.56 ppm are two sets of apparent doublets integrating for two protons describing the *para*-bromo substituted benzene moiety. Additionally the coumarin-like aromatic moiety was assigned three signals between 7.11 and 6.94 ppm. These include a doublet at 6.94 ppm with a small coupling constant of 2.1 Hz implying long range coupling. Additionally, a convoluted doublet and doublet of doublets, latter having a matching small coupling constant of 2.1 Hz, were observed between 7.11 and 7.06 ppm. These three signals are highlighted in purple in **figure 4**. These findings alongside HRMS confirmation of the molecular ion for this compound and additional ^{13}C NMR evidence confirmed that compound **5** had been successfully synthesised.

Chapter 1 Synthesis and Imaging of Fluorescent Dietary Compound Analogues

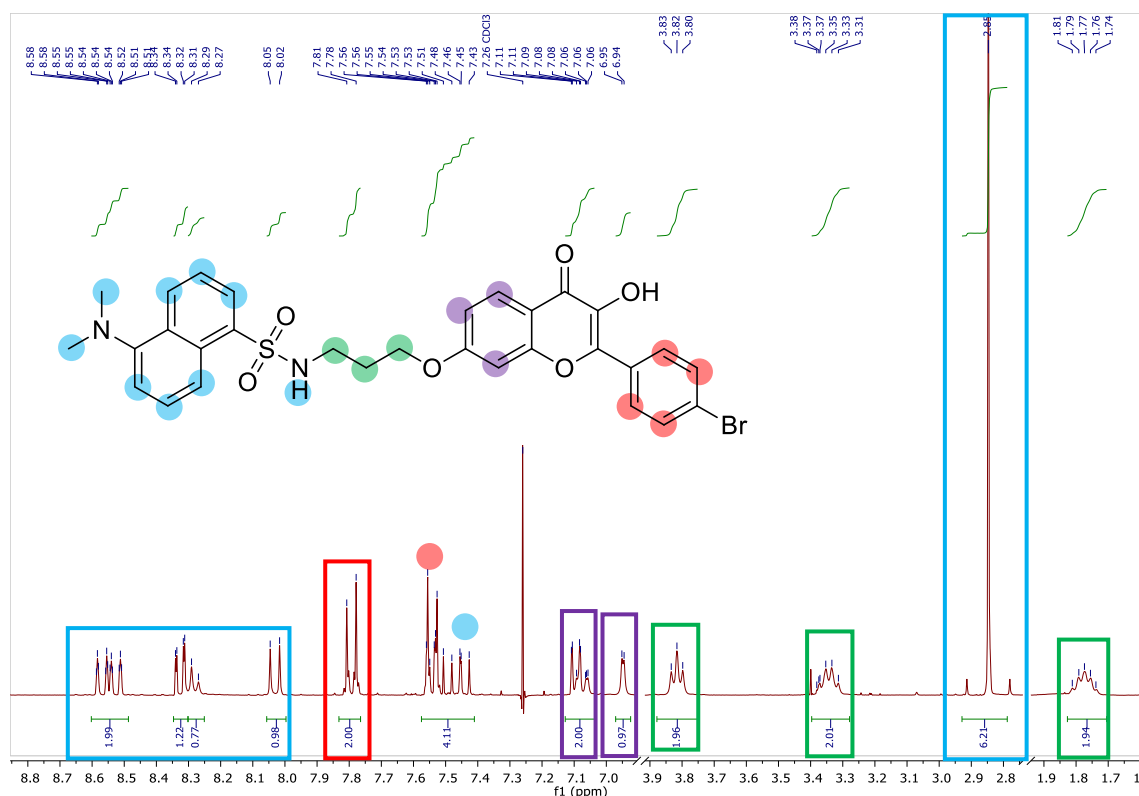


Figure 4 ^1H NMR spectrum of the target BrFis analogue **5** in Chloroform-*d* at 300 MHz.

BIOLOGICAL EVALUATION

With the probes DFKA **4** and DBrFis **5** in hand, their activity in the biological setting was tested. This was important as significant differences between the probe and their parent compound invalidates the probe as representative. After these analyses the probes were used in confocal microscopy studies to determine where they localise within cancer cells, as a representation of where the parent compounds localise. This assists in determining the mechanism of action for the parent compounds.

SUMMARY OF METHODS

MTT CYTOTOXICITY ASSAY

The 3-(4,5-dimethylthiazol-2-yl)-2,5-diphenyltetrazolium bromide (MTT) cellular viability assay measures the formation of formazan crystals via UV spectrometry. The cleavage of the yellow MTT reagent, forming a strongly absorbing purple product, occurs due to the metabolic activity of living cells. The amount of living cells can therefore be correlated to the absorbance of 595 nm light. The assay can in this way be used to determine the concentration of a drug necessary for 50% of the cells to be viable (IC_{50}). This value describes the relative activity of a drug and allows for comparisons to be made.

A dilution series in dimethyl sulphoxide (DMSO) of the analysed compounds was made from 200 μM to 0.01 μM , halving the concentration of the previous solution in each increment.

Chapter 1 Synthesis and Imaging of Fluorescent Dietary Compound Analogues

These solutions were then incubated in triplicate with a constant concentration of cells. Cell lines tested were A549 lung cancer and MDA-MB-231 breast cancer cell lines. Experiments were performed in triplicate and data gathered had curves fitted via logistic regression analysis. Data was represented as the logarithm of the concentration used versus the absorbance of 595 nm light. IC_{50} values were then determined from the resulting sigmoidal curves.

CONFOCAL MICROSCOPY

Chambered cover glass plates were charged with 30 000 cells per well and allowed to settle overnight. Cells were treated with a solution of the fluorescent probe in DMSO and incubated overnight, not exceeding 0.1 % DMSO in cells. Half an hour prior to viewing, cells were treated with commercially available live tracking dyes.

RESULTS

MTT ASSAY ANALYSIS

Across several repeated experiments the labelled flavanol and chalcone both showed excellent comparison to the unlabelled counterparts. Naturally occurring Flavokawain A was slightly more potent than its labelled cousin, whereas the reverse was observed for the labelled and unlabelled flavanol. When tested against the A549 lung cancer and MDA-MB-231 breast cancer cell lines, both labelled compounds compared well against their non-labelled counterparts. The natural compound, Flavokawain A and the fluorescently labelled analogue were tested. After analysis, as described in **figures 5** and **6**, DFKA displayed IC_{50} values of 187 and 91 μ M for the A549 and MDA-MB-231 cell lines respectively (**figure 5**). In comparison to naturally occurring FKA this is a two to three-fold decrease in activity, depending on the cell line. This may imply that FKA has a specific target such as a protein and is sensitive to modification. Other explanations for this loss in activity may lie in the chalcone's ability to be oxidised. Removing the phenolic group found in the parent compound and replacing it with the ether linkage as per the probe, compound **4** may lose its phenolic type anti-oxidant behaviour, reducing its effectiveness. Additionally, the bulk that the tag introduces into the probe may also hinder the compound, introducing steric interactions not present in the parent compound. However, these explanations are speculative and require further study. DBrFis **5** displayed IC_{50} values of 9 and 10 μ M for the A549 and MDA-MB-231 cell lines respectively; fractions of the activity of the parent compound **3**. This may be due to the modification of the phenol, once again. It is possible that the phenolic group is deprotonated to some degree in the biological system and this may reduce the compound's ability to cross hydrophobic, lipid membranes. The difference in activity between the compounds of interest and their fluorescent derivatives is within a tolerable range for imaging experiments to be valid. Should the values have deviated by more than an order of magnitude the results could be skewed by this property.

Chapter 1 Synthesis and Imaging of Fluorescent Dietary Compound Analogues

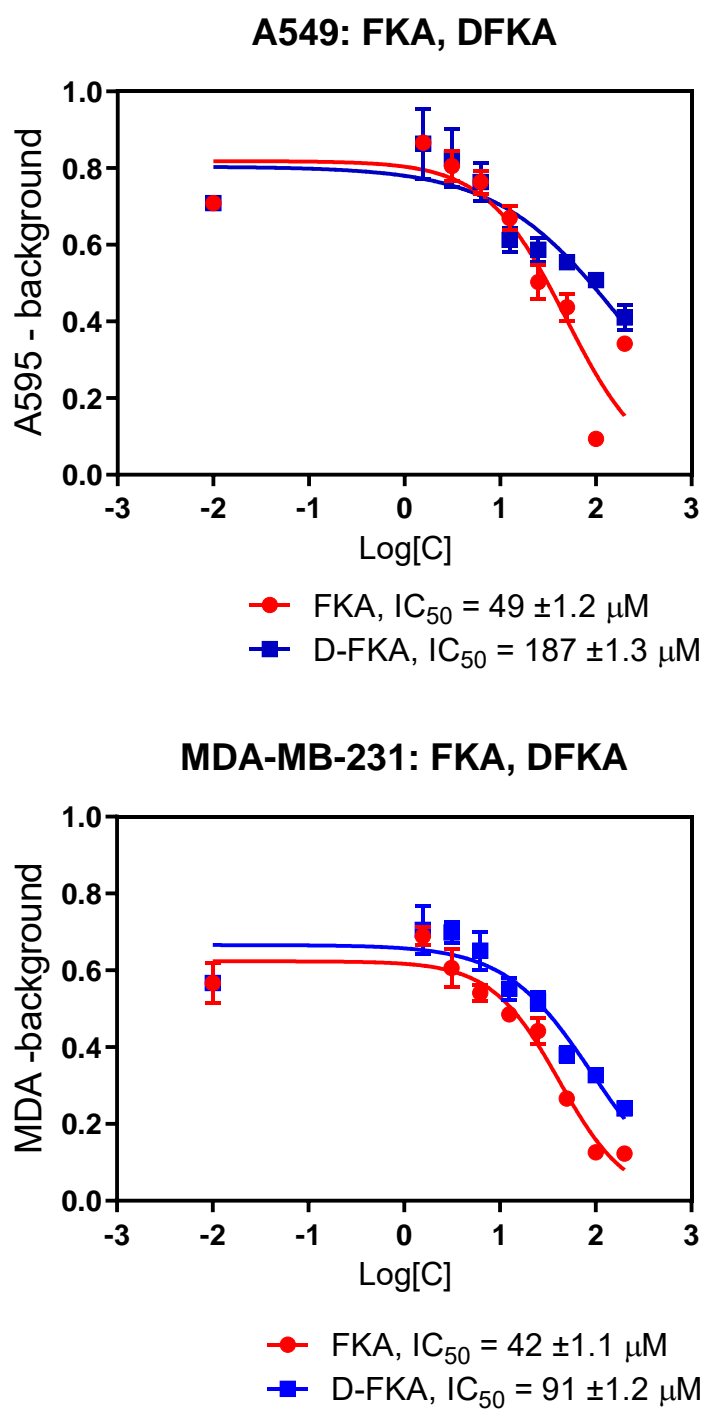


Figure 5 Dose response curves for absorbance vs log[C] as measured by MTT for compound **4** and FKA.

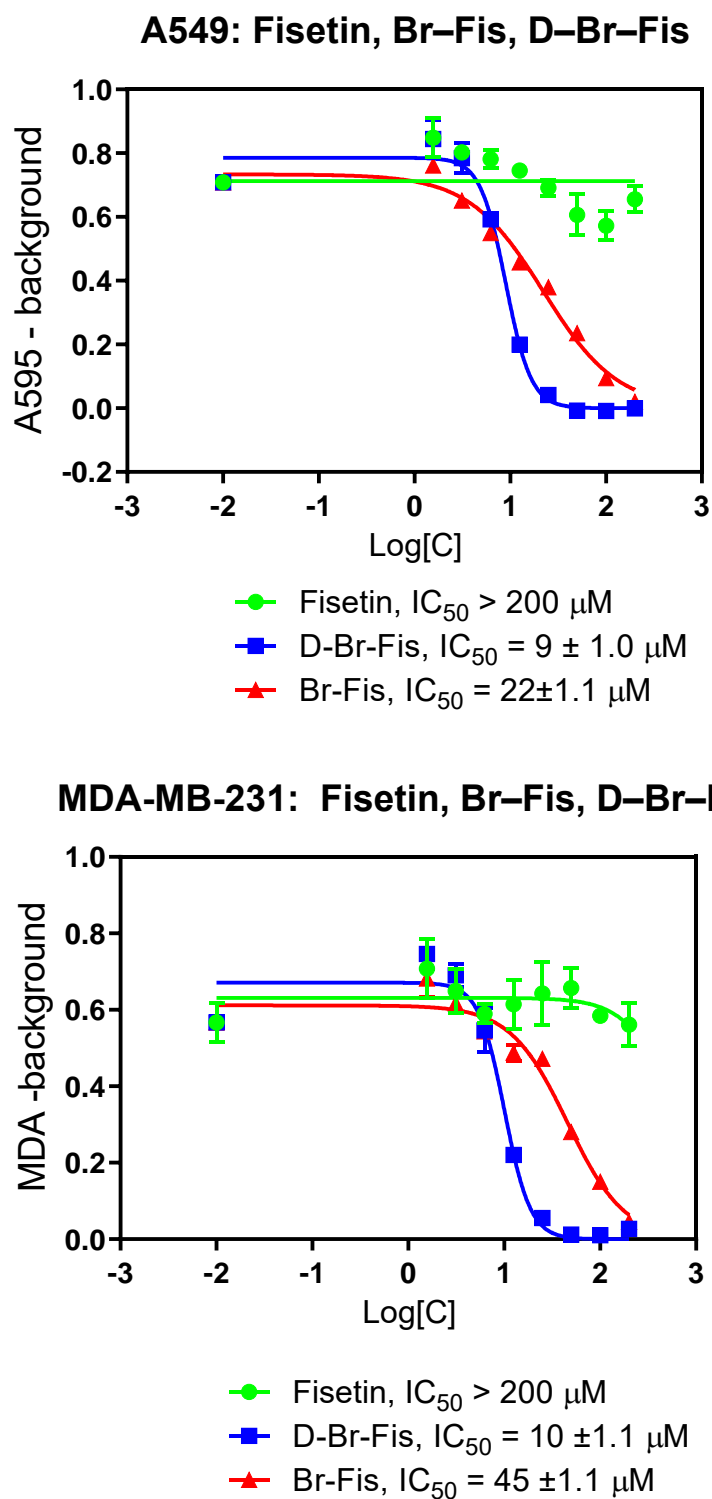


Figure 6 Dose response curves for absorbance vs log[C] as measured by MTT for compound **5**, fisetin and BrFis. Fisetin **2** has strong anti-oxidant properties and interferes with the MTT assay resulting in an IC_{50} value that is not representative of the true activity.

Chapter 1 Synthesis and Imaging of Fluorescent Dietary Compound Analogues

CONFOCAL STUDIES

The labelled FKA compound was incubated with MDA-MB-231 cells at a 50 μM concentration, against several live tracking dyes, staining for mitochondria, lysosome and endoplasmic reticulum (ER). These findings are visualised in **figure 7**. The compound was found to colocalise in only one of these organelles, the ER (**figure 7, xv**). Commercial ER-Tracker™ Red was used to stain the ER of the cells and a colocalization study was performed between the tracker and compound **4**. **Figure 9** highlights in yellow the pixels where wavelengths associated with the fluorescence wavelengths of both the probe **4** and the commercial tracker are detected. This implies that both compounds are detected in the same region. **Figure 10** shows the number of pixels overlapping between the two channels, red and blue; quadrant 3 describes pixels above background signal thresholds. This quadrant describes the number of colocalised pixels visually as a diagonal trend. As can be seen in **figure 10** the majority of the signals from both the tracker and the probe, **4**, are colocalised; residing in quadrant 3. Pearson's and Mander's coefficients for these plots are 0.34 and 0.75 respectively. These values describe the ratio of overlapped pixels between the two wavelengths observed. Pearson's coefficient ranges from -1 to 1 and describes the ratio between the two wavelengths observed, corrected by the average pixel intensity. However, for images where the average pixel intensity is quite high, this analysis is skewed and does not accurately describe the colocalization. A value of 1 describes perfect colocalization, and -1 describing the opposite scenario. Positive values of this coefficient describe colocalization. Mander's coefficient describes the colocalization as a value from 0 to 1 as a weighted average with values closer to 1 describing more colocalization. Both values confirm colocalization of the flavokawain probe **4** with the ER. Analysis of the DBrFis probe, **5**, resulted in values of 0.11 and 0.52 for the Pearson and Mander analyses respectively. The **figures 11** and **12** describe overlapped pixels highlighted in yellow and localisation map respectively. Though these analyses do show colocalization between the probe and the ER, they are only just exceeding the threshold. This may be due to the high potency of the probe; low treatment concentrations may be below the threshold for detecting the fluorophore effectively. The negative results for both probes **4** and **5** when tested support the findings for the ER, ruling out the interaction of the probes with the cellular dyes as no colocalization was found in the instances where mitotracker and lysotracker were utilised. Finally, the control dansyl tag compound, **20**, produced no noticeable signals confirming that the fluorophore is not responsible for the localisation observed. The synthesis of the dansyl control compound is detailed in the next section.

Chapter 1 Synthesis and Imaging of Fluorescent Dietary Compound Analogues

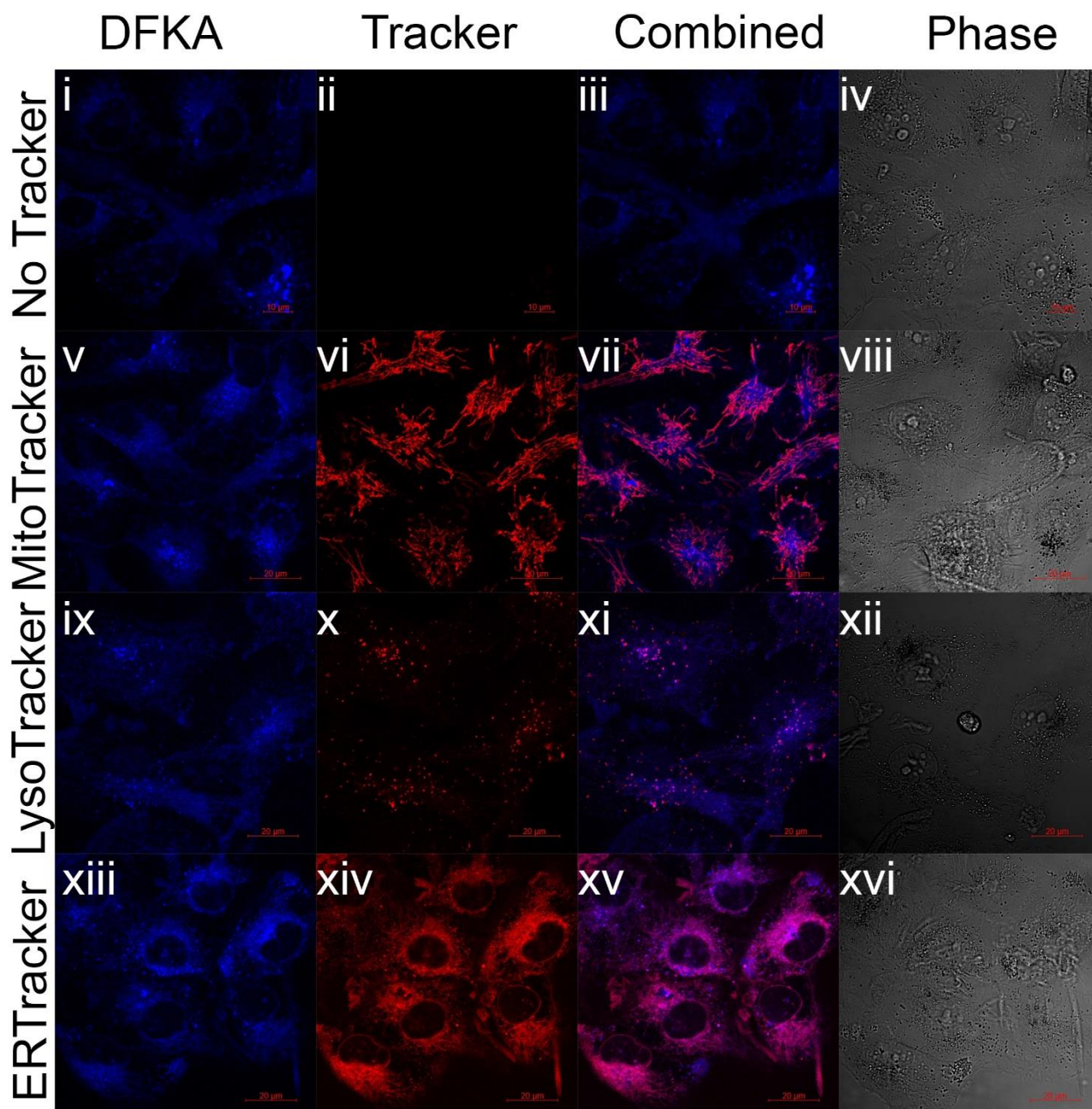


Figure 7 Confocal microscopy study of DFKA **4** and commercial live cell dyes. Columns represent from left to right, blue channel (wavelengths corresponding to the dansyl tag fluorescence emission spectrum), red channel (wavelengths corresponding to the tracking dye fluorescence emission spectrum), overlay of both red and blue channels, and the phase or visible, white light image. Rows represent the trackers used; colocalization can be seen very well in **xv** as the blue and red channels mix to form a magenta or pink colour. This colour mixing provides a speculative suggestion towards colocalization and was confirmed as true colocalization using the analyses described in **figures 8** and **9**.

Chapter 1 Synthesis and Imaging of Fluorescent Dietary Compound Analogues

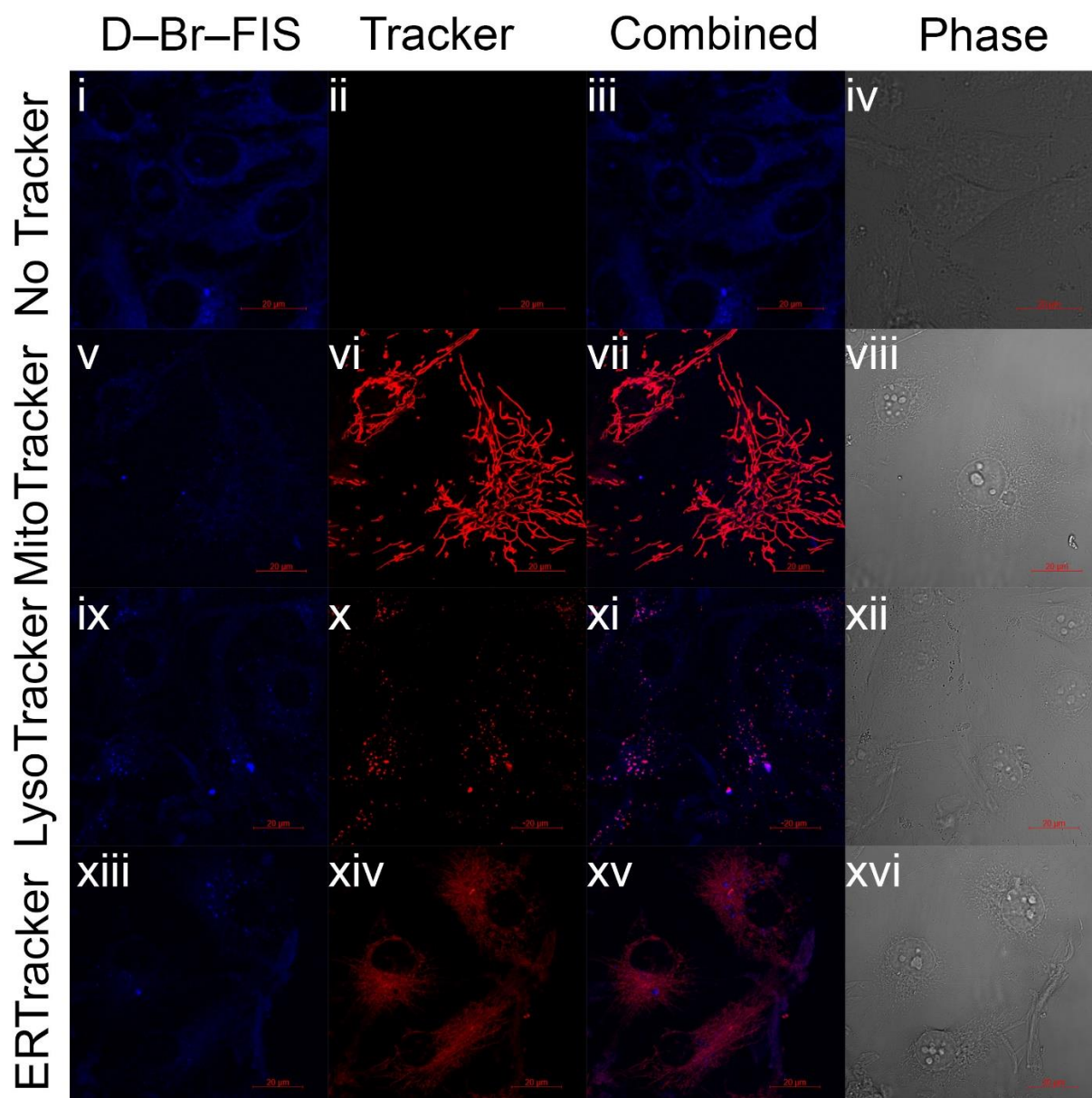


Figure 8 Confocal microscopy study of DBrFis **5** and commercial live cell dyes. Columns represent from left to right, blue channel (wavelengths corresponding to the dansyl tag fluorescence emission spectrum), red channel (wavelengths corresponding to the tracking dye fluorescence emission spectrum), overlay of both red and blue channels, and the phase or visible, white light image. Rows represent the trackers used; colocalization can be seen in frame **xv** as the blue and red channels mix to form a magenta or pink colour. However, this signal is very weak in comparison to the previous figure and can not be seen as clearly visually.

Chapter 1 Synthesis and Imaging of Fluorescent Dietary Compound Analogues

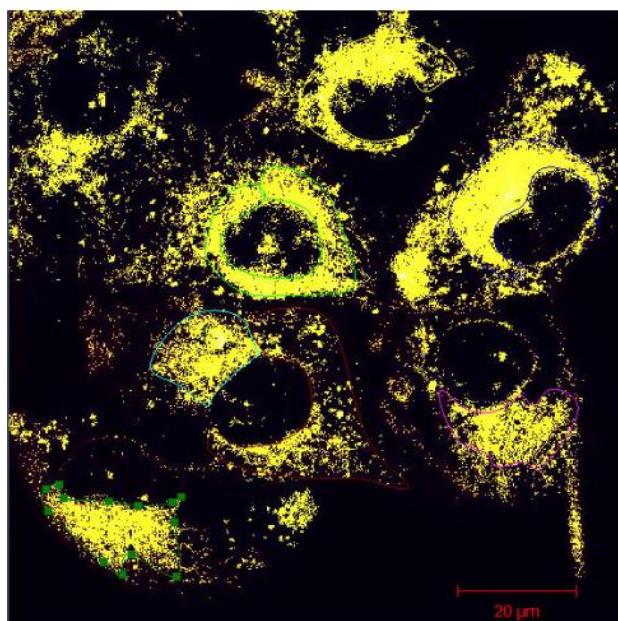


Figure 9 Image of cells treated with DFKA **4**, and ERTracker. Pixels containing information from both blue (DFKA probe **4**) and red (ERTracker) are highlighted in yellow.

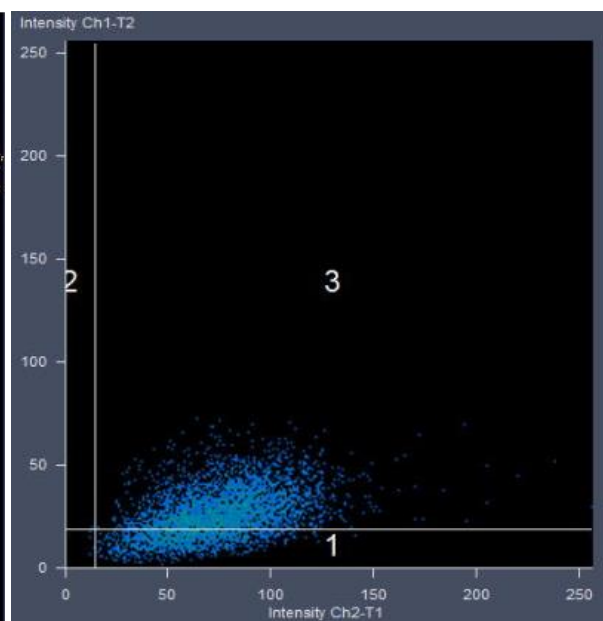


Figure 10 Colocalization map for the study of DFKA **4** (figure 7) between the ER and the probe. Pearson = 0.34; Mander = 0.75. Most of the signals are described by quadrant 3, confirming colocalization.

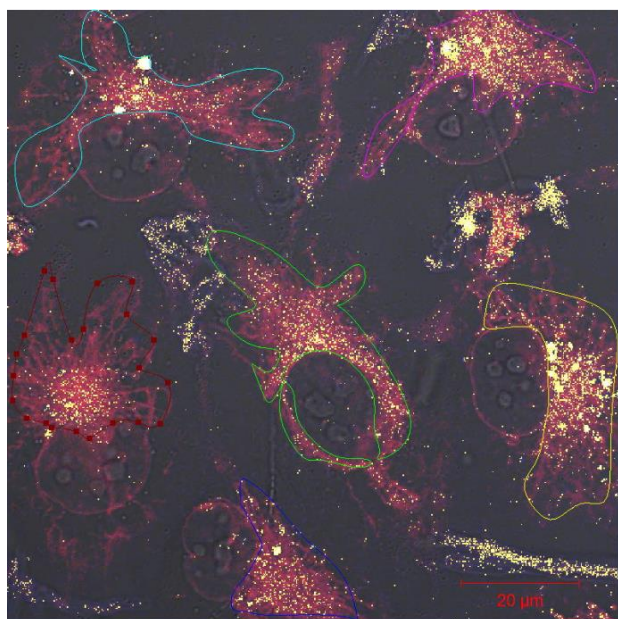


Figure 11 Image of cells treated with DBrFis **5**, and ERTracker. Pixels containing information from both blue (DBrFis probe **5**) and red (ERTracker) are highlighted in yellow.

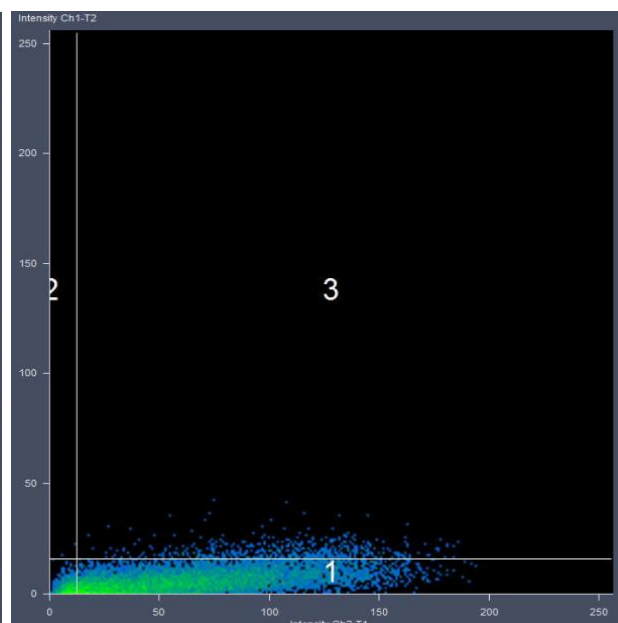


Figure 12 Colocalization map for the study of DBrFis **5**, (figure 8) between the ER and the probe. Pearson = 0.11; Mander = 0.52. Some of the signals are described by quadrant 3, suggesting some colocalization.

Chapter 1 Synthesis and Imaging of Fluorescent Dietary Compound Analogues

VALIDITY OF THE PROBES

A salient point to be discussed is the validity of the probes. Should the fluorophore drastically alter the observed activity of the compound, the localisation of the probe in cells would be invalid as an analogue for the natural compounds they represent. The activity of the compounds relative to their unlabelled counterparts, though altered is within an acceptable margin. Relevant control studies also eliminate the possibility that the fluorophore is responsible for the localisation seen. Additionally, the control compounds synthesised containing no pharmacophore reveal that the fluorophore does not contribute to any localisation. Thus, there is a good degree of confidence in the findings that these compounds are indeed localising in the endoplasmic reticulum.

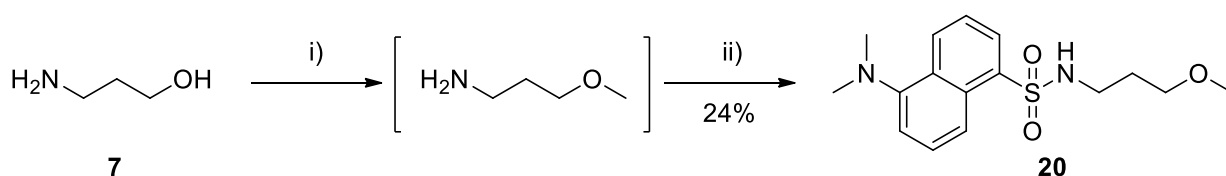
CONTROL COMPOUND

The methyl ether of compound **8** was synthesized in order to simulate the fluorophore and ether linkage. Investigating this portion of the target molecules, DFKA **4** and DBrFis **5**, in isolation was an important control study to perform. This ensures the effect of the fluorophore and the linker was negligible in comparison to the probes. The control compound was synthesized in a two-step, one flask procedure (**scheme 5**). Due to the low boiling and water solubility of one of the intermediates in this synthesis, a one flask protocol was performed. 1,3-propanolamine **7** was treated with NaH in THF and subsequently methylated using dimethylsulphate, as described by Kashima and coworkers.⁹ The resulting mixture was filtered of solids, the solids washed with DCM and the organic phase collected. The solvent was then removed carefully at room temperature *in vacuo* to avoid losing the methylated intermediate described in **scheme 5** which was not isolated. This crude mixture was then dissolved in DCM and commercially available dansyl chloride was then added at -10 °C in a single portion and left to stir overnight, warming to room temperature. This resulted in four distinct fluorescent products which were then separated by column chromatography. The desired product **20** was isolated and confirmed by ¹H and ¹³C NMR spectroscopy, where the additional aromatic signals were confirmed, as well as IR spectroscopy which confirmed the presence of the sulphonamide N–H. The control compound, **20** and the dansyl alcohol, **8** were used to investigate the influence of the fluorophore and linker assembly and to eliminate them as a cause of the colocalization. The control probes showed no colocalization with the ER (**figure 14**) and supports the biologically inert nature of the tag. This implies the natural product component of the probes are responsible for the majority of the localisation within the cell which was observed.

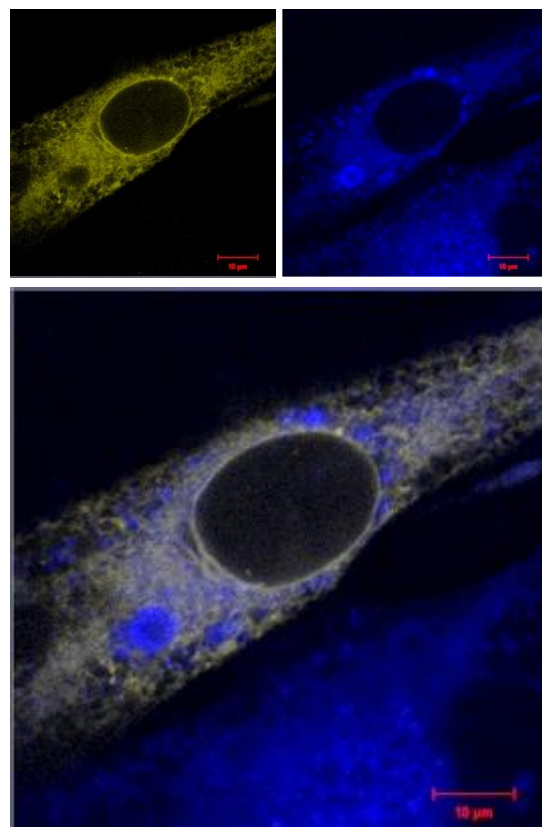
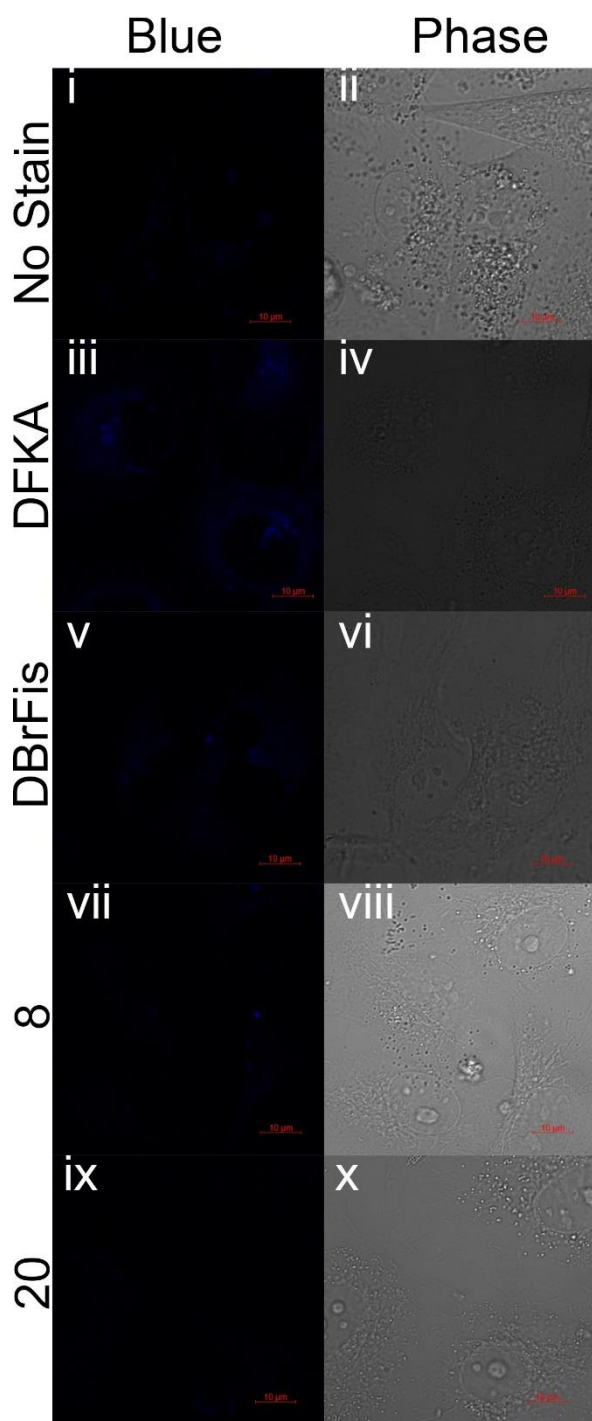
CONTROL COLOCALIZATION STUDIES

Yellow fluorescent protein (YFP) expressing MDA–MB–231 cells were incubated with the probes, **4** and **5**, and imaged (**figure 13**). The mutant cells express the fluorescent protein

Chapter 1 Synthesis and Imaging of Fluorescent Dietary Compound Analogues



Scheme 5 Synthesis of dansyl and linker assembly control compound. Conditions: i) NaH (1 eq), Me₂SO₄ (1 eq), THF, rt, 2 h; ii) dansyl Chloride (0.8 eq), Et₃N (1.2 eq), DCM, rt, 6 h.



▲ **Figure 13** YFP expressing MDA–MB–231 cells highlight the ER with yellow fluorescence; DFKa **4** colocalises with the ER to show a white glow, supplementing initial observations.

◀ **Figure 14** Blue channel and bright field (phase) images of (top to bottom) untreated cells, DFKa **4**, DBrFis **5**, the dansyl alcohol precursor **8**, and the methyl ether analogue **20**. In this group of images fluorescence can be seen for the probes **4** and **5** (iii–vi), however not for the control compounds **9** and **20** (vii–x).

Chapter 1 Synthesis and Imaging of Fluorescent Dietary Compound Analogues

which collects in the endoplasmic reticulum serving as a non-chemical staining method to recognise the ER. The probes were found to colocalise with the ER of the YFP expressing cells, confirming the colocalization results found in the previous studies. This also eliminates the possibility that the probes interact with the organelle stains used.

CONCLUSIONS

Both target compounds **4** and **5** have successfully been synthesised and confirmed by a variety of techniques. Their biological activity seems to mimic that of their parent compounds within a tolerable range and can be considered as insightful probes representing the natural products from which they have been derived. The labelled FKA analogue **4** has been imaged successfully and provides bright fluorescence suitable for confocal microscopy. Unfortunately, the same cannot be extended to the labelled DBrFis analogue **5**. The decrease in IC_{50} of the compound as a result of the labelling, although providing insight into improving the compound further, is detrimental to the imaging characteristics of the probe. The low concentrations of the pharmacophore also lower the concentration of the fluorophore below a critical threshold required for acceptable fluorescence. Despite this, the probe was visible enough to image, however provided limited colocalization information. Overall, both probes collected in the endoplasmic reticulum. Further studies are necessary to understand exactly how this stress occurs; the compounds may be interrupting protein folding or interacting with specific targets located within the ER. In either case the compounds can conclusively be located in the ER and provides an additional piece of the puzzle in elucidating their mechanism of action.

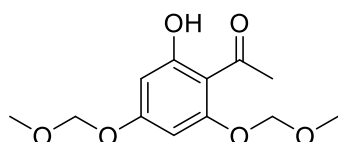
REFERENCES

- (1) Taylor, J. B.; Triggle, D. J. *Compr. Med. Chem. II* **1991**, 10 (4), 449–461. <https://doi.org/10.1002/qsar.19910100410>.
- (2) Panche, A. N.; Diwan, A. D.; Chandra, S. R. Flavonoids: An Overview. *J. Nutr. Sci.* **2016**, 5. <https://doi.org/10.1017/jns.2016.41>.
- (3) Tang, Y.; Simoneau, A. R.; Xie, J.; Shahandeh, B.; Zi, X. Effects of the Kava Chalcone Flavokawain A Differ in Bladder Cancer Cells with Wild-Type versus Mutant P53. *Cancer Prev. Res.* **2008**, 1 (6), 439–451. <https://doi.org/10.1158/1940-6207.CAPR-08-0165>.
- (4) Kaschula, C. H.; Hunter, R.; Cotton, J.; Tuveri, R.; Ngarande, E.; Dzobo, K.; Schäfer, G.; Siyo, V.; Lang, D.; Kusza, D. A.; et al. The Garlic Compound Ajoene Targets Protein Folding in the Endoplasmic Reticulum of Cancer Cells. *Mol. Carcinog.* **2016**, 55 (8), 1213–1228. <https://doi.org/10.1002/mc.22364>.
- (5) Zhenting, D.; She, X.; Ma, J.; Wang, Z.; Wu, H.; Li, Y.; Pan, X. A Facile Synthetic Route to Two Chalcones. *J. Chem. Res.* **2004**, 17 (2), 45–46.
- (6) Sabarwal, A.; Agarwal, R.; Singh, R. P. Fisetin Inhibits Cellular Proliferation and Induces Mitochondria-Dependent Apoptosis in Human Gastric Cancer Cells. *Mol. Carcinog.* **2017**, 56 (2), 499–514. <https://doi.org/10.1002/mc.22512>.

Chapter 1 Synthesis and Imaging of Fluorescent Dietary Compound Analogues

- (7) Pan, M. H.; Ho, C. T. Chemopreventive Effects of Natural Dietary Compounds on Cancer Development. *Chem. Soc. Rev.* **2008**, 37 (11), 2558–2574. <https://doi.org/10.1039/b801558a>.
- (8) Rodriguez-Fernandez, E.; Manzano, J.; Alonso, A.; Almendral, M.; Perez-Andres, M.; Orfao, A.; Criado, J. Fluorescent Cisplatin Analogues and Cytotoxic Activity. *Curr. Med. Chem.* **2009**, 16 (32), 4314–4327. <https://doi.org/10.2174/092986709789578169>.
- (9) Kashima, C.; Harada, K.; Omote, Y. The Influence of a Base on the Methylation of Aminoalcohols. *Can. J. Chem.* **1985**, 63 (2), 288–290. <https://doi.org/10.1139/v85-048>.
- (10) Zhen, X. H.; Quan, Y. C.; Peng, Z.; Han, Y.; Zheng, Z. J.; Guan, L. P. Design, Synthesis, and Potential Antidepressant-like Activity of 7-Prenyloxy-2,3-Dihydroflavanone Derivatives. *Chem. Biol. Drug Des.* **2016**, 87 (6), 858–866. <https://doi.org/10.1111/cbdd.12717>.

EXPERIMENTAL

2, 4-Dimethoxymethyl-6-hydroxylacetophenone 11

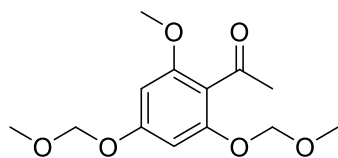
In a two neck round bottom flask equipped with a magnetic stirrer bar, was prepared a solution of trihydroxyacetophenone, (1000 mg, 5.37mmol, 1 eq) in acetone (30 mL). To this was added K_2CO_3 (5.68 g, 42.9 mmol, 8 eq) and allowed to stir for 0.5 h. To this solution was then added dropwise methoxymethyl chloride (1.00 mL, 13.4 mmol, 2.5 eq). After addition the solution was heated to reflux for 2 h, stirring. The solution was then cooled and filtered. The filtered solution was then evaporated *in vacuo*. The resulting solid was purified by column chromatography eluting with 5 - 30% EtOAc in hexanes to give the title compound, 743 mg, 54% as a sticky colourless oil. Spectral data collected for this compound compared well with reported literature values.⁵

1H NMR (400 MHz, Chloroform-*d*) δ 13.71 (s, 1H), 6.26 (d, J = 2.3 Hz, 1H), 6.24 (d, J = 2.3 Hz, 1H), 5.25 (s, 2H), 5.17 (s, 2H), 3.52 (s, 3H), 3.47 (s, 3H), 2.65 (s, 3H).

^{13}C NMR (101 MHz, Chloroform-*d*) δ 203.3, 166.9, 163.5, 160.4, 107.1, 97.2, 94.6, 94.1, 56.8, 56.5, 33.1.

IR (ATR, cm^{-1}) 2959 (O-H), 1590 (C=O)

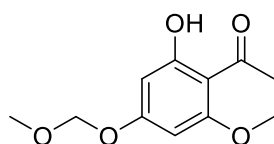
Chapter 1 Synthesis and Imaging of Fluorescent Dietary Compound Analogues

2,4-Dimethoxymethyl-6-methoxyacetophenone 12

In a two neck round bottom flask was prepared a solution of 2, 4-Dimethoxymethyl-6-hydroxylacetophenone (717 mg, 2.73 mmol, 1 eq) in acetone. To this was added K_2CO_3 (4.33 g, 32.76 mmol, 12 eq) and allowed to stir for 0.5 h. To this solution was added dimethylsulphate (0.62 mL, 6.55 mmol, 2.4 eq) dropwise. Once the addition was complete the solution was heated to reflux, and allowed to stir vigorously for 24 h. The reaction was then quenched with water (50 mL) and this mixture was extracted with diethyl ether (3×30 mL). The organic layers were collected and dried over $MgSO_4$. The solvent was filtered and evaporated *in vacuo* and the product purified by column chromatography eluting with 5 - 20% EtOAc in hexanes to give the title compound, 692 mg, 94% as a colourless oil. Spectral data collected for this compound compared well with reported literature values.⁵

1H NMR (400 MHz, Chloroform-*d*) δ 6.42 (d, $J = 2.0$ Hz, 1H), 6.28 (d, $J = 2.0$ Hz, 1H), 5.13 (s, 2H), 5.10 (s, 2H), 3.75 (s, 3H), 3.44 (s, 3H), 3.42 (s, 3H), 2.44 (s, 3H).

^{13}C NMR (101 MHz, Chloroform-*d*) δ 210.7, 201.5, 159.6, 157.8, 155.3, 115.7, 95.8, 94.7, 94.4, 93.8, 69.4, 56.2, 56.1, 55.7, 53.8, 32.4, 31.6, 29.2.

2-Methoxy-4-methoxymethyl-6-hydroxyl acetophenone 13

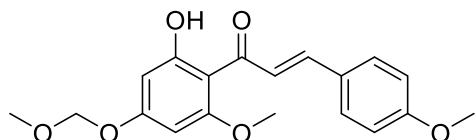
A two neck round bottom flask was prepared with a solution in methanol (2 mL) of 2,4-Dimethoxymethyl-6-methoxyacetophenone (108 mg, 0.398 mmol, 1 eq). To this was added a catalytic amount of I_2 (1 mg, 1% w/w) and allowed to stir for 2 h at rt. The reaction was quenched with a saturated aqueous solution of sodium thiosulphate (10 mL). The methanol was then removed under vacuum and the resulting solution extracted with ethyl acetate (3×30 mL). The organic layer was collected and dried over $MgSO_4$. The solution was then filtered and the solvent removed *in vacuo*. The resulting solid was then purified using column chromatography with elution gradient of 10 - 40% EtOAc in hexanes. Pure fractions were evaporated to dryness to afford the title compound as a white solid, 56 mg, 63% yield as a white solid. Spectral data collected for this compound compared well with reported literature values.⁵

Chapter 1 Synthesis and Imaging of Fluorescent Dietary Compound Analogues

^1H NMR (400 MHz, Chloroform-*d*) δ 13.84 (s, 1H), 6.21 (d, J = 2.3 Hz, 1H), 6.03 (d, J = 2.3 Hz, 1H), 5.18 (s, 2H), 3.87 (s, 3H), 3.48 (s, 3H), 2.61 (s, 4H).

^{13}C NMR (101 MHz, Chloroform-*d*) δ 203.4, 167.2, 163.7, 163.1, 106.7, 96.4, 94.1, 91.4, 56.5, 55.7, 33.1

IR (ATR, cm^{-1}) 2952 (O-H), 1589 (C=O)

2'-Hydroxyl-4'-methoxymethyl-4, 6'-dimethoxy chalcone 14

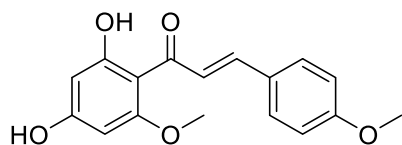
In an inert atmosphere, a two neck round bottom flask was prepared containing 2-Methoxy-4-methoxymethyl-6-hydroxyl acetophenone (100 mg, 0.440 mmol, 1 eq). To this was added a solution of KOH (500 mg), H_2O (1.00 mL) and ethanol (0.500 mL) and allowed to stir until homogeneous. To this solution was added *p*-anisaldehyde (59.0 mg, 0.440 mmol) in 0.5 mL ethanol. This solution was allowed to stir at rt for 24 h. It was noted the solution gradually gained an orange hue. The reaction was quenched with water (5 mL) and 1 M HCl was then added dropwise until acidic. Addition of acid caused a milky orange-yellow precipitate to form. This solution was extracted with ethyl acetate (3 \times 30 mL). The organic layers were collected, washed with saturated brine solution and dried over MgSO_4 . The solvent was then removed under vacuum and the product purified by column chromatography with elution gradient of 5 - 60% EtOAc in hexanes. Pure fractions were evaporated to dryness to afford the title compound as a yellow solid, 151 mg, 66% yield. Spectral data collected for this compound compared well with reported literature values.⁵

^1H NMR (300 MHz, Chloroform-*d*) δ 14.15 (s, 1H), 7.79 (s, 2H), 7.56 (d, J = 9.0 Hz, 2H), 6.93 (d, J = 8.5 Hz, 2H), 6.26 (d, J = 2.5 Hz, 1H), 6.07 (d, J = 2.5 Hz, 1H), 5.20 (s, 3H), 3.93 (s, 4H), 3.85 (s, 3H), 3.49 (s, 3H).

^{13}C NMR (75 MHz, Chloroform-*d*) δ 193.3, 168.3, 164.0, 163.1, 161.9, 143.1, 130.6, 128.8, 125.6, 114.9, 107.5, 97.1, 94.6, 92.3, 57.0, 56.4, 55.9.

IR (ATR, cm^{-1}) 2936 (O-H), 1580 (C=O)

Chapter 1 Synthesis and Imaging of Fluorescent Dietary Compound Analogues

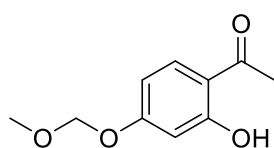
2', 4'-Dihydroxy-4, 6'-dimethoxy chalcone 15

To a solution of 2'-Hydroxyl-4'-methoxymethyl-4, 6'-dimethoxy chalcone (75.5 mg, 0.219 mmol, 1 eq) in methanol (5 mL) was added 3 M HCl (1.5 mL) in an inert atmosphere. This solution was heated to reflux and left stirring for 0.5 h. The solution was then allowed to cool to rt and extracted with ethyl acetate three times. The combined organic layer was washed with saturated brine solution and then dried over MgSO_4 . The solvent was then removed under vacuum and the residue purified by flash column chromatography with elution gradient of 5 - 70% EtOAc in hexanes. Pure fractions were evaporated to dryness to afford the title compound as an orange solid, 49 mg, 75% yield. Spectral data collected for this compound compared well with reported literature values.⁵

^1H NMR (600 MHz, Chloroform-*d*) δ 14.28 (s, 1H), 7.78 (s, 2H), 7.56 (d, J = 8.7 Hz, 2H), 6.93 (d, J = 8.8 Hz, 2H), 6.03 (d, J = 2.3 Hz, 1H), 5.95 (d, J = 2.4 Hz, 1H), 3.93 (s, 3H), 3.86 (s, 3H), 2.18 (s, 1H).

^{13}C NMR (151 MHz, Chloroform-*d*) δ 192.8, 168.0, 163.3, 162.5, 161.5, 142.7, 130.2, 128.4, 125.2, 114.5, 106.6, 96.9, 91.1, 56.1, 55.5.

IR (ATR, cm^{-1}) 3940 (O-H), 1623 (C=O)

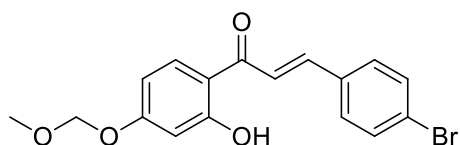
1-[2-Hydroxy-4-(methoxymethoxy)phenyl]ethan-1-one 17

In a two neck round bottom flask, equipped with a magnetic stirrer bar, was prepared a solution of 2,4-dihydroxyacetophenone, (10.0 g, 65.7 mmol, 1 eq) in acetone (400 mL). To this was added K_2CO_3 (26.1 g, 197 mmol, 3 eq.) and allowed to stir for 0.5 h. To this solution was then added dropwise methoxymethyl chloride (7.97 g, 98.6 mmol, 1.5 eq). After addition the solution was heated to reflux for 2 h, stirring. The solution was then cooled and filtered. The filtered solution was then evaporated *in vacuo*. The resulting solid was purified by column chromatography eluting with 5 - 30% EtOAc in hexanes. Pure fractions were collected and evaporated to dryness affording the title compound, 10.2 g, 79% yield as a colourless oil. Spectral data collected for this compound compared well with reported literature values.¹⁰

Chapter 1 Synthesis and Imaging of Fluorescent Dietary Compound Analogues

^1H NMR (400 MHz, Chloroform-*d*) δ 12.60 (s, 1H), 7.64 (d, J = 8.8 Hz, 1H), 6.59 (d, J = 2.4 Hz, 1H), 6.54 (dd, J = 8.9, 2.4 Hz, 1H), 5.20 (s, 1H), 3.47 (s, 3H), 2.56 (s, 3H).

^{13}C NMR (151 MHz, Chloroform-*d*) δ 202.69, 164.78, 163.52, 132.32, 114.70, 108.12, 103.70, 93.94, 56.32, 26.23.

(*E*)-3-(4-Bromophenyl)-1-[2-hydroxy-4-(methoxymethoxy)phenyl]prop-2-en-1-one 18

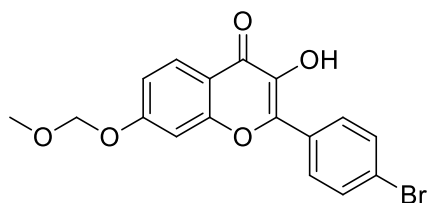
A two neck round bottom flask was prepared containing 1-[2-hydroxy-4-(methoxymethoxy)phenyl]ethan-1-one (10.2 g, 51.9 mmol, 1 eq). To this was added a solution of 50% w/w KOH (60 mL), and ethanol (300 mL) and allowed to stir until all the starting material had dissolved. To this solution was added a solution of *p*-bromobenzaldehyde (9.60 g, 51.9 mmol, 1 eq.) in ethanol (100 mL). This solution was allowed to stir at rt for 24 h. The reaction was quenched with water (100 mL) and 1 M HCl was then added dropwise until acidic. Addition of acid caused a milky precipitate to form. This suspension was extracted three times with ethyl acetate (3 x 100 mL). The organic layers were collected, washed with saturated brine solution (3 x 50 mL) and dried over MgSO_4 . The solvent was then removed under vacuum and the product purified by column chromatography eluting with 5 - 80% EtOAc in hexanes. Pure fractions were collected and evaporated to dryness affording the title compound, 15.8 g, 84% yield as an off white solid. Spectral data collected for this compound compared well with reported literature values.¹⁰

^1H NMR (300 MHz, Chloroform-*d*) δ 13.19 (s, 1H), 7.84 (d, J = 1.8 Hz, 1H), 7.81 (d, J = 8.3 Hz, 1H), 7.59 – 7.48 (m, 5H), 6.65 (d, J = 2.4 Hz, 1H), 6.59 (dd, J = 8.9, 2.5 Hz, 1H), 5.23 (s, 2H), 3.49 (s, 3H).

^{13}C NMR (75 MHz, Chloroform-*d*) δ 191.87, 166.43, 163.95, 143.30, 133.81, 132.41, 131.45, 130.02, 125.16, 121.00, 115.01, 108.50, 104.14, 94.19, 56.60.

MS (ESI+) predicted for $\text{C}_{17}\text{H}_{15}\text{BrO}_4$ [$\text{M}+\text{H}^+$]: 363.0234, found 363.0029.

Chapter 1 Synthesis and Imaging of Fluorescent Dietary Compound Analogues

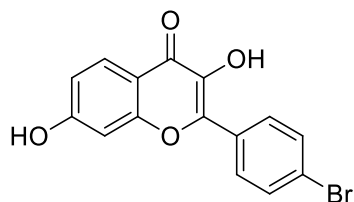
2-(4-Bromophenyl)-3-hydroxy-7-(methoxymethoxy)-4H-chromen-4-one 19

A two neck round bottom flask was prepared containing (*E*)-3-(4-bromophenyl)-1-[2-hydroxy-4-(methoxymethoxy)phenyl]prop-2-en-1-one (16.0 g, 44.1 mmol, 1 eq) and dissolved in 3 M KOH (50 mL) and further diluted in methanol (100 mL). This mixture was stirred vigorously at rt for 30 min. The solution was then cooled to 0 °C and a solution of 30% w/w hydrogen peroxide (110 mL) added slowly. The mixture was then allowed to warm to rt and stirred for 4 h. Addition of acid caused a milky precipitate to form. This suspension was extracted three times with ethyl acetate (3 x 100 mL). The organic layers were collected, washed with saturated brine solution (3 x 50 mL) and dried over MgSO₄. The solvent was then removed under vacuum and the product purified by column chromatography eluting with 5 - 100% EtOAc in hexanes. Pure fractions were collected and evaporated to dryness affording the title compound, 3.98 g, 24% yield as an off white solid.

¹H NMR (300 MHz, DMSO-*d*₆) δ 9.74 (s, 1H), 8.16 (d, *J* = 8.8 Hz, 2H), 8.02 (d, *J* = 8.9 Hz, 1H), 7.75 (d, *J* = 8.8 Hz, 2H), 7.33 (d, *J* = 2.3 Hz, 1H), 7.12 (dd, *J* = 8.9, 2.2 Hz, 1H), 5.37 (s, 2H), 3.43 (s, 3H).

¹³C NMR (75 MHz, DMSO-*d*₆) δ 177.59, 166.21, 161.22, 148.72, 144.35, 136.76, 135.81, 134.49, 131.59, 128.28, 121.11, 120.55, 108.06, 99.26, 61.28.

MS (ESI⁺) predicted for C₁₇H₁₃BrO₅ [M+H⁺]: 377.0026, found 377.0022.

2-(4-Bromophenyl)-3,7-dihydroxy-4H-chromen-4-one 3

A two neck round bottom flask was charged with 2-(4-bromophenyl)-3-hydroxy-7-(methoxymethoxy)-4H-chromen-4-one (2.93 g, 7.76 mmol, 1 eq) and dissolved in methanol (200 mL). To this solution was added 3 M HCl (25 mL). This solution was then heated to reflux and left stirring for 0.5 h. The solution was then allowed to cool to rt and extracted with ethyl acetate (3 x 200 mL). The combined organic layer was washed with saturated brine solution and then dried over MgSO₄. The solvent was then removed under vacuum and the crude

Chapter 1 Synthesis and Imaging of Fluorescent Dietary Compound Analogues

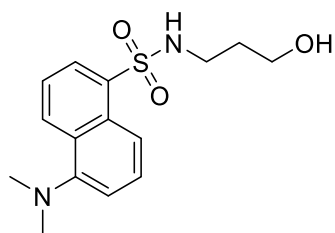
product was recrystallized from hot methanol (150 mL) to yield the title compound, 2.31 g, 90% as an off-white solid.

^1H NMR (300 MHz, $\text{DMSO}-d_6$) δ 10.87 (s, 1H), 9.58 (s, 1H), 8.12 (d, J = 8.8 Hz, 2H), 7.94 (d, J = 8.6 Hz, 1H), 7.74 (d, J = 8.8 Hz, 2H), 6.97 – 6.90 (m, 2H).

^{13}C NMR (75 MHz, $\text{DMSO}-d_6$) δ 172.32, 162.71, 156.51, 142.99, 138.83, 131.55, 130.74, 129.25, 126.61, 122.89, 115.04, 114.25, 102.01.

MS (ESI+) predicted for $\text{C}_{15}\text{H}_9\text{BrO}_4$ [$\text{M}+\text{H}^+$]: 332.9764, found 332.9767.

5-(Dimethylamino)-*N*-(3hydroxypropyl)naphthalene-1-sulfonamide 6



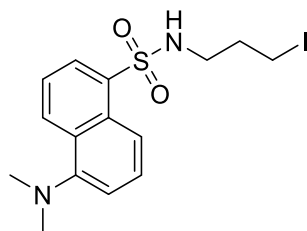
A two neck round bottom flask was prepared containing a solution of dansyl chloride (500 mg, 1.85 mmol, 1 eq) and triethylamine (374 mg, 3.70 mmol, 2 eq) in DCM (15 mL). This solution was cooled to 0 °C, followed by addition of 1,3-aminopropanol (208 mg, 2.78 mmol, 1.5 eq) in DCM (5 mL). The reaction was monitored by TLC and was quenched after 18 h by dissolution with DCM (50 mL) once starting material was no longer observed. The reaction was quenched by addition of NaHCO_3 (10 mL). The product was extracted with DCM (3 x 50 mL) and the collected organic layers were washed with saturated brine solution and then dried over MgSO_4 . The solvent was then removed under vacuum and the residue purified by column chromatography eluting with 10 – 80% EtOAc in hexanes to afford a white solid, 558 mg, 98% yield. Spectral data collected for this compound compared well with reported literature values.⁴

^1H NMR (600 MHz, Chloroform-*d*) δ 8.54 (d, J = 8.5 Hz, 1H), 8.28 (d, J = 8.6 Hz, 1H), 8.24 (dd, J = 7.3, 1.1 Hz, 1H), 7.59 – 7.49 (m, 2H), 7.18 (d, J = 7.5 Hz, 1H), 5.35 (t, J = 6.1 Hz, 1H), 3.65 (q, J = 5.1 Hz, 3H), 3.04 (q, J = 6.2 Hz, 2H), 2.89 (s, 5H), 1.88 (s, 1H), 1.63 (p, J = 5.9 Hz, 2H).

^{13}C NMR (151 MHz, Chloroform-*d*) δ 152.1, 134.7, 130.5, 130.1, 129.7, 129.7, 128.5, 123.3, 118.8, 115.3, 60.6, 45.5, 41.2, 31.6.

IR (ATR, cm^{-1}) 3501 (N-H), 3150 (O-H), 1307 (R_2SO_2)

Chapter 1 Synthesis and Imaging of Fluorescent Dietary Compound Analogues

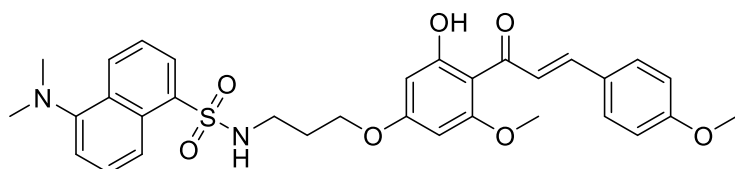
5-(Dimethylamino)-*N*-(3-iodopropyl)naphthalene-1-sulfonamide 9

A solution of 5-(Dimethylamino)-*N*-(3hydroxypropyl)naphthalene-1-sulfonamide (455 mg, 1.48 mmol, 1 eq) in DCM (10 mL) was prepared under a nitrogen atmosphere. This solution was cooled to 0 °C, followed by addition of imidazole (150 mg, 2.21 mmol, 1.5 eq), triphenylphosphine (580 mg, 2.21 mmol, 1.5 eq) and I₂ (561 mg, 2.21 mmol, 1.5 eq) in the order stated. The solution was allowed to reach room temperature, stirring, and was quenched with saturated aqueous sodium thiosulphate solution. The solution was then extracted with DCM (3 x 50 mL) and the organic layer washed with saturated brine solution and then dried over MgSO₄. The solvent was then removed under vacuum and the residue purified by column chromatography eluting with 0 – 40% EtOAc in hexanes to afford a luminous green-yellow fluorescent sticky oil, 600 mg, 97% yield. Spectral data collected for this compound compared well with reported literature values.⁴

¹H NMR (600 MHz, Chloroform-*d*) δ 8.56 (ddd, *J* = 8.5, 1.1 Hz, 1H), 8.29 – 8.24 (m, 2H), 7.61 – 7.51 (m, 2H), 7.22 – 7.17 (m, 1H), 4.78 (t, *J* = 6.4 Hz, 1H), 3.08 – 2.97 (m, 4H), 2.90 (s, 6H), 1.88 (p, *J* = 6.5 Hz, 2H).

¹³C NMR (151 MHz, Chloroform-*d*) δ 152.1, 134.3, 130.6, 129.9, 129.8, 129.5, 128.5, 123.1, 118.4, 115.2, 60.3, 45.3, 43.4, 32.8.

IR (ATR, cm⁻¹) 3289 (N-H), 1139 (R₂SO₂)

(*E*)-5-(Dimethylamino)-*N*-(3-(3-hydroxy-5-methoxy-4-(3-(4-methoxyphenyl)acryloyl)phenoxy)propyl)naphthalene-1-sulfonamide 4

To a two neck round bottom flask was added 2', 4'-Dihydroxy-4, 6' -dimethoxy chalcone (11 mg, 0.036 mmol, 1 eq) in DMF (1.0 mL). To this solution was added Cs₂CO₃ (14 mg, 0.043 mmol, 1.2 eq) and allowed to stir for 0.5 h. It was observed the solution turned from a pale orange to a deep amber colour. To this solution was added 5-(Dimethylamino)-*N*-(3-iodopropyl)naphthalene-1-sulfonamide (14.9 mg, 0.036 mmol, 1 eq). The solution was stirred

Chapter 1 Synthesis and Imaging of Fluorescent Dietary Compound Analogues

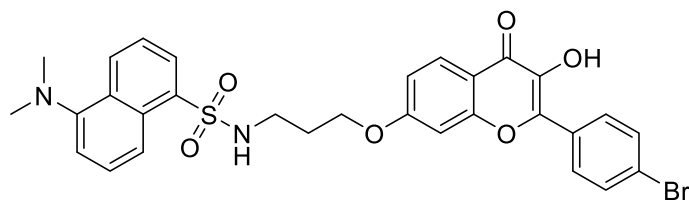
at room temperature for 24 h and then quenched with water (10 mL). The resulting solution was then extracted with ethyl acetate (3 x 20 mL). The organic layer was then washed generously with water (5 x 10 mL), and once more with a saturated brine solution (10 mL). The organic layer was then collected and dried over MgSO_4 . The solvent was then evaporated under vacuum and the resulting residue was purified by column chromatography eluting with 0 – 50% EtOAc in hexanes to afford the title compound as an orange oil, 12 mg, 57% yield.

^1H NMR (400 MHz, Chloroform- d) δ 14.33 (s, 1H), 8.51 (ddd, J = 8.5, 1.1 Hz, 1H), 8.26 (dd, J = 7.3, 1.2 Hz, 2H), 7.79 (s, 2H), 7.56 (d, J = 8.8 Hz, 2H), 7.50 (ddd, J = 8.6, 7.4, 2.3 Hz, 2H), 7.14 (dd, J = 7.6, 1.0 Hz, 1H), 6.93 (d, J = 8.8 Hz, 1H), 5.83 (dd, J = 8.9, 2.3 Hz, 2H), 5.02 (t, J = 6.2 Hz, 1H), 3.89 (s, 3H), 3.85 (s, 3H), 3.12 (q, J = 6.4 Hz, 2H), 2.86 (s, 6H), 1.88 (p, J = 6.1 Hz, 2H), 0.91 – 0.82 (m, 2H).

^{13}C NMR (101 MHz, Chloroform- d) δ 192.58, 168.11, 164.70, 162.38, 161.39, 152.06, 142.57, 134.27, 130.62, 130.12, 129.85, 129.82, 129.52, 128.48, 128.25, 125.04, 123.07, 118.40, 115.18, 114.37, 106.41, 94.30, 91.22, 65.43, 55.86, 55.39, 45.36, 40.56, 28.82.

MS (ESI+) predicted for $\text{C}_{32}\text{H}_{35}\text{N}_2\text{O}_7\text{S}$ [$\text{M}+\text{H}^+$]: 591.2165, found 591.2175.

***N*-{3-[(2-(4-Bromophenyl)-3-hydroxy-4-oxo-4H-chromen-7-yl)oxy]propyl}-5-(dimethylamino)naphthalene-1-sulfonamide 5**



Under an inert atmosphere, to a two neck round bottom flask was added 2-(4-bromophenyl)-3,7-dihydroxy-4H-chromen-4-one (50 mg, 0.15 mmol, 1 eq) in DMF (3.0 mL). To this solution was added Cs_2CO_3 (59 mg, 0.18 mmol, 1.2) and allowed to stir for 0.5 h. To this solution was added 5-(Dimethylamino)-*N*-(3-iodopropyl)naphthalene-1-sulfonamide (63 mg, 0.15 mmol). The solution was stirred at room temperature for 24 h and then quenched with water (15 mL). The resulting solution was then extracted with ethyl acetate (3 x 20 mL). The organic layer was then washed generously with water (5 x 10 mL), and once more with a saturated brine solution (10 mL). The organic layer was then collected and dried over MgSO_4 . The solvent was then evaporated under vacuum and the resulting residue was purified by column chromatography eluting with 0 – 50% EtOAc in hexanes to afford the title compound as a brown oil, 39 mg, 42% yield.

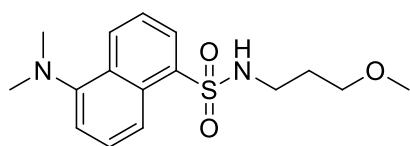
^1H NMR (300 MHz, Chloroform- d) δ 8.57 (ddd, J = 8.6, 0.9 Hz, 1H), 8.53 (ddd, J = 8.5, 1.1 Hz, 1H), 8.33 (dd, J = 7.3, 1.3 Hz, 1H), 8.28 (d, J = 6.5 Hz, 1H), 8.03 (d, J = 8.8 Hz, 1H), 7.79 (d, J =

Chapter 1 Synthesis and Imaging of Fluorescent Dietary Compound Analogues

8.8 Hz, 2H), 7.54 (d, J = 8.8 Hz, 2H), 7.51 – 7.41 (m, 2H), 7.12 – 7.05 (m, 2H), 6.95 (d, J = 2.1 Hz, 1H), 3.82 (t, J = 5.4 Hz, 2H), 3.34 (q, J = 6.3 Hz, 2H), 2.85 (s, 3H), 1.77 (p, J = 10.7, 5.6 Hz, 2H).

^{13}C NMR (75 MHz, Chloroform- d) δ 207.1, 174.8, 161.9, 157.0, 154.6, 151.7, 139.8, 136.2, 131.87, 129.97, 129.93, 129.77, 129.67, 129.53, 128.86, 127.90, 127.56, 125.37, 123.25, 119.8, 117.3, 115.3, 115.1, 102.8, 68.9, 45.4, 40.9, 40.1, 30.9, 29.4.

MS (ESI+) predicted for $\text{C}_{30}\text{H}_{28}\text{N}_2\text{O}_6\text{SBr}$ [$\text{M}+\text{H}^+$]: 623.0851, found 623.0845.

5-(Dimethylamino)-N-(3-methoxypropyl)naphthalene-1-sulfonamide 20

A two-neck flask was charged with sodium hydride 60% dispersion in mineral oil (614 mg, 16 mmol, 1 eq) and dissolved in THF (10 mL) and cooled to 0 °C. To this solution was added 1,3-aminopropanol (1.20 g, 16 mmol, 1 eq) in THF (5 mL) dropwise. This mixture was allowed reach rt with vigorous stirring for 30 min. To this solution was then added dimethyl sulphate (2.02 g, 16 mmol, 1 eq) in THF (5 mL) dropwise at rt. After the addition was completed the solution was stirred at rt for an additional 1 h. Once complete the solvent was removed under reduced pressure resulting in a clear oily residue. This residue was then dissolved in DCM (40 mL) and triethyl amine (1.62 g, 16 mmol 1 eq) was added and the solution cooled to 0 °C. Subsequently, dansyl chloride (1.00 g, 10 mmol, 0.62 eq) was added in a single portion. The mixture was stirred vigorously and allowed to reach rt over 6 h. The mixture was then quenched by dissolution with DCM (50 mL) and water (50 mL) was added. The resulting solution was then extracted with DCM (3 x 50 mL). The organic layer was then washed with a saturated brine solution (50mL). The organic layer was then collected and dried over MgSO_4 . The solvent was then evaporated under vacuum and the resulting residue was purified by column chromatography eluting with 0 – 100% EtOAc in hexanes to afford the title compound as a yellow oil, 1.24 g 24% yield over two steps.

^1H NMR (400 MHz, Chloroform- d) δ 8.52 (ddd, J = 8.6, 1.1 Hz, 1H), 8.29 (ddd, J = 8.7, 0.9 Hz, 1H), 8.23 (dd, J = 7.3, 1.3 Hz, 1H), 7.52 (ddd, J = 14.9, 8.6, 7.4 Hz, 2H), 7.17 (dd, J = 7.6, 0.9 Hz, 1H), 5.50 (t, J = 5.8 Hz, 1H), 3.26 (t, J = 5.6 Hz, 2H), 3.14 (s, 3H), 2.98 (q, J = 5.9 Hz, 2H), 2.87 (s, 6H), 1.64 (p, J = 5.8 Hz, 2H).

^{13}C NMR (101 MHz, Chloroform- d) δ 151.83, 134.32, 130.42, 130.25, 130.18, 129.35, 128.18, 123.23, 119.56, 115.33, 58.87, 46.42, 45.46, 34.39, 30.01.

MS (ESI+) predicted for $\text{C}_{16}\text{H}_{23}\text{N}_2\text{O}_3\text{S}$ [$\text{M}+\text{H}^+$]: 323.1429, found 323.1428.

TOWARDS A BRØNSTED ACID CATALYSED ENANTIOSELECTIVE SYNTHESIS OF 4-AZA-PODOPHYLOTOXIN

INTRODUCTION

A gracious opportunity was offered through Stellenbosch University and the Erasmus Mundus program for a short-term collaboration with Leipzig University over three months. The Schneider research group kindly extended their facilities and expertise and a project was designed as an intersection of research interests between the work of the sending and receiving groups.

PODOPHYLLOTOXIN

Podophyllotoxin is a naturally occurring lignan compound which can be isolated from *Podophyllum* plant species *P. hexandrum* and *P. peltatum*, the latter having the common names of American mandrake and mayapple.¹ This compound exhibits exceptional cytotoxic activity and has been used various applications, including the successful treatment of several cancers.¹

Additionally, semi-synthetic derivatives of this compound, known as etoposide and teniposide, have been used in the clinic as successful anti-cancer drugs.¹ It should be noted that the natural product and the semi-synthetic derivatives have wildly different biological targets. Whereas podophyllotoxin targets tubulin, etoposide and teniposide are topoisomerase II poisons but both display anti-cancer activity.² However, all these compounds display several limitations such as serious side effects and the development of resistance.³ The complexity of the molecule, with its four stereogenic centers also poses a serious synthetic challenge, and as such the majority of podophyllotoxin containing treatments are derived from plant material extracts.⁴

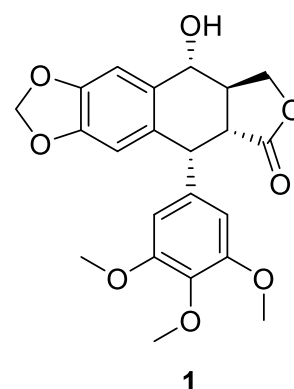


Figure 1
Podophyllotoxin1

MECHANISM OF ACTION

Podophyllotoxin and its derivatives, etoposide and teniposide, interrupt two distinct biological functions² depending on their functionalisation. These interruptions both ultimately lead to cell death. The naturally occurring podophyllotoxin inhibits the formation of tubulin which in turn prevents cell division.⁵ Tubulins are a class of proteins which form structural elements of the cytoskeleton which are known as microtubules. As a broad description these structures

Chapter 2 Towards a Brønsted Acid Catalysed Enantioselective Synthesis of 4-azapodophyllotoxin

govern intracellular transport and, important to the context of podophyllotoxin, are key components of mitotic spindles.⁵ These structures form a key step in cell division and uncontrolled division is a hallmark of cancers.⁵ Intentional control over this process allows the pharmacopeia an important tool for controlling and mitigating cancers. The other target is an enzyme known as topoisomerase II.¹ This enzyme is part of cellular DNA management and inhibition can lead to DNA damage which ultimately triggers apoptosis pathways.¹ The natural product derivatives discussed can interrupt the enzyme-DNA complex from completing its function, causing damage.

AZA-ANALOGUES

As previously discussed, clinical application of podophyllotoxin has several limitations and side effects. Gastrointestinal issues are prevalent during treatment, as well as a high toxicity to healthy cells.³ The four stereocenters lead to a prohibitively complicated synthesis pathway in order to replicate the natural product, counting against the product as a viable medicine.⁴ Plant sources therefore are the major source of the compound. However, 4-azapodophyllotoxins, with only one stereogenic centre, display equal if not higher biological activities while being synthetically much less challenging.⁶ It should be noted however, that this remaining stereocenter has a marked effect on the activity of the compound. The work of Magedov *et. al.* shows that a single enantiomer is responsible for the activity of the compound class, with the other being essentially inactive.⁷ Despite this fact, racemic mixtures still display excellent activities.⁶ Control over this centre would allow for a true description of the class's capabilities and therapeutic value. Enantiopure samples could show similar activities at lower dosages, an important factor in determining the therapeutic index of pharmaceuticals. Additionally, the structure is quite tolerant to modification outside of the dihydroquinoline lactone offering a wide range of possibilities for optimisation as a drug candidate.⁶

ORTHO-QUINONE METHIDES AND THEIR AZA ANALOGUES

Ortho quinone methides (oQM's) have been known about for over 100 years but have only recently been "tamed" as useful intermediates for synthesis.⁸ The reactivity of these intermediates can be attributed to the 1-oxabutadiene system they contain which can be formed by several methods such as thermolysis, oxidation, photolysis and most relevant to this discussion, acid- and base-mediated processes.⁹ These systems are highly reactive electrophiles, any suitable nucleophile adding to this Michael acceptor is encouraged by the reestablishment of aromaticity. Other modes of reactivity which have been explored are [4 + 2] cycloadditions and electrocyclizations; however, the Michael acceptor properties are most relevant to the scope of this discussion. These intermediates are highly reactive, driven by the stability of the products formed after aromatisation, requiring the intermediate to be

Chapter 2 Towards a Brønsted Acid Catalysed Enantioselective Synthesis of 4-azapodophylotoxin

generated *in situ*.⁸ This requires the design of the starting oQM generating fragment, generation method and nucleophile to be designed in concert as each variable may pose restrictions on the other.

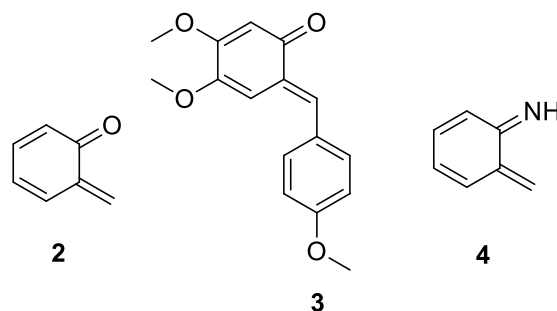
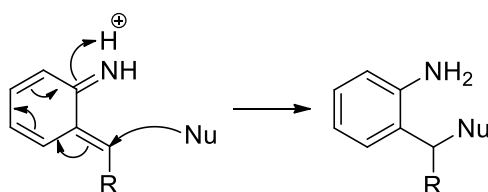


Figure 2 The *ortho* quinone methide moiety **2**; (E)-3,4-dimethoxy-6-(4-methoxybenzylidene)cyclohexa-2,4-dien-1-one **3** is one of the few bench stable oQMs; The *ortho* quinone methide imine moiety **4**.



Scheme 1 Nucleophilic attack on the Michael accepting position of the oQMI fragment results in bond formation and rearomatization. Reestablishment of aromaticity greatly contributes to the reactivity of quinone methide chemistry.

Similar chemistry can be performed on ortho quinone methide imines (oQMIs), the aza analogues of the systems described above.¹⁰ The aniline-derived oQMIs are decidedly less reactive than their phenolic cousins; however provide additional opportunities for forming *N*-functionalised products.¹¹

CHIRAL CONTROL OVER *N*-HETEROCYCLES DEMONSTRATED BY SCHNEIDER AND COWORKERS

Axial chirality arises from the non-planar arrangement of four groups about an axis.¹² Allenes, spiro compounds and biarenes are examples of systems that can be described as axially chiral. In biaryl systems steric effects can force one of the paired aromatic moieties to ‘twist’ out of the plane of the other. Viewing biaryls side on, one can visualise a tetrahedron over the molecule with the nearest and furthest atoms acting as vertices. From this the absolute configuration can be described by Cahn-Ingold-Prelog rules and assigned as R or S. This can also be referred to as helicity and the enantiomers can also be described as having M or P helicity.

Chapter 2 Towards a Brønsted Acid Catalysed Enantioselective Synthesis of 4-azapodophylotoxin

Axially chiral binaphthyl phosphoric acids or BINOL-PA's have been demonstrated by Schneider and coworkers to form oQMs⁹ and oQMIs¹¹ via acid-mediated dehydration of benzydrylic alcohols as a viable and versatile synthetic strategy; transferring chiral information to products formed from these intermediates.

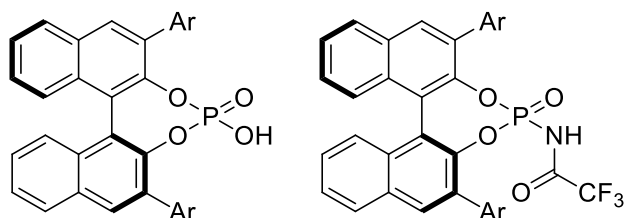


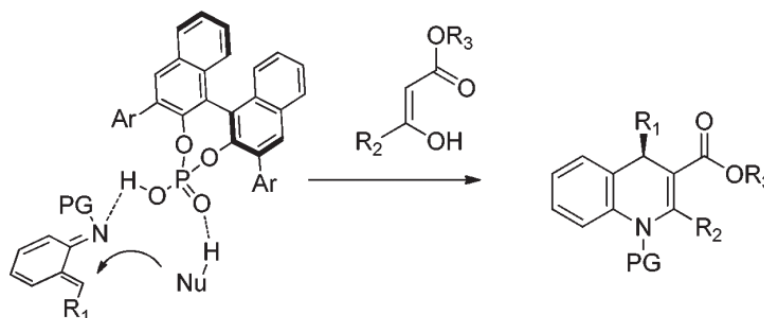
Figure 3 BINOL phosphoric acid (PA) and *N*-triflyl amide (NTf) Brønsted acid catalysts used by the Schneider working group.

Generating oQMI's in this fashion allows for reaction with several classes of nucleophiles with enamides,¹³ β -dicarbonyls and enolisable aldehydes¹⁰ being demonstrated as synthetically useful by the group. Enantiomerically-enriched tetrahydroacridines, 1-4-dihydroquinoline-3 carboxylates and diaryl dihydrocoumarins were produced respectively from these nucleophiles as a sample of the methods developed by the group. The researchers propose that the chiral information is transferred from the catalyst by a hydrogen bonded transition state. Consider the case of an oQMI aminobenzhydrylic alcohol precursor and a β -dicarbonyl nucleophile. The phosphoric acid mediates dehydration of the alcohol and hydrogen bonds to the formed oQMI. An additional hydrogen bond pair can be formed between the β -dicarbonyl enol and phosphoric acid shown in **scheme 2**. They propose that the steric demand of the bulky functionalisation of the BINOL-PA organises these components in such a way as to promote conjugate addition of the enol to the oQMI from a single face, while the other is adequately blocked off. After this addition the re-formed aniline is available for intramolecular cyclisation to the aminor. Subsequent acid mediated dehydration forms the final unsaturated heterocycles. A library of functionalisations have been demonstrated on both the oQM fragments as well as the various nucleophiles tolerated by the process. As a result the group has demonstrated a versatile and well described method for the enantioselective formation of six membered functionalised heterocycles.¹¹

Of particular interest for this discussion is the use of β -dicarbonyls to form dihydroquinoline-3 carboxylates. The lactone moiety of 4-azapodophylotoxins is a critical pharmacophore and commercially available tetronic acid is routinely used to introduce this group synthetically.¹⁴ Tetronic acid is a β -dicarbonyl lactone that exists primarily as its enol form. Schneider and coworkers have demonstrated enantiomeric control with cyclic β -dicarbonyls and ketoesters,¹¹ however tetronic acid specifically has not been demonstrated at the time of

Chapter 2 Towards a Brønsted Acid Catalysed Enantioselective Synthesis of 4-azapodophyllotoxin

writing. It would be reasonable to propose tetronic acid as a suitable nucleophile with respect to the functional groups tolerated.



Scheme 2 The Schneider working group proposes this transition state for the formation of dihydroquinoline-3 carboxylates formed by nucleophilic attack of the enolate on the Michael accepting methide of the oQMI. This model proposes the steric demand of the aryl groups organises the transition state so as to achieve the enantioenriched product.

Reproduced from Hodik and Schneider.¹¹

AIM

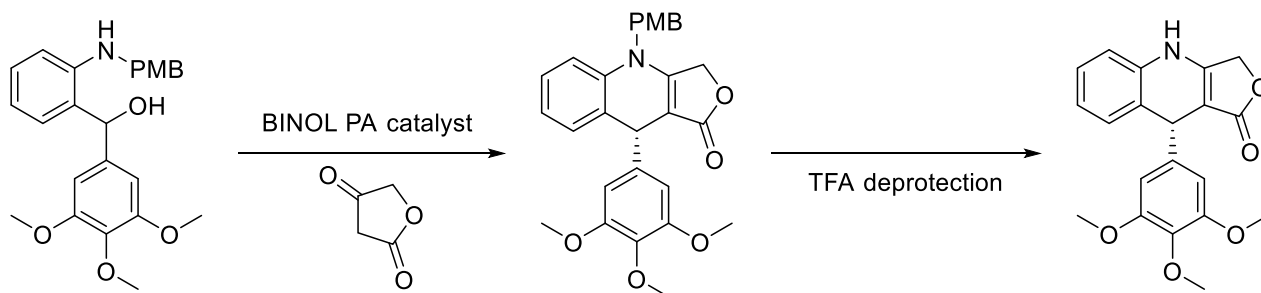
Since the Schneider group has demonstrated enantiomeric control over the formation of 6 membered *N*-heterocycles, the question was posed if the methods and expertise developed within the group could be applied to the formation of 4-aza-podophyllotoxins. Control over the available stereocenter and its marked effect on the biological activity of this class of compounds seemed to be a logical and worthwhile investigation.

RETROSYNTHESIS

As described previously, electron rich aromatic systems capable of forming orthoquinone methides and their aza analogues tend to form more readily than electron poor systems. At times these species can be bench stable, despite the disruption of aromaticity. This is particularly well noted in systems where electron donating methoxy groups are situated *para* to the moieties required for this chemistry to occur. Considering this, the dioxolane ring present in podophyllotoxin and its discussed analogue raised concerns of added complexity.

As such a model system was proposed as per **scheme 3**, to determine the viability of chiral Brønsted acids to perform the intended transformation. The initial target fragments were heavily influenced by the previous successes and knowledge of the Schneider group; a protected anilino-benzhydrylic alcohol is required to form the desired oQMI. Using tetronic acid as a nucleophile in combination with the BINOL-PA catalysts the group has at its disposal is proposed to reach the intended, enriched target which can be deprotected.

Chapter 2 Towards a Brønsted Acid Catalysed Enantioselective Synthesis of 4-azapodophylotoxin

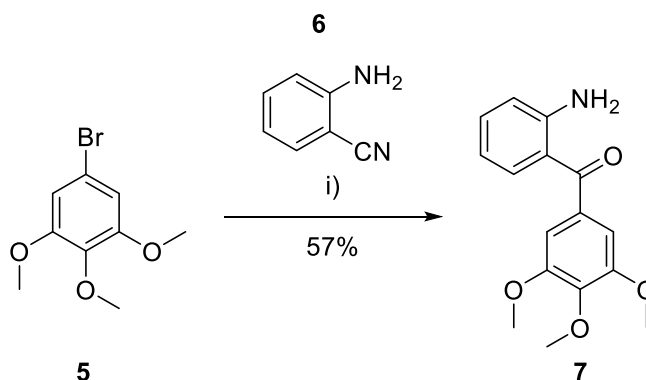


Scheme 3 Proposed synthetic strategy to achieve enantioenriched 4-azapodophylotoxins.

RESULTS AND DISCUSSION

MODEL SUBSTRATE SYNTHESIS

The required benzhydrylic alcohol fragment was achieved over the following three transformations and was synthesised as per literature procedure.¹⁰



Scheme 4 Conditions: i) **5** (3.5 eq), Mg (3.5 eq), **6** (1 eq), THF, refl., 24 h.

The first intermediate was achieved by a formation of 3,4,5 trimethoxyphenyl magnesium bromide in THF and subsequent nucleophilic attack of the Grignard reagent on 2-aminobenzonitrile, described in **Scheme 4**. Upon complete consumption of the nitrile, the resulting imine was hydrolyzed in an acidic aqueous environment to afford the desired ketone **7** in an acceptable yield. The structure of this compound was confirmed with ¹H NMR (**figure 4**) and HRMS being the key analyses. Methoxy groups were easily identified at 3.91 and 3.86 ppm, appearing as intense singlets. Four signals representing four protons in different aromatic environments were observed with splitting patterns consistent with ortho-substituted benzenes. A singlet integrating for two protons was assigned to the remaining trimethoxy substituted symmetrical benzene.

Chapter 2 Towards a Brønsted Acid Catalysed Enantioselective Synthesis of 4-azapodophylotoxin

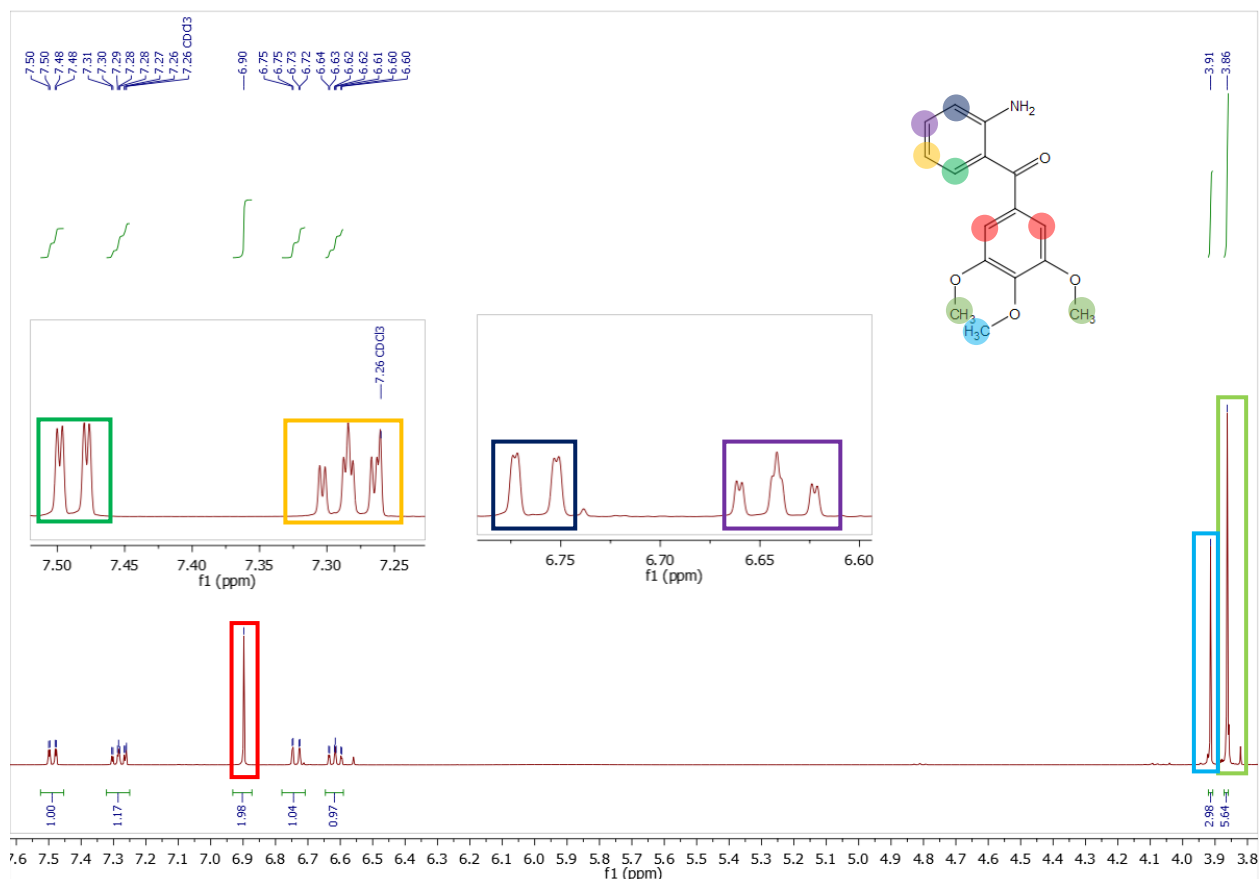
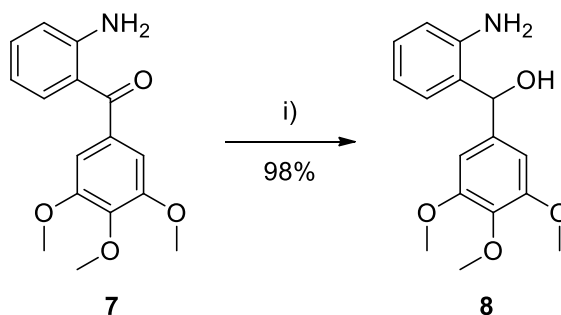


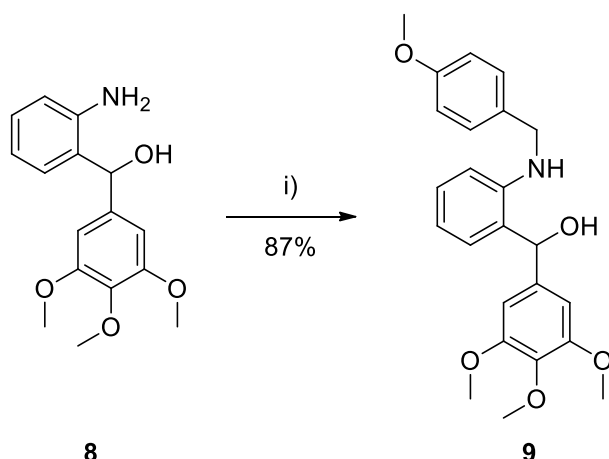
Figure 4 ^1H NMR of compound **7** was completely assigned and subsequent spectra were assigned relative to this initial value.



Scheme 5 Reduction of benzophenone. Conditions i) NaBH_4 (0.98 eq), EtOH/EtOAc (3:1), 0°C – rt, 4 h.

This benzophenone was then reduced with NaBH_4 in a mixed ethanol/ethylacetate solvent system to the corresponding alcohol in excellent yield. The appearance of a single proton at 5.77 ppm in the ^1H NMR spectrum was assigned to the now formed benzylic proton and in combination with the confirmed mass of the compound via HRMS the analysis was in good agreement with literature.¹¹

Chapter 2 Towards a Brønsted Acid Catalysed Enantioselective Synthesis of 4-azapodophylotoxin



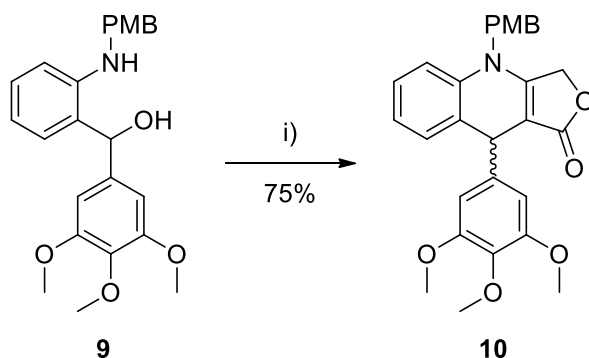
Scheme 6 Protection of aniline benzyhydrilic alcohol. Conditions i) AcOH (2.8 eq), anisaldehyde (1.2 eq), NaCNBH₄ (1.2 eq), 3Å molecular sieves, MeOH, 0 °C – rt, 3 h.

Furthermore this (2-aminophenyl)(3,4,5-trimethoxyphenyl)methanol fragment was protected by reductive amination with *p*-anisaldehyde. This afforded the desired PMB protected aminoalcohol in good yield of 87%. The target benzhydrylic alcohol was confirmed with ¹H NMR where the additional benzylic protons and pair of doublets integrating for two protons each at 7.10 ppm and 6.82 ppm denoting the anisole moiety. HRMS analysis was key to confirming the additional mass added to the molecule. The overall yield was calculated to be 49% over 3 steps. The initial Grignard addition reaction severely limits what has the potential to be a highly efficient synthesis. However, this route was deemed satisfactory for the purposes of the study.

PROOF OF CONCEPT

In order to establish the viability of tetronic acid as a suitable nucleophile to form the desired 4-azapodophylotoxin analogue catalysed by a Brønsted acid and is shown in **scheme 7**. As mentioned previously, acid mediated elimination of the benzydrylic alcohol leads to the formation of the reactive oQMI fragment. This electrophile then can receive the enol nucleophile, in this case tetronic acid. Subsequent enamine formation between the aniline and carbonyl of the tetronic acid moiety results in the desired heterocyclic ring formation. The catalyst loading, solvent and proportion of nucleophile was based on conditions shown to be previously successful within the Schneider research group on similar systems.¹¹

Chapter 2 Towards a Brønsted Acid Catalysed Enantioselective Synthesis of 4-azapodophylotoxin



Scheme 7 Generating the *o*-quinone methide imine via acid mediated dehydration with *p*-toluenesulphonic acid, investigating the viability of tetronic acid as a nucleophile. Conditions
i) tetronic Acid (1.2 eq), *p*-TSA (0.1 eq), DCM, rt, 18 h.

INITIAL CHIRAL CATALYST SCREENING

The conditions and catalysts described in **Table 1** were screened using commercially available tetronic acid as the required 1,3-dicarbonyl nucleophile to form compound **10**.

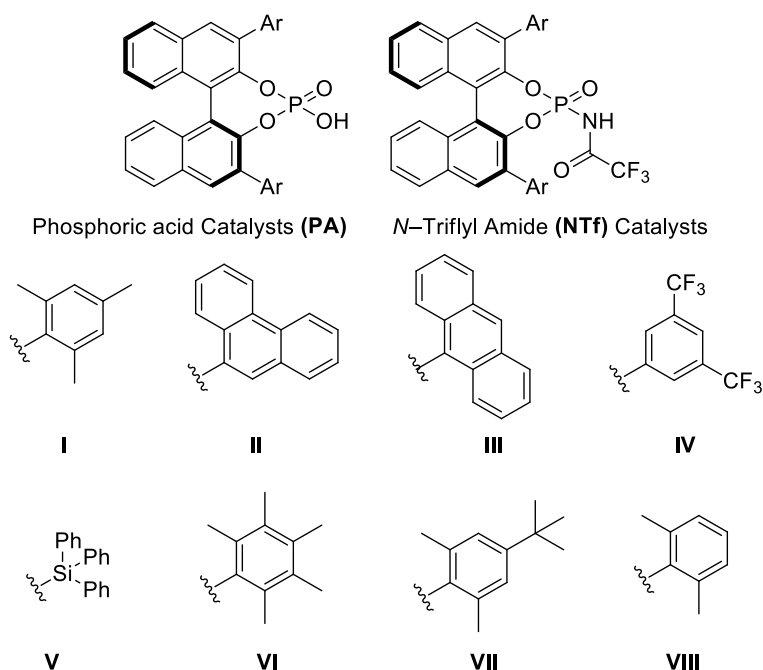


Figure 9 The chiral BINOL catalysts used within this study can be described as either phosphoric acids (PA) or *N*-triflyl amides (NTf). These can be further distinguished by their aryl substituents labelled I–VII. The catalysts will be referred to in this manner e.g. PA (I).

In the first entry in the table above *p*-toluenesulfonic acid was used to acquire a racemic mixture of the intended product. The optimum separation was achieved by HPLC using a CHIRALPAK® IB column, 250 x 4,6 mm, 5 μ m particle size eluting with 1:1 isopropanol:hexane over 45 min.

Chapter 2 Towards a Brønsted Acid Catalysed Enantioselective Synthesis of 4-azapodophylotoxin

Entries 2 and 3 of **Table 1** were performed after this to determine the effect of having a standard phosphoric acid as compared to the more acidic *N*-triflyl amide functionalised phosphoric acid catalysts. The catalysts showed little difference in performance in terms of yield, however, it was noted that the additional acidity of the *N*-triflyl amides encouraged the formation of by-products which ultimately complicated chromatography.

Moving forward standard phosphoric acid catalysts were preferred as a result. An array of catalysts was then screened simultaneously, entries 4 -6. Each resulted in racemic mixtures with comparable yields, raising suspicions about the assumptions made in the experimental set up. Two control experiments were then performed, separating the effect of the catalyst and drying agents – entries 7 & 8. Again, racemic mixtures of the intended product were formed in yields within the range seen previously raising concerns over an uncontrolled racemic background reaction. It should be noted that the chiral BINOL phosphoric acids have a pKa in DMSO in the range of 3.77 – 4.22,¹⁵ whereas tetrionic acid has a pKa in DMSO of 3.78.¹⁶

Table 1 Initial conditions investigating BINOL–PA catalysts (**5**) to acquire enantiomerically enriched 4–azapodophylotoxins. Binol phosphoric acid (PA) or *N*–Triflylamide (NTf) catalysts with various aryl substitutions were screened and powdered 4Å molecular sieve (MS) was used to trap the water generated.

| | Acid | Additives | Solvent | Temperature | Reaction Time | Product | Yield % |
|----|-------------------------------|-----------|---------|-------------|---------------|---------|---------|
| 1 | <i>p</i> TSA.H ₂ O | – | DCM | RT | 18 h | Rac. | 75 |
| 2 | PA (I) | 4Å MS | DCM | RT | 48 h | Rac. | 72 |
| 3 | NTf (II) | 4Å MS | DCM | RT | 48 h | Rac. | 68 |
| 4 | PA (III) | 4Å MS | DCM | RT | 48 h | Rac. | 65 |
| 5 | PA (IV) | 4Å MS | DCM | RT | 48 h | Rac. | 70 |
| 6 | PA (V) | 4Å MS | DCM | RT | 48 h | Rac. | 65 |
| 7 | – | 4Å MS | DCM | RT | 48 h | Rac. | 67 |
| 8 | – | – | DCM | RT | 48 h | Rac. | 64 |
| 9 | PA (I) | NaH | DCM | RT | 36 h | Rac. | 71 |
| 10 | NTf IDPI | 4Å MS | DCM | RT | 24 h | Rac. | 73 |

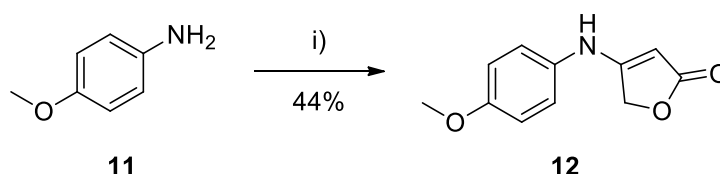
This would imply that the tetrionic acid is acidic enough to catalyse the reaction without the need for external assistance. Entries 9 and 10 detail efforts to negate the acidity of tetrionic acid. The former involved the formation of the sodium salt by deprotonation sodium hydride in the hope that the acidity and subsequent chiral control over the resulting product would come solely from the acid catalyst, however this was not the case. The latter attempt involved the use of the most acidic catalyst readily available, the imidodiphosphorimidate (IDPI)

Chapter 2 Towards a Brønsted Acid Catalysed Enantioselective Synthesis of 4-azapodophylotoxin

developed by List and coworkers¹⁷ in order to outcompete the racemic background reaction which was also unsuccessful. From these observations it was concluded that the tetronic acid issued a fundamental challenge for the transfer of chiral information of the catalyst.

SYNTHESIS OF ENAMINE TETRONIC ACID ANALOGUE

The work of Shi and co-workers¹⁸ details the use of BINOL axially chiral phosphoric acids to perform the singular addition of enamine nucleophiles to reactive electrophilic species; transferring chiral information using BINOL PA catalysts. One of the nucleophiles demonstrated suited our efforts sufficiently, the synthesis of this analogue is detailed below.



Scheme 8 Enaminone tetronic acid analogue described by Shi and coworkers.¹⁸ which was compatible with BINOL-PA catalysts. Conditions: i) ethyl 4-chloroacetoacetate (1.0 eq), AcOH (1.1 eq), toluene, refl., 8 h.

Formation of the desired enamine containing lactone was achieved via reflux of 4-methoxyaniline and ethyl 4-chloroacetoacetate in acidified toluene. The resulting product precipitated out of solution and was used without further purification. The product's insolubility in a variety of solvents forced a solvent change in further investigations. It should also be noted that the anisidine moiety was used simply because of previous compatibility demonstrated by Shi *et. al.* with the organocatalysts used in this study. Due to time constraints on the project, determining an optimized fragment was implausible. Within their work, Shi and coworkers demonstrated the singular addition of an enamine such as **12**; moieties which allowed for later hydrolysis of the enamine were valued less in their study. However, labile fragments such as those rejected by Shi would encourage the final ring closure intended to form 4-azapodophylotoxins. The electron rich nature of the 4-methoxy aniline makes it a poor leaving group in this application. However, noticing trends within the work of Schneider, aromatic bulkiness tends to favor a more organized transition state with the organocatalysts used, resulting in higher enantiomeric ratio values. From these two pieces of information a reasonable future step in the optimization of this reaction would be to incorporate a bulky electron poor aromatic amine to form the desired enamine. A simple halogenated aniline could be a reasonable starting point for this optimization.

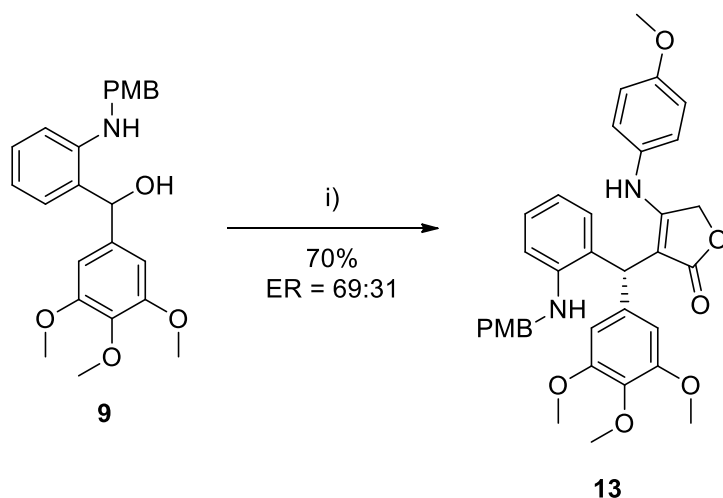
FURTHER SCREENING

Using the enamine analogue of tetronic acid **12** the conditions described in **Table 2** were tested. Keeping the conditions as consistent as possible with the first round of experiments,

Chapter 2 Towards a Brønsted Acid Catalysed Enantioselective Synthesis of 4-azapodophylotoxin

DCM was used as a solvent. It was quickly noted that the enamine was not soluble enough in this solvent, even at elevated temperatures described in entry 2. A small solubility study was performed, and it was found the enamine was soluble in DMSO and 1,4-dioxane.

Subsequent experiments were therefore performed in dioxane. Despite these efforts the addition of the enamine to the *o*QMI substrate **9** did not occur. A Lewis acid mediated strategy was then attempted, entry 5, which did yield some product. The identity of this complex mixture was not elucidated fully; however, mass spectrum evidence suggests the addition of the enamine had occurred.



Scheme 9 Single addition of enamine **12** to the model substrate **9**. Conditions: i) **12** (1.2 eq), mesityl BINOL-PA (0.1 eq), MgSO₄ (20 mg/mL), dioxane, rt, 48 h.

Table 2 Conditions using enaminone analogue **12** as a nucleophile, and various chiral BINOL-phosphoric acid (PA) catalysts.

| | Acid | Additive | Solvent | Temp | Reaction Time | Product |
|-----------|---------------------|-------------------|---------|------|---------------|--|
| 1 | PA (I) | 4Å MS | DCM | RT | 48 Hr | No Reaction |
| 2 | PA (I) | 4Å MS | DCM | 50 C | 24 Hr | No Reaction |
| 3 | PA (I) | 4Å MS | Dioxane | RT | 48 Hr | No Reaction |
| 4 | NTf (II) | 4Å MS | Dioxane | RT | 48 Hr | No Reaction |
| 5 | Sc(Tf) ₃ | 4Å MS | Dioxane | RT | 48 Hr | Inconclusive NMR, Positive MS |
| 6 | PA (I) | MgSO ₄ | Dioxane | RT | 48 Hr | Single addition of enamine 60:40 ER – 68%, 5% conversion to 10 after 4 days |
| 7 | PA (IV) | MgSO ₄ | Dioxane | RT | 48 Hr | Rac – 71% |
| 8 | PA (VI) | MgSO ₄ | Dioxane | RT | 48 Hr | Single Addition of Enamine 69:31 ER – 70% |
| 9 | PA (VII) | MgSO ₄ | Dioxane | RT | 48 Hr | Single Addition of Enamine 60:40 ER – 65% |
| 10 | PA (VIII) | MgSO ₄ | Dioxane | RT | 48 Hr | Single Addition of Enamine 60:40 ER – 68% |

Chapter 2 Towards a Brønsted Acid Catalysed Enantioselective Synthesis of 4-azapodophylotoxin

Empowered by these findings a solution was devised. An early paper on BINOL phosphoric acids describes certain reactions being catalysed by the corresponding magnesium phosphate complex, rather than the BINOL phosphoric acid itself. This was noted when changing the drying agent required for the reaction from MgSO_4 to molecular sieves. Certain reactions failed when the latter was introduced. As such, entry 6 **table 2** was attempted, whereby simply changing the drying agent to MgSO_4 yielded the first positive result of the series. This set of conditions allowed for the single addition of the enamine **13** in acceptable yield.

Most importantly, chiral information was transferred, resulting in a 60:40 enantiomeric ratio (*ER*) value (**Scheme 9**). Separation of the enantiomers was achieved by HPLC using a CHIRALPAK® IA column, 250 x 4,6 mm, 5 μm particle size eluting with 1:4 isopropanol:hexane over 45 min. The reaction was repeated and allowed to continue for an additional 2 days and it was also found that the final acid-catalysed ring closure did occur, albeit very slowly. We propose that the nature of the electron rich enamine as previously discussed discourages the completion of the ring closure by means of a poor leaving group. Entries 7-10 investigating the effect of the catalyst on the *ER* were then conducted, finding that the pentamethylphenyl derived catalyst to be most effective for this application. These last four entries lend themselves tentatively to the notion that greater steric bulk may organise the transition state favouring one enantiomer over the other.

CONCLUSION

The five membered lactone of the highly biologically active 4-azapodophylotoxin class of compounds is a critical pharmacophore. This moiety was successfully incorporated into the structure of a model azapodophylotoxin compound exploiting orthoquinone methide chemistry. Additionally, chiral information, albeit in a moderate fashion, was also successfully transferred from an axially chiral phosphoric acid catalyst to the final product.

It was determined that using tetronic acid as a nucleophile was not compatible with the phosphoric acid catalysts used. The acidity of tetronic acid allows for a racemic background reaction to occur, circumventing the chiral catalyst's ability to transfer of chiral information to the product. This challenge was addressed via the formation of an enamine analogue of tetronic acid via *p*-methoxy aniline. Initial, moderate, stereochemical control over the chiral centre of the model 4-azapodophylotoxin compound was established and sets a starting point for further optimisation efforts.

FUTURE WORK

Several limitations arise from these initially successful conditions which should be addressed. The solubility of the enamine lactone limits solvent choice and works directly against the intended elimination and product formation. This fragment should be optimised by exploring

Chapter 2 Towards a Brønsted Acid Catalysed Enantioselective Synthesis of 4-azapodophyllotoxin

bulky, electron poor amines which should balance between facilitating the elimination and assisting in the organisation of the transition state while bound to the catalyst. Furthermore, it should be determined what exact role the magnesium sulphate is playing in the reaction. Synthesis of the corresponding magnesium phosphate of a selected catalyst should be carried out and another drying agent used to determine which is the active species of catalyst. From this point, the catalyst and solvent system can be optimised until satisfactory yields and enantiomeric excesses are achieved.

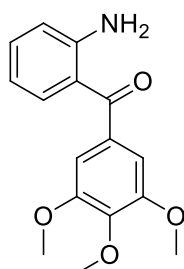
REFERENCES

- (1) Gordaliza, M.; García, P. A.; Miguel Del Corral, J. M.; Castro, M. A.; Gómez-Zurita, M. A. Podophyllotoxin: Distribution, Sources, Applications and New Cytotoxic Derivatives. *Toxicon* **2004**, *44* (4), 441–459. <https://doi.org/10.1016/j.toxicon.2004.05.008>.
- (2) Xu, H.; Lv, M.; Tian, X. A Review on Hemisynthesis, Biosynthesis, Biological Activities, Mode of Action, and Structure-Activity Relationship of Podophyllotoxins: 2003- 2007. *Curr. Med. Chem.* **2008**, *16* (3), 327–349. <https://doi.org/10.2174/092986709787002682>.
- (3) Madec, D.; Mingoia, F.; Prestat, G.; Poli, G. N-Substituted Tetronamides as Ambident Nucleophilic Building Blocks for the Synthesis of New 4-Aza-2,3-Didehydropodophyllotoxins. *Synlett* **2008**, No. 10, 1475–1478. <https://doi.org/10.1055/s-2008-1078429>.
- (4) Stadler, D.; Bach, T. Concise Stereoselective Synthesis of (-)-Podophyllotoxin by an Intermolecular Iron(III)-Catalyzed Friedel-Crafts Alkylation. *Angew. Chemie - Int. Ed.* **2008**, *47* (39), 7557–7559. <https://doi.org/10.1002/anie.200802611>.
- (5) Hanahan, D.; Weinberg, R. A. Hallmarks of Cancer: The next Generation. *Cell* **2011**, *144* (5), 646–674. <https://doi.org/10.1016/j.cell.2011.02.013>.
- (6) Jeedimalla, N.; Flint, M.; Smith, L.; Haces, A.; Minond, D.; Roche, S. P. Multicomponent Assembly of 4-Aza-Podophyllotoxins: A Fast Entry to Highly Selective and Potent Anti-Leukemic Agents. *Eur. J. Med. Chem.* **2015**, *106*, 167–179. <https://doi.org/10.1016/j.ejmech.2015.10.009>.
- (7) Magedov, I. V.; Frolova, L.; Manpadi, M.; Bhoga, U. D.; Tang, H.; Evdokimov, N. M.; George, O.; Hadje Georgiou, K.; Renner, S.; Getlik, M.; et al. Anticancer Properties of an Important Drug Lead Podophyllotoxin Can Be Efficiently Mimicked by Diverse Heterocyclic Scaffolds Accessible via One-Step Synthesis. *J. Med. Chem.* **2011**, *54* (12), 4234–4246. <https://doi.org/10.1021/jm200410r>.
- (8) Spanka, M.; Schneider, C. Phosphoric Acid Catalyzed Aldehyde Addition to in Situ Generated O-Quinone Methides: An Enantio- and Diastereoselective Entry toward Cis-3,4-Diaryl Dihydrocoumarins. *Org. Lett.* **2018**, *20* (16), 4769–4772. <https://doi.org/10.1021/acs.orglett.8b01865>.
- (9) Gebauer, K.; Reuß, F.; Spanka, M.; Schneider, C. Relay Catalysis: Manganese(III) Phosphate Catalyzed Asymmetric Addition of β -Dicarbonyls to Ortho-Quinone Methides Generated by Catalytic Aerobic Oxidation. *Org. Lett.* **2017**, *19* (17), 4588–4591. <https://doi.org/10.1021/acs.orglett.7b02185>.
- (10) Kretzschmar, M.; Hodík, T.; Schneider, C. Brønsted Acid Catalyzed Addition of Enamides to Ortho-Quinone Methide Imines—An Efficient and Highly Enantioselective Synthesis of Chiral Tetrahydroacridines. *Angew. Chemie - Int. Ed.* **2016**, *55* (33), 9788–9792.

Chapter 2 Towards a Brønsted Acid Catalysed Enantioselective Synthesis of 4-azapodophyllotoxin

- <https://doi.org/10.1002/anie.201604201>.
- (11) Hodík, T.; Schneider, C. Brønsted Acid-Catalyzed, Enantioselective Synthesis of 1,4-Dihydroquinoline-3-Carboxylates: Via in Situ Generated Ortho -Quinone Methide Imines. *Org. Biomol. Chem.* **2017**, *15* (17), 3706–3716. <https://doi.org/10.1039/c7ob00488e>.
 - (12) Parmar, D.; Sugiono, E.; Raja, S.; Rueping, M. Complete Field Guide to Asymmetric BINOL-Phosphate Derived Brønsted Acid and Metal Catalysis: History and Classification by Mode of Activation; Brønsted Acidity, Hydrogen Bonding, Ion Pairing, and Metal Phosphates. *Chem. Rev.* **2014**, *114* (18), 9047–9153. <https://doi.org/10.1021/cr5001496>.
 - (13) Zhao, L.; Li, J.; Li, Y.; An, Y.; Shi, L. Experimental Section. **2008**.
 - (14) Tratat, C.; Giorgi-Renault, S.; Husson, H. P. A Multicomponent Reaction for the One-Pot Synthesis of 4-Aza-2,3-Didehydropodophyllotoxin and Derivatives. *Org. Lett.* **2002**, *4* (19), 3187–3189. <https://doi.org/10.1021/ol0200908>.
 - (15) Christ, P.; Lindsay, A. G.; Vormittag, S. S.; Neudörfl, J. M.; Berkessel, A.; O'Donoghue, A. C. PKa Values of Chiral Brønsted Acid Catalysts: Phosphoric Acids/Amides, Sulfonyl/Sulfonyl Imides, and Perfluorinated TADDOLs (TEFDDOLs). *Chem. - A Eur. J.* **2011**, *17* (31), 8524–8528. <https://doi.org/10.1002/chem.201101157>.
 - (16) Perez, G. V; Perez, A. L. Organic Acids without a Carboxylic Acid Functional Group Group I: Phenolic-Type Acids. *J. Chem. Educ.* **2000**, *77* (7), 910–915. <https://doi.org/10.1021/ed077p910>.
 - (17) List, B.; Schreyer, L.; Properzi, R. IDPi Catalysis. *Angew. Chemie Int. Ed.* **2019**, *58*. <https://doi.org/10.1002/anie.201900932>.
 - (18) Zhou, L. J.; Zhang, Y. C.; Jiang, F.; He, G.; Yan, J.; Lu, H.; Zhang, S.; Shi, F. Enantioselective Construction of Cyclic Enaminone-Based 3-Substituted 3-Amino-2-Oxindole Scaffolds via Catalytic Asymmetric Additions of Isatin-Derived Imines. *Adv. Synth. Catal.* **2016**, *358* (19), 3069–3083. <https://doi.org/10.1002/adsc.201600508>.

EXPERIMENTAL

(2-Aminophenyl)(3,4,5-trimethoxyphenyl)methanone 7

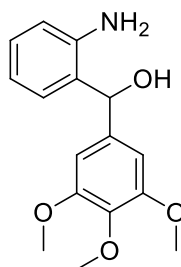
To a flame dried flask equipped for reflux was added magnesium (49.2 mg, 2.02 mmol, 3.5 eq) and THF (2 mL) and allowed to stir for 30 min at rt. 3,4,5-trimethoxy bromobenzene (500 mg, 2.02 mmol, 3.5 eq) was then added in THF (5 mL) and allowed to stir for 3 h at reflux. The solution was then cooled to rt and 2-aminobenzonitrile (68.3 mg, 0.578 mmol, 1 eq) was subsequently added dropwise in THF (2 mL) over 5 minutes. This solution was then allowed

Chapter 2 Towards a Brønsted Acid Catalysed Enantioselective Synthesis of 4-azapodophylotoxin

to stir at rt overnight, after which TLC analysis showed complete consumption of the nitrile. Once this was noted, 2 M aqueous HCl (30 mL) was then added at rt. After this addition the reaction mixture was heated to reflux for an additional 2 hr. The mixture was then cooled and neutralised with 1 M aqueous NaOH solution and extracted with EtOAc (3 × 30 mL). The organic fractions were collected and dried over MgSO₄, filtered and solvent was removed under reduced pressure. Purification of this residue was achieved by flash column chromatography with elution gradient of 5 - 20% EtOAc in hexanes. Pure fractions were evaporated to dryness to afford the title compound as a yellow oil, 94 mg, 57% yield. Spectral data collected for this compound compared well with reported literature values.¹¹

¹H NMR (400 MHz, Chloroform-*d*) δ 7.51 (dd, *J* = 8.0, 1.6 Hz, 1H), 7.31 (ddd, *J* = 8.5, 7.1, 1.6 Hz, 1H), 6.92 (s, 2H), 6.76 (dd, *J* = 8.3, 1.1 Hz, 1H), 6.64 (ddd, *J* = 8.1, 7.1, 1.1 Hz, 1H), 3.94 (s, 3H), 3.89 (s, 6H).

¹³C NMR (101 MHz, Chloroform-*d*) δ 198.0, 152.8, 150.8, 140.8, 135.1, 134.2, 134.1, 118.2, 117.0, 115.5, 106.8, 60.9, 56.2.

(2-Aminophenyl)(3,4,5-trimethoxyphenyl)methanol 8

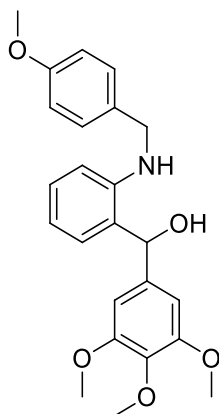
A flask containing a solution of (2-aminophenyl)(3,4,5-trimethoxyphenyl)methanone (660 mg, 2.29 mmol, 1 eq) in EtOH/EtOAc (4.6 mL, 3:1) was prepared under a N₂ atmosphere and cooled to 0 °C. To this flask was added portionwise NaBH₄ (82.6 mg, 2.18 mmol, 0.98 eq) and allowed to stir until homogeneous. The solution was then allowed to warm to rt over 4 hrs. Consumption of the starting material was monitored by TLC analysis. Upon complete consumption of the starting material the reaction mixture was quenched with sat. brine solution (10 mL) and extracted with ethyl acetate (3 × 30 mL). The organic fraction was collected and evaporated under reduced pressure. Purification of the crude product was achieved by flash column chromatography with elution gradient of 20 - 40% EtOAc in petroleum ether. Pure fractions were evaporated to dryness to afford the title compound as a white solid, 648 mg, 98% yield. Spectral data collected for this compound compared well with reported literature values.¹¹

¹H NMR (300 MHz, Chloroform-*d*) δ 7.12 (ddd, *J* = 7.6, 1.6 Hz, 1H), 7.00 (dd, *J* = 7.6, 1.6 Hz, 1H), 6.74 (ddd, *J* = 7.5, 1.2 Hz, 1H), 6.68 (dd, *J* = 7.9, 1.2 Hz, 1H), 6.62 (d, *J* = 0.7 Hz, 2H), 5.77 (s, 1H), 3.84 (s, 3H), 3.80 (s, 6H).

Chapter 2 Towards a Brønsted Acid Catalysed Enantioselective Synthesis of 4-azapodophylotoxin

^{13}C NMR (75 MHz, Chloroform-*d*) δ 153.2, 137.7, 128.9, 128.5, 127.5, 118.5, 116.9, 103.6, 74.8, 60.8, 56.1.

MS (ESI+) predicted for $\text{C}_{16}\text{H}_{19}\text{NO}_4\text{Na}$ $[\text{M}+\text{Na}^+]$: 312.1206, found 312.1223.

{2-[(4-Methoxybenzyl)amino]phenyl}(3,4,5-trimethoxyphenyl)methanol 9

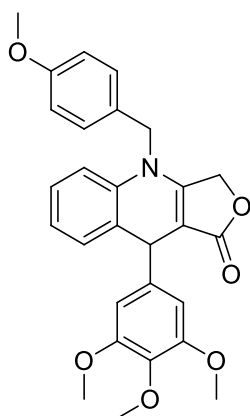
A solution of (2-aminophenyl)(3,4,5-trimethoxyphenyl)methanol (1.32 g, 4.55 mmol, 1 eq), acetic acid (766 mg, 12.7 mmol, 2.8 eq) and anisaldehyde (742 mg, 5.45 mmol, 1.2 eq) in methanol (22 mL). This solution was allowed to stir at rt for 30 min until the complete consumption of the starting aniline was observed by TLC. The solution was then cooled to 0 °C and NaCNBH_3 (400 mg, 6.36 mmol, 1.2 eq) was added in a single portion and the solution was allowed to reach rt and stirred for 3 hr. The mixture was then quenched with 2M KH_2PO_4 solution (10 mL) and extracted with EtOAc (3 \times 30 mL). The organic fractions were collected and washed with sat. brine and sat NaHCO_3 solutions. Thereafter the organic fraction was collected and evaporated under reduced pressure and the resulting residue was purified by column chromatography eluting with 5 - 30% EtOAc in PE. Pure fractions were collected and evaporated to dryness affording the title compound, 1.62 g, 87% yield. Spectral data collected for this compound compared well with reported literature values.¹¹

^1H NMR (400 MHz, Chloroform-*d*) δ 7.19 (ddd, J = 8.0, 7.4, 1.6 Hz, 1H), 7.10 (d, J = 8.6 Hz, 2H), 7.04 (dd, J = 7.5, 1.6 Hz, 1H), 6.82 (d, J = 8.7 Hz, 2H), 6.73 – 6.65 (m, 2H), 6.58 (d, J = 0.7 Hz, 2H), 5.78 (s, 1H), 4.19 (s, 2H), 3.86 (s, 3H), 3.79 (s, 3H), 3.74 (s, 6H).

^{13}C NMR (101 MHz, Chloroform-*d*) δ 158.9, 153.4, 146.4, 137.9, 137.3, 131.3, 129.4, 128.8, 128.6, 126.9, 116.9, 114.1, 114.1, 111.8, 103.6, 75.5, 61.0, 56.1, 55.4, 47.5.

MS (ESI+) predicted for $\text{C}_{24}\text{H}_{27}\text{NO}_5\text{Na}$ $[\text{M}+\text{Na}^+]$: 432.1781, found 432.1807.

Chapter 2 Towards a Brønsted Acid Catalysed Enantioselective Synthesis of 4-azapodophylotoxin

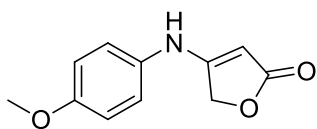
4-(4-Methoxybenzyl)-9-(3,4,5-trimethoxyphenyl)-4,9-dihydrofuro[3,4-b]quinolin-1(3H)-one 10

A solution of {2-[(4-methoxybenzyl)amino]phenyl}(3,4,5-trimethoxyphenyl)methanol (40.9 mg, 0.10 mmol, 1 eq), *p*-toluene sulfonic acid (17.2 mg, 0.01 mmol, 10% catalyst loading), powdered 4Å molecular sieves (30 mg), and tetronic acid (15 mg, 0.15 mmol) in DCM (1.0 mL) was prepared in a sealed tube and stirred at the specified temperatures and times. Thereafter the solution was then dried of solvent under reduced pressure and the products purified by column chromatography eluting with 2% MeOH in DCM. Fractions containing the desired product were collected and evaporated of solvent under reduced pressure to afford the title compound, 35.4 mg, 75% yield.

^1H NMR (400 MHz, Chloroform-*d*) δ 7.20 – 7.08 (m, 4H), 7.06 – 6.96 (m, 1H), 6.92 (d, J = 8.2 Hz, 1H), 6.86 (d, J = 8.8 Hz, 2H), 6.42 (s, 2H), 5.17 (s, 1H), 4.91 – 4.71 (m, 4H), 3.79 (s, 3H), 3.78 (s, 3H), 3.76 (s, 6H).

^{13}C NMR (101 MHz, Chloroform-*d*) δ 172.7, 159.5, 158.2, 153.3, 141.8, 137.6, 136.8, 131.9, 128.1, 127.0, 127.0, 125.8, 124.39, 114.8, 114.1, 105.2, 98.9, 65.4, 60.9, 56.1, 55.5, 48.9, 40.5.

MS (ESI+) predicted for $\text{C}_{28}\text{H}_{27}\text{NO}_6$ Na $[\text{M}+\text{Na}^+]$: 496.1731, found 496.1755.

4-[(4-Methoxyphenyl)amino]furan-2(5H)-one 12

A solution of 4-methoxyaniline (615.7 mg, 5.00 mmol) in toluene (15 mL) was prepared in a two neck flask equipped for reflux. To this solution was added acetic acid (0.300 ml, 5.24 mmol) at rt. Subsequently ethyl 4-chloroacetoacetate (0.676 ml, 5.00 mmol) was added dropwise and the resulting solution was heated under reflux which was maintained for 8 hr. The solution was then allowed to cool to room temperature and the resulting precipitate was

Chapter 2 Towards a Brønsted Acid Catalysed Enantioselective Synthesis of 4-azapodophylotoxin

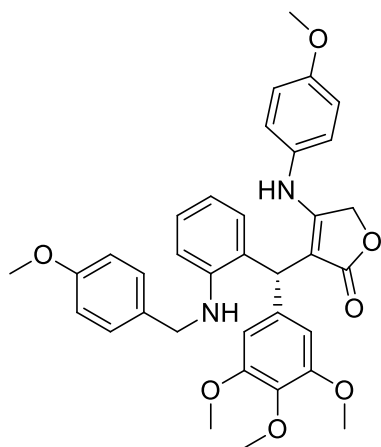
then filtered and washed with cold EtOH. This afforded the title compound, 451 mg, 44% yield spectroscopically pure and was used without further purification. Spectral data collected for this compound compared well with reported literature values.¹⁸

¹H NMR (400 MHz, DMSO-*d*₆) δ 9.61 (s, 1H), 7.13 (d, *J* = 9.0 Hz, 1H), 6.93 (d, *J* = 9.0 Hz, 1H), 5.09 (s, 1H), 4.82 (d, *J* = 0.8 Hz, 2H), 3.73 (s, 3H).

¹³C NMR (101 MHz, DMSO-*d*₆) δ 175.0, 163.6, 155.4, 133.2, 120.6, 114.6, 82.0, 67.8, 55.3.

MS (ESI+) predicted for C₁₁H₁₁NO₃ Na [M+Na⁺]: 228.0631, found 228.0664.

3-{[2-((4-Methoxybenzyl)amino)phenyl](3,4,5-trimethoxyphenyl)methyl}-4-[(4-methoxyphenyl)amino]furan-2(5H)-one 13



A solution of {2-[(4-methoxybenzyl)amino]phenyl}(3,4,5-trimethoxyphenyl)methanol (40.9 mg, 0.100 mmol, 1 eq), 4-[(4-methoxyphenyl)amino]furan-2(5H)-one (30.8 mg, 0.15 mmol, 1.5 eq), mesityl BINOL-PA (0.01 mmol, 10% catalyst loading), in 1,4-dioxane (1 ml) and MgSO₄ (20 mg/mL) was stirred for 48 hr at rt. The resulting solution was then evaporated under reduced pressure and the residue was subjected to column chromatography eluting with 2% MeOH in DCM. Fractions containing the desired product were collected and evaporated of solvent under reduced pressure to afford the title compound, 41.7 mg, 70% yield and 69:31 ER.

¹H NMR (400 MHz, Chloroform-*d*) δ 7.20 (t, *J* = 7.7 Hz, 1H), 6.99 (d, *J* = 8.7 Hz, 2H), 6.89 (s, 1H), 6.78 (d, *J* = 9.0 Hz, 2H), 6.73 (d, *J* = 8.0 Hz, 2H), 6.57 (d, *J* = 8.8 Hz, 1H), 6.48 (s, 2H), 5.26 (s, 1H), 4.76 (d, *J* = 15.6 Hz, 1H), 4.60 (d, *J* = 15.7 Hz, 1H), 4.22 (s, 1H), 3.85 (s, 2H), 3.77 (s, 3H), 3.75 (s, 6H).

¹³C NMR (101 MHz, Chloroform-*d*) δ 174.8, 162.1, 158.8, 157.7, 153.7, 145.4, 137.2, 135.3, 131.1, 130.7, 129.3, 128.5, 128.3, 125.4, 124.1, 118.0, 114.9, 114.0, 111.9, 105.5, 96.1, 66.0, 60.9, 56.2, 55.6, 55.2, 47.3, 42.4.

Chapter 2 Towards a Brønsted Acid Catalysed Enantioselective Synthesis of 4-azapodophylotoxin

MS (ESI+) predicted for $C_{35}H_{36}N_2O_7 Na$ $[M+Na^+]$: 619.2414, found 619.2438.

SULFONYL FLUORIDES AS EGFR INHIBITORS

INTRODUCTION

Epidermal growth factor receptor (EGFR) is a transmembrane protein responsible for interfacing with extracellular factors and initiating intracellular processes linked to cell growth in humans.¹ EGFR is a kinase² and consumes adenosine triphosphate (ATP), transferring a phosphate group from the ATP to its target.² More specifically, EGFR is a receptor tyrosine kinase which phosphorylates its own tyrosine containing domain¹ in the intracellular, cytoplasmic portion of the protein when stimulated by an extracellular growth factor.¹ The binding of the external stimulus to the receptor site causes EGFR to homodimerize, activating the complex and allowing phosphorylation to occur.³ Once phosphorylated, other cytoplasmic signalling pathways are activated,³ recognising and binding to the now phosphorylated domain.⁴ For example, a signal transduction cascade pathway, known as MAPK, is activated by binding to EGFR.⁵ A full description of signal transduction is outside the scope of this work, however in short, a phosphorylation cascade is initiated after activation by a receptor, such as EGFR.⁵ Each subsequent component of the pathway recognises, binds to and is activated by the previous entity.⁶ Phosphate transfers occur at each step in the pathway, until ultimately activating a final component by phosphorylation which enters the nucleus of the cell.⁶ This goes on to influence gene transcription⁶ and can control a number

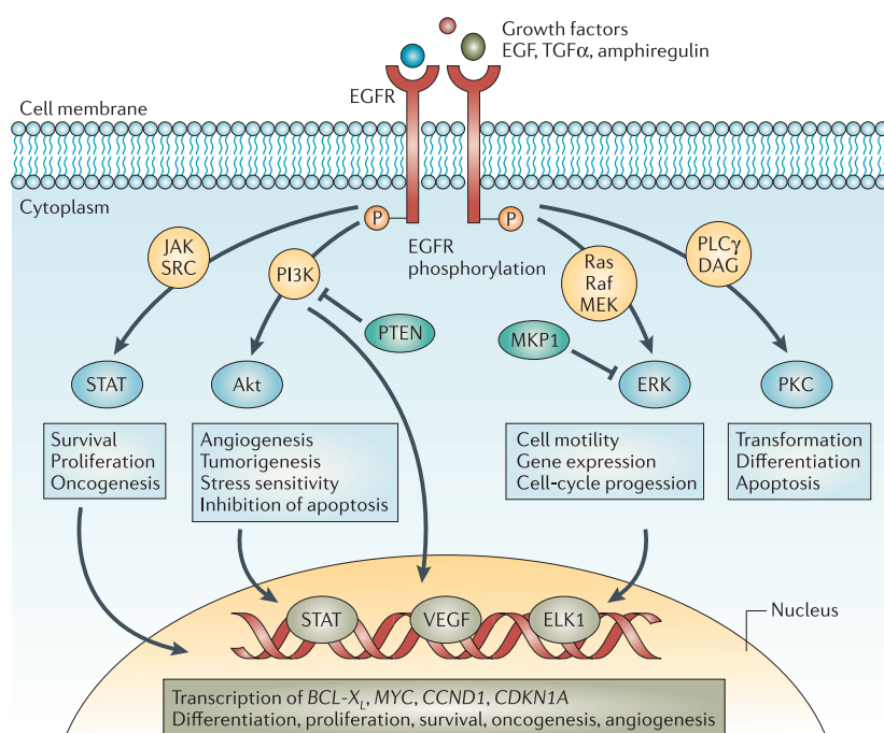


Figure 1: A simplified representation of EGFR activating cell signaling pathways associated with cell growth. Phosphorylated EGFR causes a phosphorylation cascade through pathways such as the Ras–Raf–MEK pathway responsible for gene expression. Reproduced from Nyati *et. al.*³

Chapter 3 Sulfonyl Fluorides as EGFR Inhibitors

of cellular processes⁴. The activated genes, in the case of EGFR, are associated with cell proliferation,³ inhibition of apoptosis⁴ and angiogenesis³ among others. In light of this one can see that overexpression,⁶ or other forms of overactivation,⁷ of EGFR can lead to uncontrolled cell growth or cancer.⁷ Overexpression or upregulation of EGFR is noted in several cancers such as lung and anal cancers, glioblastoma and epithelial tumours of the head and neck.⁴ Most relevant to this discussion, however, is the upregulated state of EGFR in non-small cell lung cancers (NSCLCs).²

Several mutations can lead to the upregulation of EGFR manifesting in cancers.¹ It has been shown that inhibition of EGFR in these mutant cells stops apoptosis avoidance⁶ and can be used as a therapeutic target.⁸ Several drugs were approved targeting EGFR and had some degrees of success.⁹ However, a theme of treatment and resistance has arisen with treatment of 1st generation inhibitors encouraging the formation of resistant EGFR mutant strains.⁸ This process has occurred several times, with mutations acting synergistically; making older generations of drugs completely ineffective.⁸ One of the most recent mutations to be overcome by medicinal chemistry is the T790M mutation.¹⁰ This mutation entails the substitution of a threonine residue with a methionine at position 790 of the enzyme.¹¹ This alters the binding pocket where ATP binds to EGFR,¹¹ the target site for many EGFR inhibitors.³ The mutation alters the binding affinity of the drugs targeting this binding site, rendering them less effective.³ 3rd generation drugs use covalent modifiers, such as acrylamides,¹² to bind to residues such as lysine and cystine to combat this.¹² Nucleophilic attack of the enzyme residues on the electrophiles forms a covalent bond between the active catalytic site of the enzyme and the drug, rendering the enzyme inactive¹². Examples of commercial drugs employing this strategy are Osimertinib¹¹ **1** and Afatinib³ **2**, which use acrylamide derivatives to target the cystine 797 residue of the catalytic site of EGFR in mutant NSCLCs.¹²

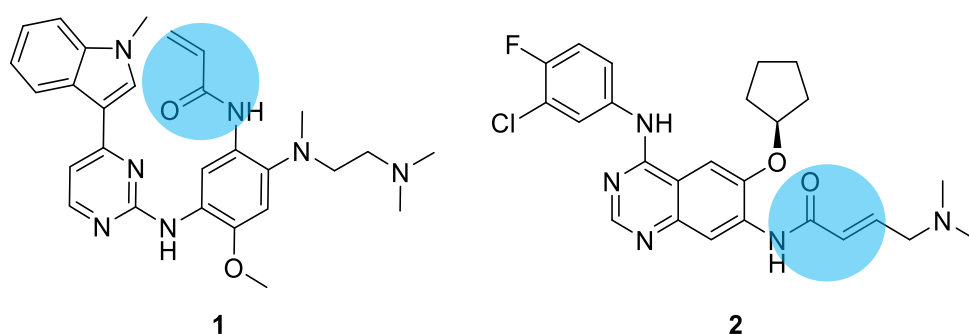


Figure 2: Osimertinib **1** and Aftinib **2** are commercially available covalent EGFR inhibitors targeting cystine 797 in the active site of the receptor with their acrylamide pharmacophores (highlighted in blue).³

However, a new mutation in addition to T790M has been observed which renders the abovementioned drugs ineffective. The C797S mutation substitutes the target cystine residue

Chapter 3 Sulfonyl Fluorides as EGFR Inhibitors

at position 797 of the receptor for a serine residue.¹² The soft thiol of the wild type's cystine residue readily performs a Michael addition to the acrylamide moiety of the drug. However, the C797S mutation's serine residue does not include a thiol, but an alcohol. This relatively harder nucleophile does not perform the Michael addition as readily due to the unfavoured hard–soft nucleophile–electrophile pair. It should be noted that certain residues critical to the function of the protein are highly conserved and are not prone to mutation. Targeting these residues, or other residues around the catalytic site of EGFR is a current theme in this field of research.⁸

Sulfonyl fluorides have been used as protein tagging electrophiles in research applications.¹³ The water stable acid halide reacts with a multitude of residues, including tyrosine phenols,¹⁴ lysine amino groups,¹³ cysteines thiols¹⁵ and serine alcohols.¹³ The reactivity is in the 'goldilocks' zone for biological systems, not so reactive as to label every available residue but not so unreactive as to face the same problems as other less reactive electrophiles. Several probes targeting these residues have been used in labelling efforts, assisting in identification and separation of proteins. These properties including water stability, reactivity and biological compatibility puts sulfonyl fluorides forward as potential covalent modifiers to replace acrylamides for cancers displaying the C797S mutation.

AIMS

This study aims to synthesise a 3rd generation core structure containing an alkyne fragment for later diversification. These pyrimidine-based inhibitors of EGFR show excellent activity against T790M mutant EGFR while sparing healthy unmutated receptors¹¹. The project aims to make a springboard for future research where these core structures can be used to provide a good platform for rapidly investigating different covalent modifiers. The core structure needs to be easily functionalised, concatenating the electrophilic modifier with the core under conditions the electrophile can tolerate. As such the copper catalysed azide–alkyne cycloaddition "click" (CuAAC)¹⁶ reaction was selected due to mild reaction conditions, biocompatibility of the triazole product it forms and its tolerance to a variety of functional groups.

Since the CuAAC reaction was chosen as the method to combine the electrophilic modifiers, or warheads, with the chosen core structure, these warheads should contain an azide moiety. As such, these warheads should be easily accessible azides also containing the warhead. This study aims to investigate sulfonyl fluorides as electrophilic warheads in the context of EGFR inhibitors.

After both the azide and alkyne fragments are achieved the study aims to find a suitable set of click conditions that tolerate both the core structure and the sulfonyl fluorides. The sulfonyl

Chapter 3 Sulfonyl Fluorides as EGFR Inhibitors

fluorides also have the potential to reject certain solvents and other reaction conditions which must be considered in the design of these conditions.

The study aims overall to access a library of electrophiles linked to a heterocyclic core structure fit for recognising kinases, and for this library to be tested in a biological context against mutant EGFR lung cancer strains. Overall, this library aims to probe chemical space around the active site of mutant EGFRs, primarily to test the viability of sulfonyl fluorides to combat the C797S mutation and secondly to possibly find new covalently modifiable residues.

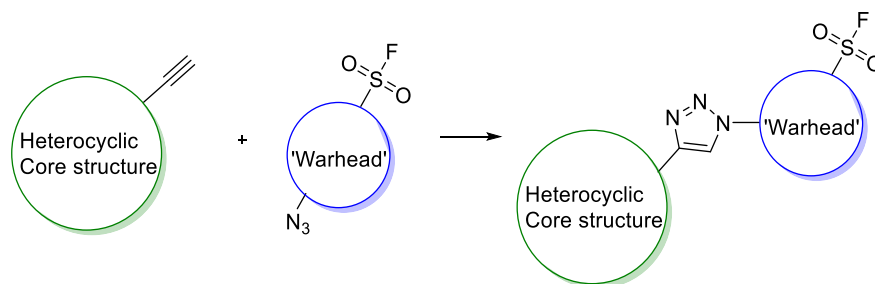


Figure 3 A simplified representation of the potential EGFR inhibitors the study aims to achieve. The 3rd generation core structure provides the driving force for delivering the covalent modifier and identifying the specific mutated EGFR protein. Sulfonyl fluorides have been selected as potentially relevant covalent modifiers.

DISCUSSION

SYNTHESIS

AZD ALKYNE CORE

As discussed, the target structure around which the project aims to be based is a 3rd generation EGFR inhibitor. AZD 9291 (Osimertinib),¹¹ developed by AstraZeneca, has passed clinical trials recently; having successfully completed an accelerated approval program due to its success.¹¹ As such, the key hinge-binding pyrimidine and methyl indole motif, optimised for the hydrophobic pocket of the mutated target, was selected as a starting point for this study. This portion of the molecule serves a key purpose – target recognition. Indolyl pyrimidine motifs were discovered to have potent kinase activity by Gompel et al.¹⁷ Investigating extracts of marine invertebrates such as *Aplidium meridianum*. Compounds isolated from these sea squirts are referred to as meridianins.¹⁷ The meridianin like core structure of AZD 9291 similarly recognises mutant kinases preferentially over the wild type enzyme, allowing the drug to include acrylamide which would otherwise be an indiscriminate electrophile.¹¹ That is to say that the core structure allows for a covalent modifier that has the potential to be quite reactive and promiscuous – a trait undesirable in a pharmaceutical. Key binding features like those present in the meridianins ensure long residence times in the active site ensuring that the electrophilic portion of the molecule reacts with its intended

Chapter 3 Sulfonyl Fluorides as EGFR Inhibitors

target.¹¹ Based on these features the meridianin core structure of AZD 9291 was chosen as a basis to attach the more electrophilic sulfonyl fluorides. Another candidate, WZ4002 also displays desirable traits like that of AZD9291 to serve as a skeleton for our efforts and will be discussed later in this document.

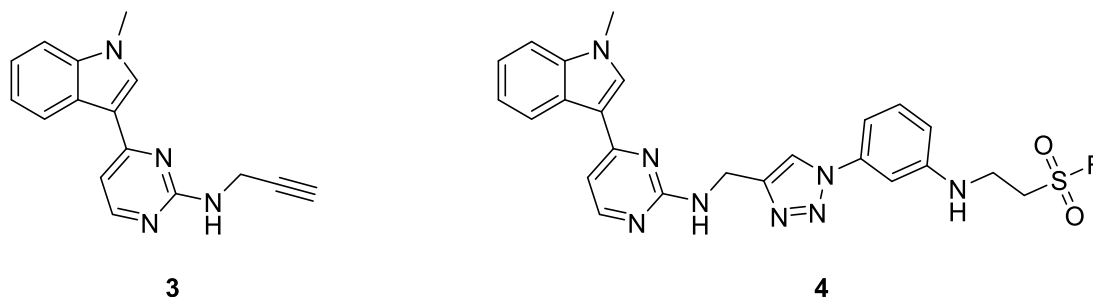
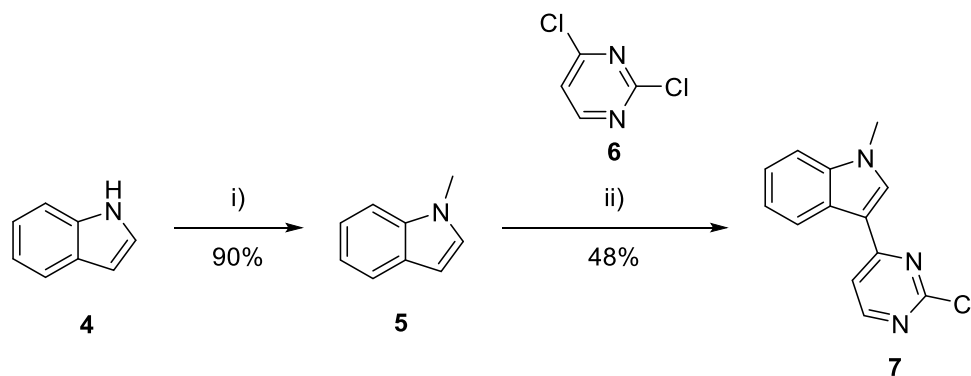


Figure 4 Target alkyne for this study **3** and Osimertinib (AZD 9291) **4** analogue

S_NAr CHLOROPYRIMIDINE STRATEGY *S_NAr*

Anilines react with chloropyrimidines to form substituted pyrimidine amines in polar solvents at elevated temperatures. *S_NAr* strategies based on this are often used in industry and reported in literature. Building on this knowledge, it was proposed that a similar reaction could occur between **7** and propargyl amine affording the desired target compound.



Scheme 1 Synthesis of 3-(2-chloropyrimidin-4-yl)-1-methyl-1H-indole **7**, proposed starting material for the target **3**. Conditions i) NaH (2.5 eq), MeI (1.3 eq), THF, -10 °C, 1 h; ii) **6** (1.1 eq), FeCl₃ (1.1 eq), DME, 60 °C, 1 h.

The initial fragment for these efforts were synthesised by NaH mediated alkylation of indole in THF to afford N-methyl indole which then arylated at the 3 position with 2, 4 dichloropyrimidine. Compound **7** was confirmed to match literature reports¹¹ for ¹H and ¹³C NMR spectra and several conditions were then attempted to directly couple propargyl amine as detailed below

Chapter 3 Sulfonyl Fluorides as EGFR Inhibitors

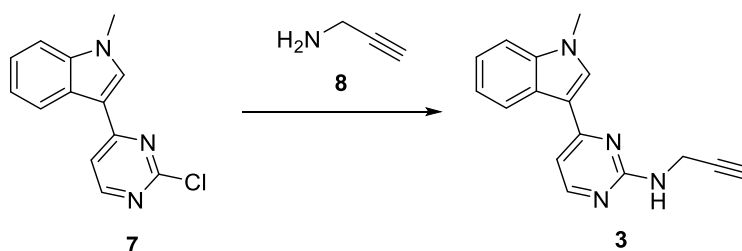
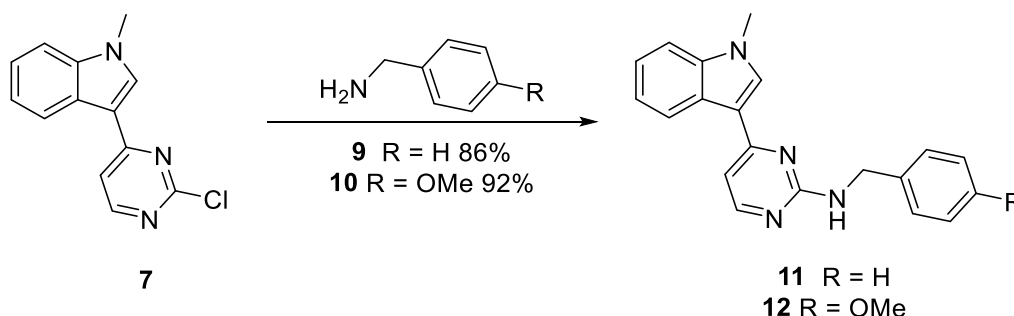
**Scheme 2** Pyrimidine amination strategy using propargyl amine **8** as a nucleophile

Table 1 A variety of conditions based on literature procedures,^{8,11} were attempted to achieve **3**, however the desired target **3** was not achieved. *Degradation of the solvent led to amination of **3** with dimethylamine as the major product. **Conditions: Cu₂O 10 mol %, TMEDA 10 mol %, K₂CO₃ 1.2 eq.

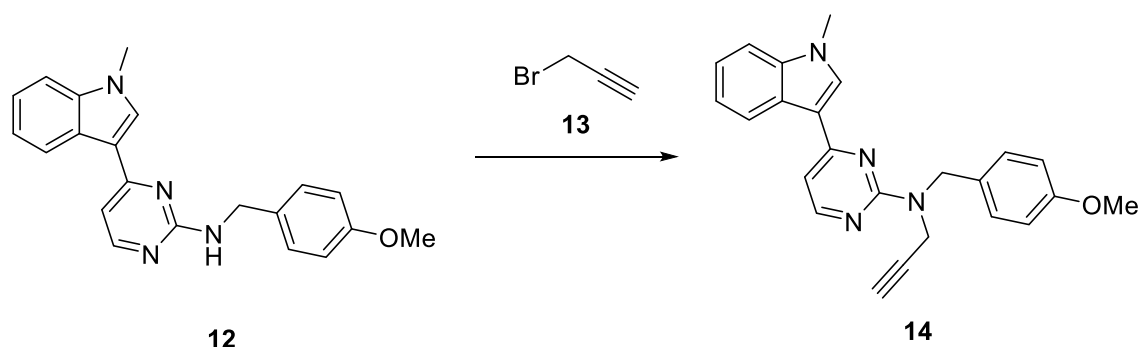
| | Eq. of 8 | Additives | Solvent | Temp | Heating | Time | Method | Conversion |
|-----------|-----------------|---------------------------------------|------------------|-------------|---------|------|-------------|------------|
| 1 | 1.1 | DIPEA 2.5 eq | THF | 66 (Refl.) | Conv | 18 h | Schlenk | N/C |
| 2 | 1.1 | DIPEA 2.5 eq | ACN | 82 (Refl.) | Conv | 18 h | Schlenk | N/C |
| 3 | 1.1 | DIPEA 2.5 eq | EtOH | 78 (Refl.) | Conv | 18 h | Sealed Tube | N/C |
| 4 | 1.1 | DIPEA 2.5 eq | EtOH | 160 | MW | 1 h | Sealed Tube | N/C |
| 5 | 1.1 | | EtOH | 160 | MW | 1 h | Sealed Tube | N/C |
| 6 | 1.1 | TsOH 10mol% | EtOH | 160 | MW | 1 h | Sealed Tube | N/C |
| 7 | 1.1 | TsOH 2.5 eq | EtOH | 160 | MW | 1 h | Sealed Tube | N/C |
| 8 | 1.1 | TsOH 10mol% | DMF | 160 | MW | 1 h | Sealed Tube | N/C * |
| 9 | 1.1 | AlCl ₃ | ACN | 82 (Refl.) | Conv | 18 h | Schlenk | N/C |
| 10 | 1.1 | KF 2 eq | H ₂ O | 100 (Refl.) | Conv | 18 h | Schlenk | N/C |
| 11 | 1.1 | KF 2 eq | H ₂ O | 175 | MW | 1 h | Sealed Tube | N/C |
| 12 | 1.1 | K ₂ CO ₃ 2,5 eq | ACN | 82 (Refl.) | Conv | 18 h | Schlenk | N/C |
| 13 | 3 | Ullmann Type** | Ethylene glycol | 60 | Conv | 18 h | Schlenk | N/C |
| 14 | 3 | Ullmann Type** | ACN | 60 | Conv | 18 h | Schlenk | N/C |

To investigate why the reaction did not proceed some model amine nucleophiles were selected and to be reacted with the meridianin-like precursor **7** shown in **Scheme 3** yielding **11** and **12** in good yields. Both products were confirmed by ¹H NMR spectroscopy.

**Scheme 3** Model studies using benzyl amines as nucleophiles. Conditions: **9** or **10** (1.2 eq), ACN, microwave irradiation, 180 °C, 1 h.

Chapter 3 Sulfonyl Fluorides as EGFR Inhibitors

Literature¹⁸ supports the findings in that the nucleophilicity of propargylamine does not allow for the reaction to proceed, where benzylamine does proceed based on its higher nucleophilicity. Benzylamines were described in these studies to be only slightly more nucleophilic than propargylamine. However, the reaction proceeds in excellent yield with only this slight increase in nucleophilicity. Literature¹¹ reports show that modification of compound **7** using an S_NAr strategy requires high temperatures, well above the boiling point of propargylamine. This may also contribute to the difficulties experienced using this strategy. Moving forward from these findings, we attempted to make use of the benzylamine derivative. Alkylation of the pyrimidinamine with propargyl bromide followed by debenzoylation was proposed. To investigate this avenue, hydrogenation conditions were attempted and failed to remove the group, even at elevated H_2 pressures. To remedy this *p*-methoxybenzylamine was used as a substitute and could easily be removed at room temperature using an excess of TFA. This led to several attempts to alkylate the pyrimidineamine to be followed by removal of the protecting group. This strategy would avoid di-alkylated byproducts and was preferred over removing PMB first.



Scheme 4 Proposed alkylation strategy for compound **12** with propargyl bromide **13**. This strategy ultimately did not produce the intended compound (**14**).

Table 2 Conditions attempted to achieve precursor **14** where deprotection would yield target compound **3**. Both conventional Schlenk techniques and sealed tube (ST) microwave heating experiments did not yield the desired product.

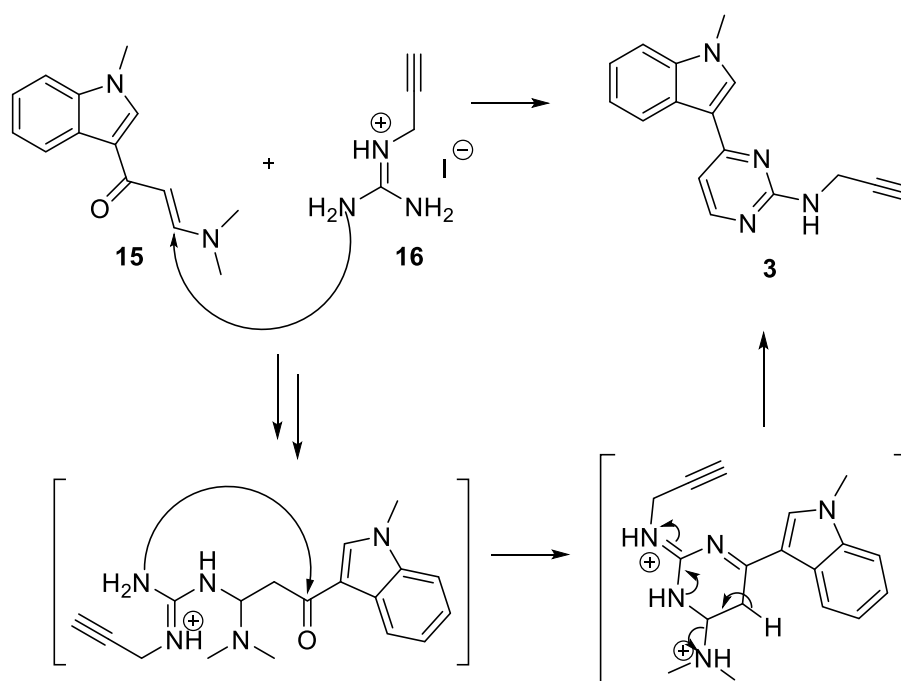
| | Eq 13 | Additives | Solvent | Temp | Technique | Time | Yield |
|---|-------|---------------------------------------|---------|----------|-----------|--------|-------|
| 1 | 1.2 | Et ₃ N 1.2 eq | DMF | 120 | MW ST | 30 min | N/C |
| 2 | 1.2 | K ₂ CO ₃ 1.2 eq | DMF | 120 | MW ST | 30 min | N/C |
| 3 | 1.2 | K ₂ CO ₃ 1.2 eq | ACN | 120 | MW ST | 30 min | N/C |
| 4 | 1.2 | NaH 1.2 eq | DMF | RT | Schlenk | 18 h | N/C |
| 5 | 5 | NaH 1.2 eq | DMF | RT | Schlenk | 18 h | N/C |
| 6 | 1.2 | <i>n</i> Bu-Li | THF | -40 – RT | Schlenk | 18 h | N/C |

Chapter 3 Sulfonyl Fluorides as EGFR Inhibitors

This strategy was not successful as can be seen in **table 2**. The conditions tested yielded no conversion, with only starting materials being observed in every case. These findings prompted the formation of a new strategy.

ALTERNATIVE SYNTHETIC STRATEGY TO AZD ALKYNE CORE

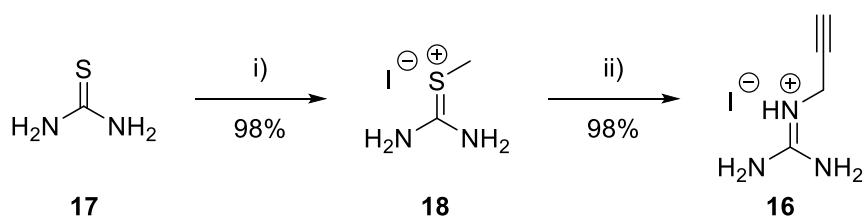
Amination and alkylation strategies failed to yield the target compound, prompting the following strategy based on the work of Rossignol et. al.¹⁹:



Scheme 5 Proposed synthesis of compound **3**, acquiring the pyrimidineamine functionality via a guanidine intermediate **16**. Some mechanistic intermediates have been omitted for clarity

Forming the pyrimidine in this way would isolate the troubled moieties in the target compound and rely on a well-studied and documented aromatisation to form the desired substituted pyrimidinamine. Literature precedents¹⁹ for aromatic and aliphatic groups tolerated in this reaction exist, prompting our next efforts.

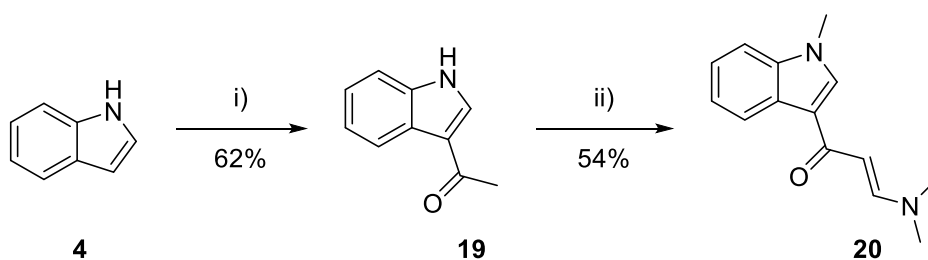
The necessary propargyl guanidine salt was synthesised as described by Aoyagi et. al.²⁰:



Scheme 6 Synthesis of propargyl guanidine fragment described by Aoyagi et. al.²⁰
Conditions: i) MeI (1.2 eq), EtOH, rt, 18 h; ii) propargylamine (1.2 eq), THF, rt, 6 h.

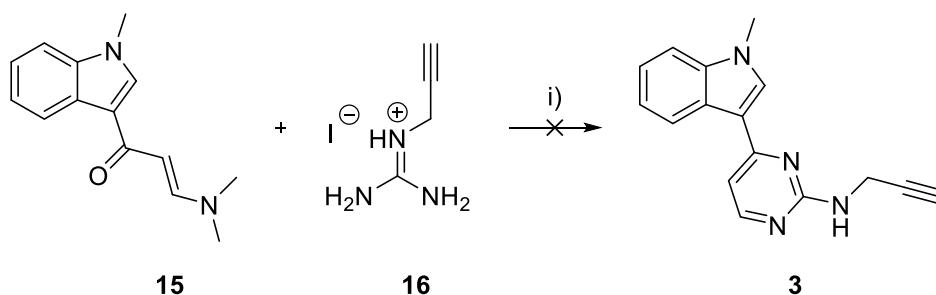
Chapter 3 Sulfonyl Fluorides as EGFR Inhibitors

Thiourea **17** was methylated using methyl iodide to yield the S-methylisothiuronium iodide salt **18**. Characterization of this compound relied on HRMS to confirm the positive ion, which matched the calculated value for **18**. The ^{13}C NMR spectrum showed two signals at 176.4 and 18.7 ppm which describe the electron poor thiocarbonyl and methyl signals respectively. ^1H NMR also showed two signals, a broad deshielded singlet at 8.88 ppm, and a sharp singlet at 2.57 ppm ascribed to the labile, symmetrical NH_2 protons and the methyl group respectively. The spectra for compound **16** were slightly more interesting, where the proton NMR spectrum showed two signals with a coupling constant of 2.5 Hz showing 4J coupling of the methylene group to the alkyne CH, where the latter appeared as a triplet at 3.36 ppm. Again, HRMS was key to confirming the compound, as the NMR spectra only describes a limited view of the molecule. The second fragment required, enaminone **20**, was synthesised over two transformations, starting with a lewis acid mediated Friedel–Crafts acetylation of indole. This was then followed by condensation and methylation by dimethylformamide dimethyl acetal (DMF–DMA), described in **scheme 7**. ^1H NMR and ^{13}C NMR spectral data for this compound matched the literature for this established synthesis.²¹



Scheme 7 enaminone fragment based on work described by Rossignol et. al.¹⁹ Conditions: i) anhydrous SnCl_4 (1.2 eq), acetic anhydride (1.0 eq), DCM/nitromethane (18:5), 0 °C, 2 h; iii) DMF–DMA (2.2 eq), DMF, microwave irradiation, 110 °C, 2 h.

Finally, the two components were subjected similar conditions described by Rossignol et. al.¹⁹



Scheme 8 i) NaOEt (1.1 eq), *i*-PrOH, 80 °C, 18 h.

Unfortunately, no transformation was observed, and the AZD target was abandoned at this point in the interest of time.

Chapter 3 Sulfonyl Fluorides as EGFR Inhibitors

WZ 4002 ALKYNE CORE SYNTHESIS

Keeping sight of the overarching goal, a 3rd generation EGFR inhibitor alkyne derivative, WZ 4002 **21** was selected to replace the meridianin motif. WZ 4002 is a 3rd generation EGFR inhibitor currently in clinical trials and has low nanomolar efficiencies, selective for L858/T790M mutant variants.⁸ It is based on a pyrimidine core hinge-binding motif and makes use of an acrylamide covalent modifier, much like AZD 9291. Prone to the same weakness against the C797S mutation, this structure provides the same springboard desired for the study. The following target structure **22** depicted in **figure 5** was proposed containing an alkyne fragment suitable for the CuAAC reaction:

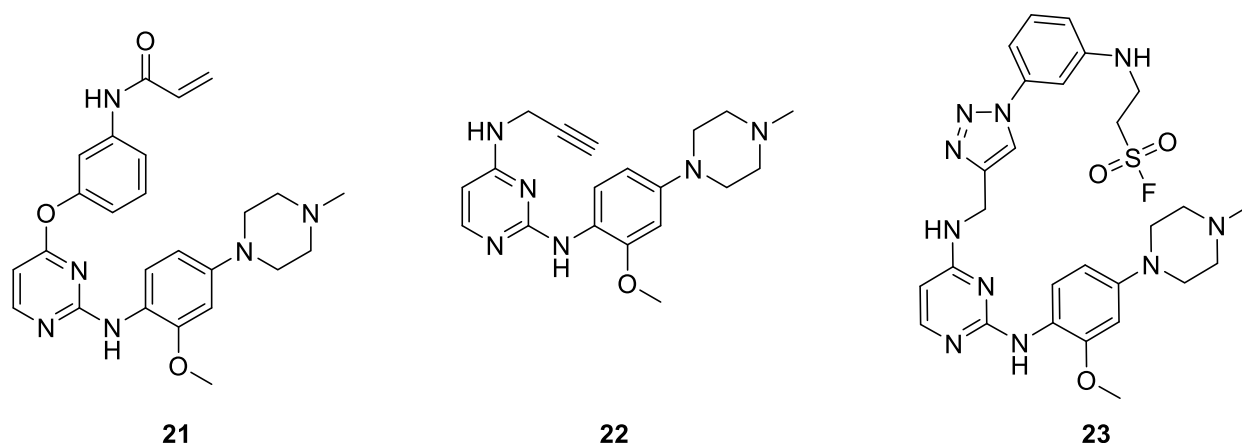
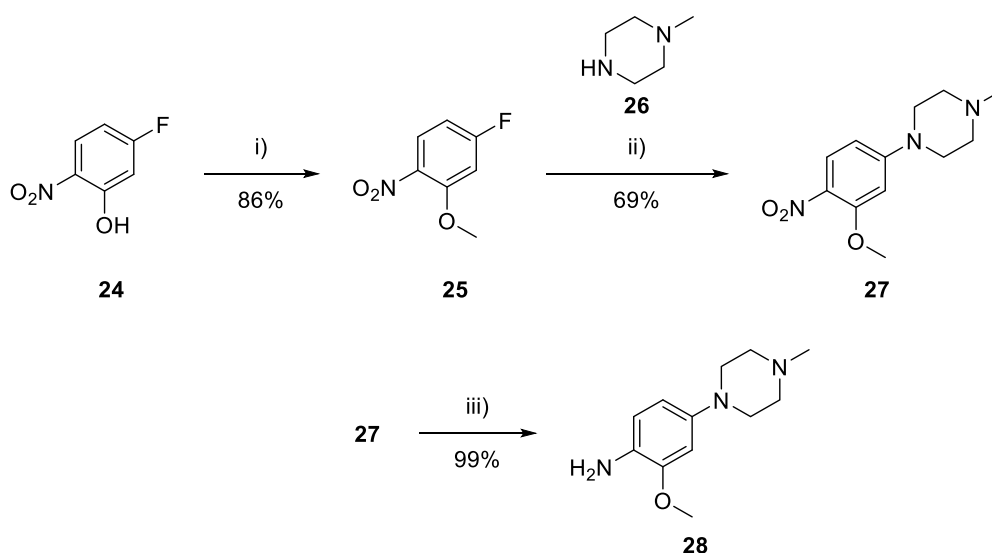


Figure 5 WZ 4002 **21** , our proposed alkyne fragment **22** and an example probe **23**

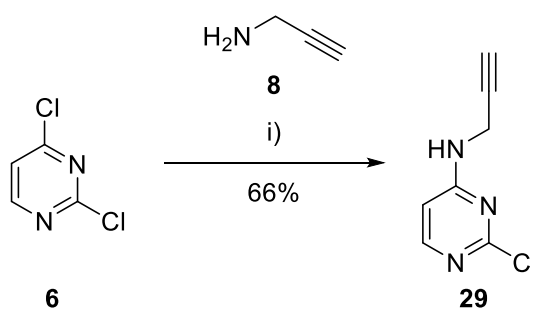
The synthesis of compound **22**, depicted in **scheme 9**, commenced with commercially available 5-fluoro-2-nitrophenol which was methylated in acetone using methyl iodide and K_2CO_3 as base in good yield. ^{13}C and 1H NMR spectroscopy revealed the additional singlet signals required for this transformation and the additional mass was confirmed by HRMS. This substrate was then reacted with N-methyl piperazine in an S_NAr displacement of the fluorine yielding a canary yellow solid. The methylene protons appeared in the 1H NMR spectrum as two broad triplets integrating for four protons each. Additionally, the relevant methyl signal was noted at 46.1 ppm and 2.34 ppm in the ^{13}C and 1H NMR spectra respectively. The final transformation was achieved by hydrogenation of the nitro group with Pd/C in methanol under a hydrogen atmosphere to yield the desired purple oily solid aniline in near quantitative yield. Catalyst was removed by filtration and washed with methanol and the organic phases collected and removed *in vacuo* to afford the aniline spectroscopically pure without further purification. The product was confirmed by IR spectroscopy and HRMS, noting a large band at 2798 cm^{-1} corresponding to an NH stretch of the newly formed aniline.

Chapter 3 Sulfonyl Fluorides as EGFR Inhibitors



Scheme 9 Synthesis of the solubilising group of WZ 4002. Conditions i) MeI (1.1 eq), K_2CO_3 (1.4 eq), acetone, refl., 3 h; ii) **26** (1.0 eq), K_2CO_3 (1.8 eq), DMF, rt, 18 h; iii) Pd/C (0.1 eq), H_2 , EtOH, rt, 18 h.

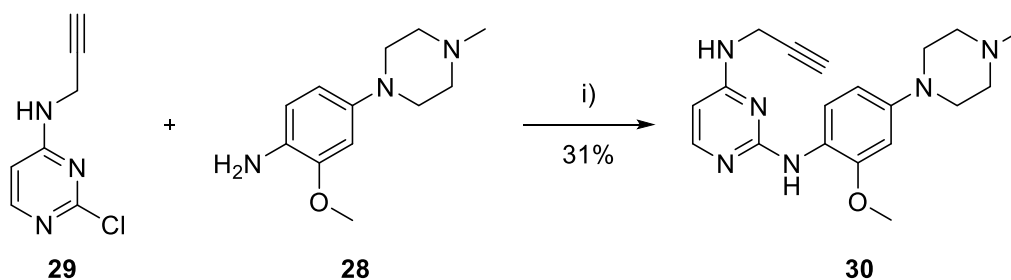
The alkyne fragment was achieved by amination with propargyl amine described in **scheme 10**. A solution of commercially available 2,4 dichloropyrimidine in ACN was prepared and to this solution an equivalent of propargylamine was added and left to stir overnight. This afforded compound **29** in 66% yield after chromatography. A characteristic triplet at 2.28 ppm in the ^1H NMR spectrum of **29** with a small coupling constant of 2.5 Hz indicative of the terminal alkyne and ^4J coupling to the methylene group nearby showed the presence of the propargyl moiety alongside the pair of aromatic doublets describing the pyrimidine. The isomer obtained can be explained by the difference in electrophilicity of the 4 position of 2,4 dichloropyrimidine as compared to that of the 2 position; where the latter is more electrophilic than the former. The increased relative electron density at the 2 position, due to the adjacent pyrimidine nitrogen atoms, significantly reduces the electrophilicity at that position. As such, the 4 position is more open to nucleophilic attack.



Scheme 10 Conditions: **8** (1.2 eq), K_2CO_3 (1.5 eq), ACN, rt, 18 h.

Chapter 3 Sulfonyl Fluorides as EGFR Inhibitors

The final step required for the synthesis of the target core structure required several attempts as noted in table 3 below.



Scheme 11 Final coupling to achieve the target WZ analogue. Conditions: i) TsOH (1.1 eq), NMP, 180 °C, 48 h.

Table 3 Microwave irradiation is conventional for this coupling however our system was prone to degradation.

| | Additive | Solvent | Time | Temp | Method | Yield |
|---|----------|----------------|------|------|-----------------------------|-------|
| 1 | TsOH | <i>n</i> -BuOH | 1 h | 120 | MW | – |
| 2 | DIPEA | <i>n</i> -BuOH | 1 h | 120 | MW | – |
| 3 | TsOH | <i>t</i> -BuOH | 1 h | 120 | MW | – |
| 4 | DIPEA | <i>t</i> -BuOH | 1 h | 120 | MW | – |
| 5 | TsOH | 2-pentanol | 1 h | 120 | MW | – |
| 6 | TsOH | NMP | 1 h | 120 | MW | 5% |
| 7 | TsOH | NMP | 1 h | 140 | MW | 8% |
| 8 | TsOH | NMP | 48 h | 140 | Conv. Heating - sealed tube | 31% |

Amination of chloro-pyrimidines is documented in literature²² to be achievable via microwave irradiation at elevated temperatures assisted by either an acid or base. Initial conditions described in **table 3** were initiated around these conditions. A high boiling alcoholic solvent is often used to facilitate the high temperatures, however the formation of insoluble tars was encouraged in our system. Finally, *N*-methylpyrrolidine (NMP) yielded the desired product however the issue of tar formation persisted. Conventional heating in NMP allowed for the optimum yield of **30**. Despite achieving the final product on small scales using the chosen acid mediated method, scaling the reaction up, even by a factor of two resulted in unsatisfactory yields. This made it impossible to acquire enough material to complete the study. Due to time limitations the process of improving the yield was stopped at this point. Losses incurred by chromatography for this product were high due to its extremely polar nature, eluting at 1:4 MeOH/DCM. The use of NMP as a solvent also complicated the purification requiring large excesses of saturated LiCl and brine solutions to remove during workup. Quantitative determination of the conversion, for example using HPLC to monitor the reaction over time, would yield useful information about where the losses are occurring.

Chapter 3 Sulfonyl Fluorides as EGFR Inhibitors

After 48 hr the pyrimidine starting material does not seem to be completely consumed however degradation products were observed to form and the reaction terminated at that point.

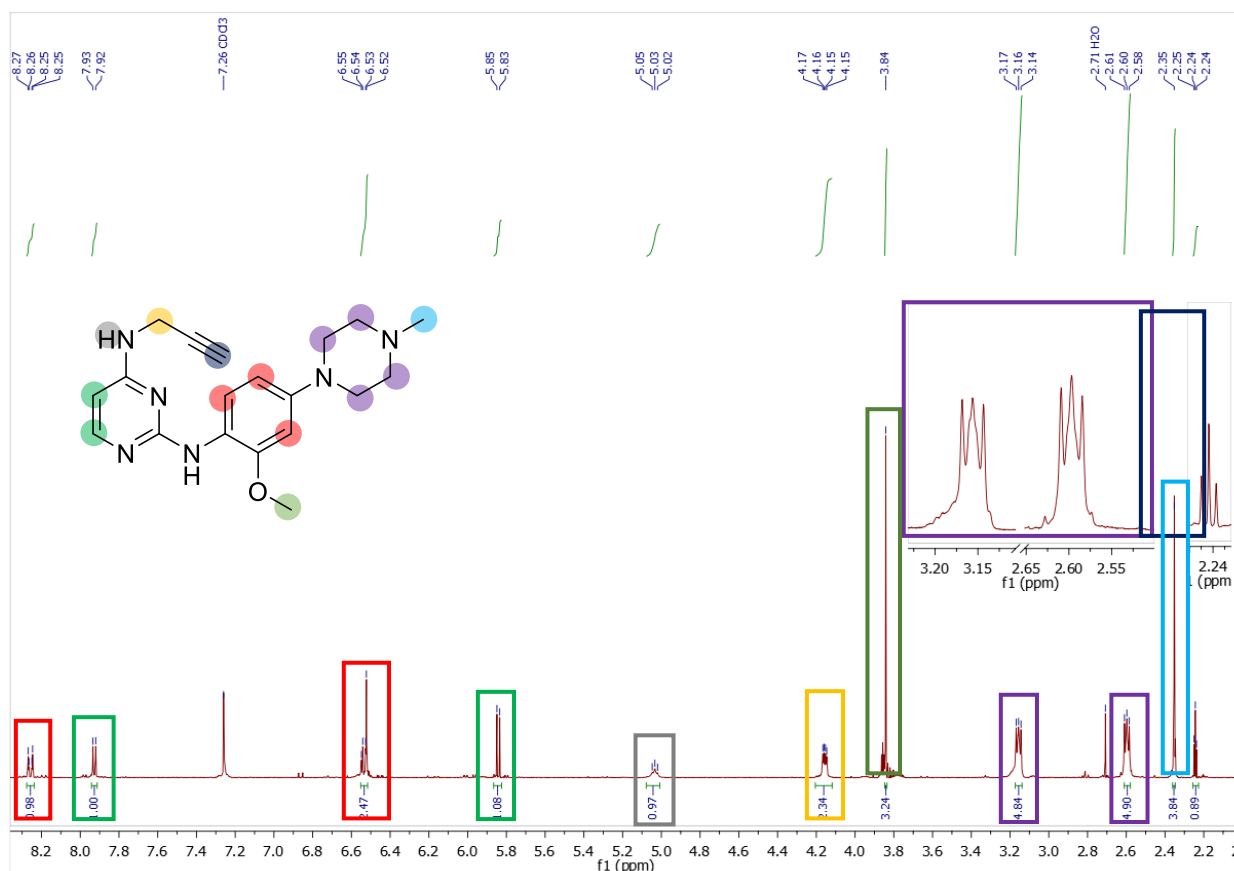


Figure 6 ¹H NMR spectrum of **30**. The majority of the spectrum was assigned with the guanidine like proton being the only unassigned feature.

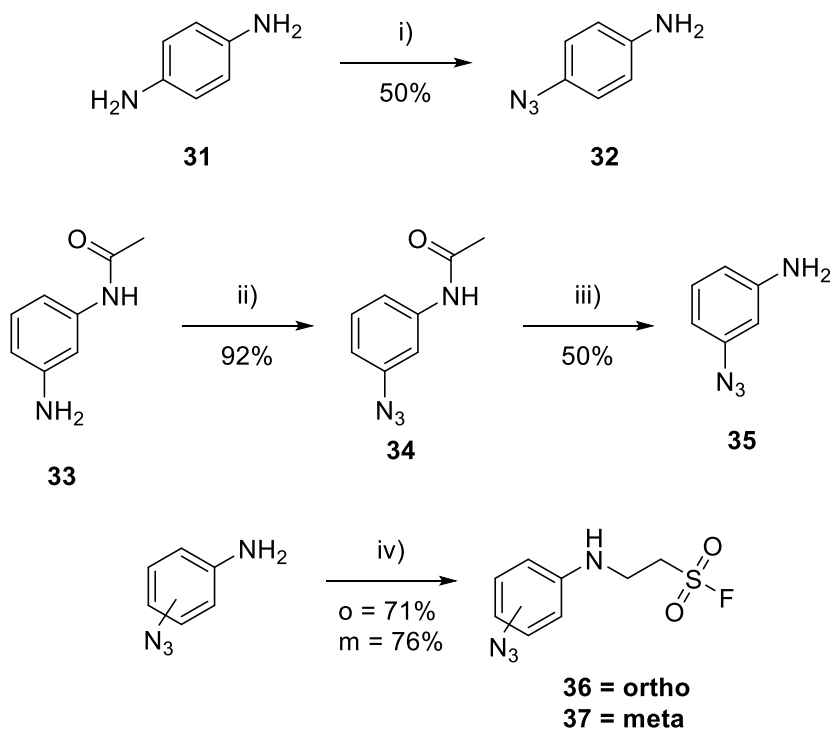
Key components from both starting fragments are present in the spectrum confirming the coupling's success. Both pyrimidine doublets, marked green, are present as well as the clear pair of apparent triplets of the piperazine ring. Importantly, the alkyne proton is visible at 2.24 ppm as a triplet and couples to the methylene doublet of doublets at 4.15 ppm indicating that the propargyl moiety has survived the harsh conditions. The carbon spectrum includes all necessary signals, accounting for the symmetry of the molecule. Finally HRMS confirms the molecular ion at 353.2090 m/z (calculated for C₁₉H₂₅N₆O [M+H⁺]: 353.2090)

WARHEAD SYNTHESIS

Azido anilines were selected as the starting point to mimic the structure of WZ4002 within the context of this study. To this end *p*-azidoaniline was synthesised by controlled diazotisation of *p*-phenylenediamine followed by nucleophilic attack of sodium azide to yield *p*-azidoaniline in **32** after aqueous workup and column chromatography. For the meta

Chapter 3 Sulfonyl Fluorides as EGFR Inhibitors

substituted variant, commercially available *m*-acetanilide was diazotised in the same manner as described previously, followed by base mediated hydrolysis of the amide, yielding compound **35** in 50% after chromatography. This protecting group is necessary due to *m*-phenylenediamine readily undergoing di-functionalisation under the same conditions described for the *para* substituted analogue. Both azidoanilines were confirmed by ^1H NMR and HRMS and compared well to literature.^{23,24}



Scheme 12 Synthesis of azidoaniline based warheads. Conditions: i) 2 M HCl, NaNO_2 (1.1 eq), NaN_3 (2.0 eq), urea (cat.), NaOAc (2.8 eq), H_2O , -10°C – rt, 30 min; ii) 2 M HCl, NaNO_2 (1.1 eq), NaN_3 (2.0 eq), urea (cat.), NaOAc (2.8 eq), H_2O , -10°C – rt, 30 min; iii) 18 M NaOH, EtOH, refl., 4 h; iv) ethenesulfonyl fluoride (1.1 eq), DMF, rt, 6 h.

These compounds were then alkylated using ethenesulfonyl fluoride in DMF at room temperature over six hours to yield the desired final compounds in good yield after chromatography. This Michael addition onto the ethene sulfonyl fluoride readily occurs and can be used as an electrophilic warhead in its own right. An example spectrum for compound **36** is displayed in Figure 9. The pair of doublets in the aromatic region are typical for *para* substituted benzenes. The aniline proton appears as a triplet lending towards confirming the alkylation, coupling to the adjacent methylene group with a coupling constant of 6.1 Hz between the two groups. Some evidence for the retention of the sulfonyl fluoride appears in the multiplet from 3.67 – 3.56 ppm. Having the general appearance of the quartet expected for this alkane chain structure, additional coupling can be seen. The fine structure contains several peaks which are unexpected for the $\text{CH}_2\text{--CH}_2$ coupling and can be explained through

Chapter 3 Sulfonyl Fluorides as EGFR Inhibitors

4J ^{19}F – ^1H coupling from the sulfonyl fluoride. This coupling can also be seen in the ^{13}C spectrum where the peak at 49.9 ppm is split with a coupling constant of 14 Hz. The cumulative effect of these couplings can be seen in the ^{19}F NMR spectrum which displays a single signal, a triplet of triplets confirming these heteronuclear couplings. Finally, IR spectrometry confirms the presence of the azide, with a strong absorbance at 2170 cm^{-1} . The meta substituted analogue, **37**, was described in the same manner.

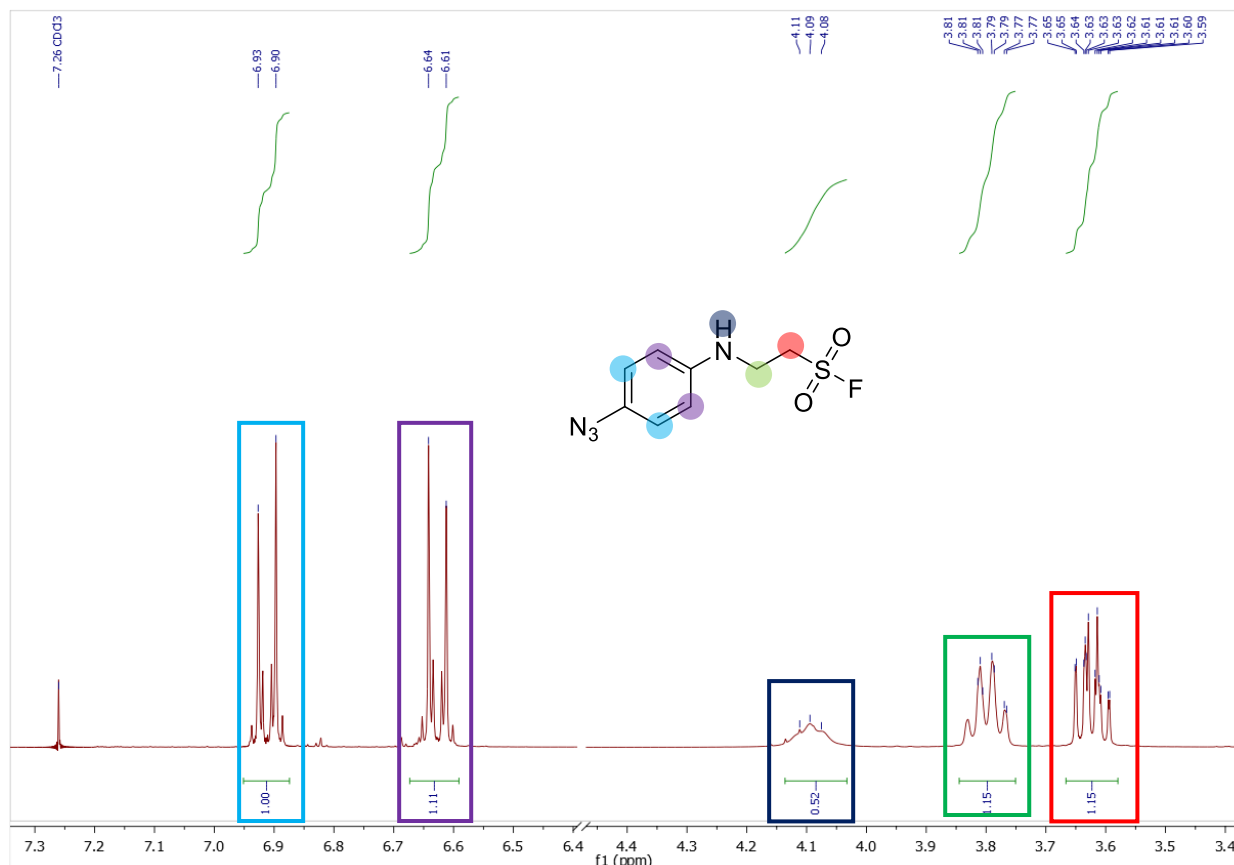
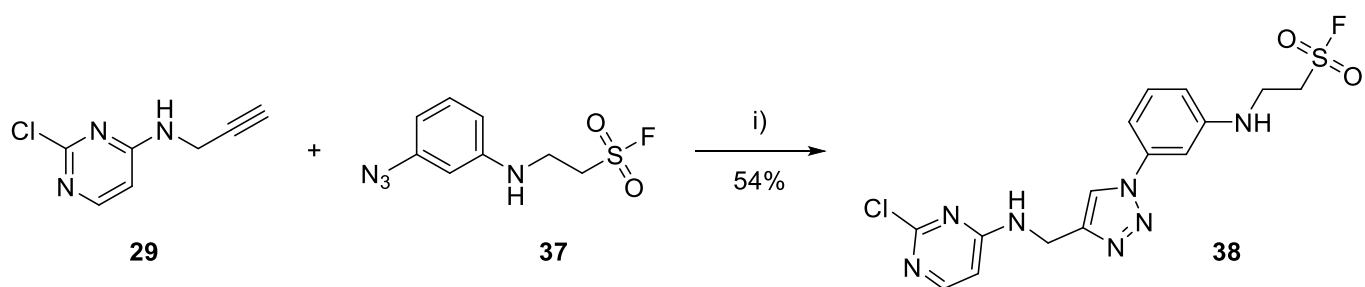


Figure 7 ^1H NMR spectrum of the azidoaniline sulfonyl fluoride containing warhead **36**.

MODEL CLICK STUDY

Due to time constraints and the limited availability of the alkyne-containing core structure a model click study was performed using the alkyne-containing pyrimidine precursor to the core and compound **37**.

Chapter 3 Sulfonyl Fluorides as EGFR Inhibitors



Scheme 13 Model click study with the alkyne containing precursor **29**. Conditions: i) $\text{Cu}(\text{OAc})_2$ (0.5 eq), Et_3N (1.5 eq), $\text{MeOH}/\text{H}_2\text{O}$ (4:1), rt, 18 h.

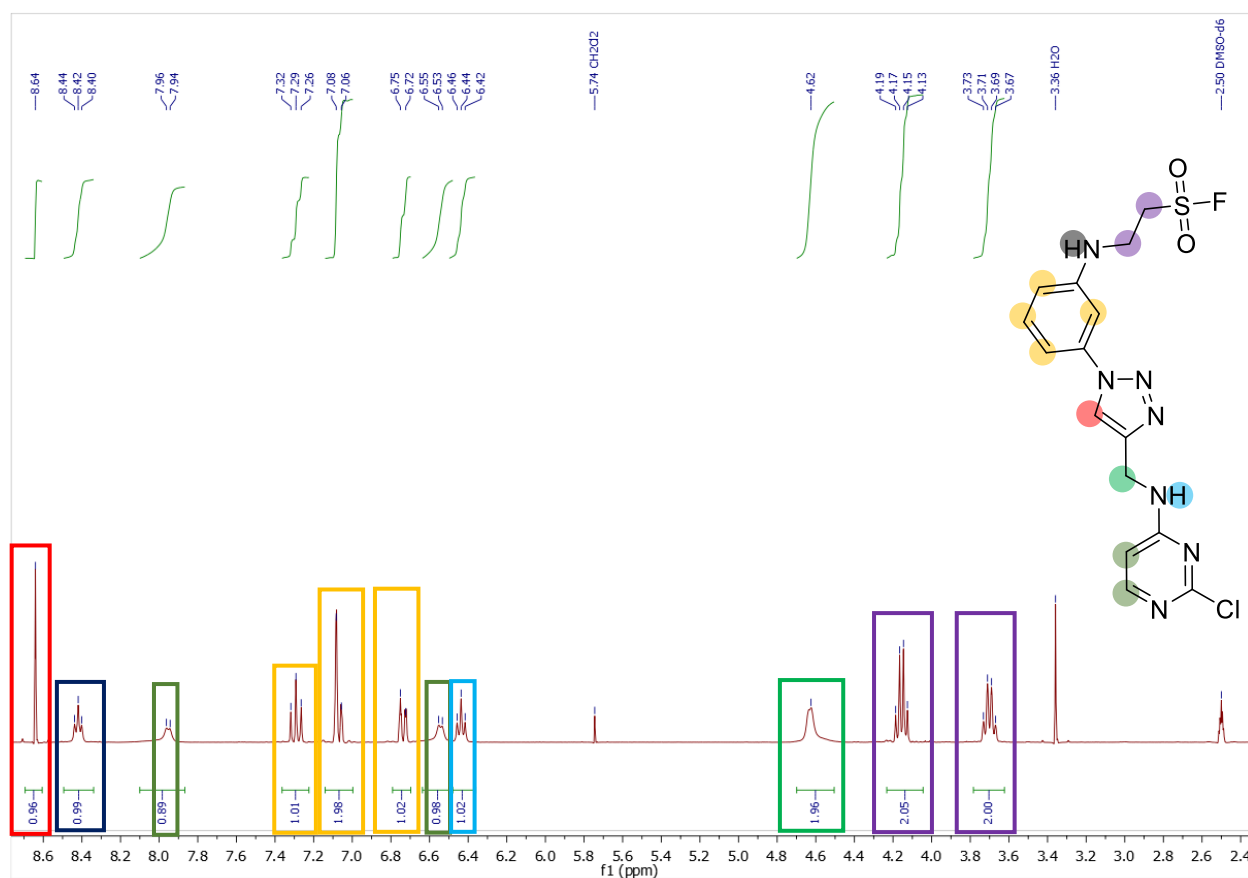


Figure 8 ¹H NMR spectrum of the click product **38**.

The more common copper sulphate/sodium ascorbate system did not yield any product for this system. However, copper(II)acetate in methanol yielded the target in acceptable yield. The CuAAC reaction requires an oxidant to maintain the active Cu(I) species. In this case methanol serves as both solvent and the oxidant to achieve the active species. In **figure 10**, the ¹H spectrum is shown for compound **38**. Substituted 1,2,3 triazoles have one proton which is highly deshielded, resulting in a characteristic downfield singlet.

Chapter 3 Sulfonyl Fluorides as EGFR Inhibitors

CONCLUSIONS

Despite difficulties, the aim of synthesising a 3rd generation heterocyclic drug core was achieved. Despite the difficulties encountered in the synthesis of the AZD9291 analogue, other strategies to achieve this target are still available for exploration. However, the timeframe of the project was not conducive to repeated attempts, and the general scope of the project was held in higher regard. The more accessible target, WZ 4002, allowed the easy formation of the alkyne leveraging the electrophilic properties halopyrimidines. Where these properties were a hindrance in the attempts to synthesise the AZD target, they were used to our advantage in the WZ synthesis. The azidoaniline model for the electrophilic warheads is easily accessible and have the potential to be easily functionalized. These initial fragments were successfully functionalised to contain alkyl sulfonyl fluorides and have the potential to be functionalised further. Finally, a model for click conditions was achieved in which all the components were tolerated to yield a combined sulfonyl fluoride and N-heterocycle containing triazole. The study is at a stage where poorly yielding reactions can be optimised and further exploration into the sulfonyl fluoride probes is easily accessible.

FURTHER STUDIES

Alkylation attempts to achieve compound **3** using propargyl bromide and a meridianin like pyrimidineamine was not investigated and could be used to achieve the intended target in theory. The reaction forming the target alkyne–core compound **30** must be optimised in order to complete the study in full. The yield is prohibitively poor in order to achieve a wide array of electrophile containing drug probes. Investigations into other reaction conditions for this S_NAr type reaction may yield more promising results. A full set of electrophilic probes should be synthesised and ‘clicked’ onto the core structure to achieve the final goal of a library of compounds with this functionality. Additionally this library should then be tested against mutant EGFR in enzymatic assays to determine how successful the concepts investigated here would be in a biological system.

REFERENCES

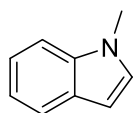
- (1) Herbst, R. S. Review of Epidermal Growth Factor Receptor Biology. *Int. J. Radiat. Oncol. Biol. Phys.* **2004**, 59 (2 SUPPL.), S21–S26. <https://doi.org/10.1016/j.ijrobp.2003.11.041>.
- (2) Yarden, Y.; Sliwkowski, M. X. Untangling the ErbB Signalling Network. *Nat. Rev. Mol. Cell Biol.* **2001**, 2 (2), 127–137. <https://doi.org/10.1038/35052073>.
- (3) Nyati, M. K.; Morgan, M. A.; Feng, F. Y.; Lawrence, T. S. Integration of EGFR Inhibitors with Radiochemotherapy. *Nat. Rev. Cancer* **2006**, 6 (11), 876–885. <https://doi.org/10.1038/nrc1953>.
- (4) Wee, P.; Wang, Z. Epidermal Growth Factor Receptor Cell Proliferation Signaling Pathways. *Cancers (Basel)*. **2017**, 9 (5), 1–45. <https://doi.org/10.3390/cancers9050052>.
- (5) Sharma, S. V; Bell, D. W.; Settleman, J.; Haber, D. A. Epidermal Growth Factor Receptor

Chapter 3 Sulfonyl Fluorides as EGFR Inhibitors

- Mutations in Lung Cancer. *Nat. Rev. Cancer* **2007**, *7* (3), 169–181. <https://doi.org/10.1038/nrc2088>.
- (6) Bublil, E. M.; Yarden, Y. The EGF Receptor Family: Spearheading a Merger of Signaling and Therapeutics. *Curr. Opin. Cell Biol.* **2007**, *19* (2), 124–134. <https://doi.org/10.1016/j.ceb.2007.02.008>.
 - (7) Hanahan, D.; Weinberg, R. A. Hallmarks of Cancer: The next Generation. *Cell* **2011**, *144* (5), 646–674. <https://doi.org/10.1016/j.cell.2011.02.013>.
 - (8) Basu, D.; Richters, A.; Rauh, D. Structure-Based Design and Synthesis of Covalent-Reversible Inhibitors to Overcome Drug Resistance in EGFR. *Bioorganic Med. Chem.* **2015**, *23* (12), 2767–2780. <https://doi.org/10.1016/j.bmc.2015.04.038>.
 - (9) Sordella, R. Gefitinib-Sensitizing EGFR Mutations in Lung Cancer Activate Anti-Apoptotic Pathways. *Science (80-.)*. **2004**, *305* (5687), 1163–1167. <https://doi.org/10.1126/science.1101637>.
 - (10) Jiang, X. M.; Xu, Y. L.; Huang, M. Y.; Zhang, L. Le; Su, M. X.; Chen, X.; Lu, J. J. Osimertinib (AZD9291) Decreases Programmed Death Ligand-1 in EGFR-Mutated Non-Small Cell Lung Cancer Cells. *Acta Pharmacol. Sin.* **2017**, *38* (11), 1512–1520. <https://doi.org/10.1038/aps.2017.123>.
 - (11) Cross, D. A. E.; Ashton, S. E.; Ghiorghiu, S.; Eberlein, C.; Nebhan, C. A.; Spitzler, P. J.; Orme, J. P.; Finlay, M. R. V.; Ward, R. A.; Mellor, M. J.; et al. AZD9291, an Irreversible EGFR TKI, Overcomes T790M-Mediated Resistance to EGFR Inhibitors in Lung Cancer. *Cancer Discov.* **2014**, *4* (9), 1046–1061. <https://doi.org/10.1158/2159-8290.CD-14-0337>.
 - (12) Finlay, M. R. V.; Anderton, M.; Ashton, S.; Ballard, P.; Bethel, P. A.; Box, M. R.; Bradbury, R. H.; Brown, S. J.; Butterworth, S.; Campbell, A.; et al. Discovery of a Potent and Selective EGFR Inhibitor (AZD9291) of Both Sensitizing and T790M Resistance Mutations That Spares the Wild Type Form of the Receptor. *J. Med. Chem.* **2014**, *57* (20), 8249–8267. <https://doi.org/10.1021/jm500973a>.
 - (13) Zhao, Q.; Ouyang, X.; Wan, X.; Gajiwala, K. S.; Kath, J. C.; Jones, L. H.; Burlingame, A. L.; Taunton, J. Broad-Spectrum Kinase Profiling in Live Cells with Lysine-Targeted Sulfonyl Fluoride Probes. *J. Am. Chem. Soc.* **2017**, *139* (2), 680–685. <https://doi.org/10.1021/jacs.6b08536>.
 - (14) Chen, W.; Dong, J.; Plate, L.; Mortenson, D. E.; Brighty, G. J.; Li, S.; Liu, Y.; Galmozzi, A.; Lee, P. S.; Hulce, J. J.; et al. Arylfluorosulfates Inactivate Intracellular Lipid Binding Protein(s) through Chemoselective SuFEx Reaction with a Binding Site Tyr Residue. *J. Am. Chem. Soc.* **2016**, *138* (23), 7353–7364. <https://doi.org/10.1021/jacs.6b02960>.
 - (15) Dong, J.; Krasnova, L.; Finn, M. G.; Barry Sharpless, K. Sulfur(VI) Fluoride Exchange (SuFEx): Another Good Reaction for Click Chemistry. *Angew. Chemie - Int. Ed.* **2014**, *53* (36), 9430–9448. <https://doi.org/10.1002/anie.201309399>.
 - (16) Worrell, B. T.; Malik, J. A.; Fokin, V. V. Direct Evidence of a Dinuclear Copper Intermediate in Cu(I)-Catalyzed Azide-Alkyne Cycloadditions. *Science (80-.)*. **2013**, *340* (6131), 457–460. <https://doi.org/10.1126/science.1229506>.
 - (17) Gompel, M.; Leost, M.; Bal De Kier Joffe, E.; Puricelli, L.; Hernandez Franco, L.; Palermo, J.; Meijer, L. Meridianins, a New Family of Protein Kinase Inhibitors Isolated from the Ascidian Aplidium Meridianum. *Bioorganic Med. Chem. Lett.* **2004**, *14* (7), 1703–1707. <https://doi.org/10.1016/j.bmcl.2004.01.050>.
 - (18) Brotzel, F.; Ying, C. C.; Mayr, H. Nucleophilicities of Primary and Secondary Amines in Water. *J. Org. Chem.* **2007**, *72* (10), 3679–3688. <https://doi.org/10.1021/jo062586z>.

Chapter 3 Sulfonyl Fluorides as EGFR Inhibitors

- (19) Rossignol, E.; Youssef, A.; Moreau, P.; Prudhomme, M.; Anizon, F. Synthesis of Aminopyrimidylindoles Structurally Related to Meridianins. *Tetrahedron* **2007**, *63* (41), 10169–10176. <https://doi.org/10.1016/j.tet.2007.07.095>.
- (20) Aoyagi, N.; Furusho, Y.; Endo, T. Convenient Synthesis of Acyclic Guanidines from Isothiouronium Iodides and Amines without Protection of the Amino Groups. *Synlett* **2014**, *25* (7), 983–986. <https://doi.org/10.1055/s-0033-1340904>.
- (21) Fresneda, P. M.; Molina, P.; Delgado, S.; Bleda, J. A. Synthetic Studies towards the 2-Aminopyrimidine Alkaloids Variolins and Meridianins from Marine Origin. *Tetrahedron Lett.* **2000**, *41* (24), 4777–4780. [https://doi.org/10.1016/S0040-4039\(00\)00728-0](https://doi.org/10.1016/S0040-4039(00)00728-0).
- (22) Sakuma, Y.; Yamazaki, Y.; Nakamura, Y.; Yoshihara, M.; Matsukuma, S.; Nakayama, H.; Yokose, T.; Kameda, Y.; Koizume, S.; Miyagi, Y. WZ4002, a Third-Generation EGFR Inhibitor, Can Overcome Anikis Resistance in EGFR-Mutant Lung Adenocarcinomas More Efficiently than Src Inhibitors. *Lab. Invest.* **2012**, *92* (3), 371–383. <https://doi.org/10.1038/labinvest.2011.187>.
- (23) Lu, Y.; Wang, L.; Wang, X.; Xi, T.; Liao, J.; Wang, Z.; Jiang, F. Design, Combinatorial Synthesis and Biological Evaluations of Novel 3-Amino-1'-((1-Aryl-1H-1,2,3-Triazol-5-Yl)methyl)-2'-Oxospiro[Benzo[a] Pyrano[2,3-c]Phenazine-1,3'-Indoline]-2-Carbonitrile Antitumor Hybrid Molecules. *Eur. J. Med. Chem.* **2017**, *135*, 125–141. <https://doi.org/https://doi.org/10.1016/j.ejmech.2017.04.040>.
- (24) Smith, P. A. S.; Hall, J. H. Kinetic Evidence for the Formation of Azene (Electron-Deficient Nitrogen) Intermediates from Aryl Azides. *J. Am. Chem. Soc.* **1962**, *84* (3), 480–485. <https://doi.org/10.1021/ja00862a032>.
- (25) Kong, A.; Han, X.; Lu, X. Highly Efficient Construction of Benzene Ring in Carbazoles by Palladium-Catalyzed Endo-Mode Oxidative Cyclization of 3-(3'-Alkenyl)Indoles. *Org. Lett.* **2006**, *8* (7), 1339–1342. <https://doi.org/10.1021/ol060039u>.

1-Methyl-1H-indole 5

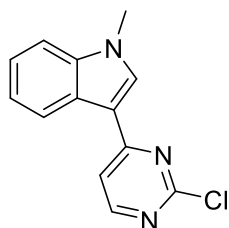
A flame dried, three neck flask, fitted with a dripping funnel, was charged with sodium hydride (60% dispersion in oil, 4.26 g, 107 mmol, 2.5 eq). To this was added THF (10 mL) and the suspension was allowed to stir for 5 min and cooled to 0°C. A solution of indole (5.00 g, 42.7 mmol, 1 eq) in 5 mL THF was prepared and dropped into the flask over 15 min and allowed to stir for an additional 1 hr at rt. A solution of methyl iodide (7.87 g, 55.5 mmol, 1.3 eq) in THF (5 mL) was prepared and was added to this flask dropwise. This mixture was then allowed to stir for an additional 1 hr at rt. The reaction mixture was quenched with sat. NH₄Cl solution (100 mL) and extracted with EtOAc (3 x 50 mL). The organic phase was collected, and the solvent removed under reduced pressure. The crude product was purified by flash column chromatography, eluting with 5 - 30% EtOAc in PE. Pure fractions were collected and evaporated to dryness affording the title compound, 4.99 g, 90% yield as a yellow oil. Spectral data collected for this compound compared well with reported literature values.²⁵

Chapter 3 Sulfonyl Fluorides as EGFR Inhibitors

^1H NMR (400 MHz, $\text{DMSO-}d_6$) δ 8.53 (d, J = 5.5 Hz, 1H), 8.50 (s, 1H), 8.40 (s, 1H), 7.82 (d, J = 5.5 Hz, 1H), 7.57 (d, J = 7.4 Hz, 1H), 7.29 (dd, J = 7.1, 1.4 Hz, 2H), 3.89 (s, 3H).

^{13}C NMR (75 MHz, $\text{DMSO-}d_6$) δ 136.8, 128.9, 128.6, 121.6, 120.9, 119.4, 109.3, 101.0, 32.9.

MS (ESI+) predicted for $\text{C}_9\text{H}_{10}\text{N}$ [$\text{M}+\text{H}^+$]: 132.0735, found 132,0813.

3-(2-Chloropyrimidin-4-yl)-1-methyl-1H-indole 7

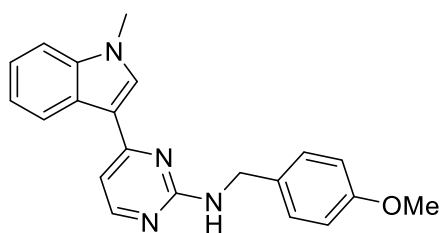
A flame-dried, 2-neck round bottomed flask was charged with 2,4-dichloropyrimidine (1.25 g, 8.39 mmol 1.1 eq) and dissolved in DME (10 mL). The resulting solution was cooled to 0 °C and FeCl_3 (1.36 g, 8.39 mmol, 1.1 eq) was added portionwise over 5 min. The solution was then allowed to warm to rt and stirred for 30 min. After recooling the solution to 0 °C, a solution of 1-methyl-1H-indole (1.00 g, 7.63 mmol, 1 eq) in DME (5 mL) was added dropwise over 10 min, where the reaction mixture developed into a red slurry. The mixture was gradually heated to 60 °C where after 1 h complete consumption of the starting material was noted by TLC. At this point the mixture was allowed to cool to rt and the solution was poured into ice cold H_2O (50 mL) while stirring. An off white precipitate was formed and washed with H_2O (3×40 mL) and MeOH (3×5 mL). Purification of the crude collected precipitate was achieved using flash column chromatography with elution gradient of 0 – 2% MeOH in DCM. Pure fractions were evaporated to dryness to afford the title compound as a white solid, 978 mg, 48% yield. Spectral data collected for this compound compared well with reported literature values.¹²

^1H NMR (300 MHz, $\text{DMSO-}d_6$) δ 8.53 (d, J = 5.5 Hz, 1H), 8.50 (s, 1H), 8.41 (dd, J = 6.8, 2.5 Hz, 1H), 7.82 (d, J = 5.5 Hz, 1H), 7.57 (dd, J = 6.7, 2.1 Hz, 1H), 7.29 (tt, J = 7.2, 5.5 Hz, 3H), 3.89 (s, 3H).

^{13}C NMR (75 MHz, $\text{DMSO-}d_6$) δ 169.7, 165.5, 163.9, 143.0, 139.9, 130.5, 128.0, 126.9, 126.8, 119.6, 116.1, 116.0, 38.5.

MS (ESI+) predicted for $\text{C}_{13}\text{H}_{11}\text{N}_3\text{Cl}$ [$\text{M}+\text{H}^+$]: 244.0642, found 244.0642

Chapter 3 Sulfonyl Fluorides as EGFR Inhibitors

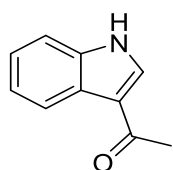
***N*-(4-Methoxybenzyl)-4-(1-methyl-1*H*-indol-3-yl)pyrimidin-2-amine 12**

A microwave vial was charged with 3-(2-chloropyrimidin-4-yl)-1-methyl-1*H*-indole (300 mg, 1.23 mmol, 1 eq) and dissolved in acetonitrile (5 mL). To this was added diisopropyl ethyl amine (175 mg, 1.35 mmol, 1.1 eq) and *p*-methoxybenzylamine (219 mg, 1.60 mmol, 1.3 eq). The mixture was then heated in a microwave reactor at 180 °C for 1 h. The solution was allowed to cool slowly to ambient temperature and then further cooled to 0 °C over 1 h. The resulting precipitate was then filtered, and the reaction solvent discarded. The filtrate was then washed with DCM (3 × 10 mL). The DCM fraction was then collected and the solvent removed under reduced pressure to yield the title compound, 389 mg, 92%.

¹H NMR (400 MHz, Chloroform-*d*) δ 8.39 (d, *J* = 7.9 Hz, 1H), 8.20 (d, *J* = 5.3 Hz, 1H), 7.72 (s, 3H), 7.39 – 7.31 (m, 3H), 7.29 (td, *J* = 7.6, 6.7, 0.8 Hz, 2H), 7.23 (td, *J* = 8.1, 6.8, 1.2 Hz, 1H), 6.90 – 6.87 (m, 2H), 5.54 (t, *J* = 4.7 Hz, 1H), 4.70 (d, *J* = 5.7 Hz, 1H), 3.82 (s, 2H), 3.80 (s, 2H).

¹³C NMR (101 MHz, Chloroform-*d*) δ 162.5, 162.4, 158.8, 157.2, 137.9, 131.7, 131.0, 128.9, 126.1, 122.5, 122.1, 121.1, 114.0, 109.7, 106.3, 55.3, 45.2, 33.2.

MS (ESI+) predicted for C₂₁H₂₁N₄O [M+H⁺]: 345.1715, found 345.1724.

1-(1*H*-Indol-3-yl)ethan-1-one 19

A flame dried three neck flask was charged with indole (1.17 g, 10.0 mmol, 1 eq) and dissolved in DCM (18 mL). To this solution was cooled to 0 °C and added anhydrous SnCl₄ (3.13 g, 12.0 mmol, 1.2 eq) dropwise where the solution turned a deep navy blue. After this addition was complete, nitromethane (5 mL) was added as cosolvent and allowed to stir for 5 min. To this suspension was then added acetic anhydride (1.02 g, 10.0 mmol, 1 eq) in DCM (2 mL) at 0 °C. The mixture was then stirred for 2 h and allowed to warm to rt. The mixture was then poured into ice cold H₂O with vigorous stirring and the resulting precipitate was filtered and the filtrate washed with EtOAc (3 × 30 mL). The organic phase was then combined and washed with saturated brine and dried over MgSO₄. This was then filtered and the solvent removed

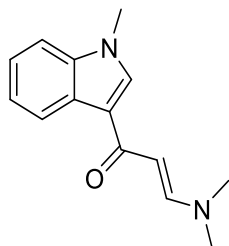
Chapter 3 Sulfonyl Fluorides as EGFR Inhibitors

under reduced pressure and the crude product was purified by column chromatography with elution gradient of 0 – 2% MeOH in DCM. Pure fractions were evaporated to dryness to afford the title compound as an off-white solid, 986 mg, 62% yield. Spectral data collected for this compound compared well with reported literature values.²¹

¹H NMR (600 MHz, DMSO-*d*₆) δ 11.91 (s, 1H), 8.30 (s, 1H), 8.19 (d, *J* = 7.5 Hz, 1H), 7.47 (d, *J* = 7.9 Hz, 1H), 7.23 – 7.15 (m, 2H), 2.45 (s, 3H).

¹³C NMR (151 MHz, DMSO-*d*₆) δ 195.7, 139.7, 137.4, 128.4, 125.8, 124.7, 124.4, 119.9, 115.2, 30.3.

MS (ESI+) predicted for C₁₀H₁₀NO [M+H⁺]: 160.0762, found 160.0761.

(*E*)-3-(Dimethylamino)-1-(1-methyl-1*H*-indol-3-yl)prop-2-en-1-one 20

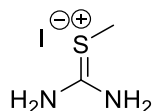
A solution of 1-(1*H*-indol-3-yl)ethan-1-one (790 mg, 4.96 mmol, 1 eq) and dimethylformamide–dimethyl acetal (2.96 g, 24.8 mmol, 5 eq) dissolved in DMF (5 mL) was prepared in a microwave vial. This was then heated to 110 °C for 2 hr in a microwave reactor whereafter it was allowed to cool to rt. Saturated brine (10 mL) and 10% w/w LiCl solution (10 mL) was then added to the solution and extracted with EtOAc (3 × 30 mL). The organic phase was collected and washed with 10% w/w LiCl solution (3 × 10 mL) and brine (3 × 10 mL) and the organic solvent removed under reduced pressure. The crude product was then subjected to flash column chromatography eluting with 0 – 10% MeOH in DCM. Pure fractions were evaporated to dryness to afford the title enamaninone as a yellow oil, 589 mg, 54% yield.²¹

¹H NMR (300 MHz, Chloroform-*d*) δ 8.42 – 8.36 (m, 1H), 7.75 (d, *J* = 12.5 Hz, 1H), 7.66 (s, 1H), 7.34 – 7.21 (m, 2H), 5.63 (d, *J* = 12.5 Hz, 1H), 3.79 (s, 3H), 2.98 (s, 6H).

¹³C NMR (75 MHz, Chloroform-*d*) δ 184.85, 151.92, 137.52, 132.98, 126.89, 122.70, 122.54, 121.52, 118.22, 109.49, 94.03, 33.34.

MS (ESI+) predicted for C₁₄H₁₆N₂O [M+H⁺]: 229.1334, found 221.1341.

Chapter 3 Sulfonyl Fluorides as EGFR Inhibitors

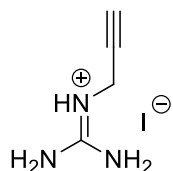
S-Methylisothiuronium iodide 18

A two neck flask was charged with thiourea (3.00 g, 39.4 mmol, 1 eq) and dissolved in ethanol (40 mL) and allowed to stir at rt for 10 min. To this solution was then added methyl iodide (6.71 g, 47.3 mmol) dropwise and allowed to stir at rt overnight. The solvent was then removed under reduced pressure to yield an off-white solid which was then subjected to high vacuum and heated to 40 °C for 18 hr. This afforded the title compound spectroscopically pure, 8.42 g, 98% yield. Spectral data collected for this compound compared well with reported literature values.²⁰

¹H NMR (300 MHz, DMSO-*d*₆) δ 8.88 (s, 4H), 2.57 (s, 3H).

¹³C NMR (75 MHz, DMSO-*d*₆) δ 176.4, 18.7.

MS (ESI+) predicted for C₂H₇N₂S [M⁺]: 91.0330, found 91.0323.

Propargylguanidine hydroiodide 16

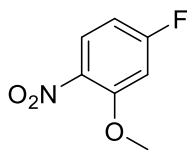
A solution of S-methylisothiuronium iodide (1.09 g, 5.00 mmol, 1 eq) in THF (4 mL) was prepared in a two neck flask and allowed to stir at rt for 10 min. A solution of propargylamine (330 mg, 6.00 mmol, 1 eq) in THF (1 mL) was then added dropwise and allowed to stir at rt for 6 hr. The solvent was then removed under reduced pressure to yield the title compound as an orange oil 1.10 g, spectroscopically pure in 98% yield with no further purification. Spectral data collected for this compound compared well with reported literature values.²⁰

¹H NMR (600 MHz, DMSO-*d*₆) δ 7.72 (s, 1H), 7.18 (s, 4H), 4.01 (d, *J* = 2.4 Hz, 2H), 3.36 (t, *J* = 2.4 Hz, 1H).

¹³C NMR (151 MHz, DMSO-*d*₆) δ 159.70, 82.1, 78.19, 33.7.

MS (ESI+) predicted for C₄H₈N₃ [M⁺]: 98.0718, found 98.0713.

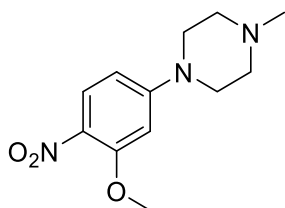
Chapter 3 Sulfonyl Fluorides as EGFR Inhibitors

4-Fluoro-2-methoxy-1-nitrobenzene 25

A three neck flask equipped for reflux was charged with K_2CO_3 (589 mg, 4.46 mmol, 1.4 eq) and 5-fluoro-2-nitrophenol (500 mg, 3.18 mmol, 1 eq) and dissolved in acetone (6.5 mL) and allowed to stir for 10 min. To this was added a solution of methyl iodide (542 mg, 3.82 mmol, 1.2 eq) in acetone (1 mL). The solution was then heated to reflux for 3 hr. After this the solution was allowed to cool to rt and filtered. The residue was washed with acetone (3×10 mL) and the organic phase was collected and the solvent removed under reduced pressure. The resulting residue was then dissolved in water (10 mL) and extracted with EtOAc (3×10 mL). The organic phase was collected and washed with sat. $NaHCO_3$ solution (3×5 mL) and then dried over $MgSO_4$. The solution was then filtered and the solvent removed under reduced pressure. The crude product was then purified by flash column chromatography eluting with 0 - 10% EtOAc in PE. Pure fractions were collected and evaporated to dryness affording the title compound, 558 mg, 86% yield as an orange oil. Spectral data collected for this compound compared well with reported literature values.⁸

1H NMR (400 MHz, Chloroform-*d*) δ 7.96 (dd, $J = 9.1, 6.0$ Hz, 1H), 6.79 (dd, $J = 10.3, 2.5$ Hz, 1H), 6.73 (ddd, $J = 9.1, 7.3, 2.5$ Hz, 1H), 3.96 (s, 3H).

^{13}C NMR (75 MHz, Chloroform-*d*) δ 167.6, 164.2, 155.3, 128.2 (d, $J = 11.3$ Hz), 107.3 (d, $J = 23.5$ Hz), 101.4 (d, $J = 27.1$ Hz), 56.8.

1-(3-Methoxy-4-nitrophenyl)-4-methylpiperazine 27

A two neck round bottom flask was charged with K_2CO_3 (535 mg, 4.05 mmol, 1.5 eq). A solution of 4-fluoro-2-methoxy-1-nitrobenzene (462 mg, 2.70 mmol, 1 eq) in DMF (2.5 mL) was then added to this and allowed to stir. A solution of *N*-methylpiperazine (270 mg, 2.70 mmol, 1 eq) in DMF (2.5 mL) was then added slowly and the resulting solution was allowed to stir for 18 hr at rt. The reaction was monitored by TLC and upon complete consumption of the starting material was quenched with brine (10 mL). This was then extracted with EtOAc (3×10 mL). The organic phase was collected and washed with 10% w/w LiCl solution (3×10

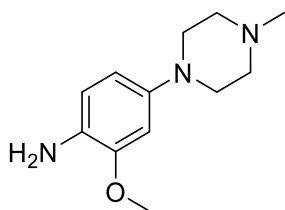
Chapter 3 Sulfonyl Fluorides as EGFR Inhibitors

mL) and brine (3×10 mL). The organic phase was then collected and dried over MgSO_4 . The solution was then filtered and the solvent removed under reduced pressure. The crude product was then subjected to flash column chromatography eluting with 0 – 10% MeOH in DCM. Pure fractions were evaporated to dryness to afford compound **27** as a yellow solid, 467 mg, 69% yield. Spectral data collected for this compound compared well with reported literature values.⁸

^1H NMR (300 MHz, Chloroform-*d*) δ 7.98 (d, $J = 9.4$ Hz, 1H), 6.41 (dd, $J = 9.4, 2.6$ Hz, 1H), 6.31 (d, $J = 2.6$ Hz, 1H), 3.93 (s, 3H), 3.40 (dd, $J = 5.1$ Hz, 4H), 2.53 (dd, $J = 5.1$ Hz, 4H), 2.34 (s, 3H).

^{13}C NMR (75 MHz, Chloroform-*d*) δ 156.43, 155.75, 128.92, 105.62, 97.20, 56.33, 54.66, 47.20, 46.18. Literature⁸ reports two peaks at 128.17 and 128.02 (101 MHz, DMSO-*d*₆) – peak at 128.92 shows these carbons as equivalent at this field strength.

MS (ESI+) predicted for $\text{C}_{12}\text{H}_{18}\text{NO}_3$ [$\text{M}+\text{H}^+$]: 252.1348, found 252.1352.

2-Methoxy-4-(4-methylpiperazin-1-yl)aniline 28

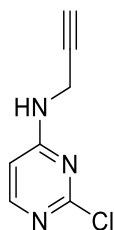
To a two neck round bottom flask was added 1-(3-methoxy-4-nitrophenyl)-4-methylpiperazine (2.19 g, 8.72 mmol, 1 eq) and dissolved in EtOH (40 mL). To this was added palladium on carbon 5% w/w (46 mg, 0.04 mmol, 0.1 eq). The system was then flushed with H_2 gas and maintained under an atmosphere of H_2 at rt for 18 hr while stirring. The suspension was then filtered and the solvent then removed under reduced pressure to afford the title compound, 1.91 g, 99% yield as a purple oily solid and was used with no further purification. Spectral data collected for this compound compared well with reported literature values.⁸

^1H NMR (300 MHz, DMSO-*d*₆) δ 6.51 (d, $J = 8.3$ Hz, 1H), 6.48 (d, $J = 2.5$ Hz, 1H), 6.28 (dd, $J = 8.4, 2.5$ Hz, 1H), 4.20 (s, 2H), 3.73 (s, 3H), 2.97 – 2.90 (m, 4H), 2.46 – 2.39 (m, 4H), 2.20 (s, 3H).

^{13}C NMR (75 MHz, Chloroform-*d*) δ 152.2, 148.5, 136.2, 119.4, 113.8, 107.1, 60.4, 60.2, 55.4, 51.0.

MS (ESI+) predicted for $\text{C}_{12}\text{H}_{20}\text{NO}$ [$\text{M}+\text{H}^+$]: 222.1606, found 222.1352.

Chapter 3 Sulfonyl Fluorides as EGFR Inhibitors

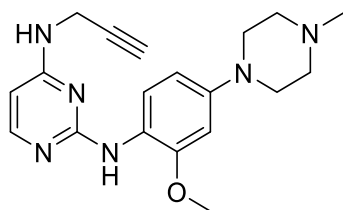
2-Chloro-1-(prop-2-yn-1-yl)pyrimidin-4-amine 29

A two neck round bottom flask was prepared with 2,4-dichloropyrimidine (1.50 g, 10.1 mmol) and K_2CO_3 (1.99 g, 15.1 mmol, 1.5 eq) and dissolved in ACN (50 mL). This solution was allowed to stir for 10 min at rt after which propargyl amine (610 mg, 11.1 mmol, 1.1 eq) in ACN (10 mL) was added slowly. The resulting mixture was allowed to stir at rt for 18 hr. The reaction mixture was then filtered and the solvent removed under reduced pressure. The crude product was then directly subjected to column chromatography eluting with 0 – 5% MeOH in DCM. Pure fractions were evaporated to dryness to afford the title compound as an off-white solid, 1.11 g, 66% yield.

1H NMR (300 MHz, Chloroform-*d*) δ 8.09 (d, J = 5.9 Hz, 1H), 6.37 (d, J = 5.9 Hz, 1H), 6.04 (s, 1H), 4.17 (d, J = 3.2 Hz, 1H), 2.28 (t, J = 2.5 Hz, 1H).

^{13}C NMR (75 MHz, Chloroform-*d*) δ 163.4, 160.1, 156.4, 105.6, 81.0, 74.0, 29.8.

MS (ESI+) predicted for $C_7H_6N_3Cl$ [$M+H^+$]: 168.0328, found 168.0336.

***N*²-[2-Methoxy-4-(4-methylpiperazin-1-yl)phenyl]-*N*⁴-(prop-2-yn-1-yl)pyrimidine-2,4-diamine 30**

A solution of 2-methoxy-4-(4-methylpiperazin-1-yl)aniline (528 mg, 2.38 mmol, 1 eq), 2-chloro-*N*-(prop-2-yn-1-yl)pyrimidin-4-amine (400 mg, 2.38 mmol, 1 eq) and TsOH (411 mg, 2.38 mmol, 1 eq) in *N*-methylpyrrolidine (2.5 mL) was prepared in a sealed tube and heated to 140 °C for 48 hr. The solution was then cooled to rt and diluted with EtOAc (5 mL). Brine (20 mL) was then added and mixed vigorously and extracted with EtOAc (3 × 20 mL). The organic phase was collected and washed with 10% w/w LiCl solution (3 × 10 mL) and brine (3 × 10 mL). The organic phase was then collected and dried over $MgSO_4$. The solution was then filtered and the solvent removed under reduced pressure. The crude product was then subjected to flash column chromatography eluting with 0 – 30% MeOH in DCM. Pure fractions

Chapter 3 Sulfonyl Fluorides as EGFR Inhibitors

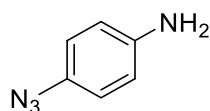
were evaporated to dryness to afford the title compound **30** as a brown oil, 260 mg, 31% yield.

^1H NMR (400 MHz, Chloroform-*d*) δ 8.26 (d, J = 9.1 Hz, 1H), 7.93 (d, J = 5.8 Hz, 1H), 6.59 – 6.48 (m, 3H), 5.84 (d, J = 5.7 Hz, 1H), 5.03 (t, J = 5.5 Hz, 1H), 4.16 (dd, J = 5.6, 2.5 Hz, 2H), 3.84 (s, 3H), 3.20 – 3.12 (m, 4H), 2.62 – 2.57 (m, 4H), 2.35 (s, 3H), 2.24 (t, J = 2.5 Hz, 1H).

^{13}C NMR (101 MHz, Chloroform-*d*) δ 162.30, 159.96, 156.41, 149.08, 146.82, 123.08, 120.02, 108.42, 100.85, 96.17, 80.30, 71.51, 55.75, 55.28, 50.35, 46.15, 30.93.

IR (ATR, cm^{-1}) 3276 (C \equiv C–H stretch), 2936 (N–H stretch), 2806 (N–H stretch)

MS (ESI+) predicted for $\text{C}_{19}\text{H}_{25}\text{N}_6\text{O}$ [$\text{M}+\text{H}^+$]: 353.2090, found 353.2090.

4-Azidoaniline 32

A two neck flask was prepared with phenylenediamine (757 mg, 7.00 mmol, 1 eq) and dissolved in 2M HCl (10 mL). A solution of sodium nitrite (580 mg, 8.40 mmol, 1.2 eq) in H_2O (2 mL) was prepared separately. The acidic solution was cooled to -10°C and the solution of sodium nitrite was added dropwise ensuring complete mixing between drops. The dark reaction mixture foamed between drops and required vigorous stirring to reincorporate the foam into solution. When the reaction mixture was homogenous, urea (50 mg, 0.83 mmol, 0.11 eq) was added in a single portion to destroy excess nitrous acid. Additionally, sodium acetate (1.65 g, 20 mmol, 2.85 eq) was added in a single portion to prevent the formation of hydrazoic acid in the following addition, and allowed to stir for 30 min at rt. The reaction mixture was cooled again to -10°C and a solution of sodium azide (910 mg, 14 mmol, 2 eq) in H_2O (3 mL) was added dropwise to the reaction mixture and allowed to stir for 30 min. The reaction mixture was then extracted with EtOAc (3×10 mL). The organic phase was collected and washed with sat. NaHCO_3 solution (3×5 mL) and then dried over MgSO_4 . The solution was then filtered and the solvent removed under reduced pressure. The crude product was then purified by flash column chromatography eluting with 0 - 30% EtOAc in PE. Pure fractions were collected and evaporated to dryness affording the title compound, 469 mg, 50% yield as a light brown crystalline solid. Spectral data collected for this compound compared well with reported literature values.²³

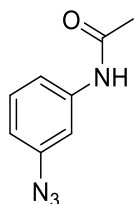
^1H NMR (300 MHz, DMSO-*d*₆) δ 6.78 (d, J = 8.3 Hz, 2H), 6.60 (d, J = 8.2 Hz, 2H), 5.14 (s, 2H).

^{13}C NMR (75 MHz, DMSO-*d*₆) δ 151.8, 131.2, 124.9, 120.2.

IR (ATR, cm^{-1}) 3392 (N–H stretch), 2104 (N=N=N stretch).

Chapter 3 Sulfonyl Fluorides as EGFR Inhibitors

MS (ESI+) predicted for $C_6H_7N_4$ $[M+H]^+$: 135.0671, found 135.0676.

***N*-(3-Azidophenyl)acetamide 34**

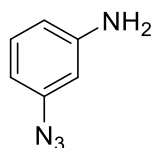
A two neck flask was prepared with acetanilide (1.05 g, 7.00 mmol, 1 eq) and dissolved in 2M HCl (10 mL). A solution of sodium nitrite (580 mg, 8.40 mmol, 1.2 eq) in H_2O (2 mL) was prepared separately. The acidic solution was cooled to $-10\text{ }^{\circ}C$ and the solution of sodium nitrite was added dropwise ensuring complete mixing between drops. Urea (50 mg, 0.83 mmol, 0.11 eq) was added in a single portion to destroy excess nitrous acid. Additionally, sodium acetate (1.65 g, 20 mmol, 2.85 eq) was added in a single portion and allowed to stir for 30 min at rt. The reaction mixture was cooled again to $-10\text{ }^{\circ}C$ and a solution of sodium azide (910 mg, 14 mmol, 2 eq) in H_2O (3 mL) was added dropwise to the reaction mixture and allowed to stir for 30 min. The reaction mixture was then extracted with EtOAc ($3 \times 10\text{ mL}$). The organic phase was collected and washed with sat. $NaHCO_3$ solution ($3 \times 5\text{ mL}$) and then dried over $MgSO_4$. The solution was then filtered and the solvent removed under reduced pressure. The crude product was then purified by flash column chromatography eluting with 0 - 30% EtOAc in PE. Pure fractions were collected and evaporated to dryness affording the title compound, 1.13 g, 92% yield as a brown oil. Spectral data collected for this compound compared well with reported literature values.²⁴

1H NMR (300 MHz, Chloroform-*d*) δ 7.69 (s, 1H), 7.31 (t, $J = 1.9\text{ Hz}$, 1H), 7.22 (d, $J = 15.9\text{ Hz}$, 1H), 7.17 (ddd, $J = 8.4, 1.4\text{ Hz}$, 1H), 6.74 (ddd, $J = 7.8, 2.0, 1.4\text{ Hz}$, 1H), 2.14 (s, 3H).

^{13}C NMR (75 MHz, Chloroform-*d*) δ 169.6, 146.2, 131.0, 130.4, 130.4, 130.4, 126.2, 126.2, 126.2, 120.1, 120.1, 120.1, 114.4, 114.4, 23.2.

IR (ATR, cm^{-1}) 3245 (N–H stretch), 2109 (N=N=N stretch), 1592 (C=O stretch)

MS (ESI+) predicted for $C_8H_9N_4O$ $[M+H]^+$: 177.0776, found 177.0782.

3-azidoaniline 35

Chapter 3 Sulfonyl Fluorides as EGFR Inhibitors

A two neck flask equipped for reflux was prepared with a solution of *N*-(3-azidophenyl)acetamide (528 mg, 3.00 mmol, 1 eq) in EtOH (3 mL). An aqueous 18M KOH solution (5 mL) was then added and the reaction mixture was heated under reflux for 4 hr. The reaction mixture was diluted with H₂O (15 mL) and extracted with EtOAc (3 × 10 mL). The organic phase was collected and washed with sat. brine solution (3 × 10 mL) and then dried over MgSO₄. The solution was then filtered and the solvent removed under reduced pressure. The crude product was then purified by flash column chromatography eluting with 0 - 30% EtOAc in PE. Pure fractions were collected and evaporated to dryness affording the title compound, 201 mg, 50% yield as a dark brown oil. Spectral data collected for this compound compared well with reported literature values.²⁴

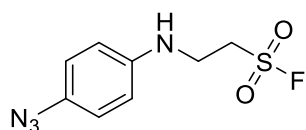
¹H NMR (300 MHz, Chloroform-*d*) δ 7.14 (t, *J* = 8.0 Hz, 1H), 6.48 (dd, *J* = 2.2, 0.6 Hz, 1H), 6.46 (d, *J* = 2.2 Hz, 1H), 6.34 (t, *J* = 2.2 Hz, 1H), 3.77 (s, 2H).

¹³C NMR (75 MHz, Chloroform-*d*) δ 147.9, 141.0, 130.5, 111.8, 109.1, 105.4.

IR (ATR, cm⁻¹) 3369 (N–H stretch), 2105 (N=N=N stretch).

MS (ESI+) predicted for C₆H₇N₄ [M+H⁺]: 135.0671, found 135.0675.

2-[(4-Azidophenyl)amino]ethane-1-sulfonyl fluoride 36



A two neck flask was charged with 4-azidoaniline (200 mg, 1.49 mmol, 1 eq) and dissolved in DMF (3 mL). Ethene sulfonyl fluoride (164 mg, 1.49 mmol, 1 eq) was dissolved in DMF (1 mL) and added at -10 °C to the reaction mixture. The mixture was allowed to stir and warm to rt over 6 hr. The reaction was quenched with brine (10 mL) and extracted with EtOAc (3 × 10 mL). The organic phase was collected and washed with 10% w/w LiCl solution (3 × 10 mL) and brine (3 × 10 mL). The organic phase was then collected and dried over MgSO₄. The solution was then filtered and the solvent removed under reduced pressure. The crude product was then subjected to flash column chromatography eluting with 0 – 10% MeOH in DCM. Pure fractions were evaporated to dryness to afford the title compound as a brown oil, 258 mg, 71% yield.

¹H NMR (300 MHz, Chloroform-*d*) δ 6.91 (d, *J* = 8.9 Hz, 1H), 6.63 (d, *J* = 8.8 Hz, 1H), 4.09 (t, *J* = 6.0 Hz, 1H), 3.80 (q, *J* = 6.1 Hz, 2H), 3.67 – 3.56 (m, 2H).

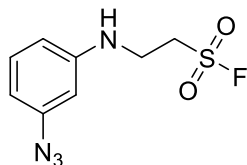
¹³C NMR (75 MHz, Chloroform-*d*) δ 143.1, 130.9, 120.5, 114.6, 49.9 (d, *J* = 14.0 Hz), 38.5.

¹⁹F NMR (282 MHz, Chloroform-*d*) δ 57.19 (tt, *J* = 4.6, 1.2 Hz).

Chapter 3 Sulfonyl Fluorides as EGFR Inhibitors

IR (ATR, cm^{-1}) 3416 (N–H stretch), 2102(N=N=N stretch), 1395 (S=O stretch)

MS (ESI+) predicted for $\text{C}_8\text{H}_{10}\text{N}_4\text{O}_2\text{FS}$ [$\text{M}+\text{H}^+$]: 245.0508, found 245.0502.

2-[(3-azidophenyl)amino]ethane-1-sulfonyl fluoride 37

A two neck flask was charged with 3-azidoaniline (200 mg, 1.49 mmol, 1 eq) and dissolved in DMF (3 mL). Ethene sulfonyl fluoride (164 mg, 1.49 mmol, 1 eq) was dissolved in DMF (1 mL) and added at $-10\text{ }^{\circ}\text{C}$ to the reaction mixture. The mixture was allowed to stir and warm to rt over 6 hr. The reaction was quenched with brine (10 mL) and extracted with extracted with EtOAc ($3 \times 10\text{ mL}$). The organic phase was collected and washed with 10% w/w LiCl solution ($3 \times 10\text{ mL}$) and brine ($3 \times 10\text{ mL}$). The organic phase was then collected and dried over MgSO_4 . The solution was then filtered and the solvent removed under reduced pressure. The crude product was then subjected to flash column chromatography eluting with 0 – 10% MeOH in DCM. Pure fractions were evaporated to dryness to afford the title compound as a brown oil, 376 mg, 76% yield.

^1H NMR (300 MHz, $\text{DMSO}-d_6$) δ 7.14 (t, $J = 8.0\text{ Hz}$, 1H), 6.47 (ddd, $J = 8.3, 2.2, 1.0\text{ Hz}$, 1H), 6.38 – 6.32 (m, 2H), 6.24 (t, $J = 6.3\text{ Hz}$, 1H), 5.33 (s, 1H), 4.09 (q, $J = 6.2\text{ Hz}$, 2H), 3.62 (qd, $J = 6.3, 1.3\text{ Hz}$, 2H).

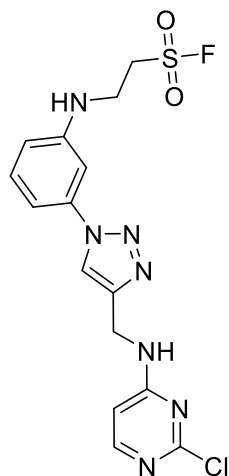
^{13}C NMR (75 MHz, $\text{DMSO}-d_6$) δ 148.9, 140.2, 130.5, 109.5, 107.1, 102.4, 49.6 (d, $J = 11.0\text{ Hz}$), 37.2.

^{19}F NMR (282 MHz, $\text{DMSO}-d_6$) δ 58.28 (t, $J = 5.9\text{ Hz}$).

IR (ATR, cm^{-1}) 3416 (N–H stretch), 2102(N=N=N stretch), 1395 (S=O stretch)

MS (ESI+) predicted for $\text{C}_8\text{H}_{10}\text{N}_4\text{O}_2\text{FS}$ [$\text{M}+\text{H}^+$]: 245.0508, found 245.0506.

Chapter 3 Sulfonyl Fluorides as EGFR Inhibitors

2-([3-(4-((2-Chloropyrimidin-4-yl)amino)methyl)-1H-1,2,3-triazol-1-yl)phenyl]amino)ethane-1-sulfonyl fluoride 38

A reaction vial was prepared with a solution of 2-((3-azidophenyl)amino)ethane-1-sulfonyl fluoride (26 mg, 0.10 mmol, 1 eq), and 2-chloro-N-(prop-2-yn-1-yl)pyrimidin-4-amine (17 mg, 0.10 mmol, 1 eq) in methanol (0.75 mL). To this was added copper(II)acetate (9 mg, 0.05 mmol, 0.5 eq) and H₂O (0.25 mL). The solution was allowed to stir vigorously for 5 min and triethylamine (15 mg, 0.15 mmol, 1.5 eq) was then added. The vial was then flushed with inert gas and sealed and the reaction mixture was allowed to stir at rt for 18 hr. The reaction mixture was then diluted with H₂O (5 mL) and extracted with EtOAc (3 × 10 mL). The organic phase was collected and washed with sat. brine solution (3 × 5 mL) and then dried over MgSO₄. The solution was then filtered and the solvent removed under reduced pressure. The crude product was then purified by flash column chromatography eluting with 0 – 15% MeOH in DCM. Pure fractions were evaporated to dryness to afford the title compound as off-white oily solid, 22 mg, 54% yield.

¹H NMR (300 MHz, DMSO-*d*₆) δ 8.64 (s, 1H), 8.42 (t, *J* = 5.6 Hz, 1H), 7.95 (d, *J* = 5.8 Hz, 1H), 7.29 (t, *J* = 8.0 Hz, 1H), 7.10 – 7.03 (m, 2H), 6.74 (dd, *J* = 8.3, 2.9 Hz, 1H), 6.54 (d, *J* = 5.8 Hz, 1H), 6.44 (t, *J* = 6.2 Hz, 1H), 4.16 (q, *J* = 6.1 Hz, 2H), 3.70 (q, *J* = 6.3 Hz, 2H).

¹³C NMR (75 MHz, DMSO-*d*₆) δ 163.2, 159.8, 155.7, 148.6, 144.7, 137.7, 130.4, 121.4, 112.8, 108.1, 105.2, 103.2, 49.6 (d, *J* = 11.0 Hz), 37.3, 35.4.

IR (ATR, cm⁻¹) 3363 (N–H stretch), 1403 (S=O stretch)

¹⁹F NMR (282 MHz, DMSO-*d*₆) δ 58.12 (t, *J* = 5.8 Hz).

MS (ESI+) predicted for C₁₅H₁₆N₇OFCIS [M+H⁺]: 412.1421, found 412.142

Chapter 4 General Practices

GENERAL PRACTICES

SOLVENTS AND REAGENTS CHEMICALS

Starting reagents and solvents used in these experiments were purchased from Alfa Aesar, Acros Organics, Sigma-Aldrich or Merck. Tetrahydrofuran and toluene were distilled under nitrogen from sodium wire/sand using benzophenone as indicator. Dichloromethane, dimethylformamide and acetonitrile were distilled under nitrogen from calcium hydride. Methanol, ethanol and isopropanol were distilled under nitrogen from magnesium turnings and catalytic iodine. Alternatively, solvents were dried for at least two days in a sealed Schlenk flask, under argon, using 3 Å, 4 Å or 5 Å molecular sieves. Triethylamine and *N,N*-diisopropylethylamine were distilled under nitrogen from potassium hydroxide. Ethyl acetate, petroleum ether and dichloromethane used for flash column chromatography was distilled under open air conditions in bulk batches.

CHROMATOGRAPHY AND PURIFICATION

Thin layer chromatography (TLC) was performed on Macherey Nagel aluminium TLC-plates, pre-coated with 0.20 mm silica gel and fluorescent indicator UV254. Visualization was performed with UV light ($\lambda = 254$ nm), iodine on silica or by spraying with KMnO_4 , *p*-anisaldehyde, ceric ammonium molybdate (CAM), ninhydrin (NIN), vanillin or bromocresol green stains followed by heating. Universal pH test paper strips were used to determine pH. Flash column chromatography was performed using Merck silica gel 60 (particle size 0.040-0.063 mm) or neutral alumina. A rotary evaporator was used to remove solvents in vacuo. High vacuum (~ 0.8 mm Hg) was used to dry products.

SPECTROSCOPY

All infrared spectra were recorded on a Thermo Nicolet FT-IR, using an Attenuated Total Reflectance (ATR) attachment. OMNIC 7.0 software was used to analyse spectra. NMR spectra were recorded on a 300 MHz Varian VNMRS (75 MHz for ^{13}C NMR, spectra 282 MHz for ^{19}F NMR spectra), 400 MHz Varian Unity Inova (101 MHz for ^{13}C NMR spectra,) or 600 MHz Varian Unity Inova (151 MHz for ^{13}C NMR spectra) at the Central Analytical Facilities (CAF) of Stellenbosch University. Chemical shifts (δ) are reported in parts per million (ppm), multiplicities are indicated as s (singlet), d (doublet), dd (doublet of doublets), t (triplet), q (quartet), m (multiplet) and coupling constants (*J*) are expressed in Hertz (Hz). ^1H and ^{13}C spectra are referenced to the residual solvent signal DMSO- d_6 (2.50 or 39.52 ppm), CDCl_3 (7.26 or 77.16 ppm) ^{19}F NMR spectra are referenced to CFCl_3 which served as the internal standard for these experiments. NMR spectra were processed using MestReNova version 12.0.0-20080. High-resolution mass spectrometry was performed using a Waters SYNAPT G2 QTOF spectrometer, in ESI positive mode, by the CAF at Stellenbosch University.

Chapter 4 General Practices

GLASSWARE AND INERT CONDITIONS

Glassware was oven dried and thereafter was placed under vacuum of ~ 0.8 mm Hg and cyclically flushed with nitrogen/argon and evacuated until it had reached room temperature. Standard Schlenk techniques were employed when necessary. All reactions were performed under a positive pressure of 2.8 kPa of 5.0 grade nitrogen or argon (Air Products). Low temperature reactions were performed in a dewar containing ice in acetone (~ -10 °C), dry ice in acetonitrile (-40 °C) or dry ice in acetone (-78 °C).

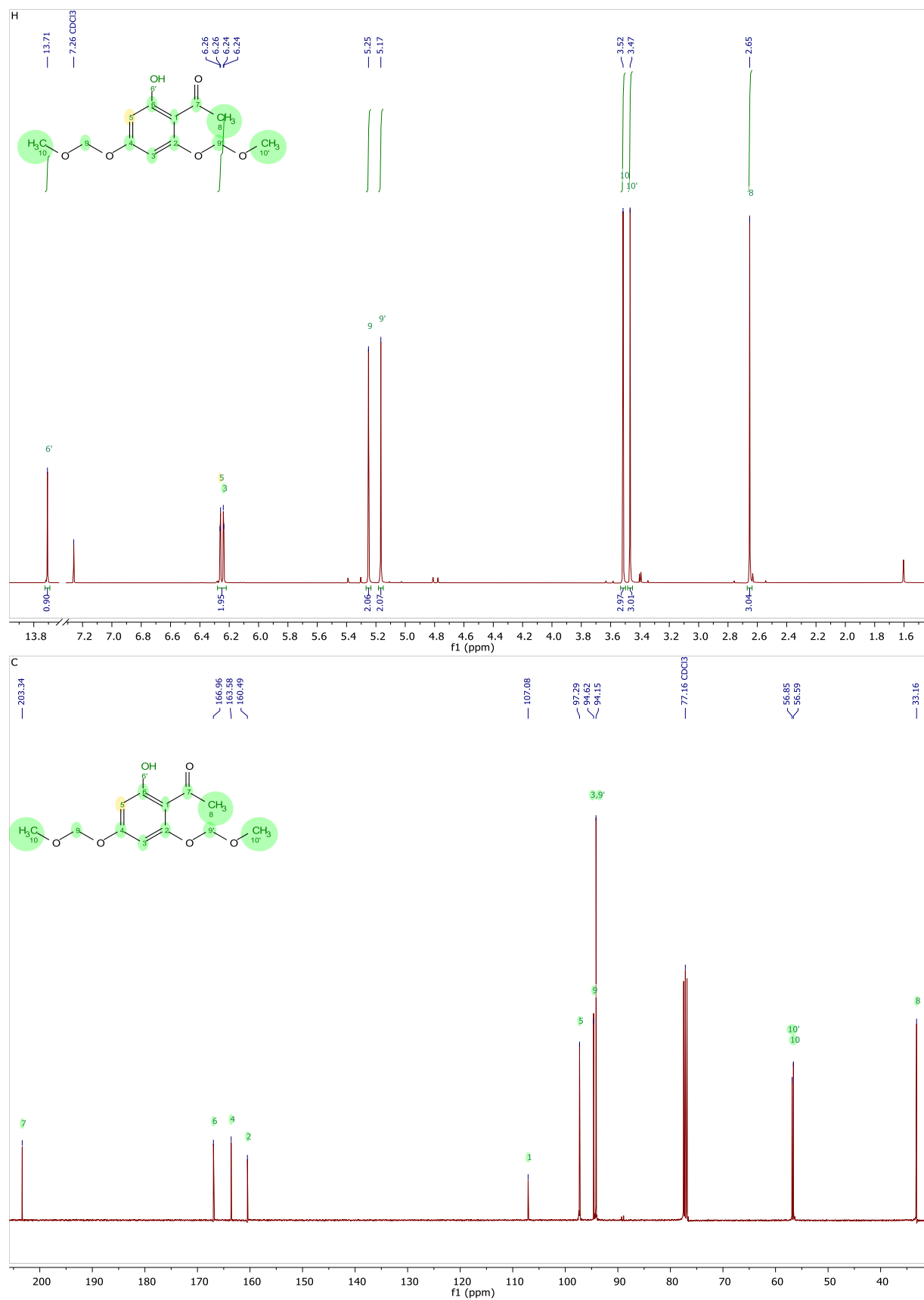
CELL CYTOTOXICITY ASSAY

The cytotoxicity of the flavonols was quantified using the standard MTT cellular viability assay. Briefly, A549 lung cancer cells were seeded at a density of 2.5×10^3 cells per well in 90 μ L DMEM growth media supplemented with 10% FBS and 2% penicillin/streptomycin in a 96-well culture dish. The cells were allowed to attach overnight and the following day 10 μ L of 2-fold dilutions (0 - 200 μ M) of the flavonol in DMSO (0.2 % v/v) was added in triplicate to the cells and incubated for 48h. Thereafter, 10 μ L of 5 mg/mL 3-(4,5-Dimethylthiazol-2-yl)-2,5-diphenyltetrazolium bromide (MTT) (Sigma- Aldrich) was added and incubated with the cells for 4 h. The resulting formazan crystals were solubilised by adding 100 μ L of 10 % sodium dodecyl sulphate (Sigma-Aldrich) to each well and incubating overnight at 37 °C. The absorbance at 595 nm was measured using a Multiskan FC multi-well reader and the data was fitted using Graphpad prism v5 using log(inhibitor) vs response (variable slope) from which a cytotoxicity IC_{50} value was obtained. All compounds were tested independently multiple times from which an average value and standard deviation was obtained.

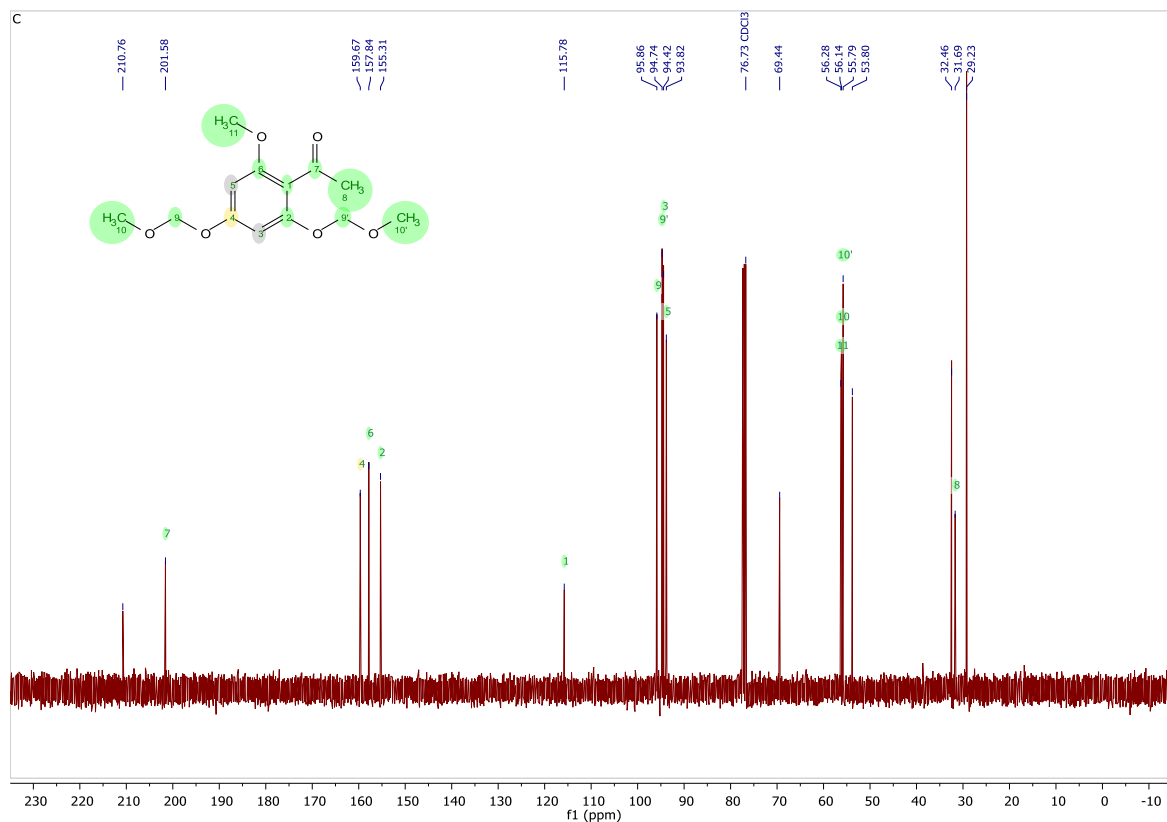
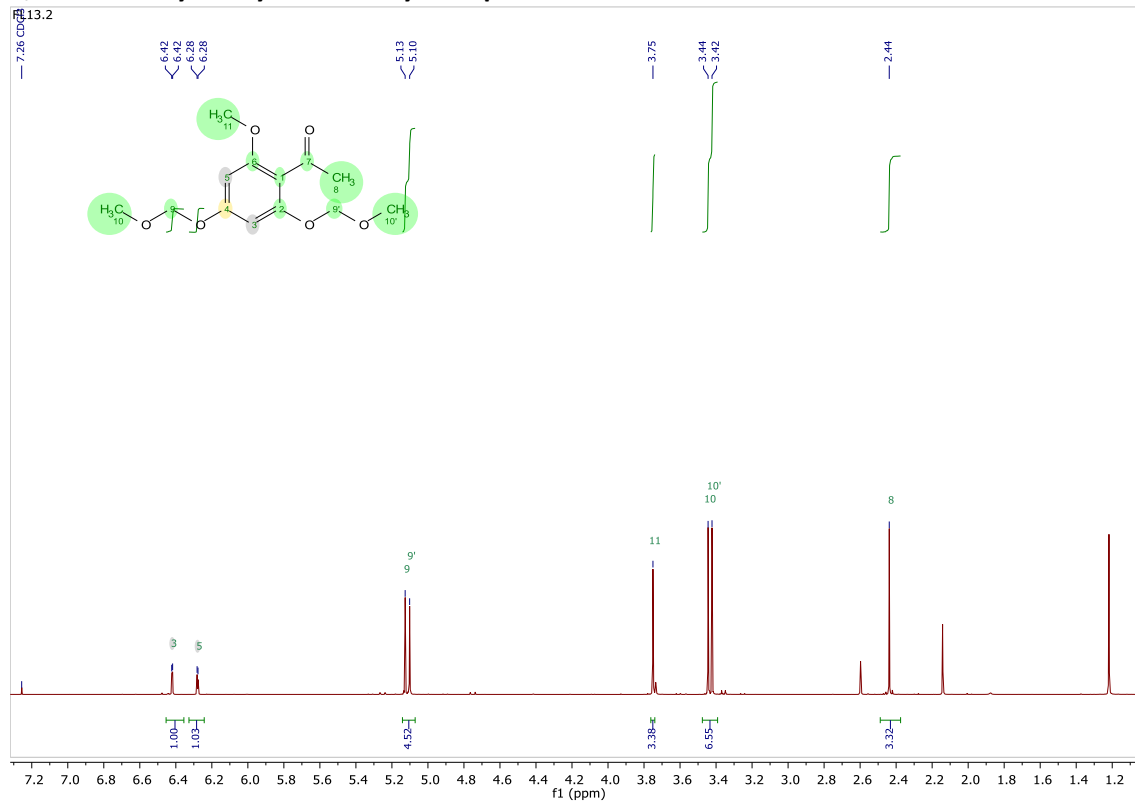
CONFOCAL MICROSCOPY

Cells were plated on chamber cover glass at a cell density of 15 000 cells/well and allowed to settle for 18 h. Cells were then treated with a stock solution of the compound being investigated in DMSO to give a final concentration of 0.1% DMSO in cells. The cells were then incubated overnight with the compound of interest. Live tracking dyes were then added to the cells half an hour prior to imaging on the confocal microscope, Zeiss LSM880 Airyscan with Fast Airyscan Module. Images and colocalization studies were performed using ZEN Black SP2.3 software. Excitation of the fluorophores was achieved using either a 405 nm DAPIlaser with a spectral emission filter tuning between 410 – 500 nm or a 561 nm solid state laser tuned between 570 – 640 nm. For viewing in wildfield epifluorescence mode a Xenon 120 UV lamp, DAPI, and CY3 filter was utilised.

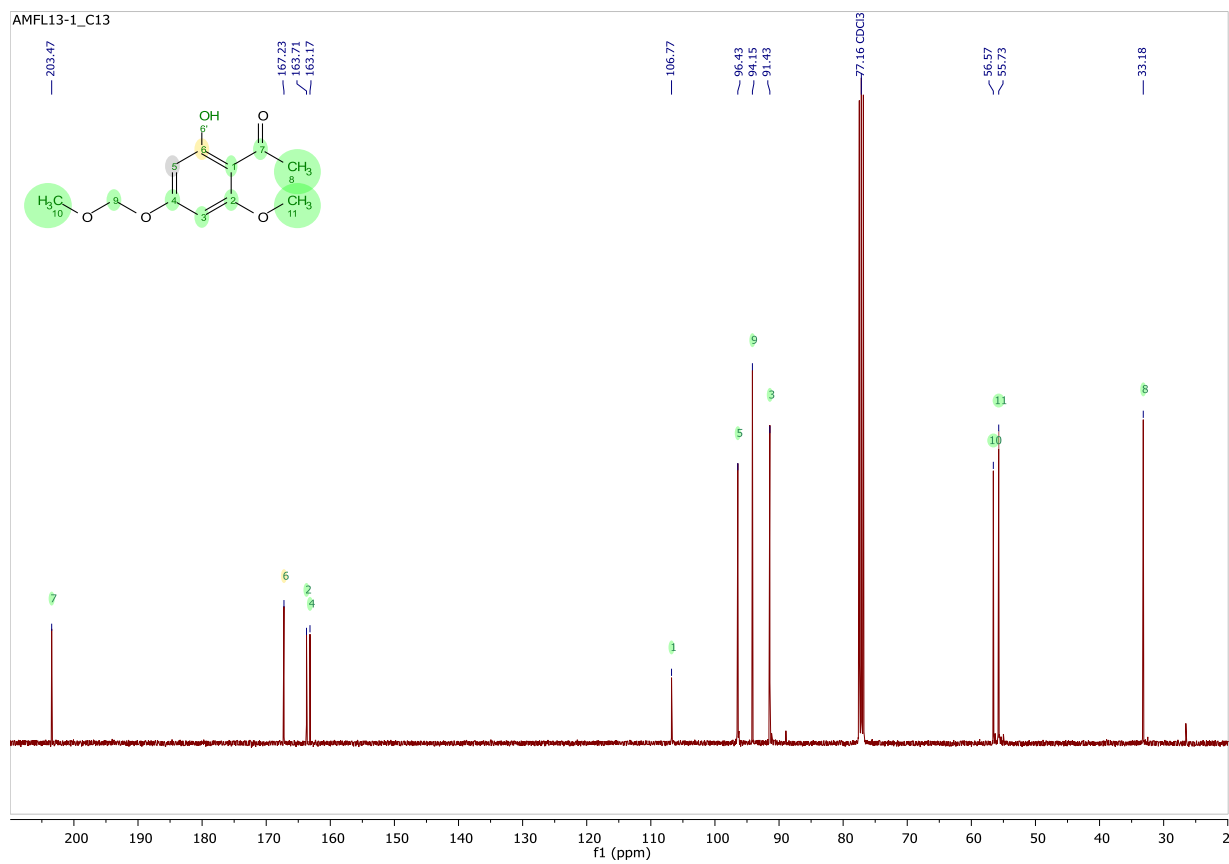
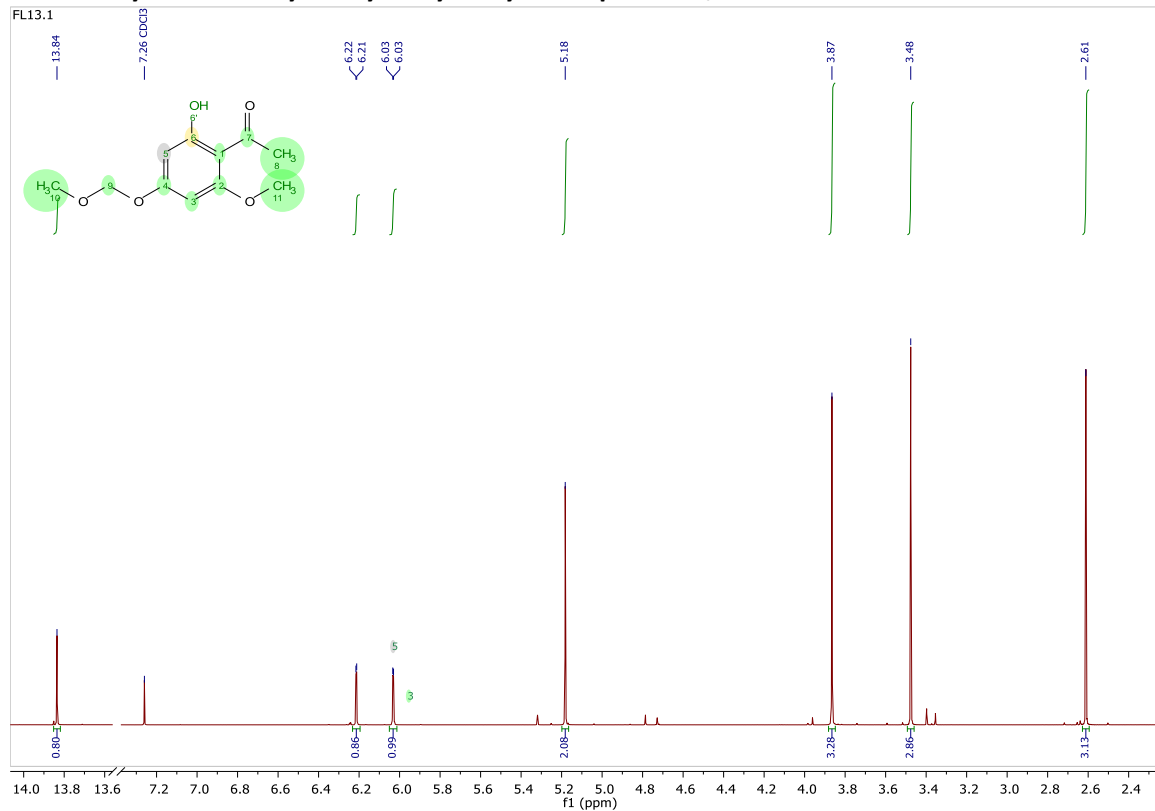
SYNTHESIS AND IMAGING OF FLUORESCENT DIETARY COMPOUND ANALOGUES

2, 4-Dimethoxymethyl-6-hydroxyacetophenone

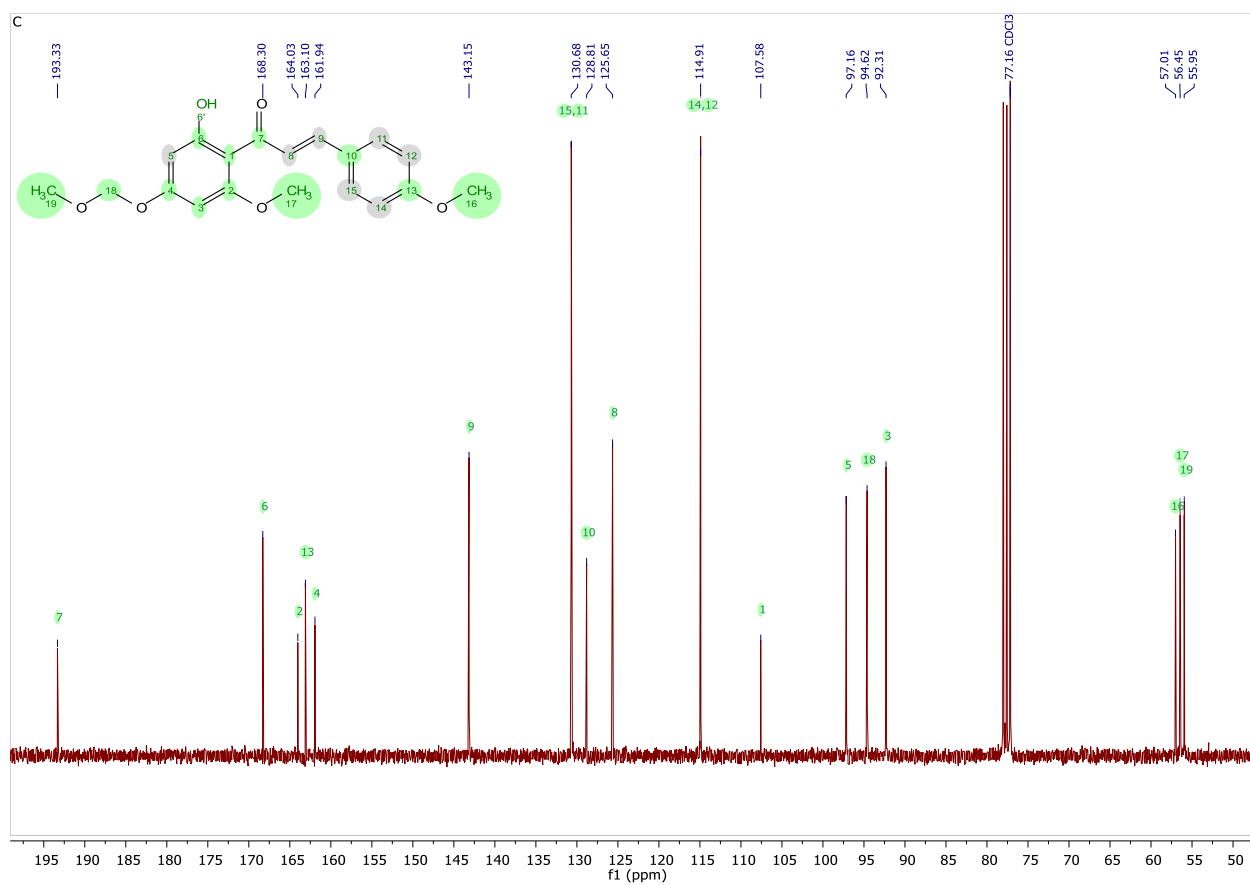
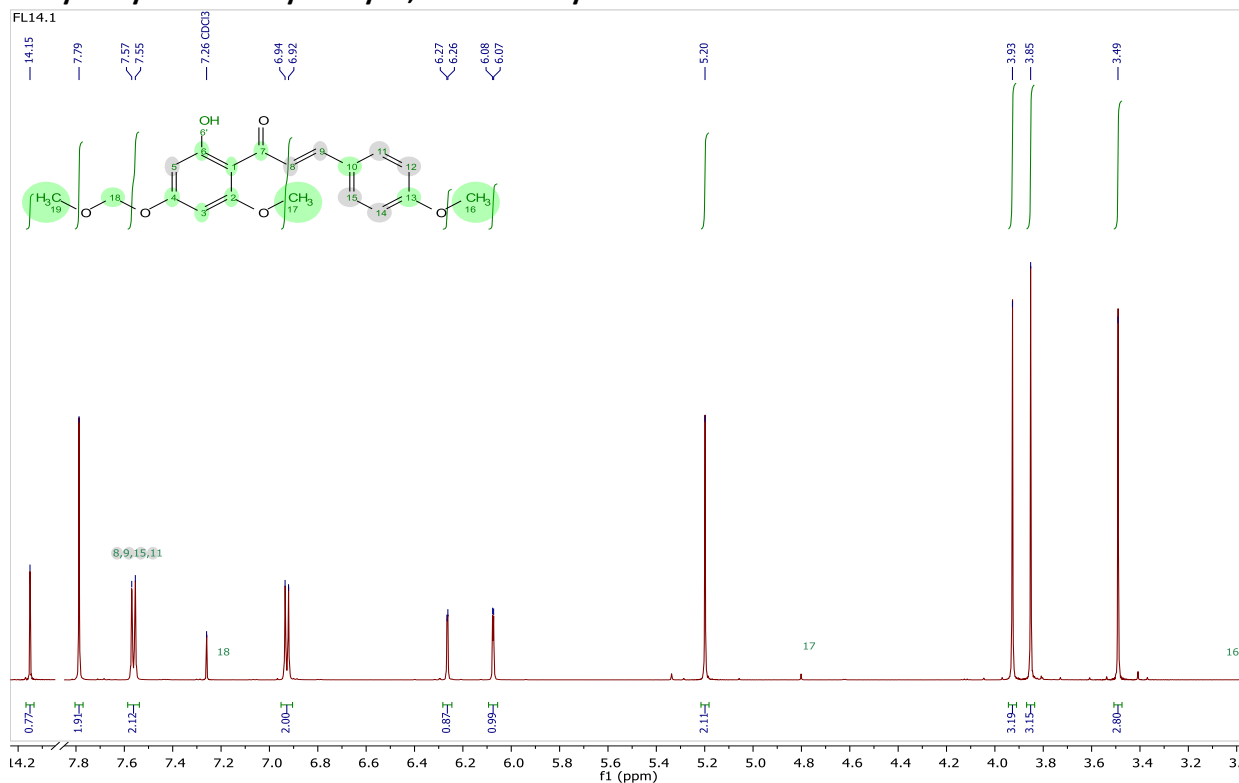
2,4-Dimethoxymethyl-6-methoxyacetophenone



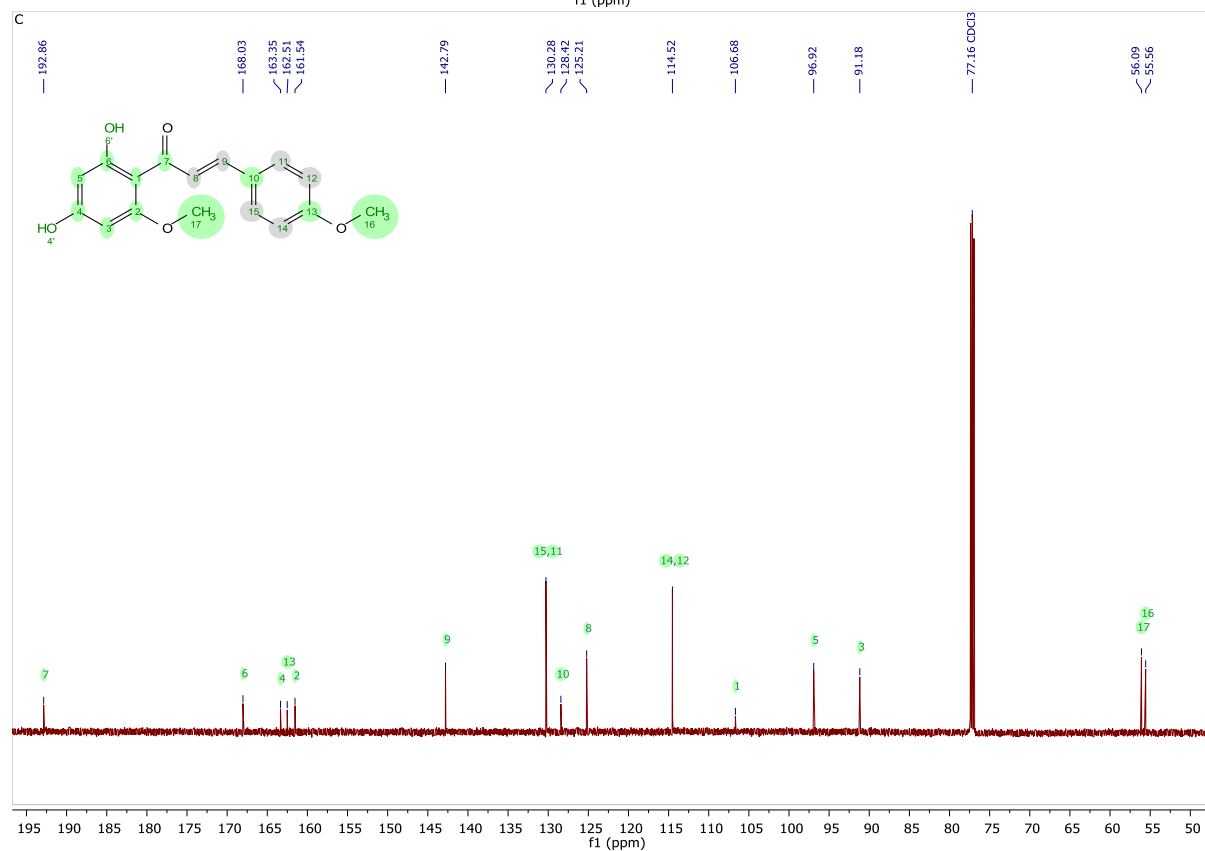
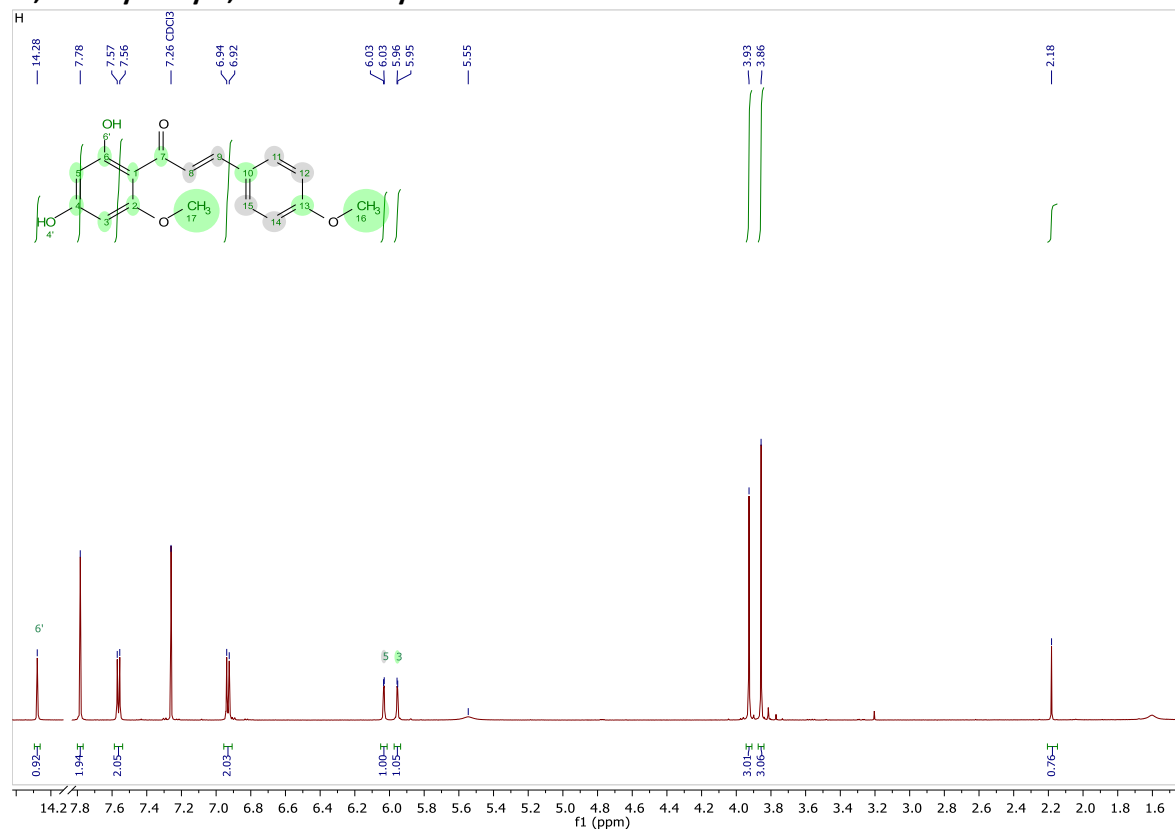
2-Methoxy-4-methoxymethyl-6-hydroxyl acetophenone,



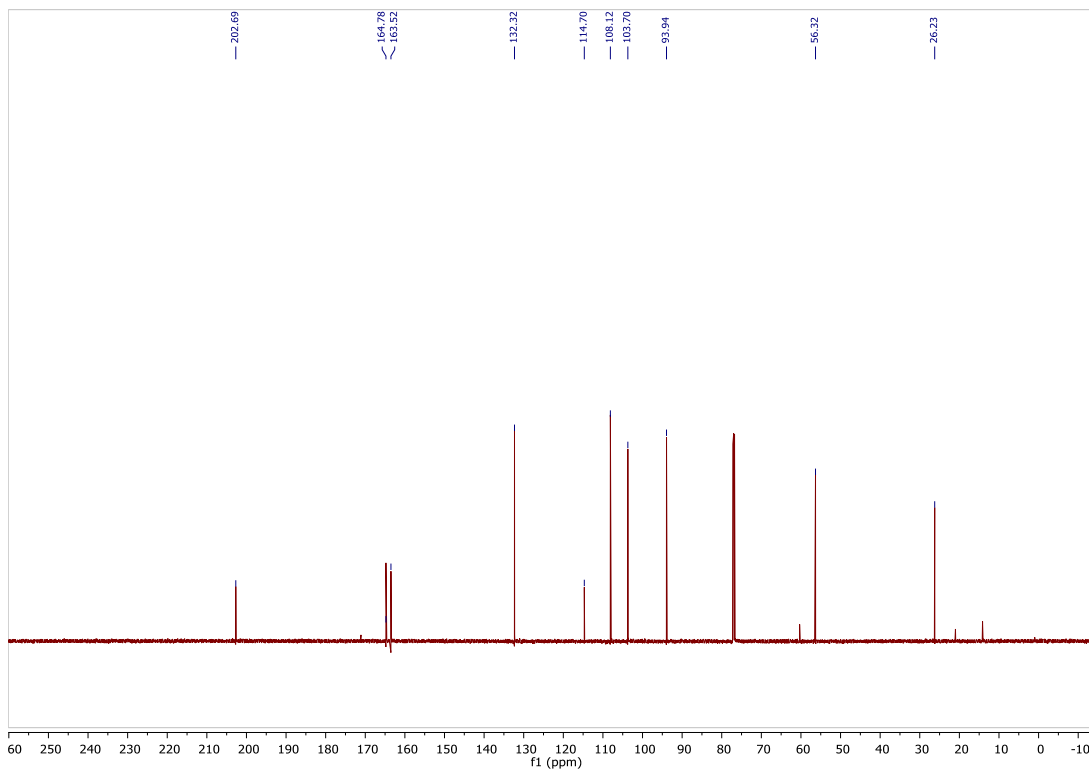
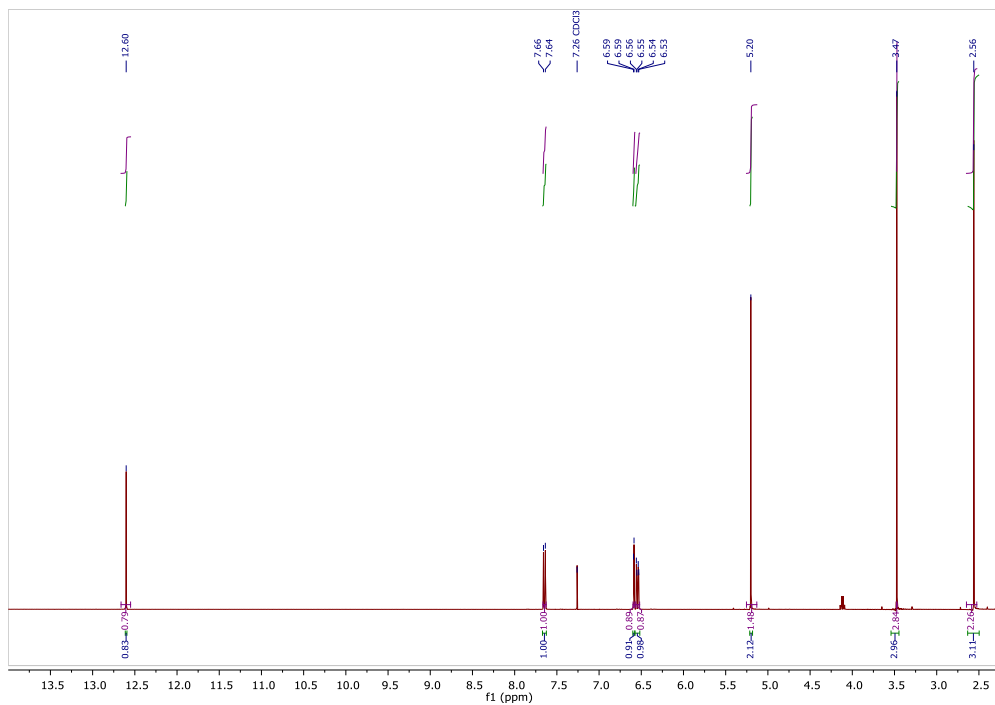
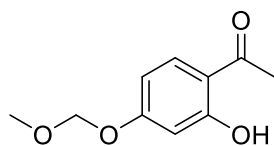
2'-Hydroxyl-4'-methoxymethyl-4, 6'-dimethoxy chalcone

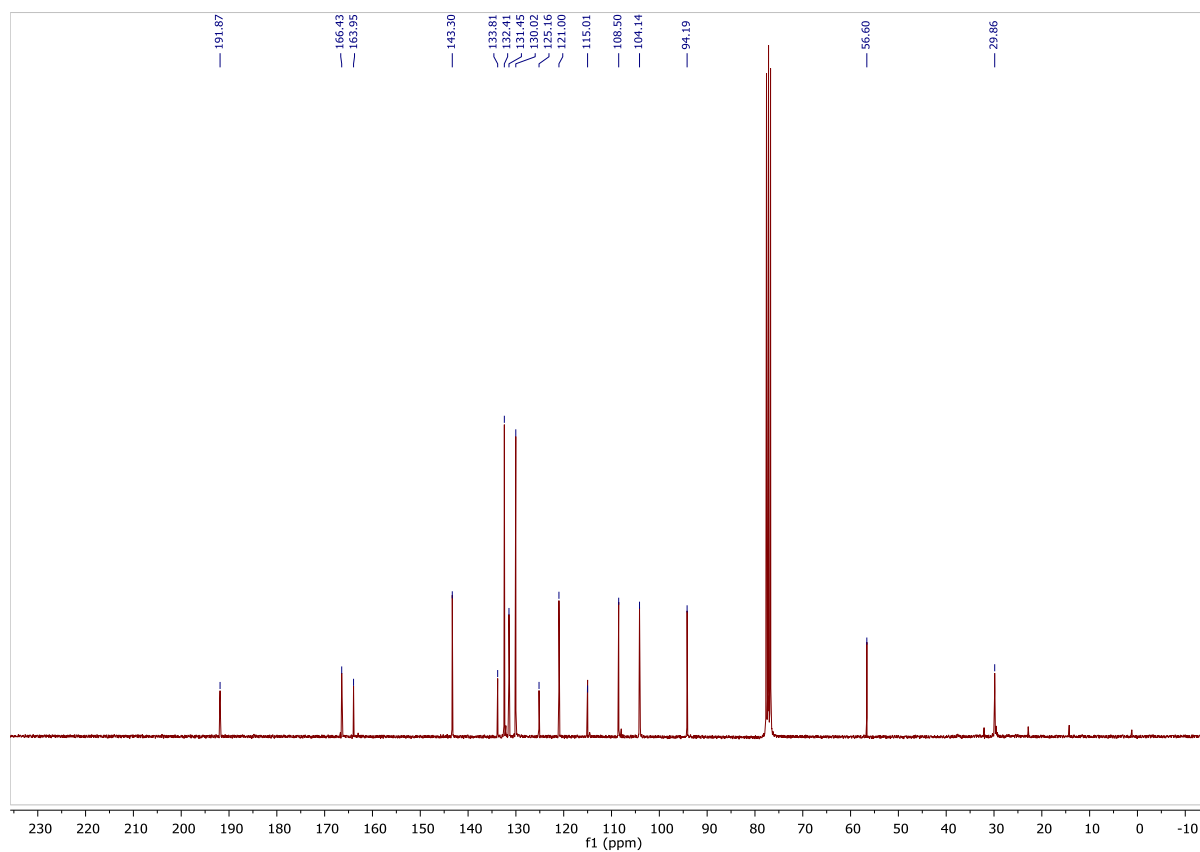
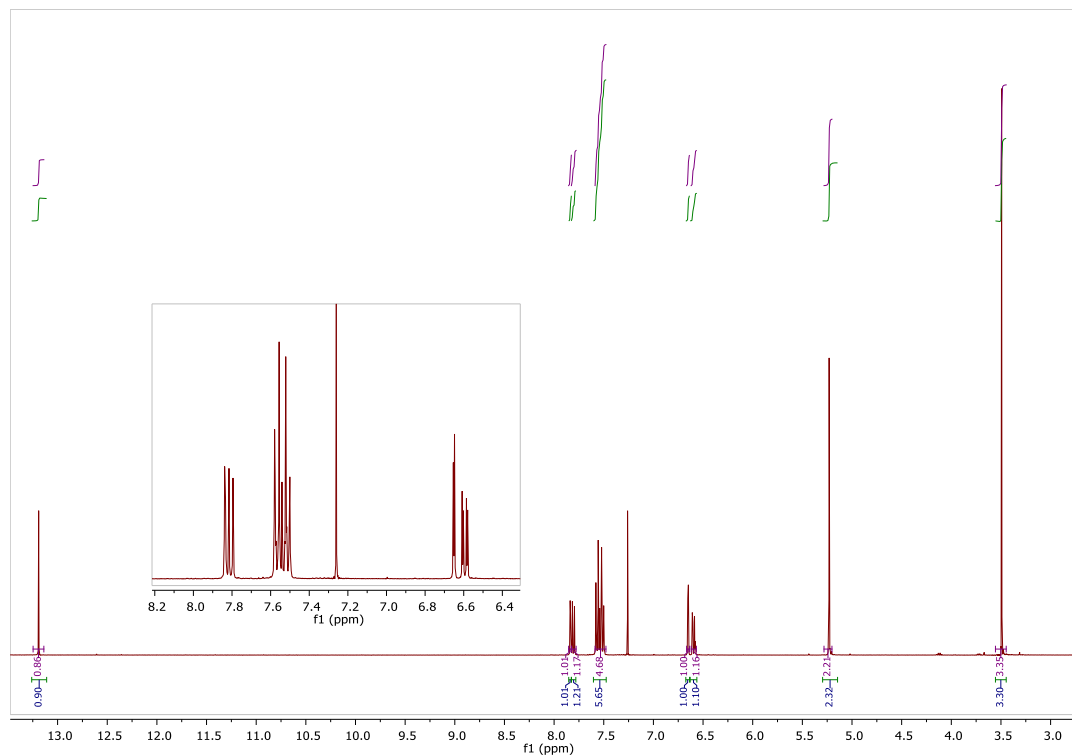
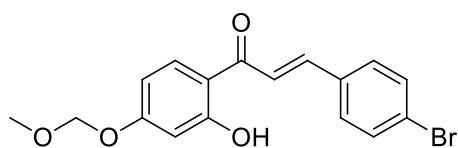


2', 4'-Dihydroxy-4, 6'-dimethoxy chalcone

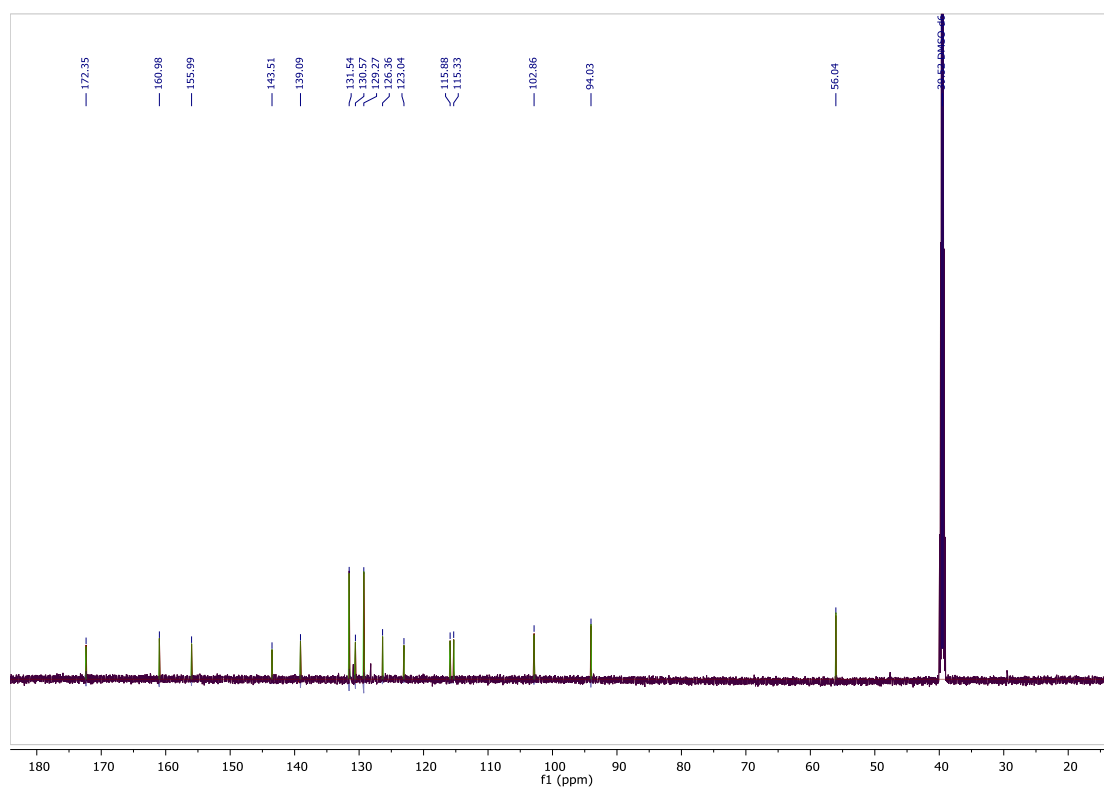
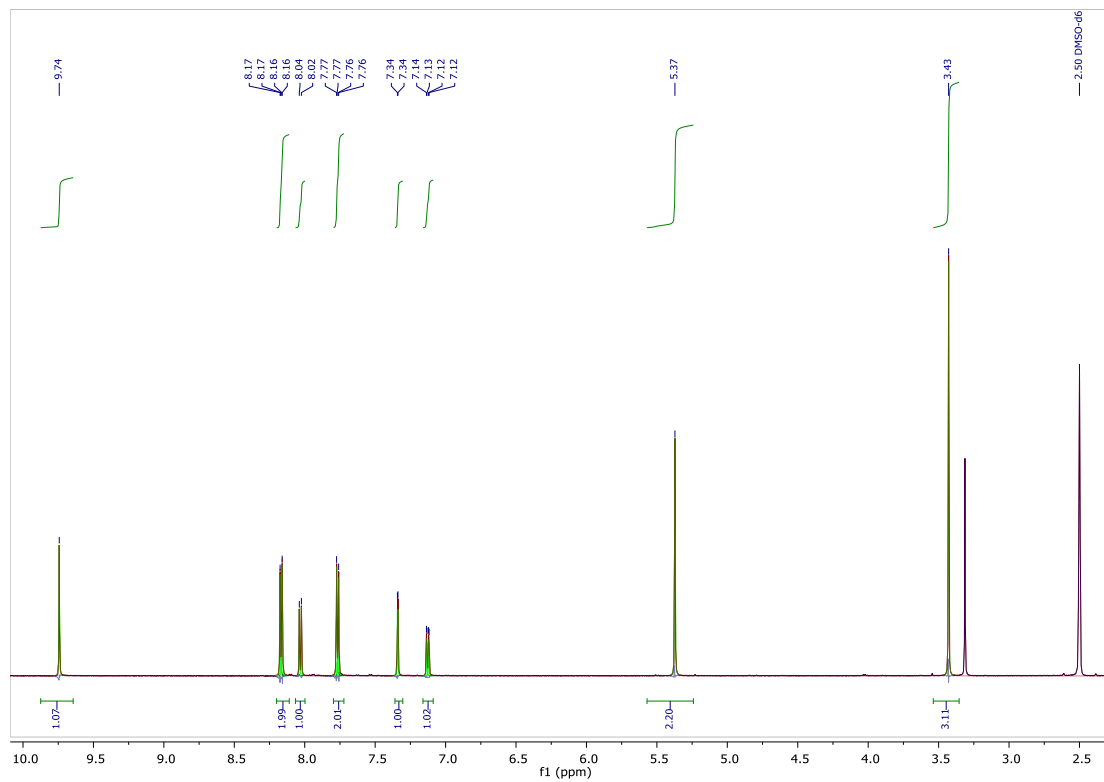
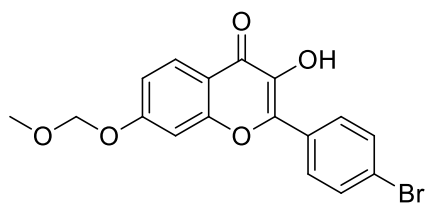


1-[2-hydroxy-4-(methoxymethoxy)phenyl]ethan-1-one

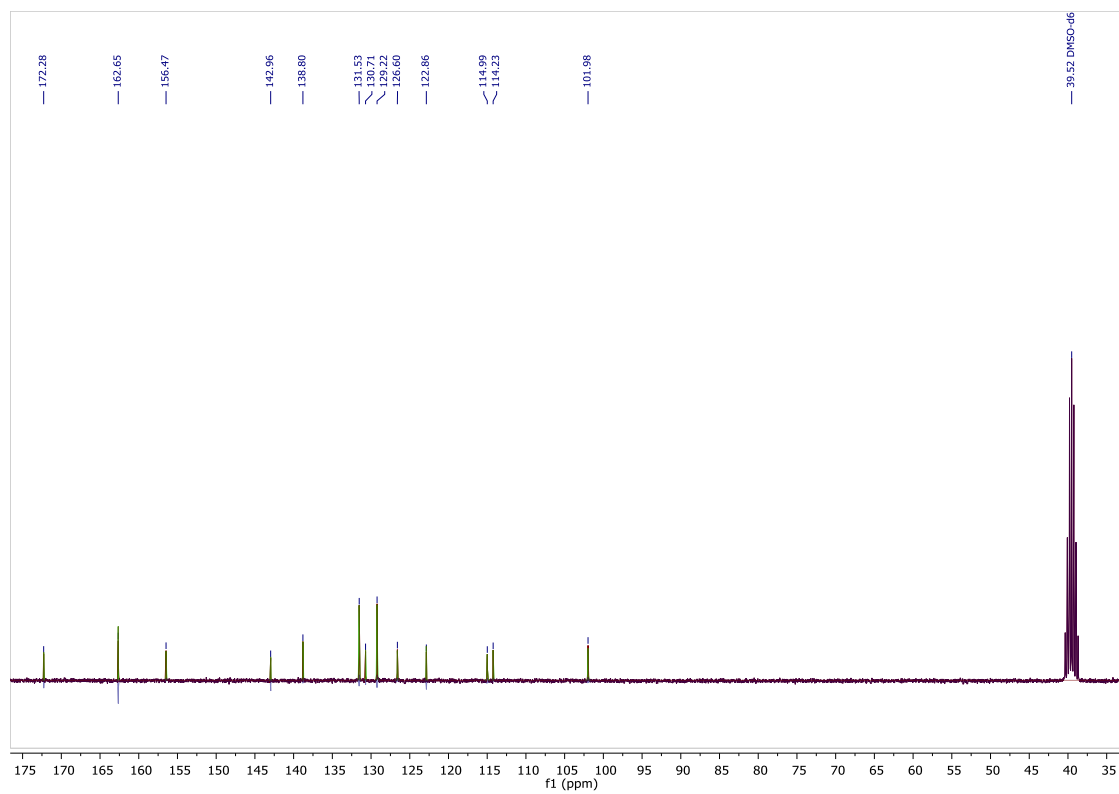
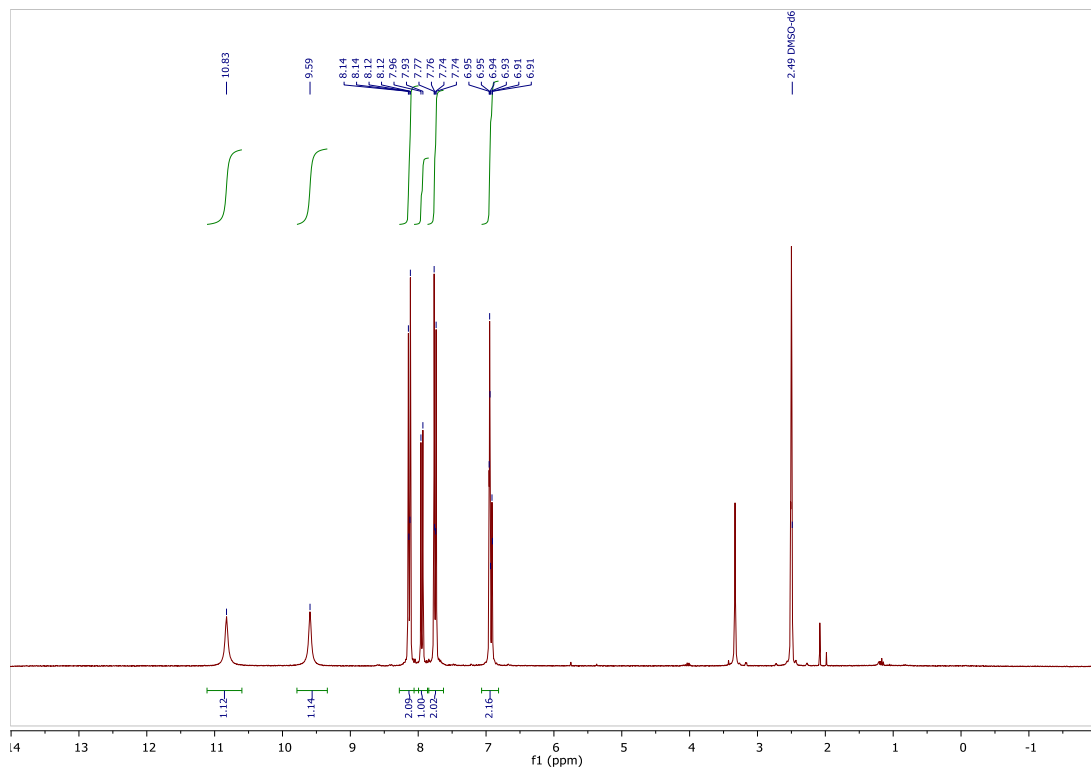
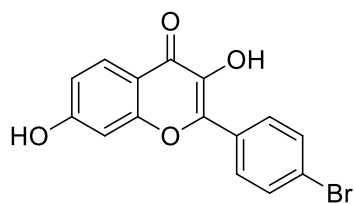


(E)-3-(4-bromophenyl)-1-[2-hydroxy-4-(methoxymethoxy)phenyl]prop-2-en-1-one

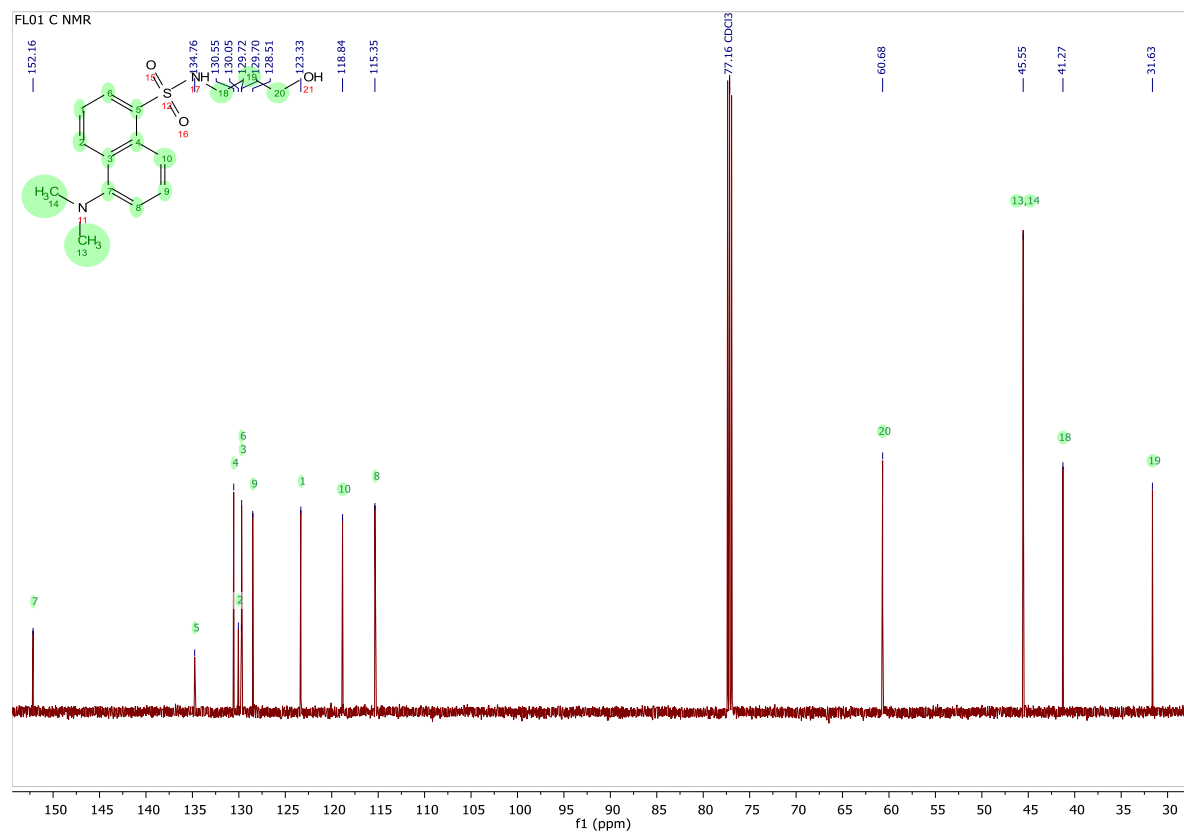
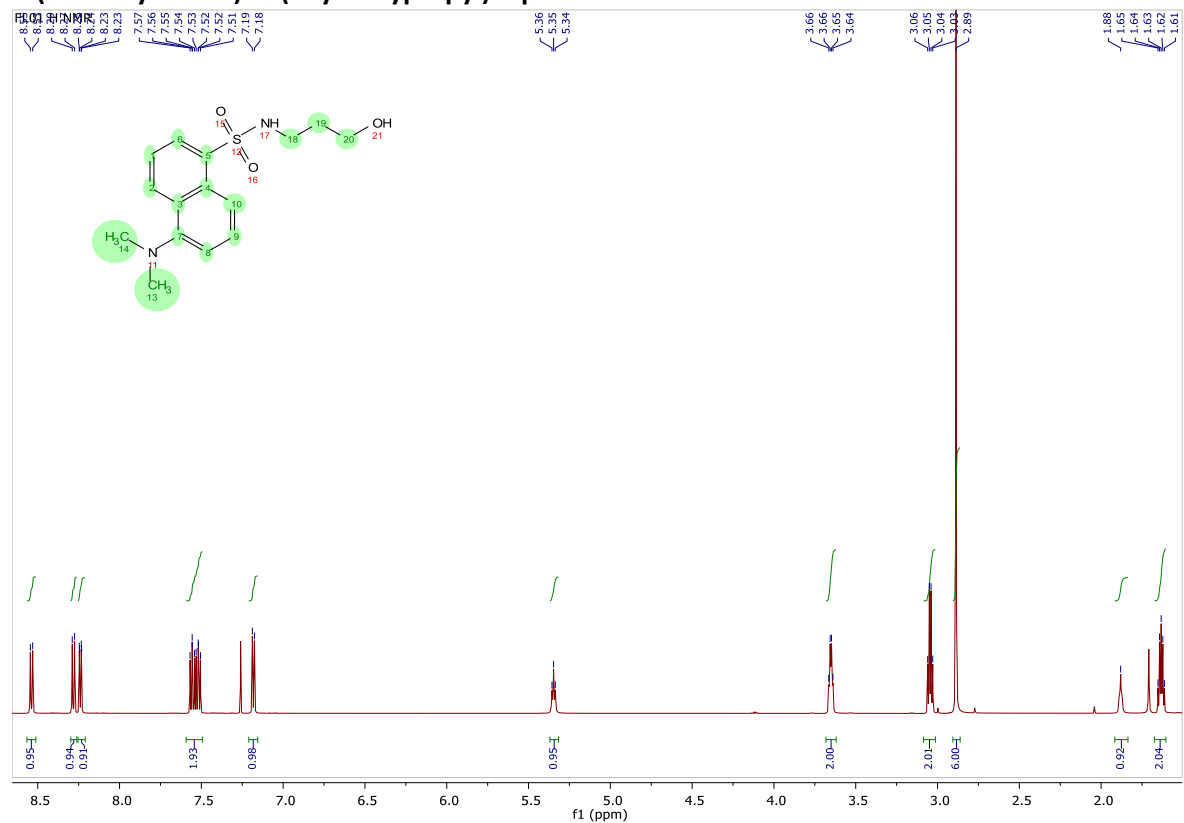
2-(4-bromophenyl)-3-hydroxy-7-(methoxymethoxy)-4H-chromen-4-one



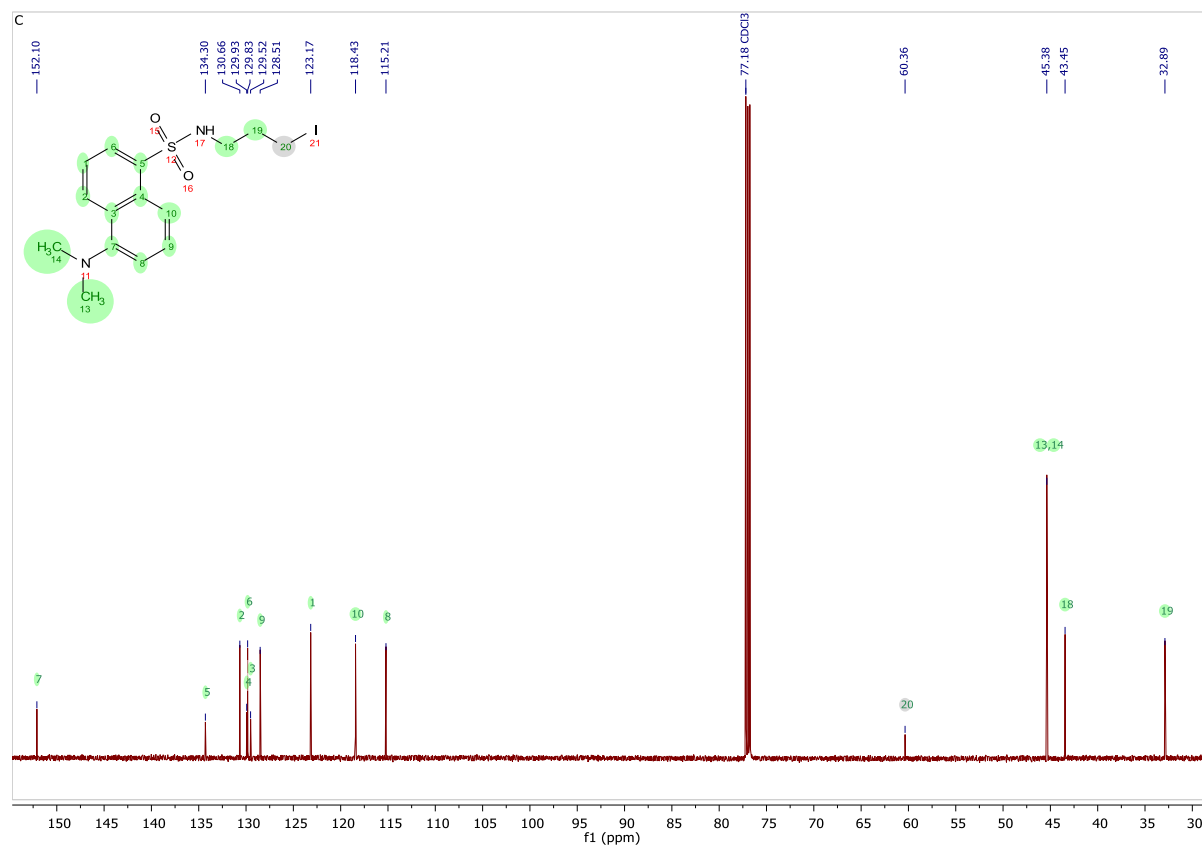
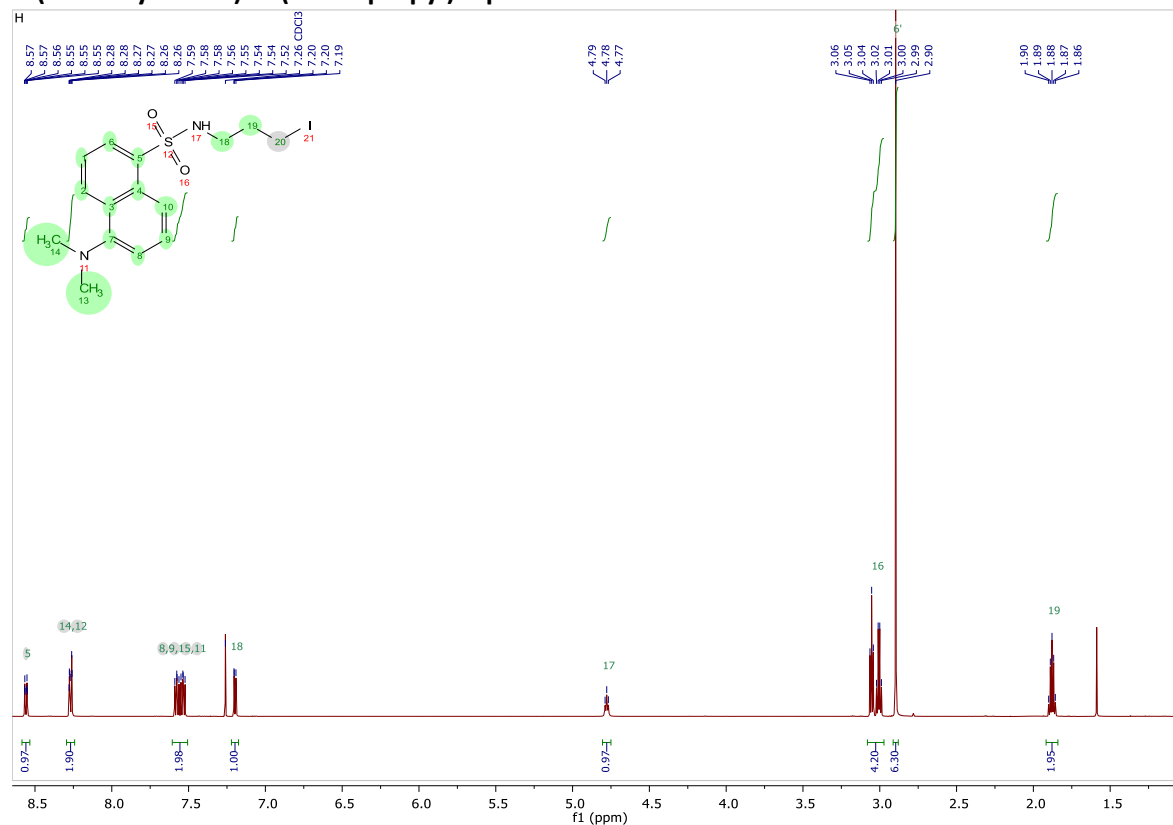
2-(4-bromophenyl)-3,7-dihydroxy-4H-chromen-4-one



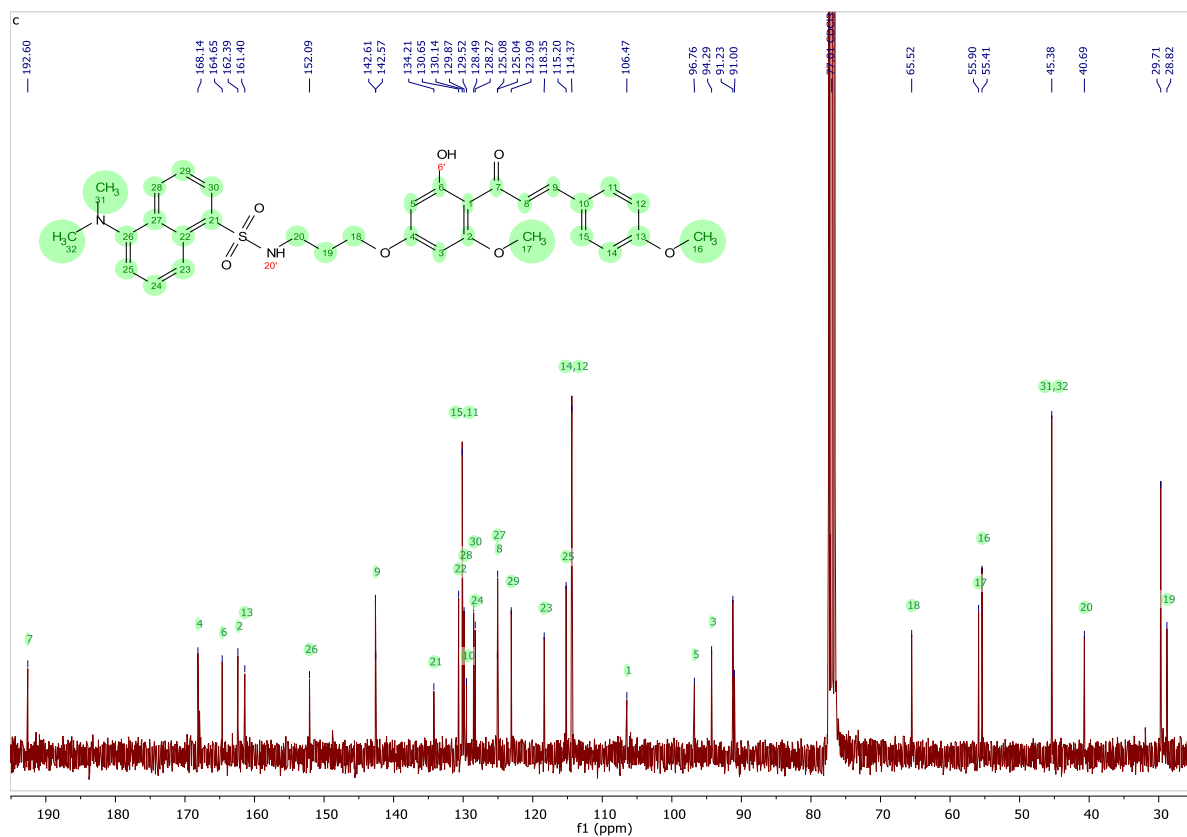
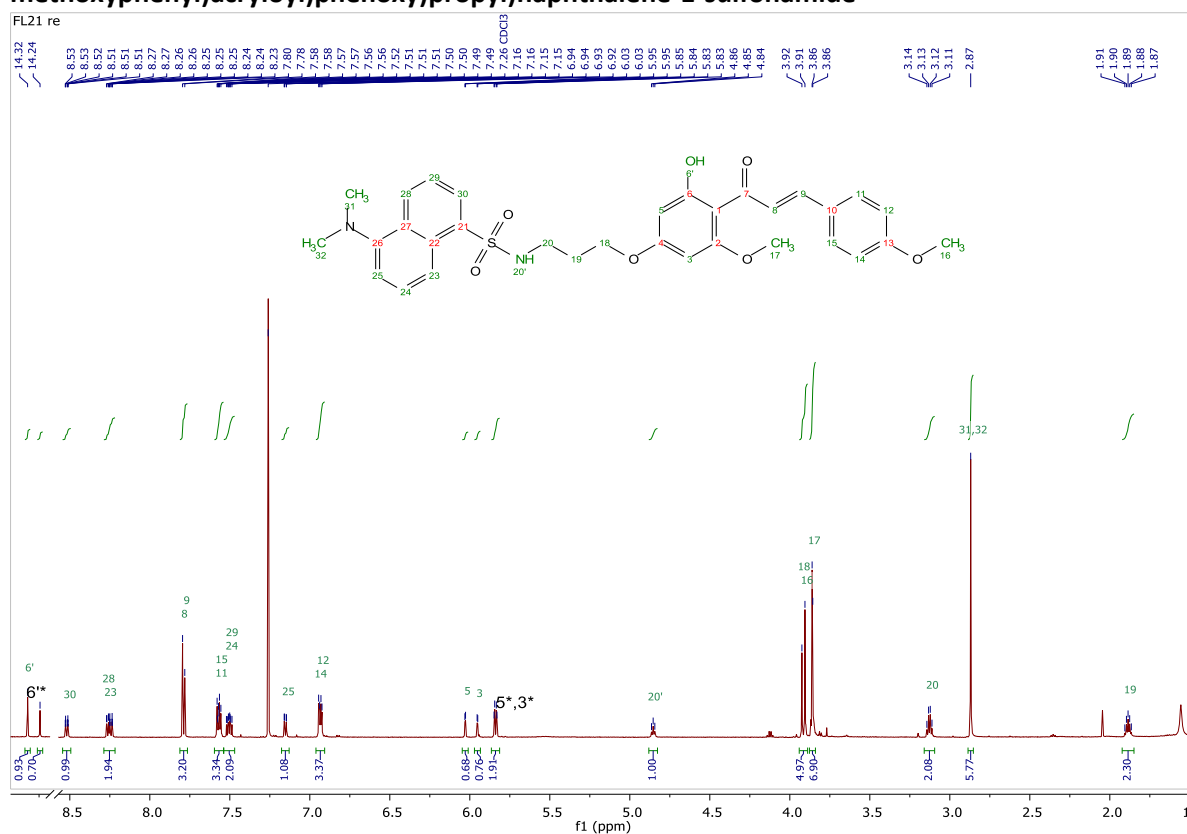
5-(Dimethylamino)-N-(3hydroxypropyl)naphthalene-1-sulfonamide



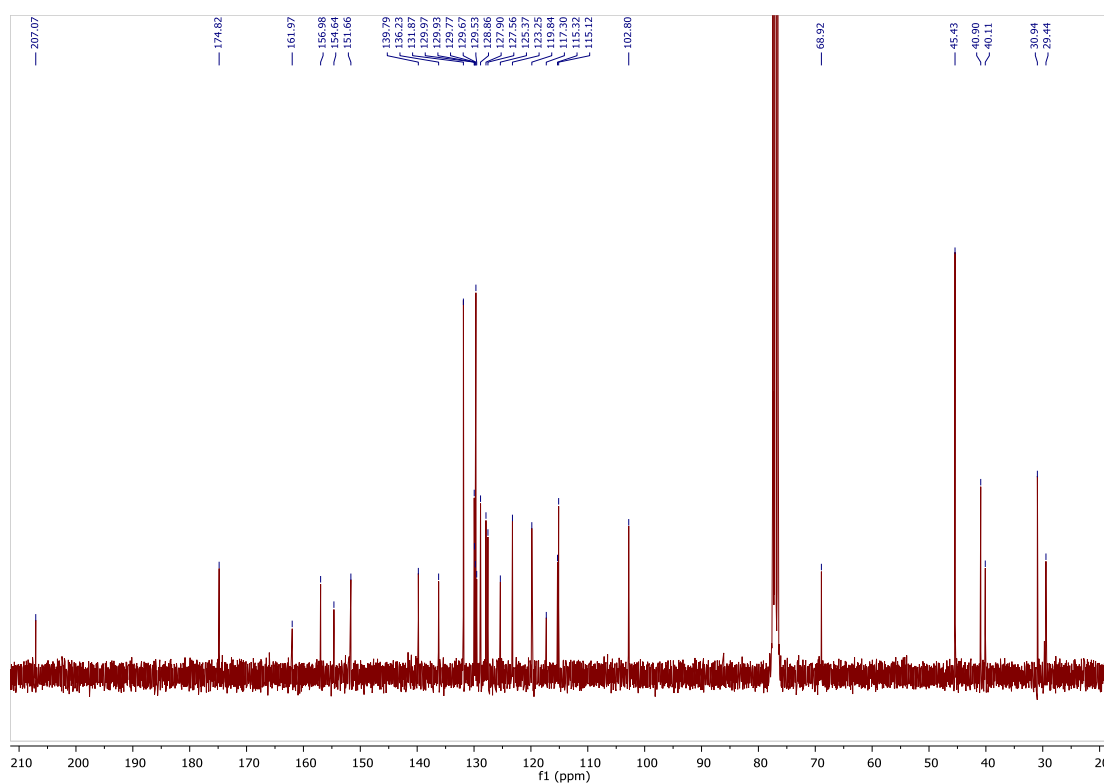
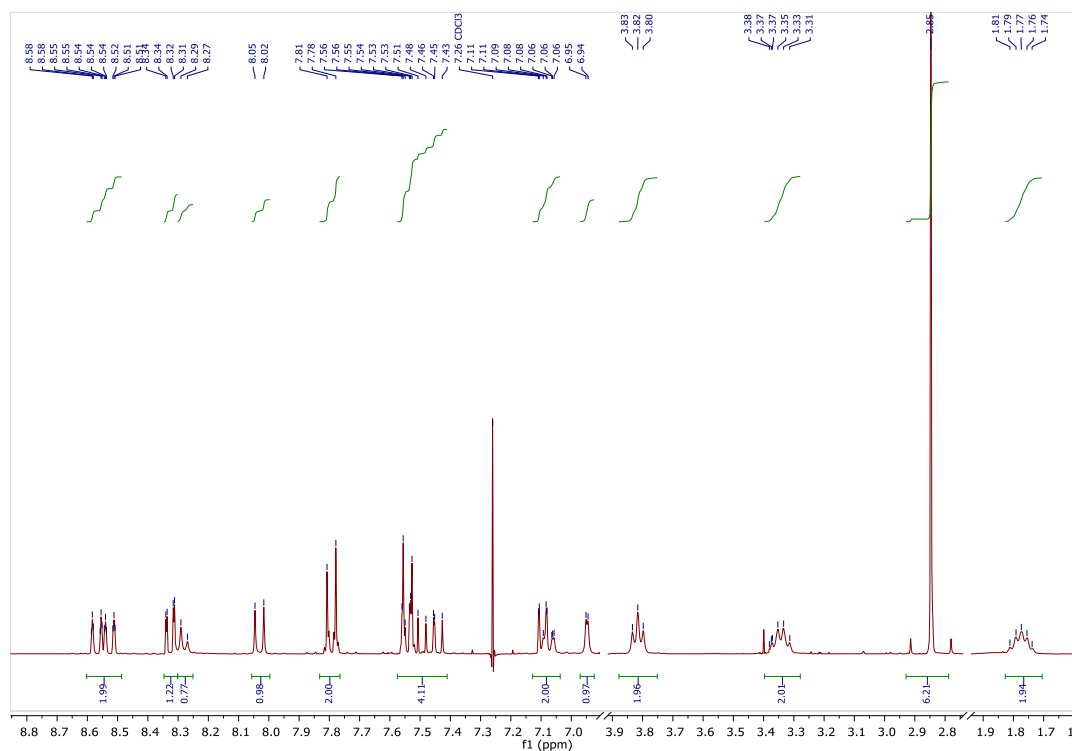
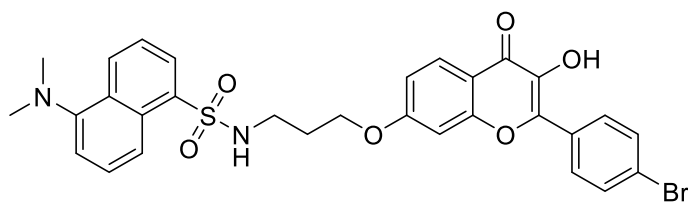
5-(Dimethylamino)-N-(3-iodopropyl)naphthalene-1-sulfonamide



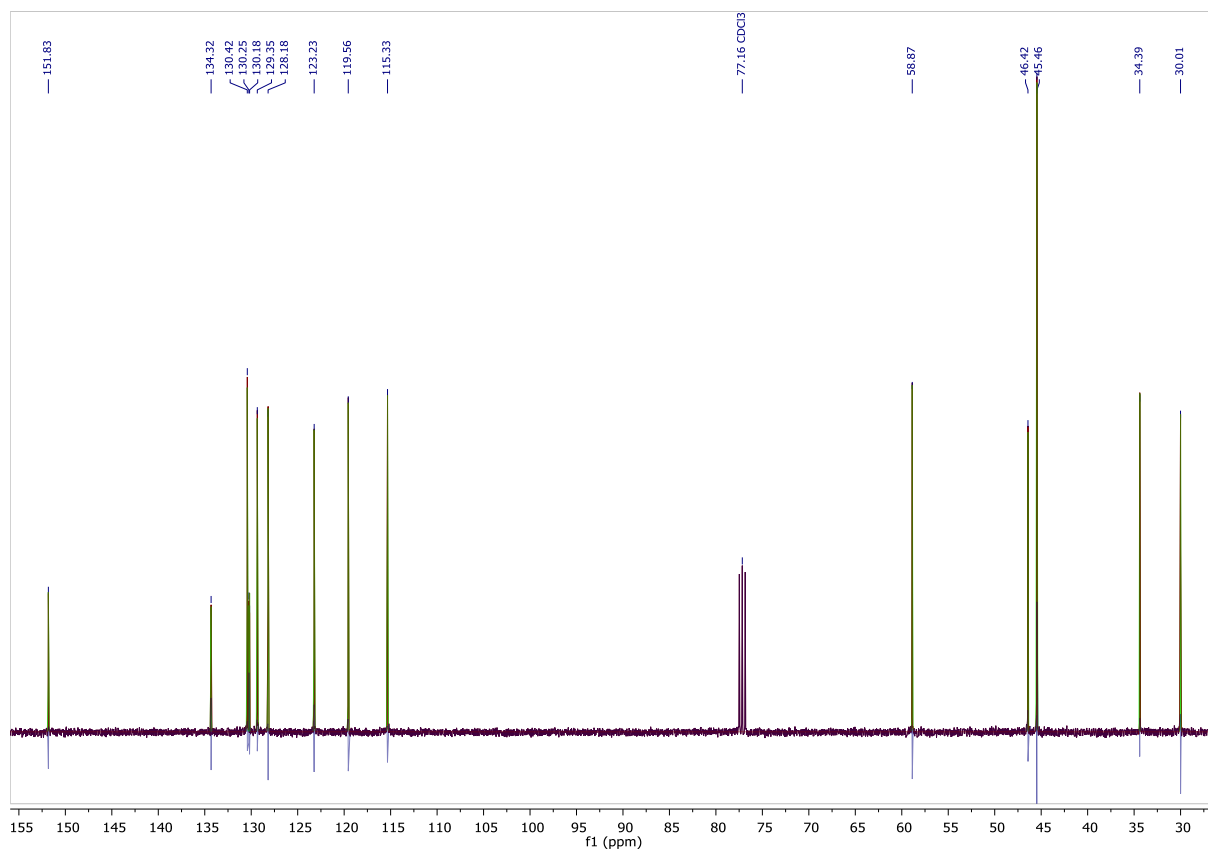
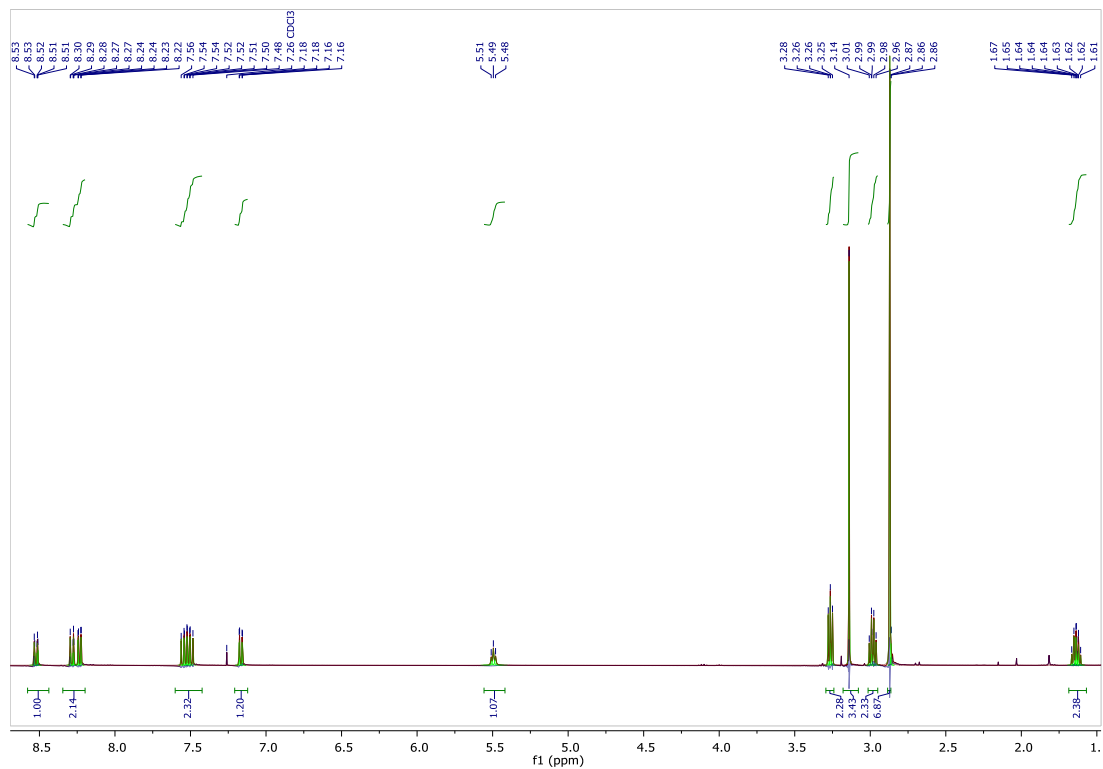
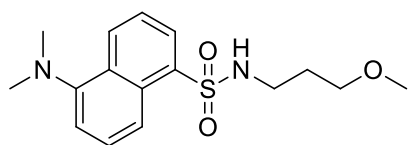
(E)-5-(dimethylamino)-N-(3-(3-hydroxy-5-methoxy-4-(3-(4-methoxyphenoxy)acryloyl)phenoxy)propyl)naphthalene-1-sulfonamide



N-{3-[(2-(4-bromophenyl)-3-hydroxy-4-oxo-4H-chromen-7-yl)oxy]propyl}-5-(dimethylamino)naphthalene-1-sulfonamide

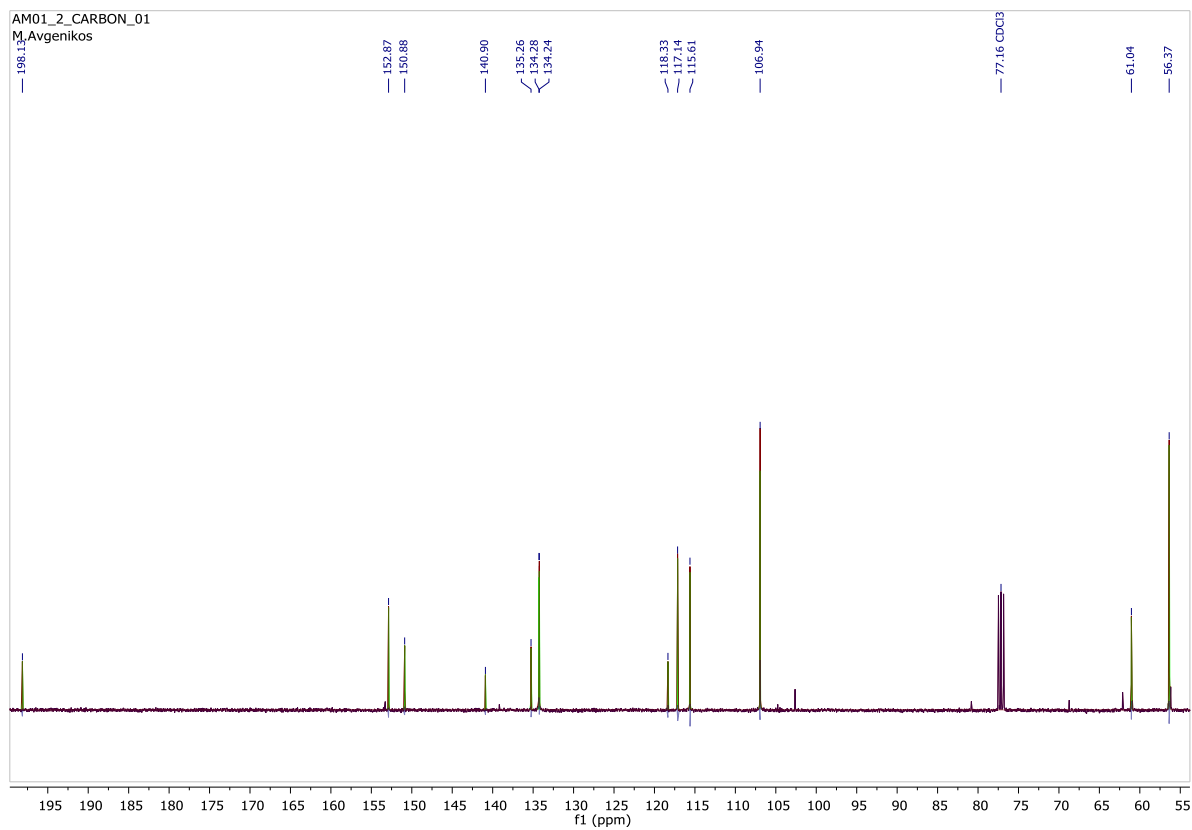
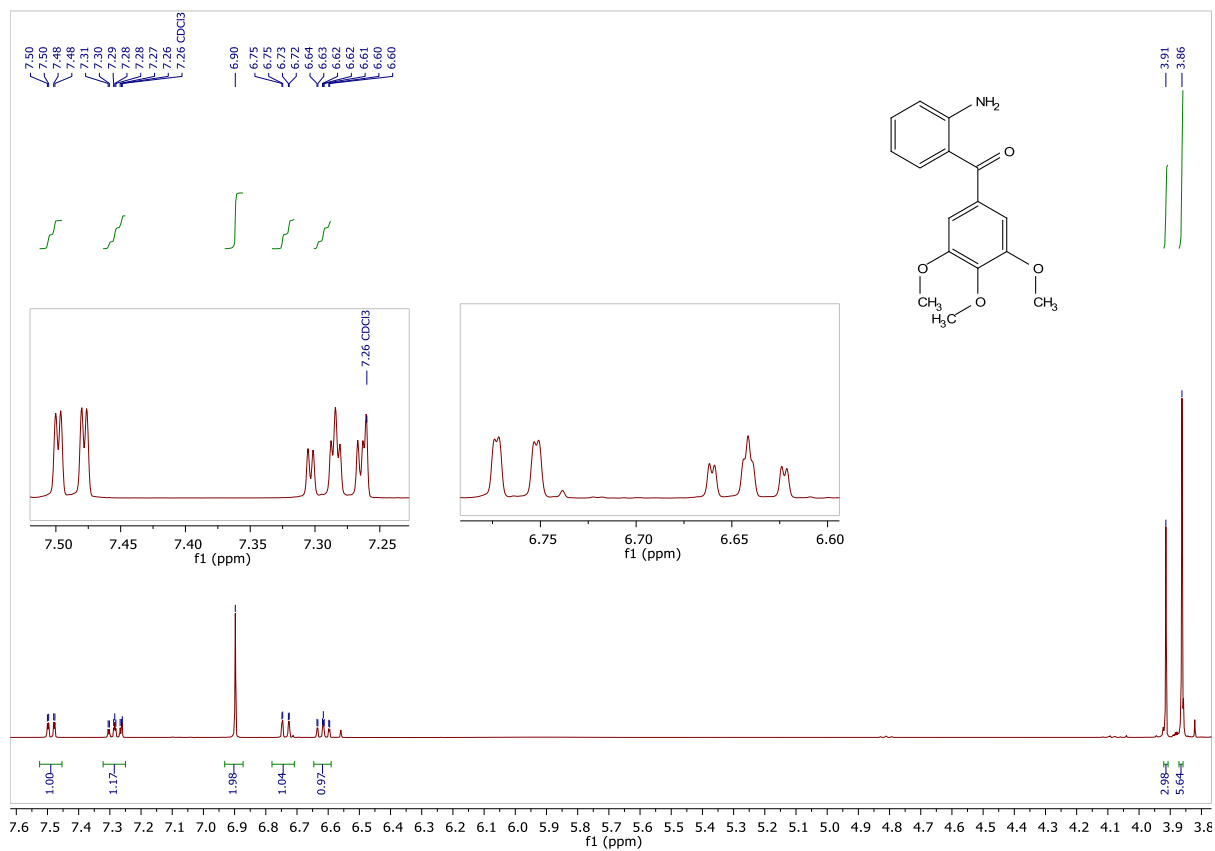


5-(dimethylamino)-N-(3-methoxypropyl)naphthalene-1-sulfonamide

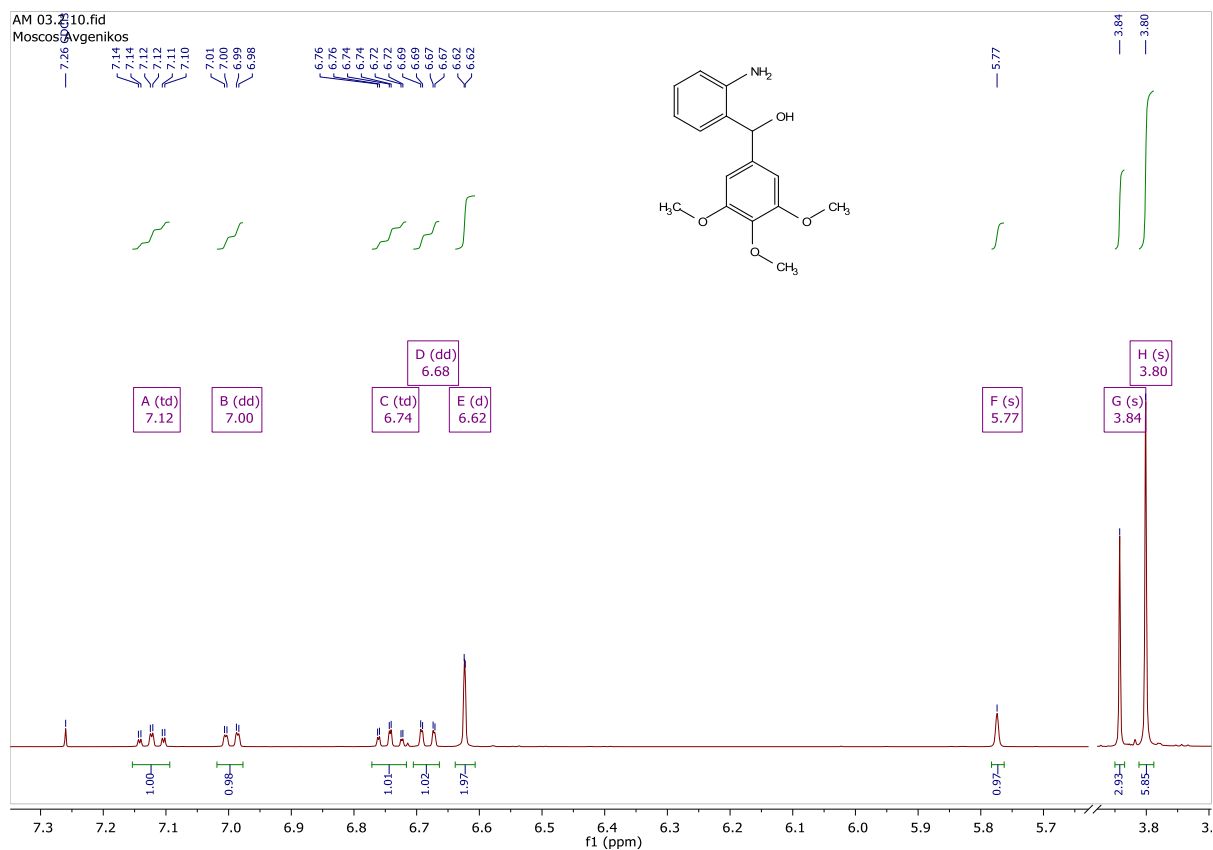
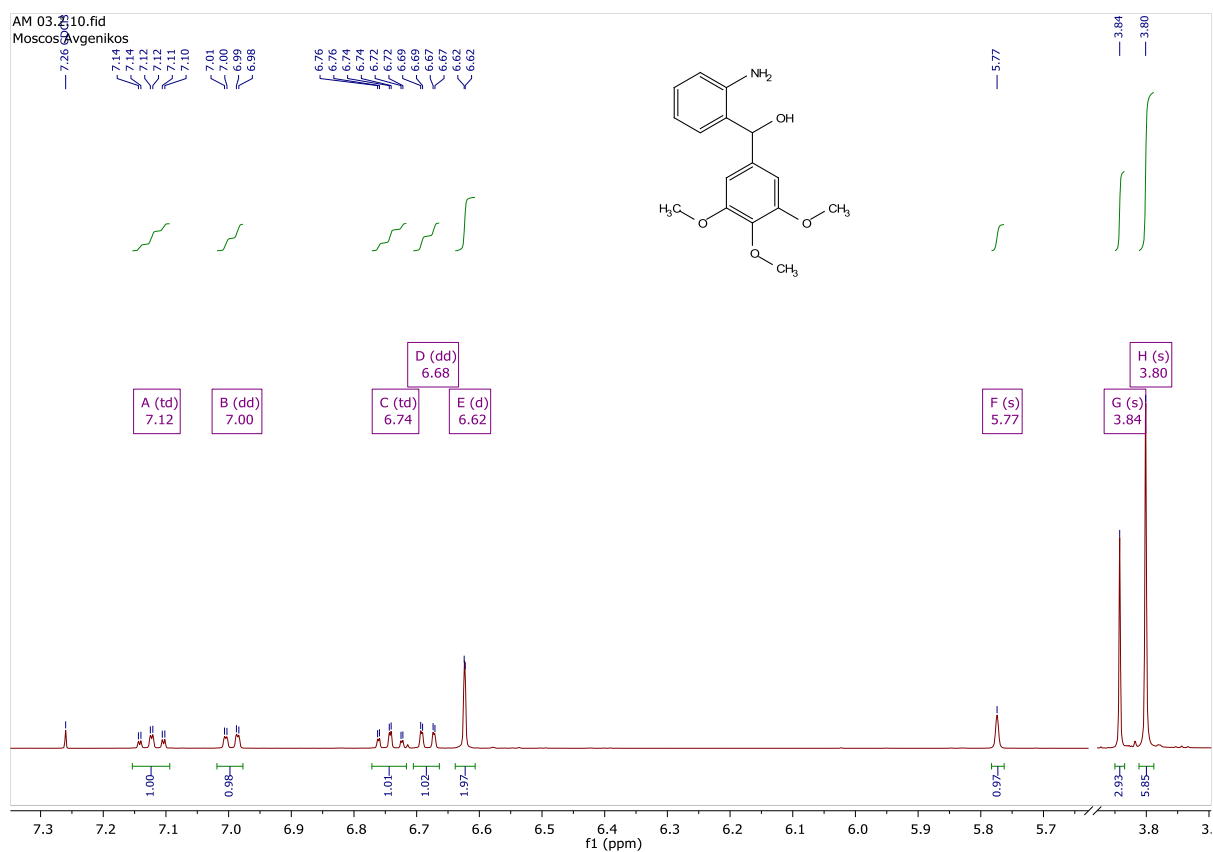


TOWARDS A BRONSTED ACID CATALYSED ENANTIOSELECTIVE SYNTHESIS OF 4-AZA- PODOPHYLOTOXIN

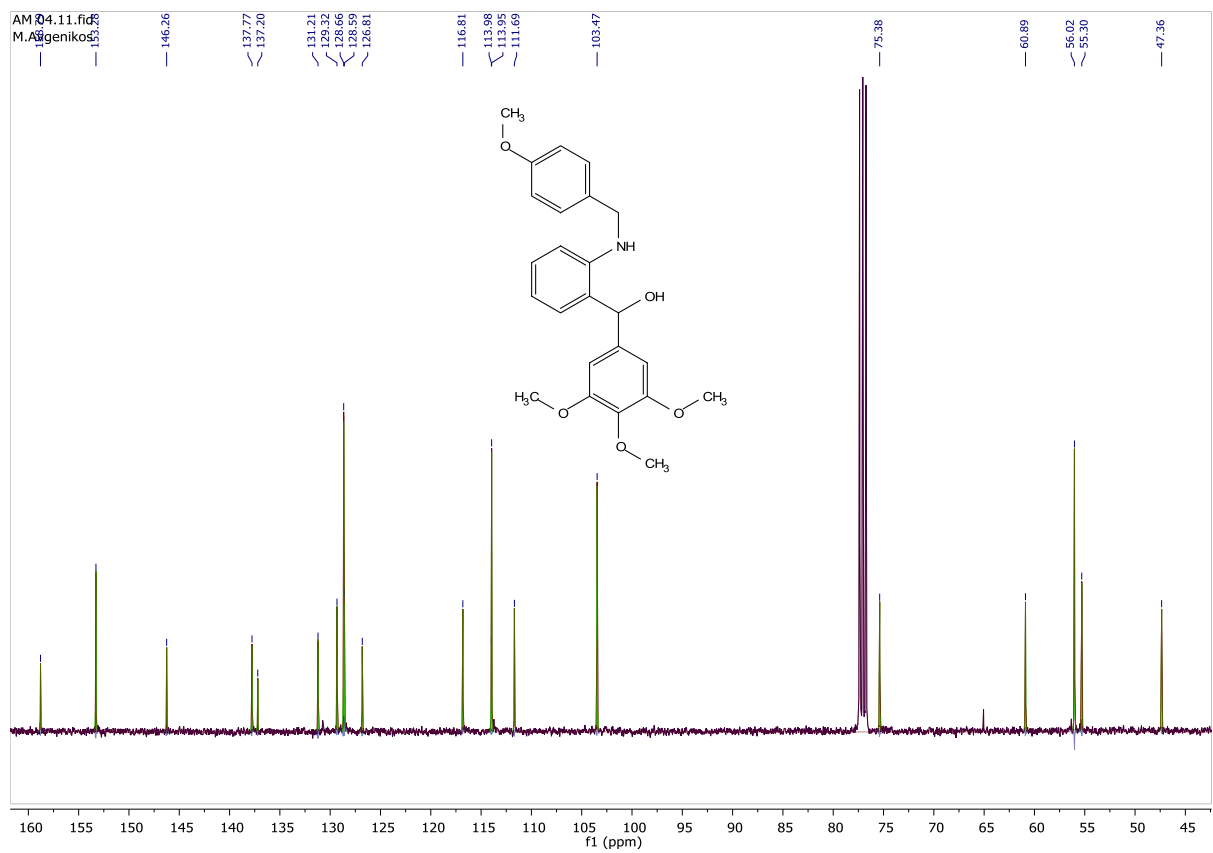
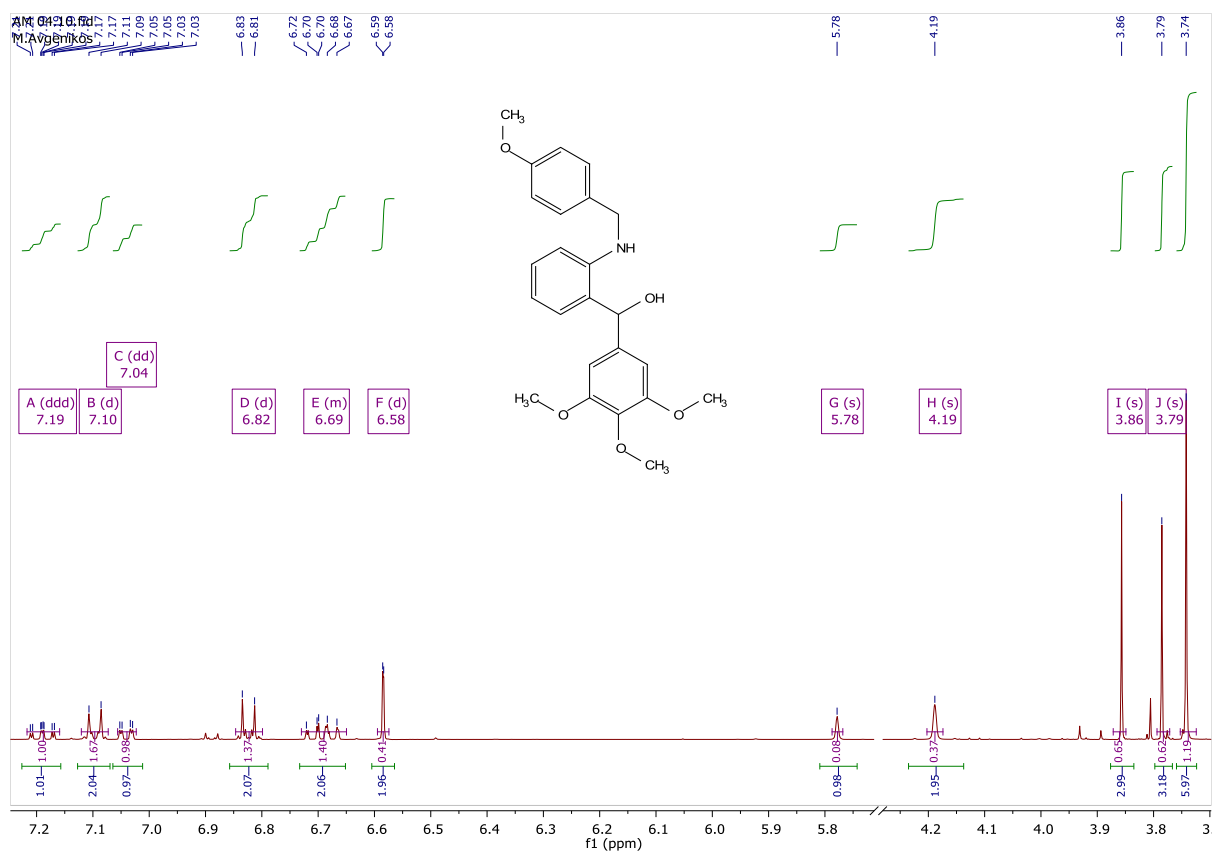
(2-aminophenyl)(3,4,5-trimethoxyphenyl)methanone



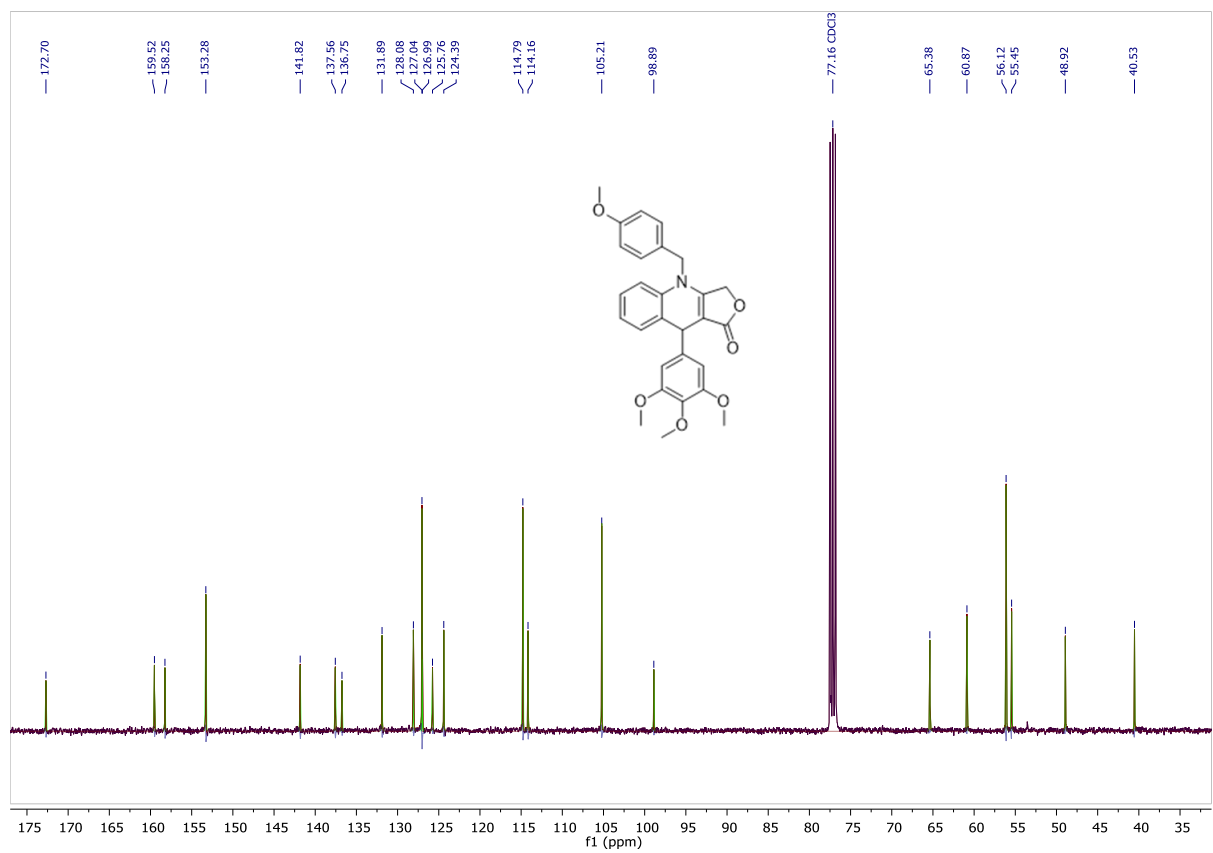
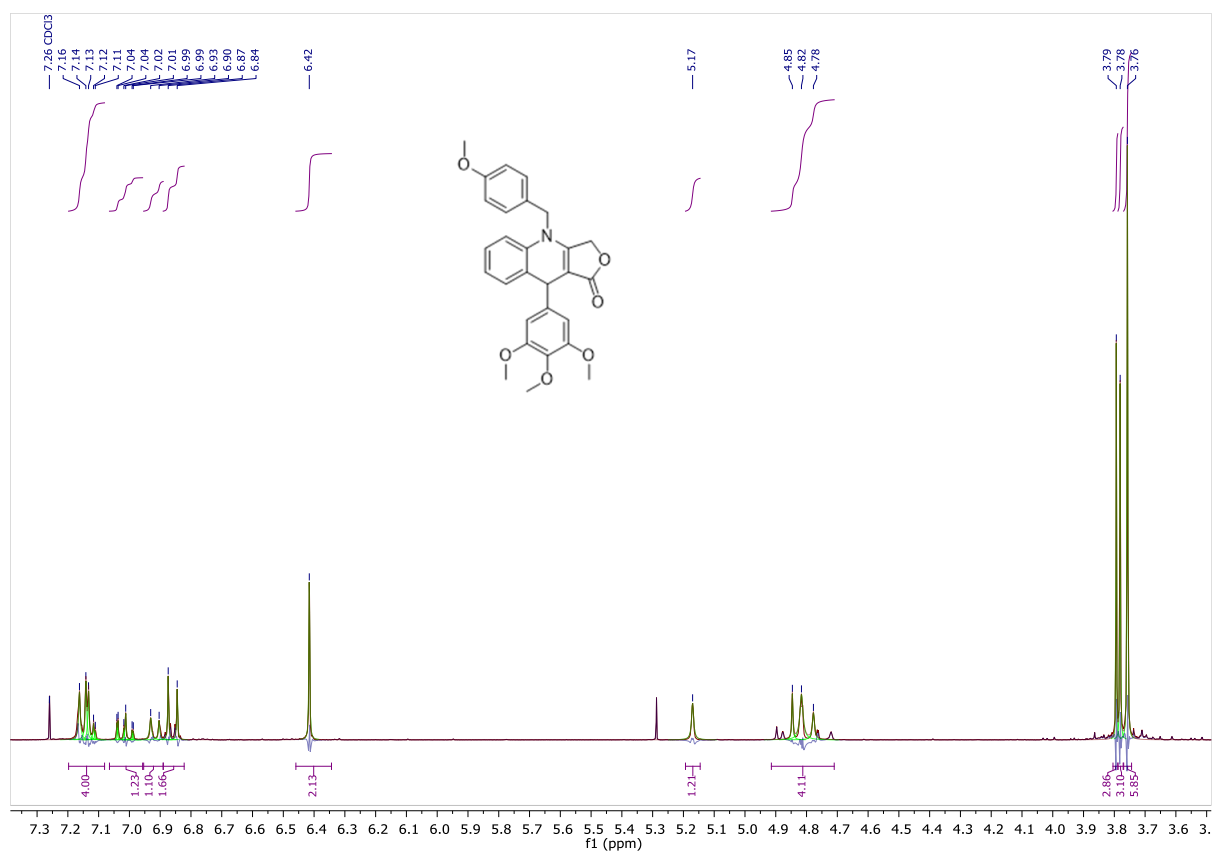
(2-aminophenyl)(3,4,5-trimethoxyphenyl)methanol



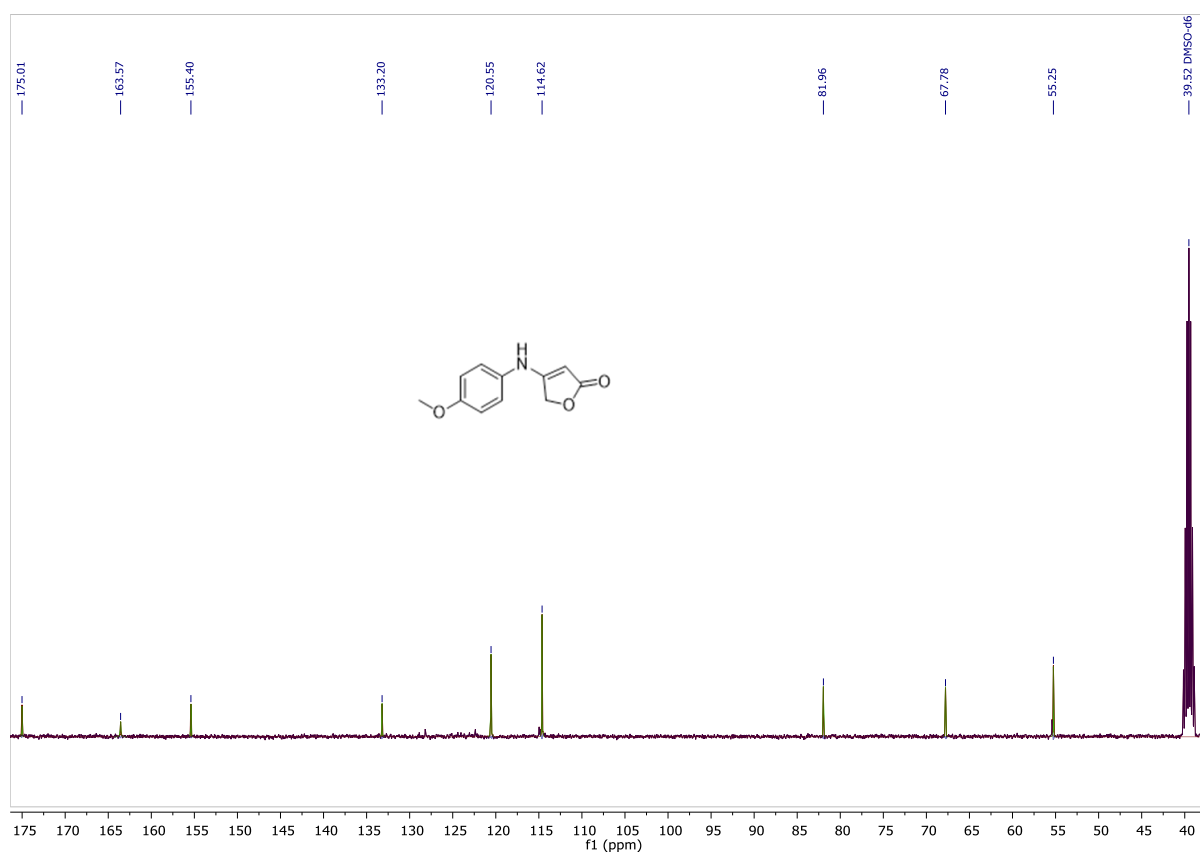
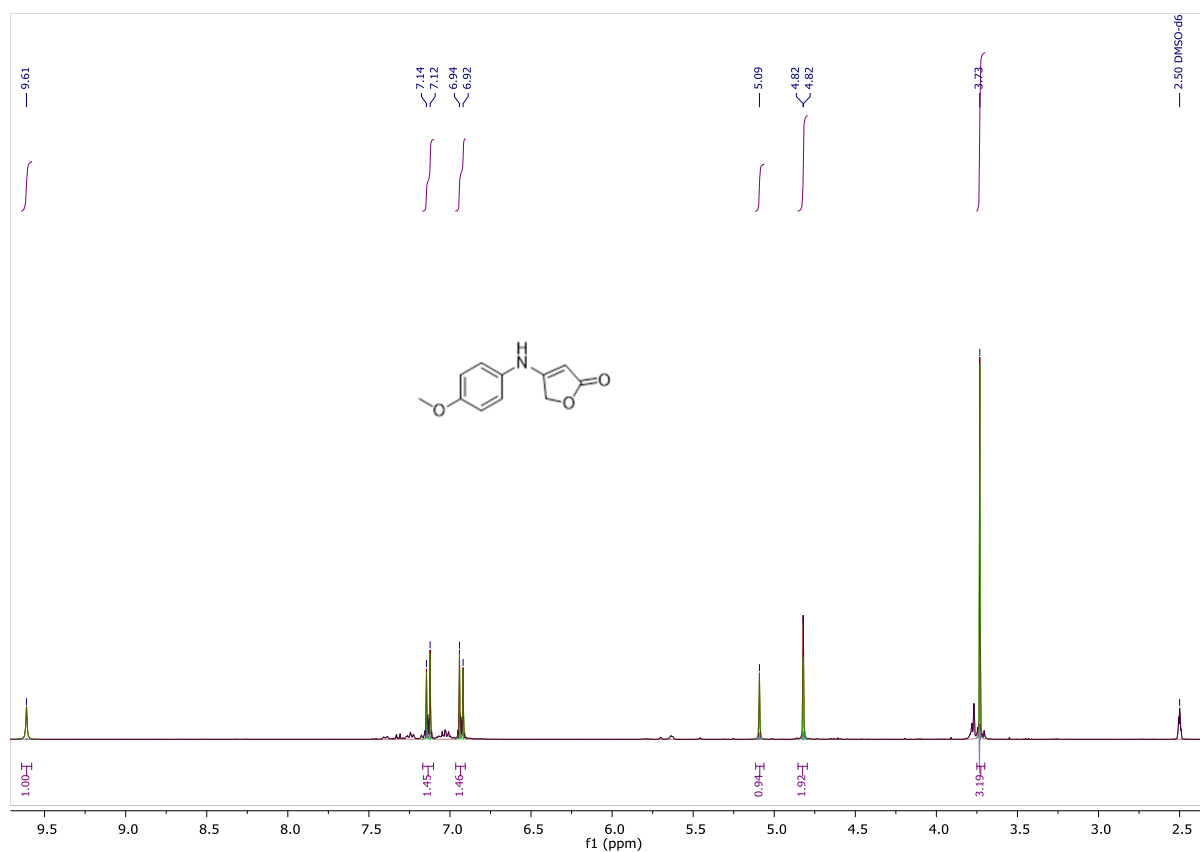
(2-((4-methoxybenzyl)amino)phenyl)(3,4,5-trimethoxyphenyl)methanol



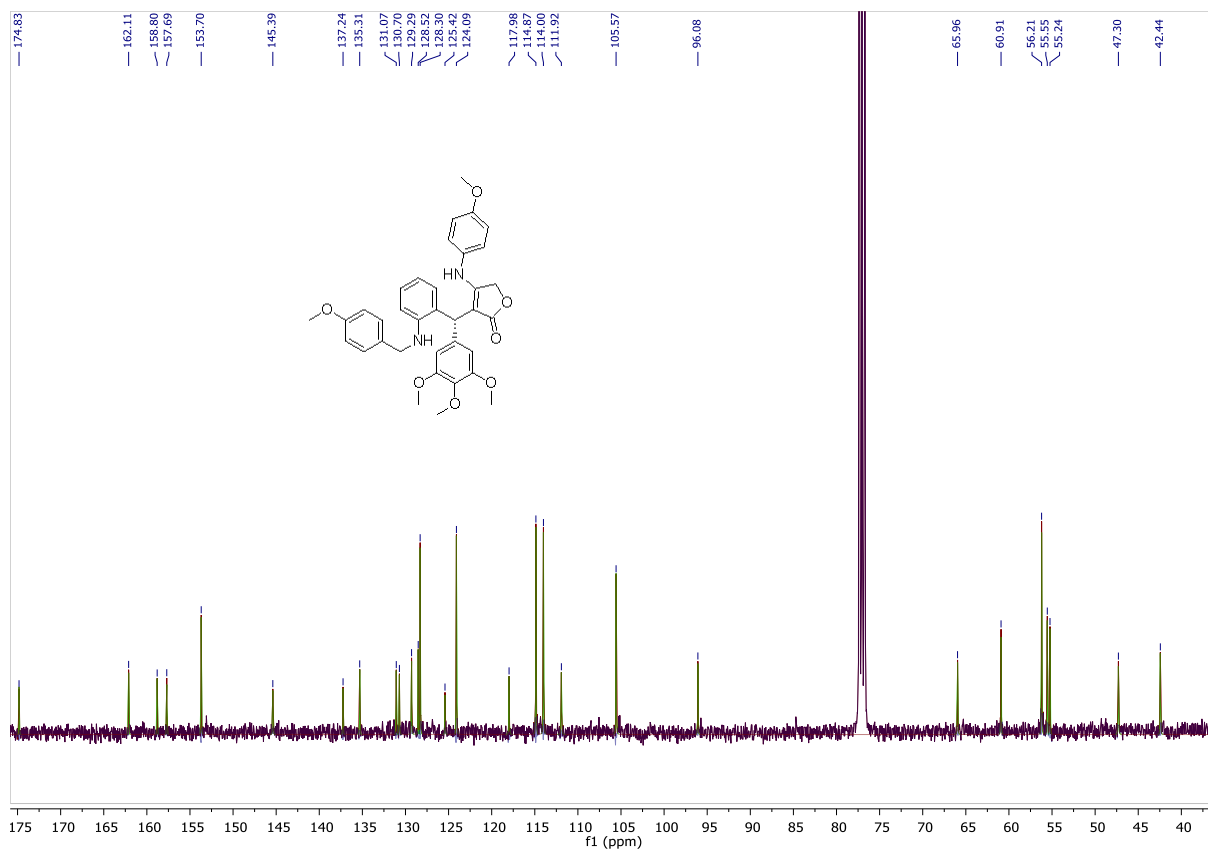
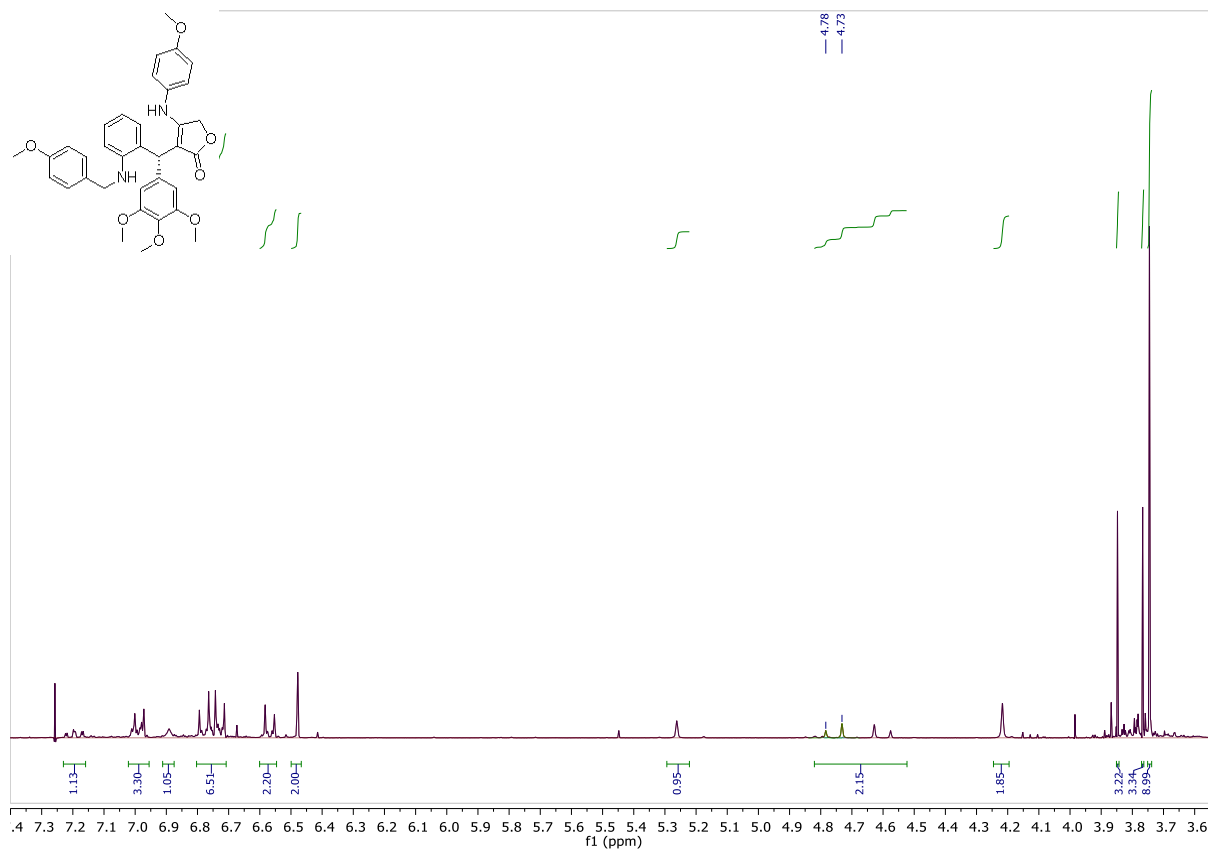
4-(4-methoxybenzyl)-9-(3,4,5-trimethoxyphenyl)-4,9-dihydrofuro[3,4-b]quinolin-1(3H)-one



4-((4-methoxyphenyl)amino)furan-2(5H)-one

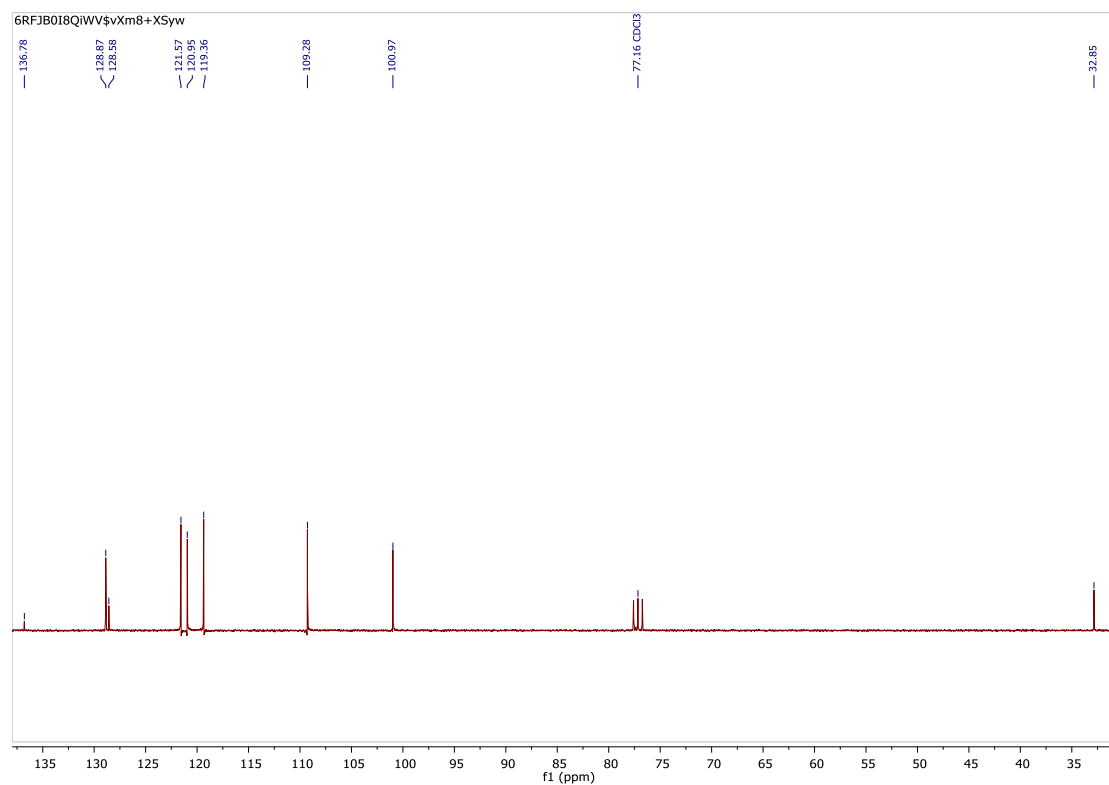
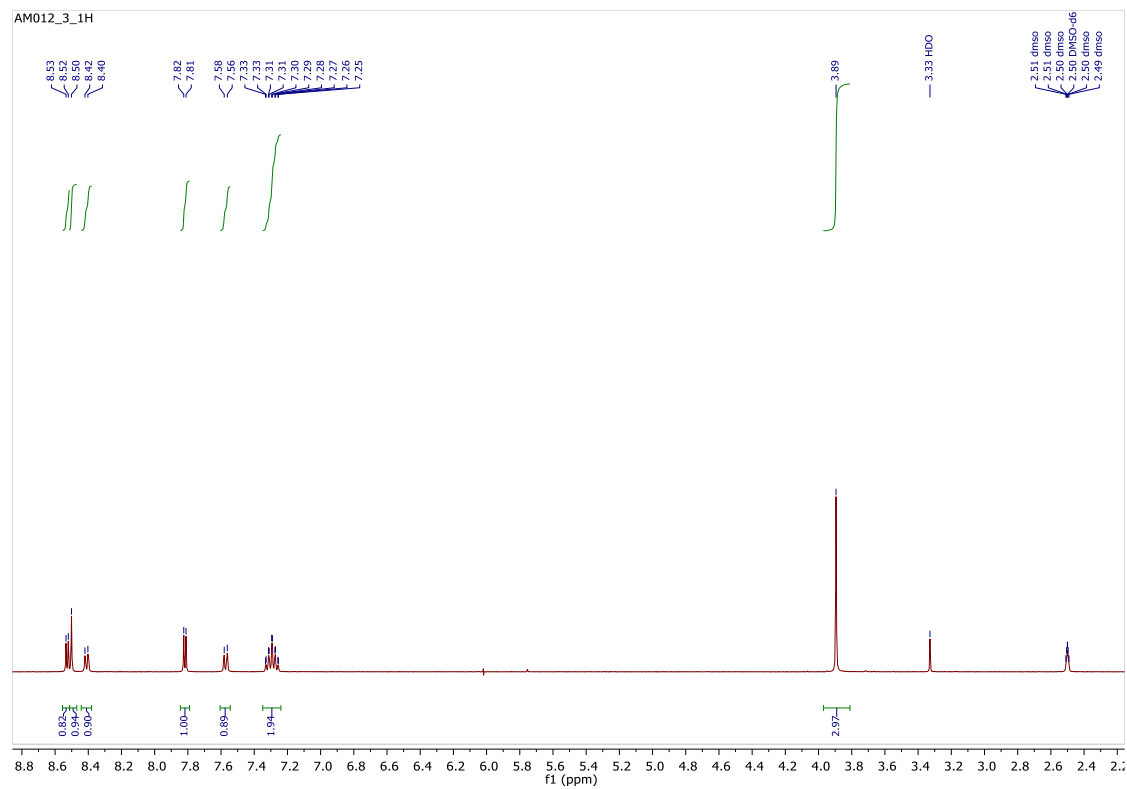
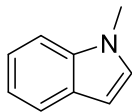


3-((2-((4-methoxybenzyl)amino)phenyl)(3,4,5-trimethoxyphenyl)methyl)-4-((4-methoxyphenyl)amino)furan-2(5H)-one

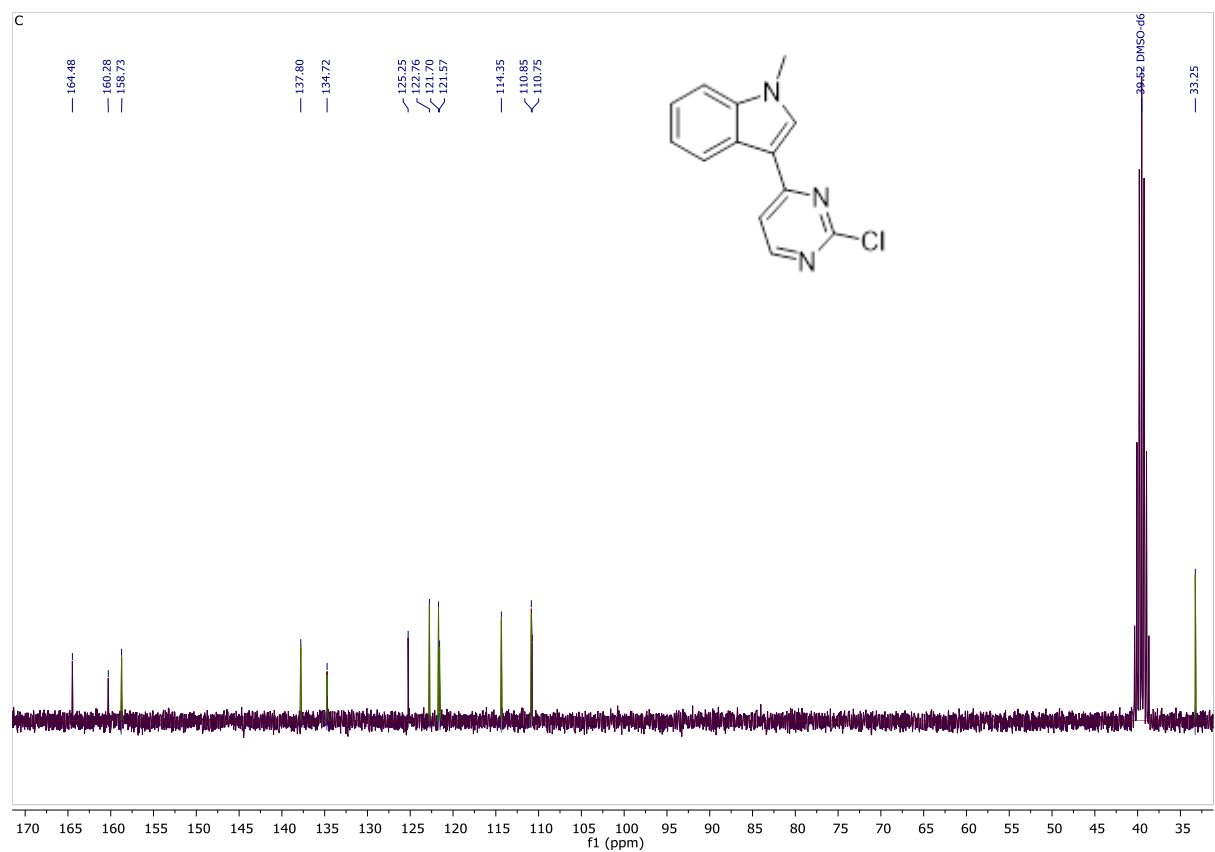
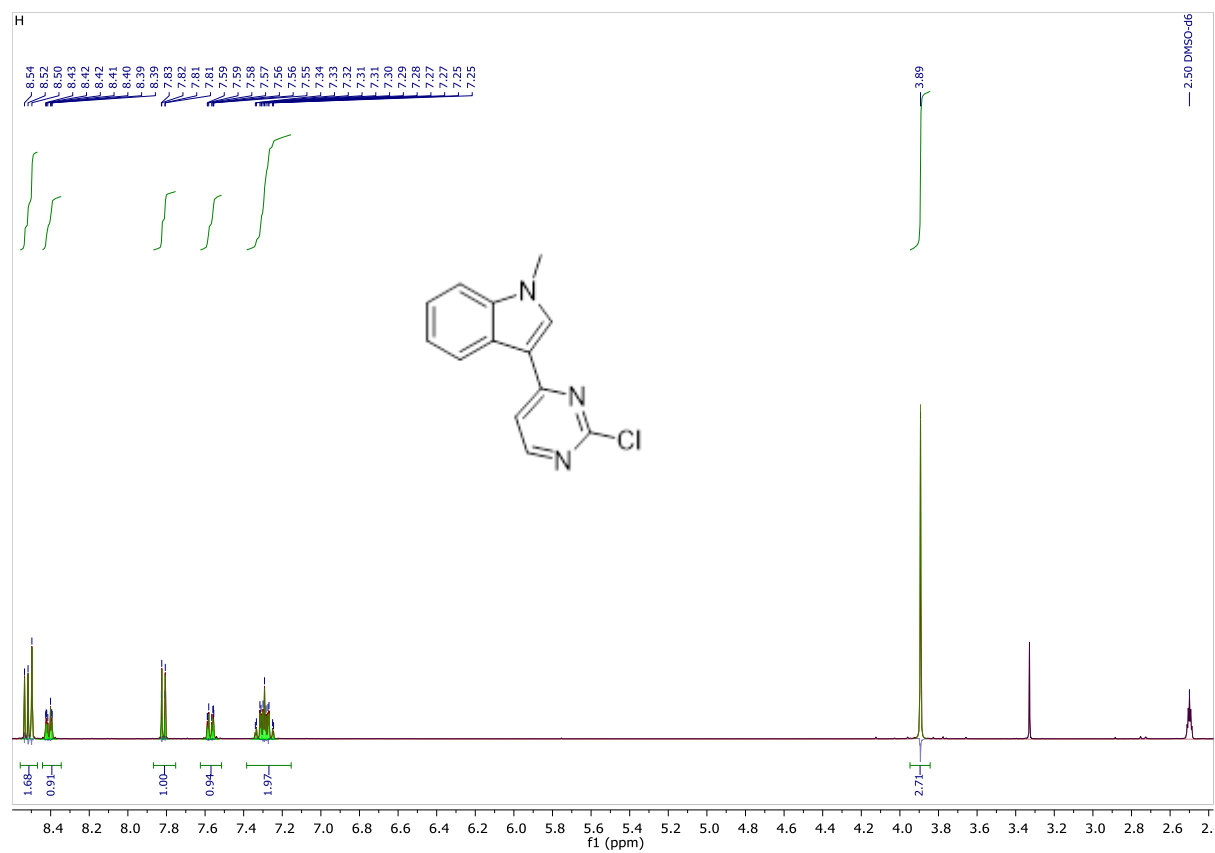


SULFONYL FLUORIDES AS EGFR INHIBITORS

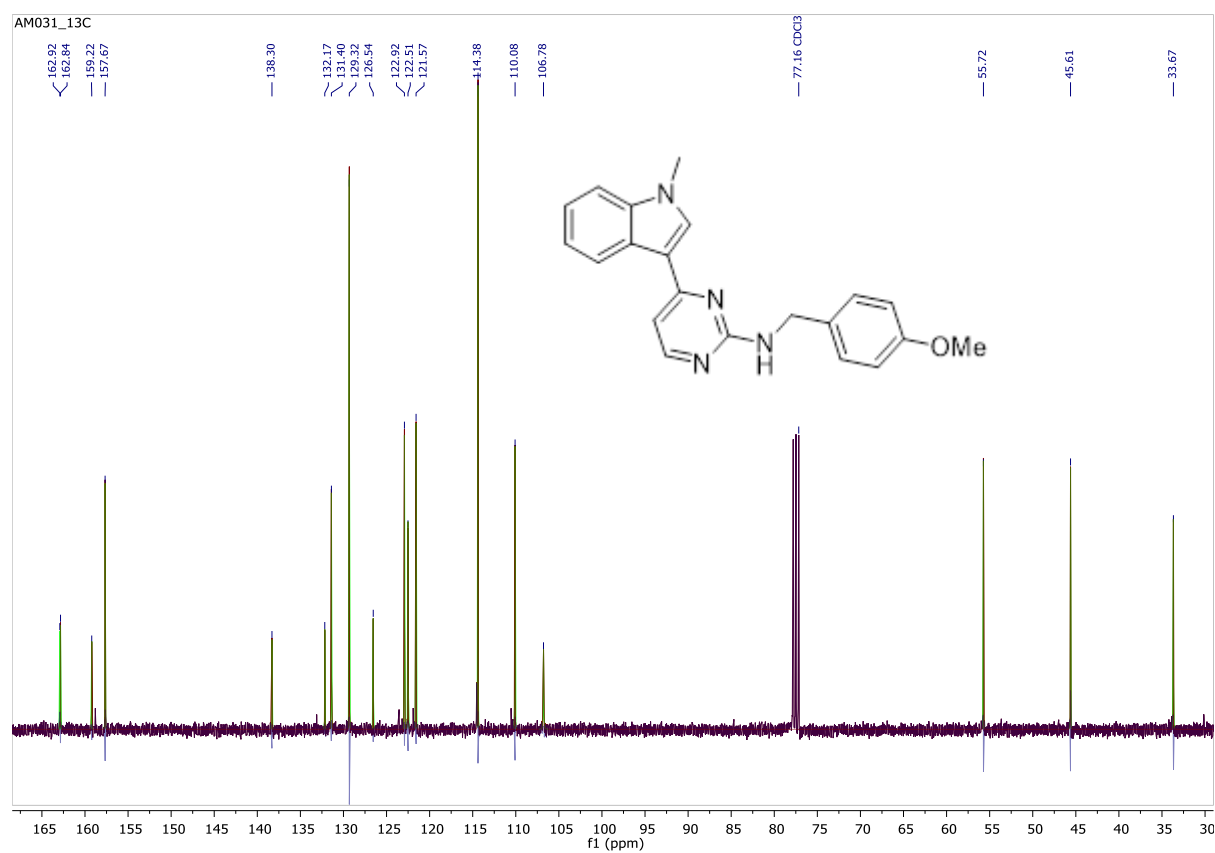
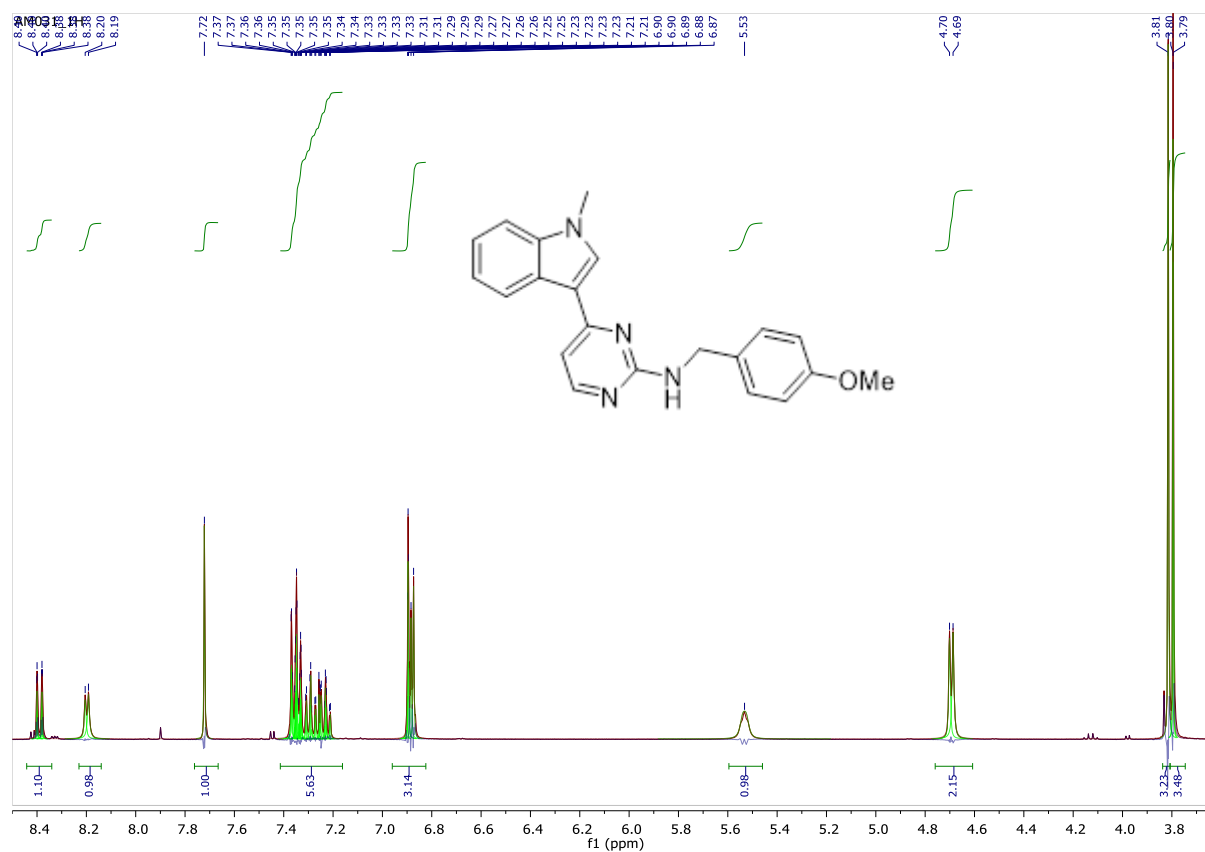
1-methyl-1H-indole



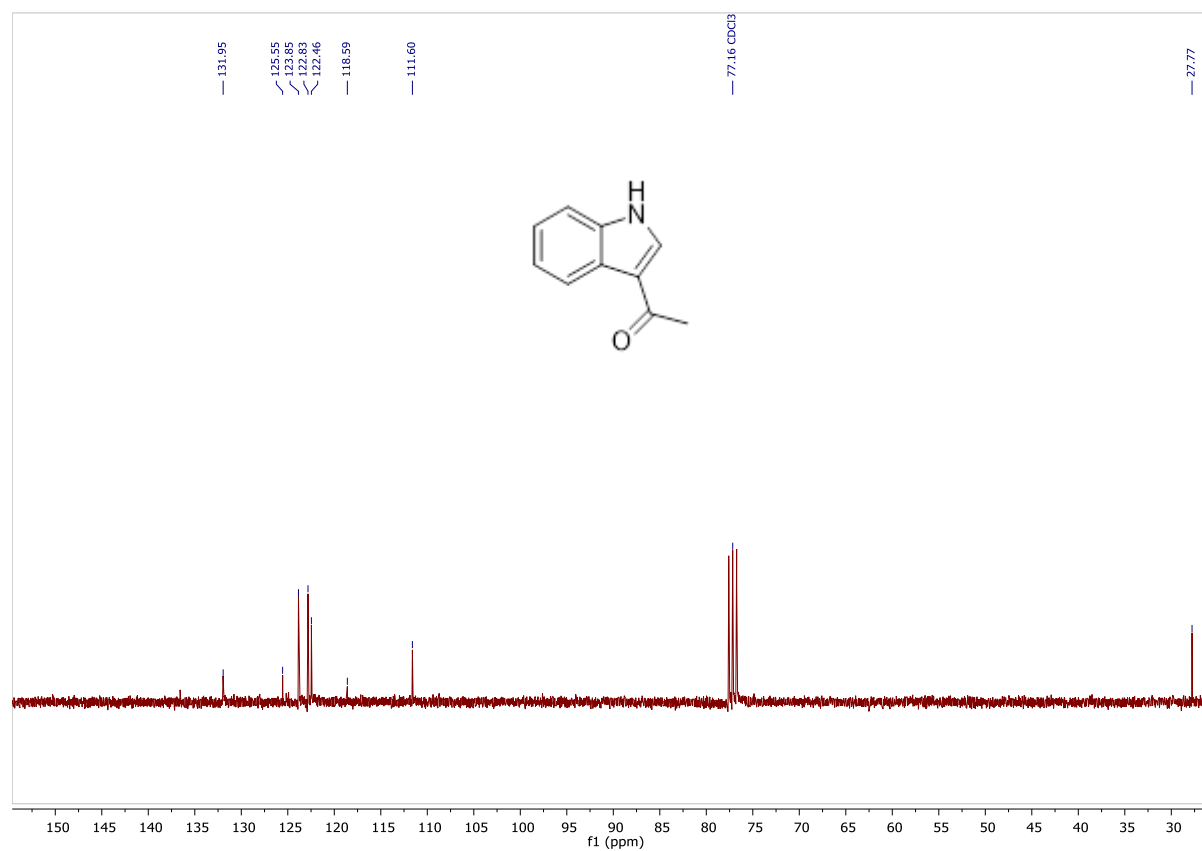
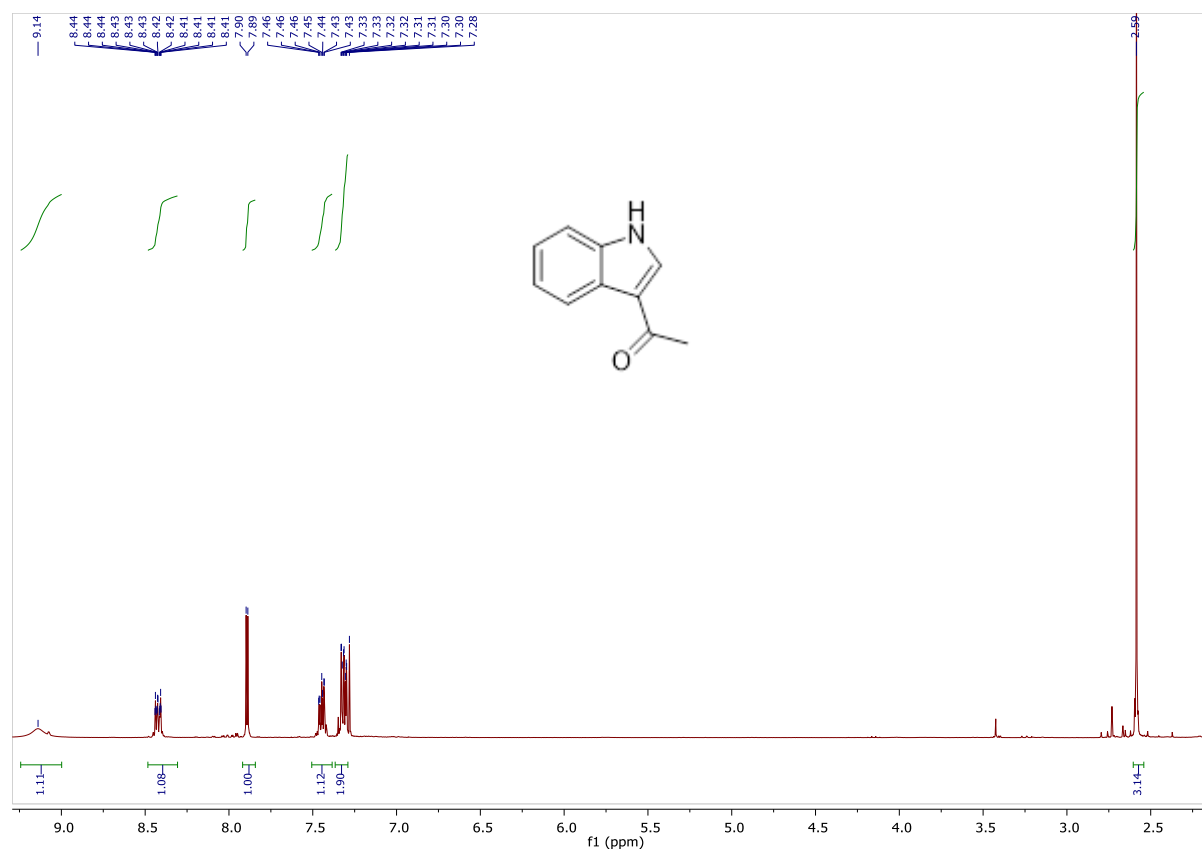
3-(2-chloropyrimidin-4-yl)-1-methyl-1H-indole



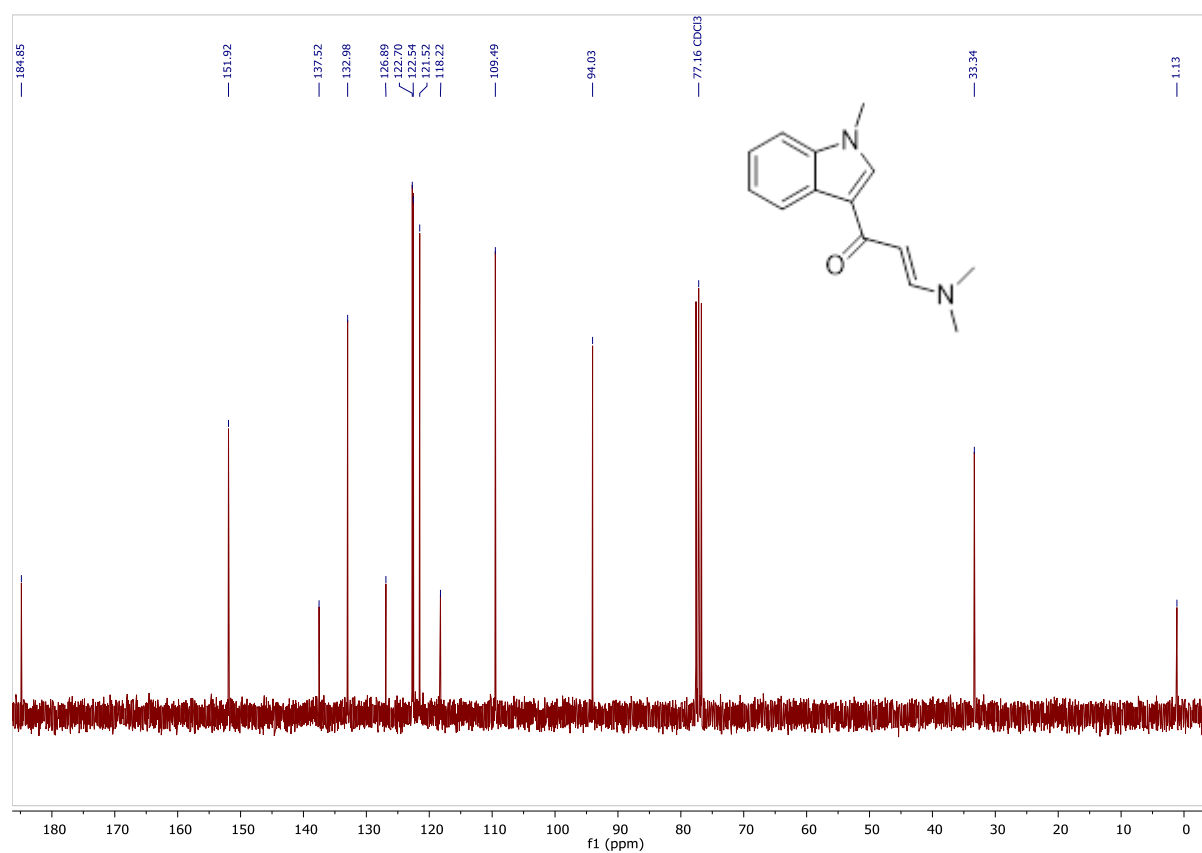
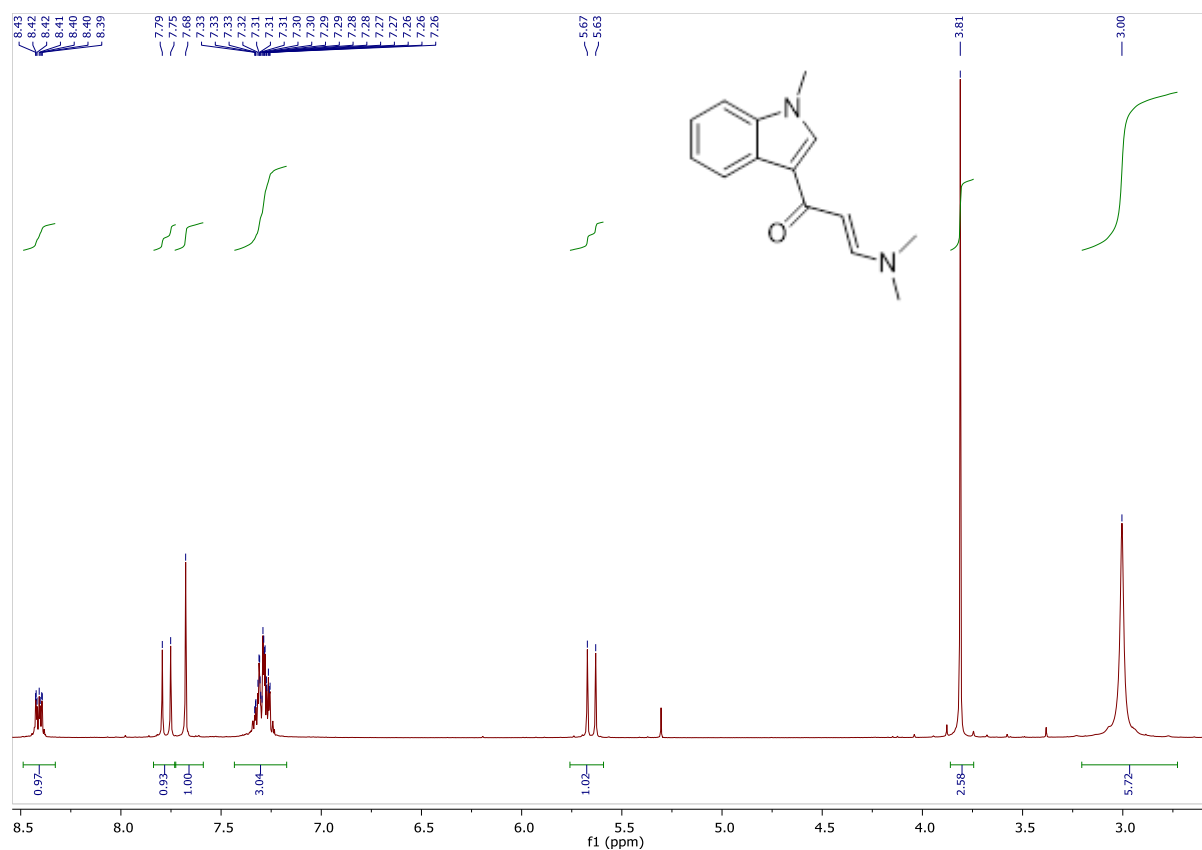
N-(4-methoxybenzyl)-4-(1-methyl-1H-indol-3-yl)pyrimidin-2-amine



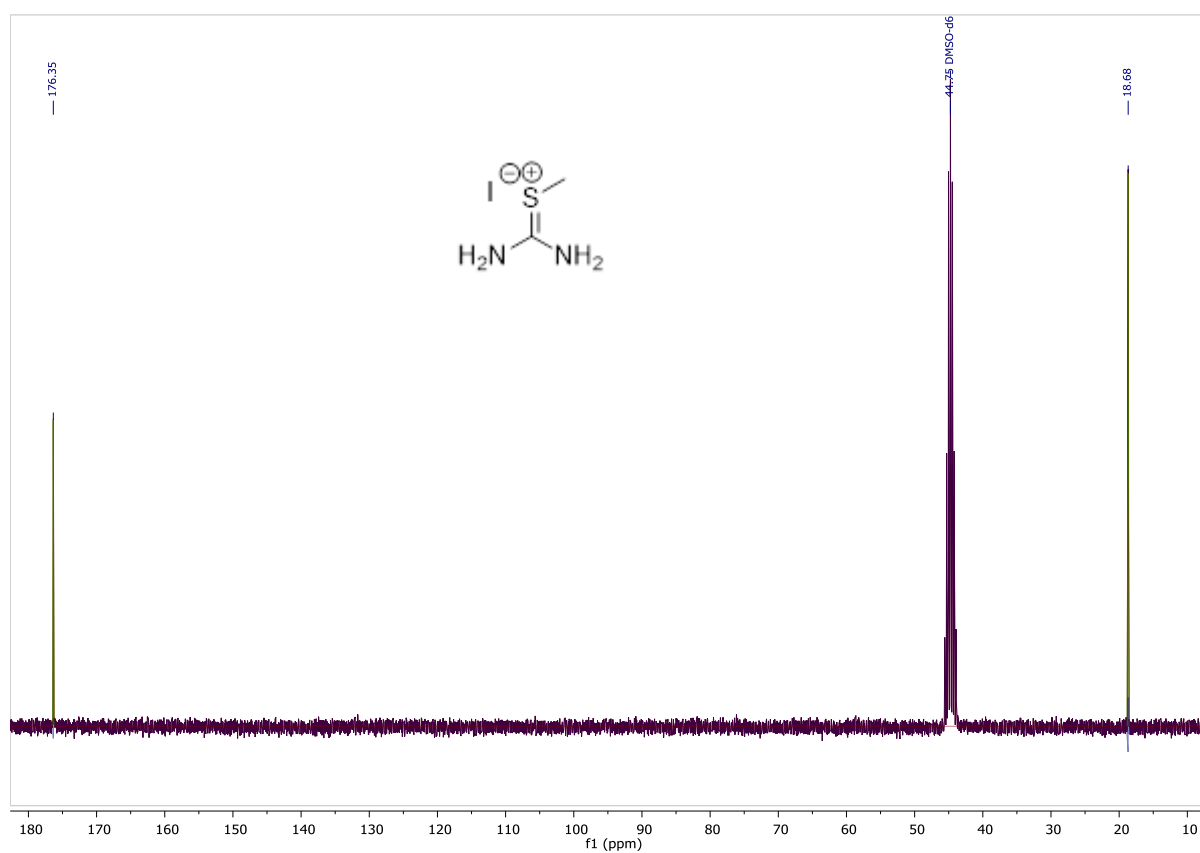
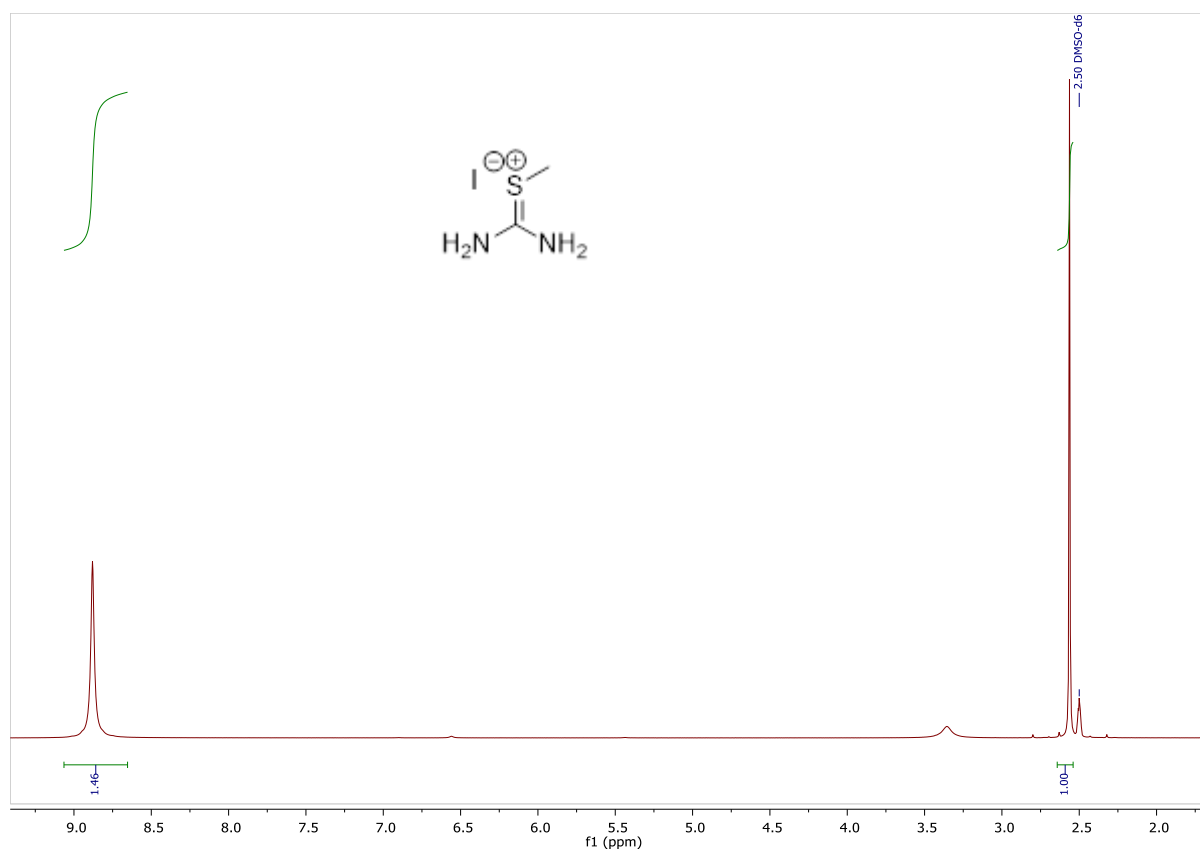
1-(1H-indol-3-yl)ethan-1-one



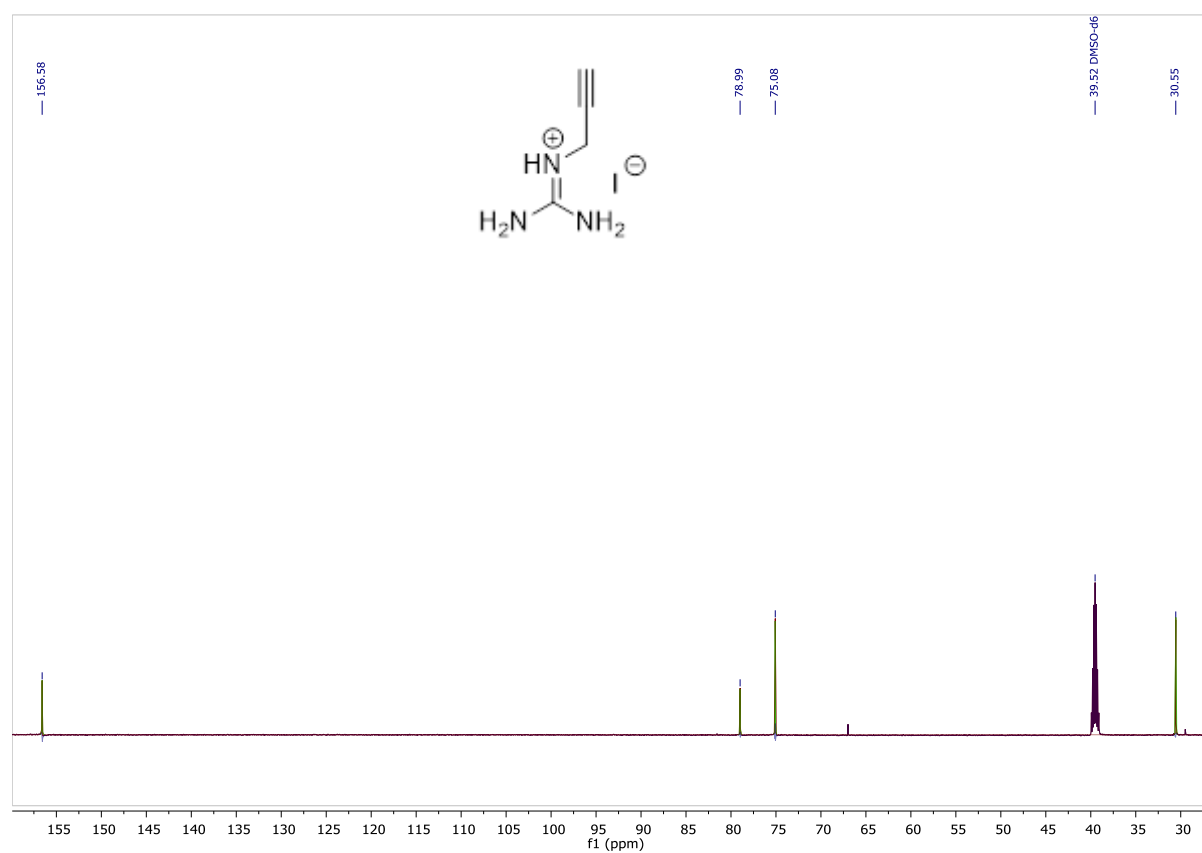
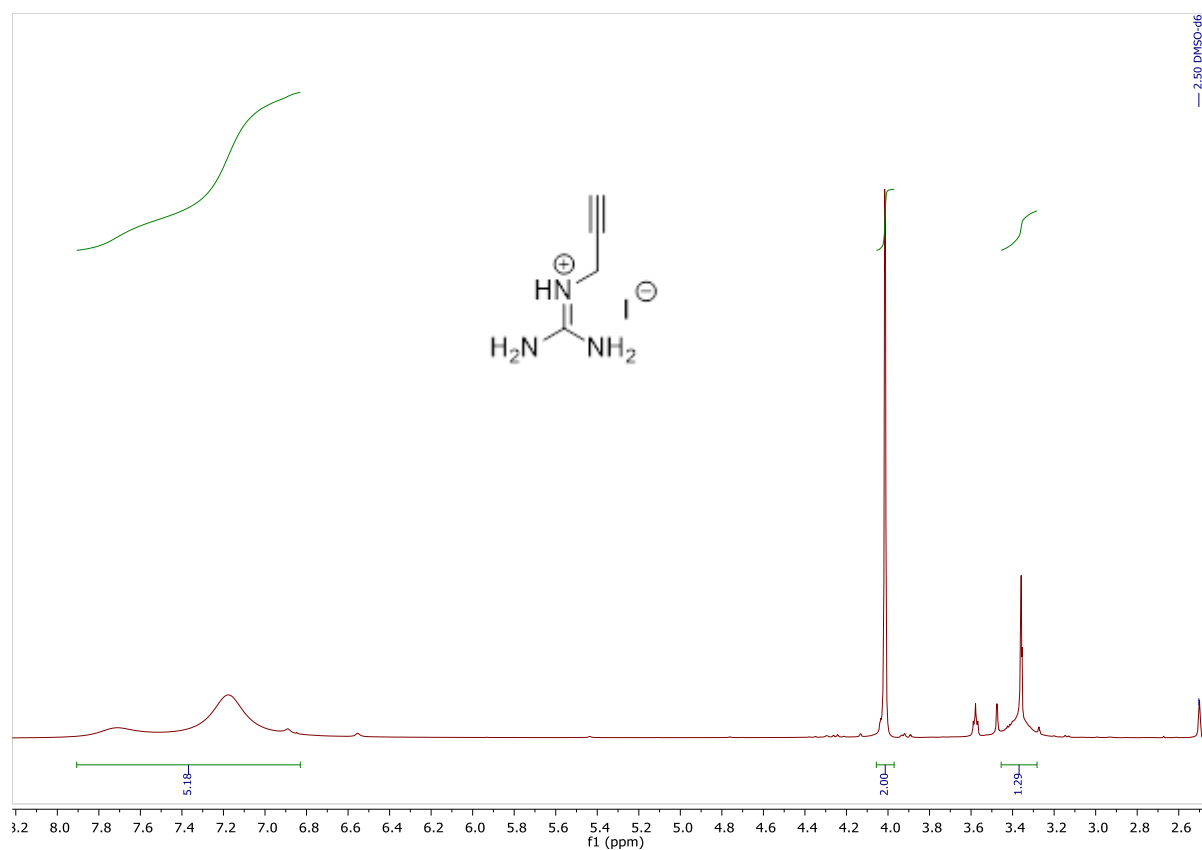
(E)-3-(dimethylamino)-1-(1-methyl-1H-indol-3-yl)prop-2-en-1-one



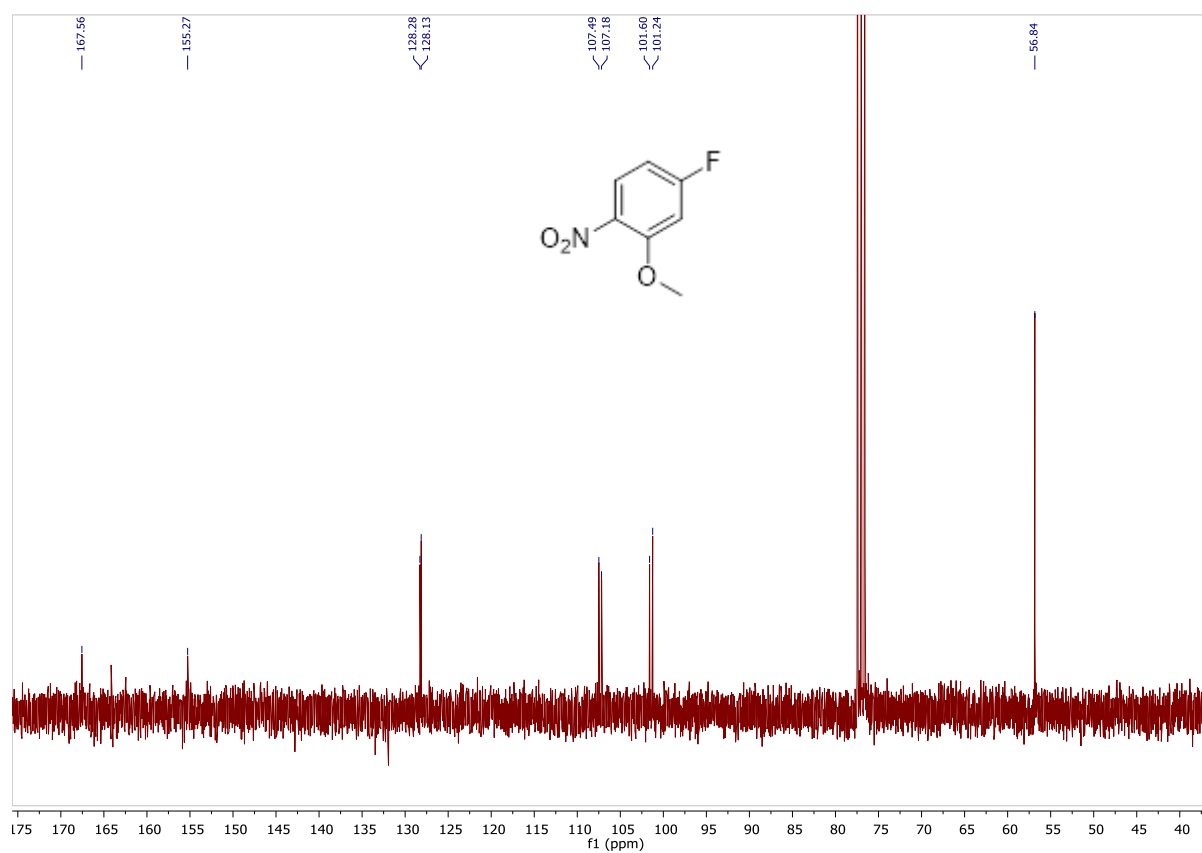
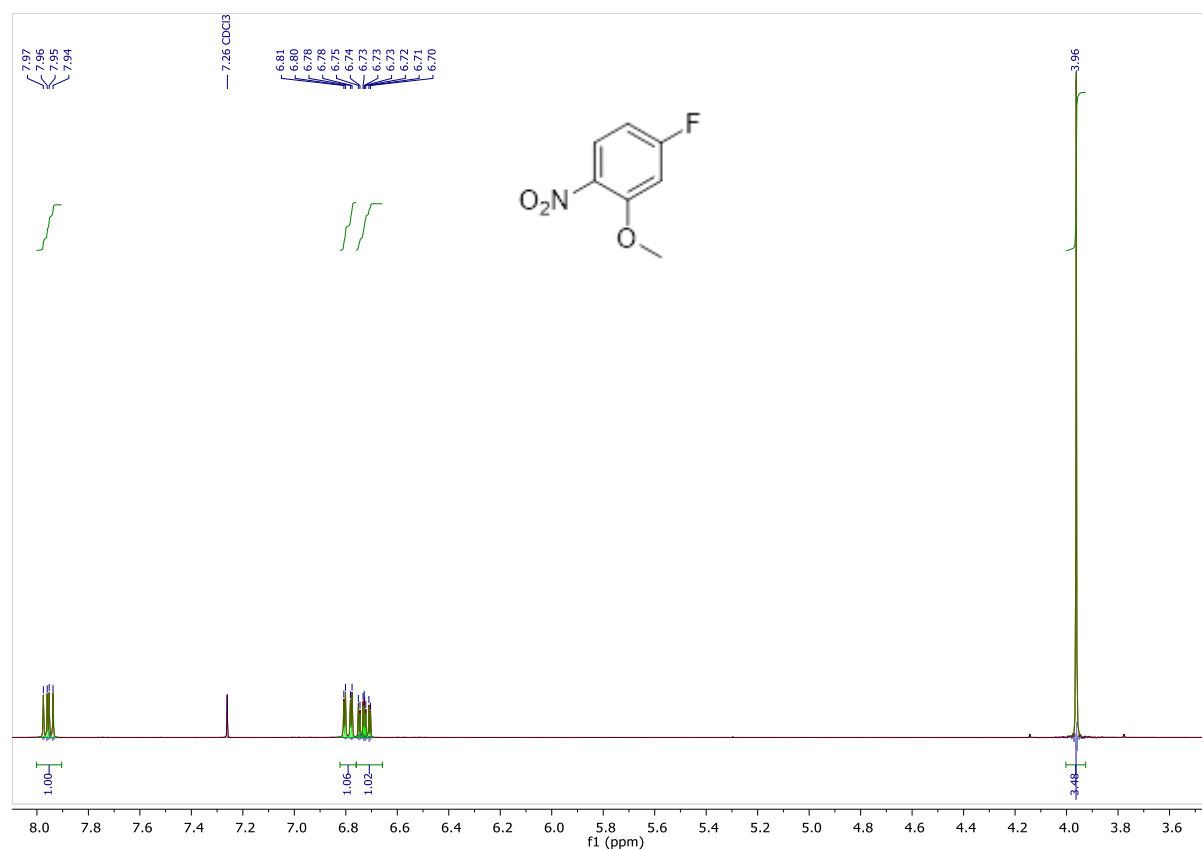
S-methylisothiuronium iodide



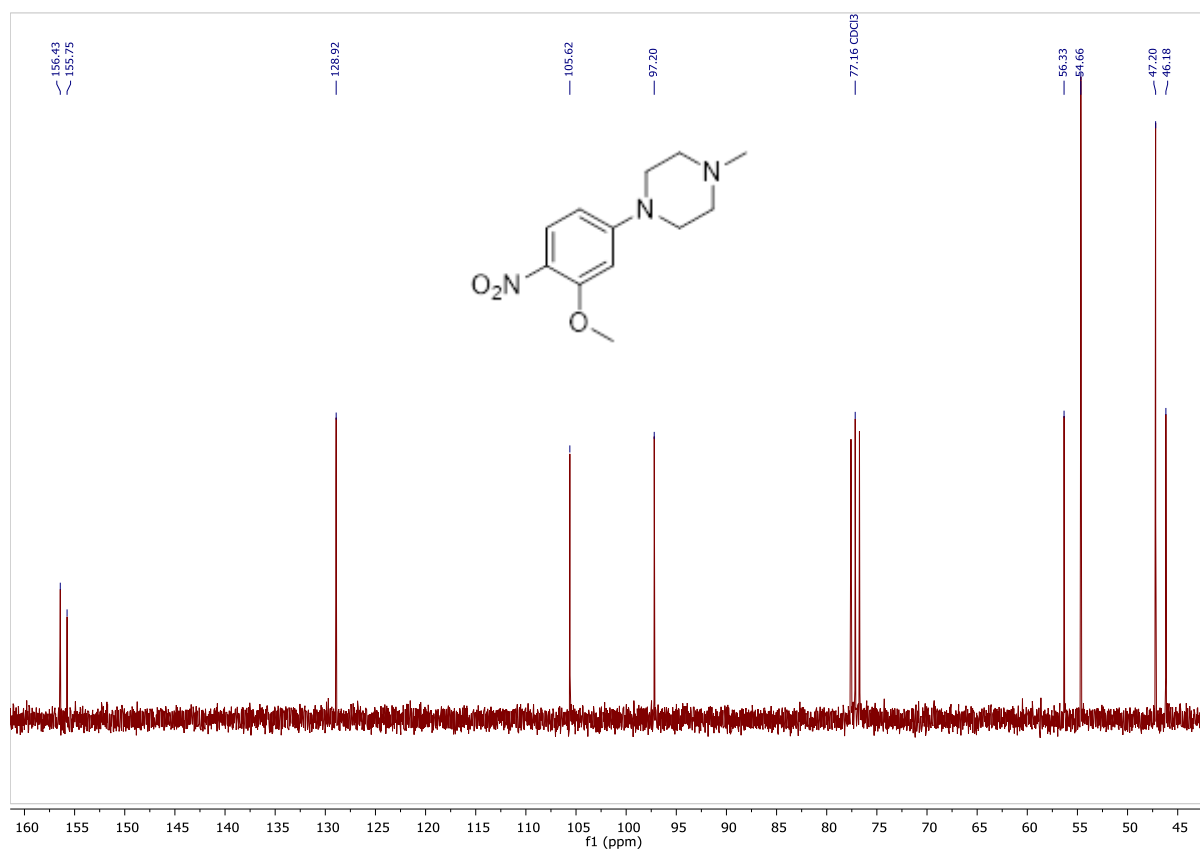
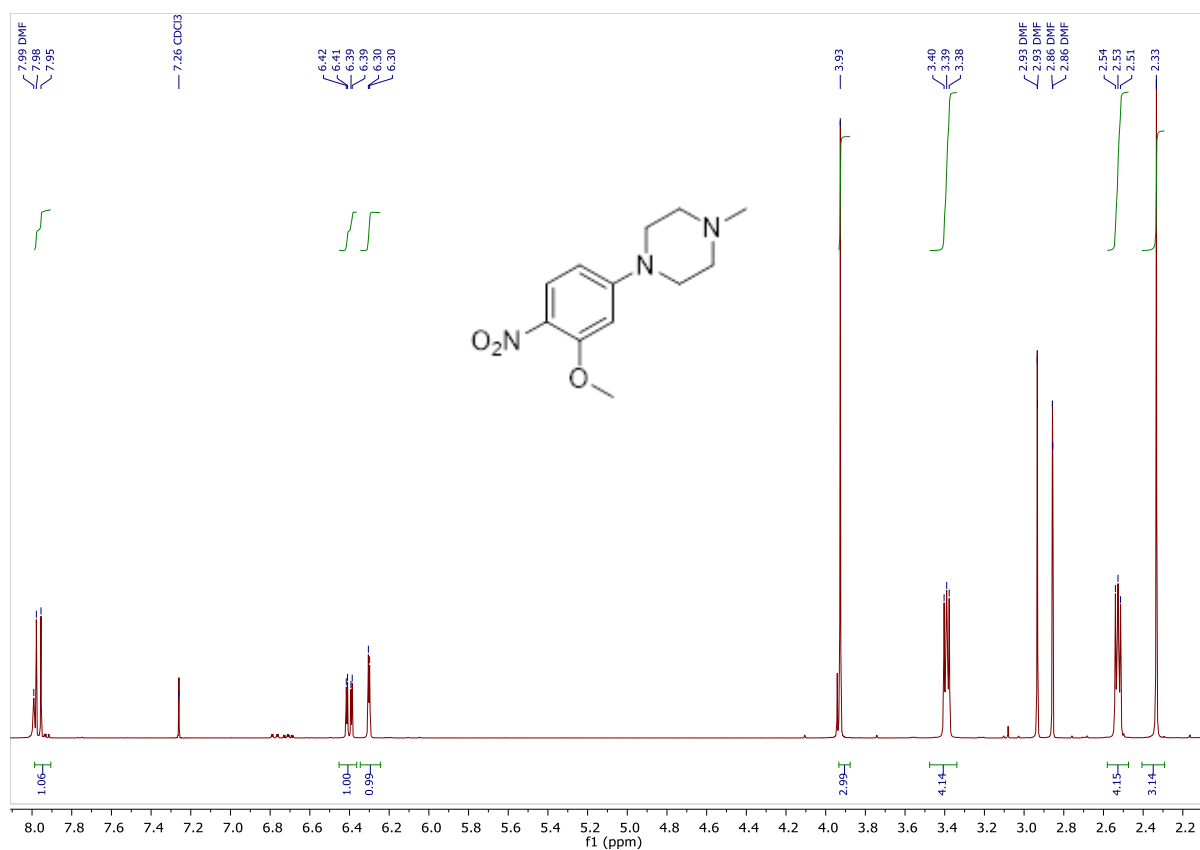
Propargylguanidine hydroiodide



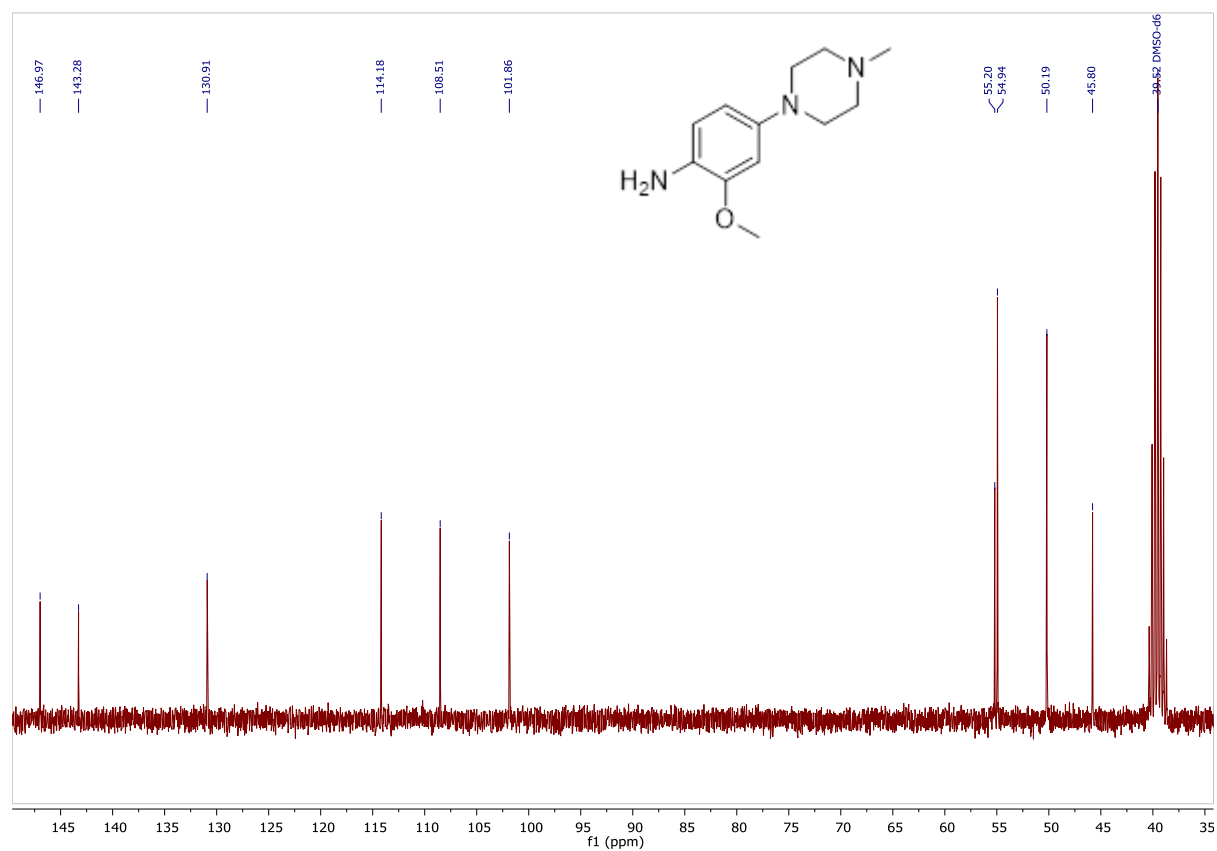
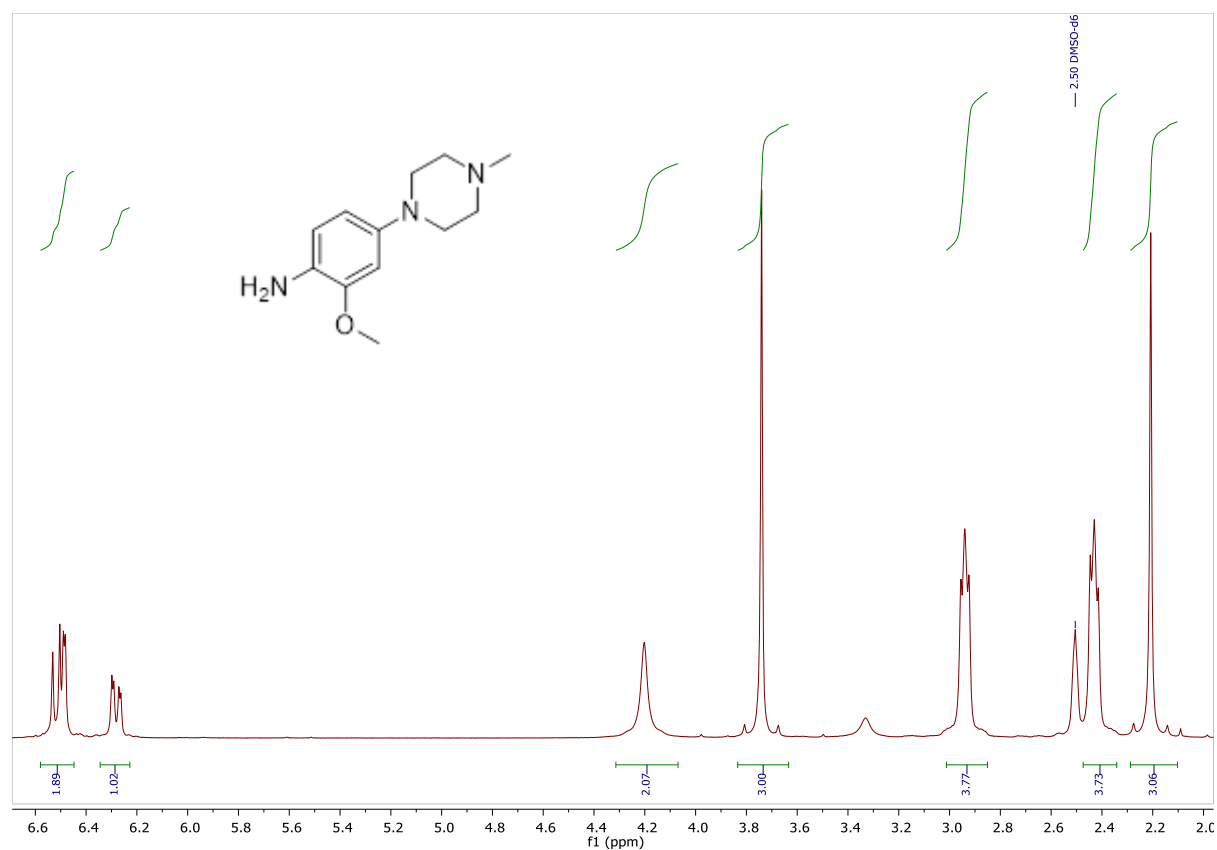
4-fluoro-2-methoxy-1-nitrobenzene



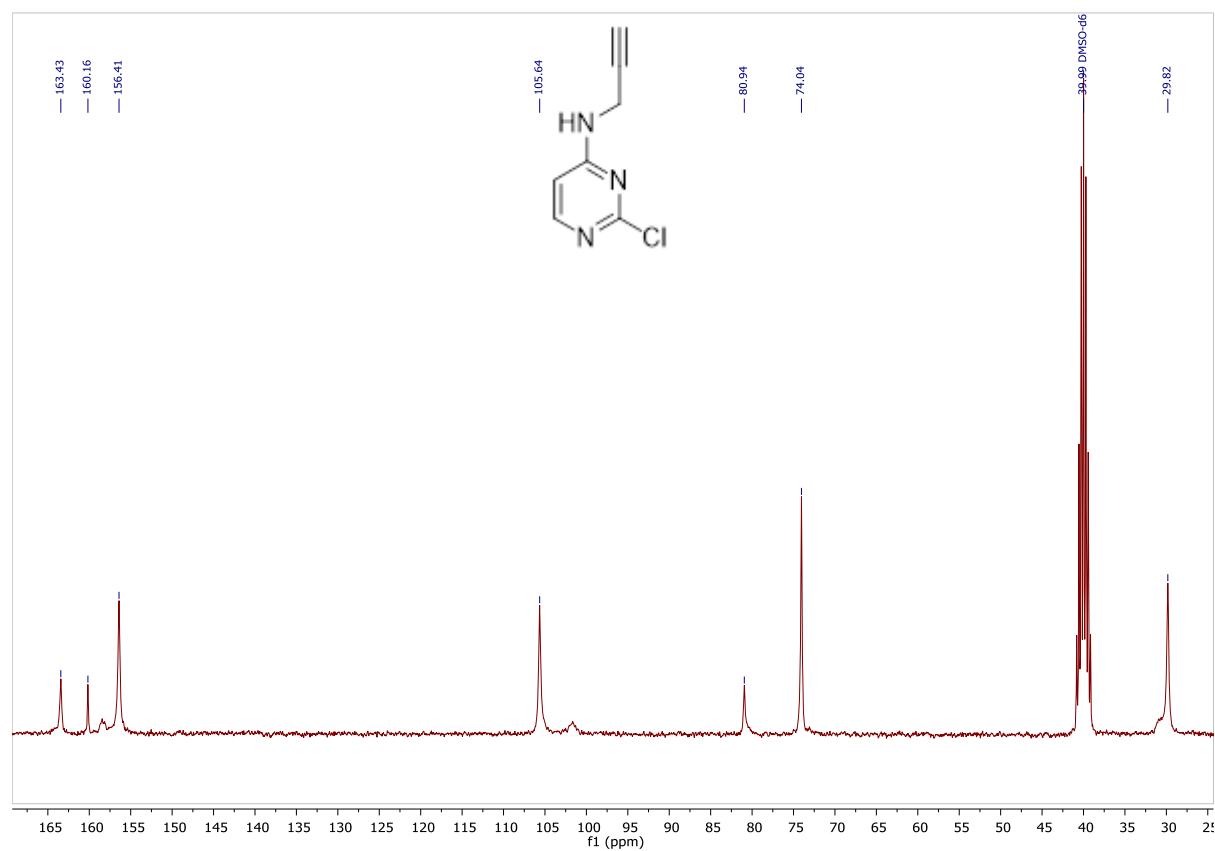
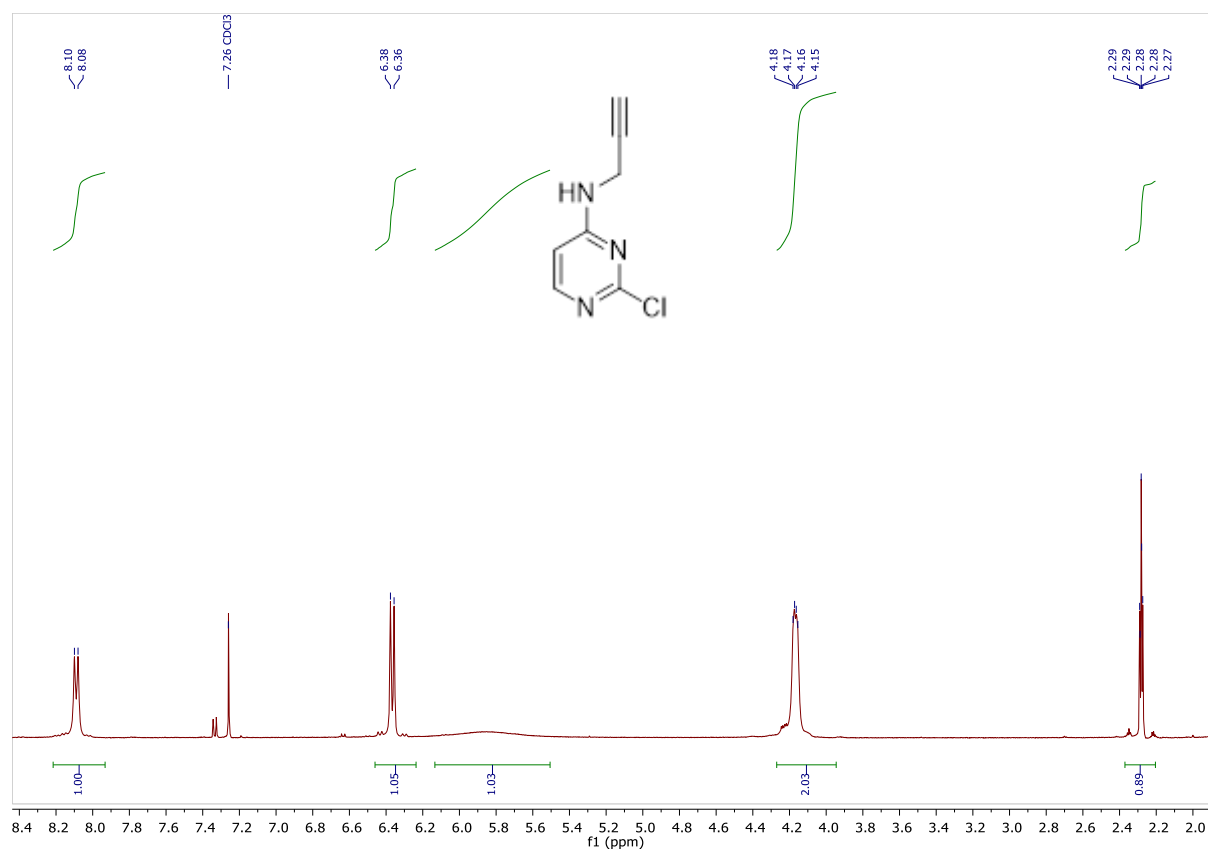
1-(3-methoxy-4-nitrophenyl)-4-methylpiperazine



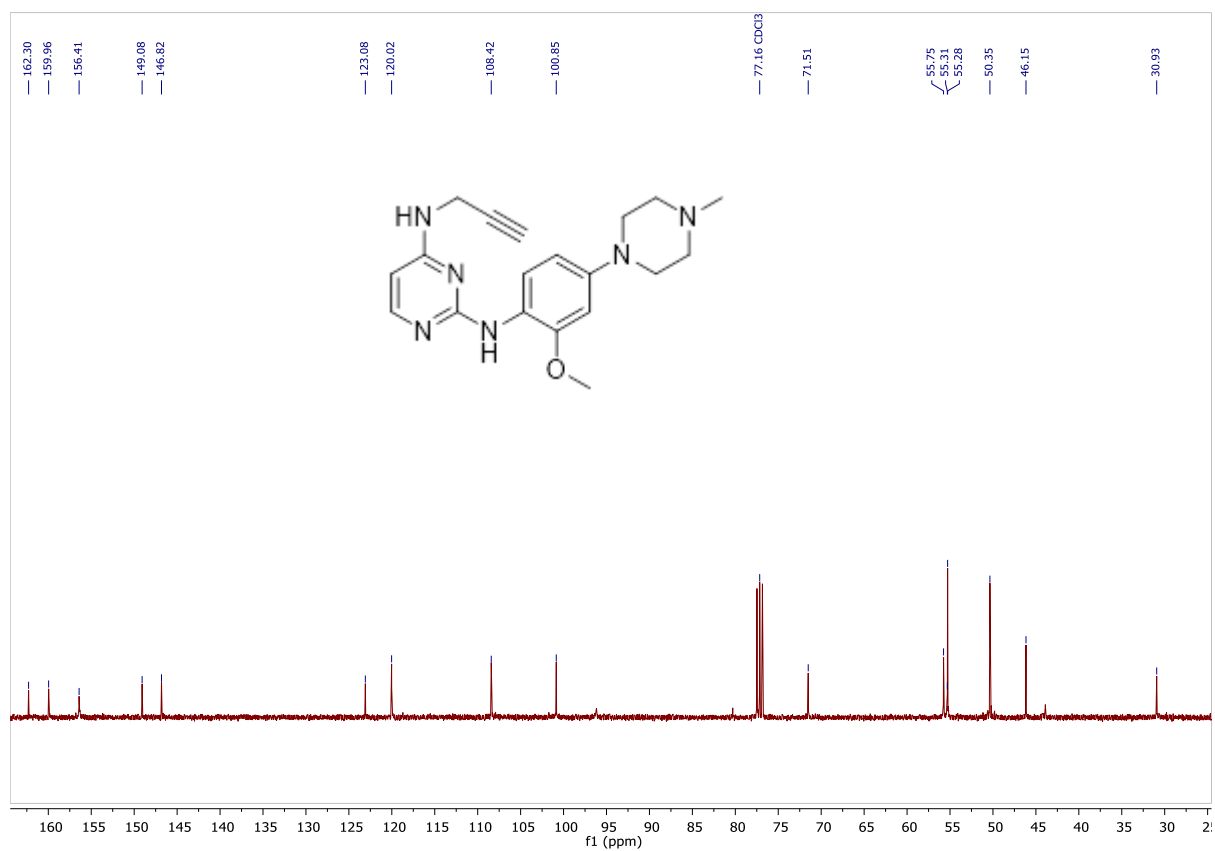
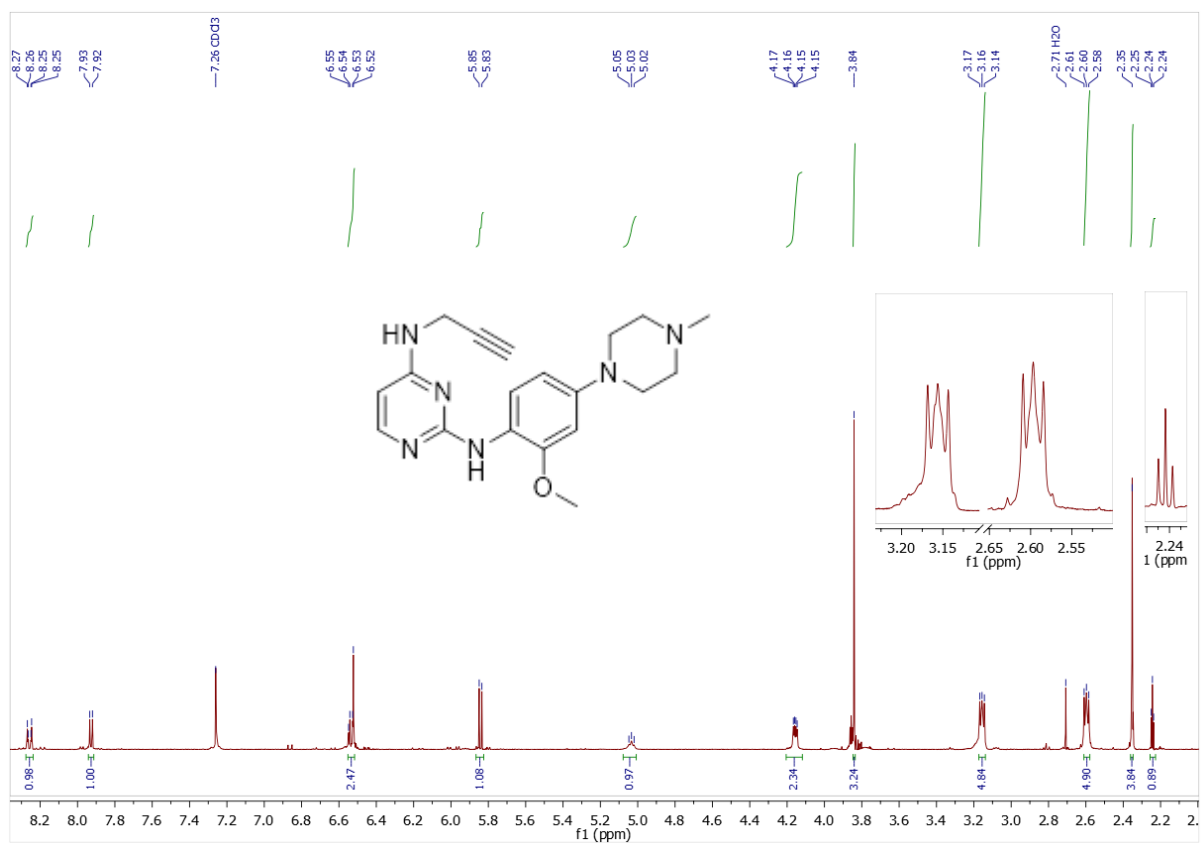
2-methoxy-4-(4-methylpiperazin-1-yl)aniline

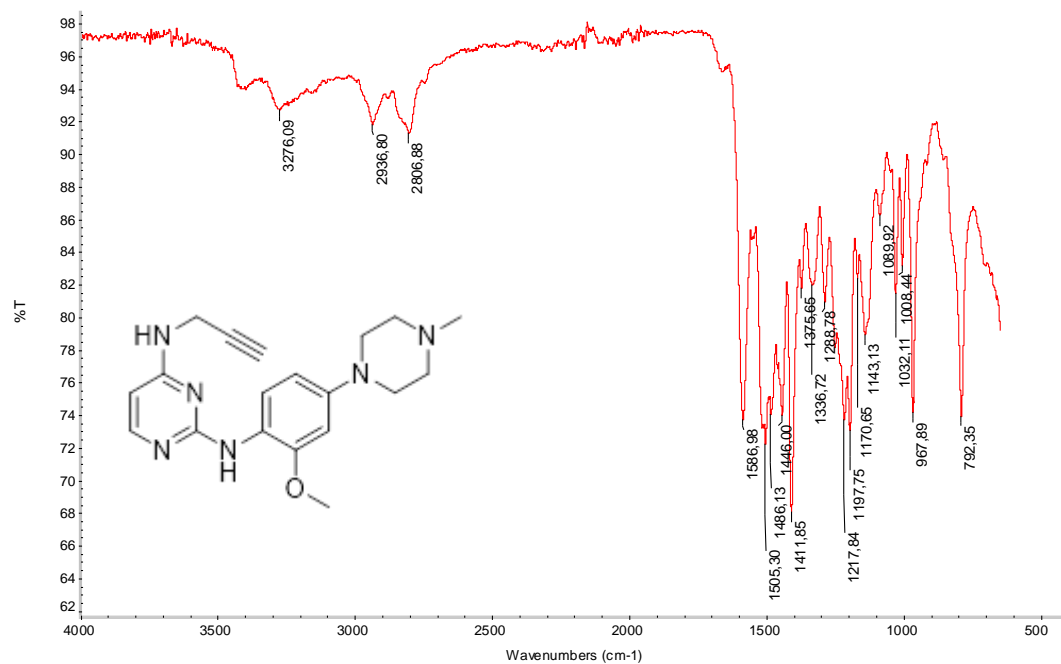


2-chloro-N-(prop-2-yn-1-yl)pyrimidin-4-amine



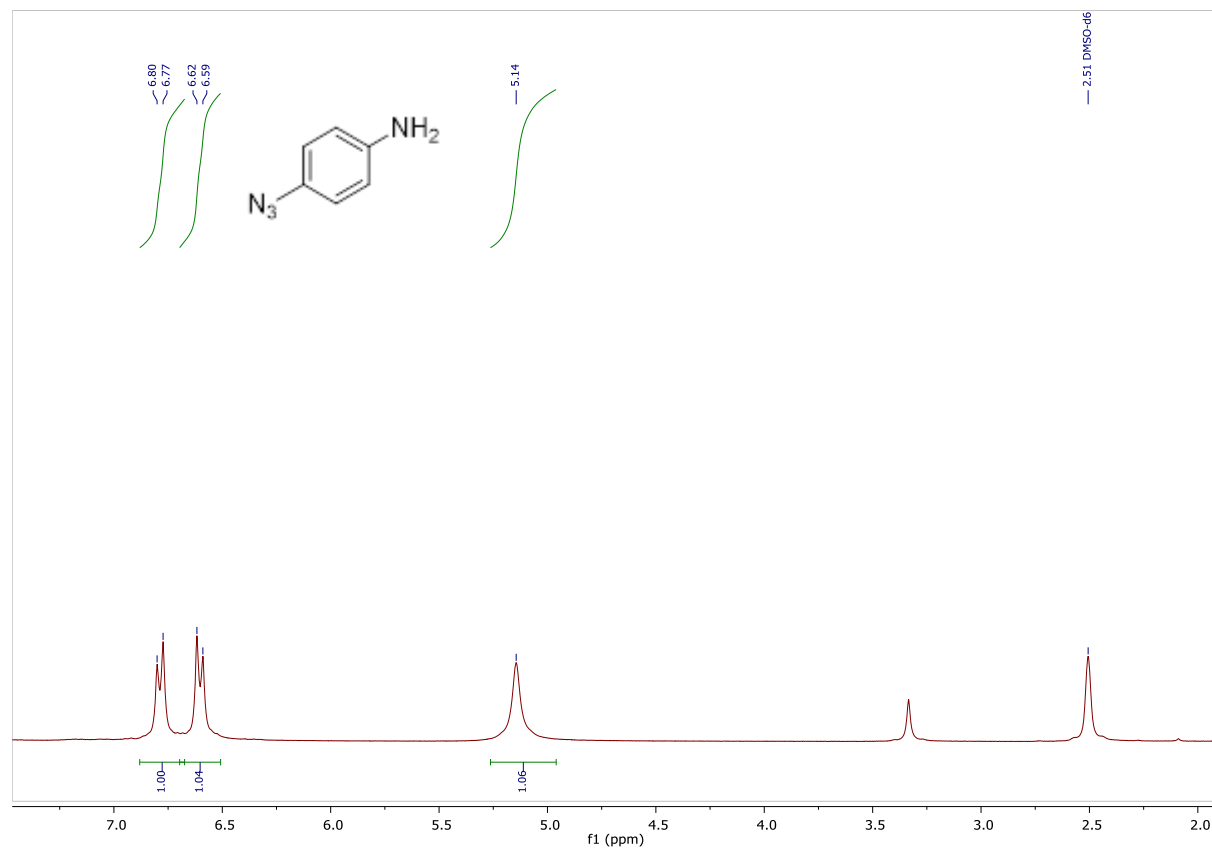
N²-(2-methoxy-4-(4-methylpiperazin-1-yl)phenyl)-N⁴-(prop-2-yn-1-yl)pyrimidine-2,4-diamine

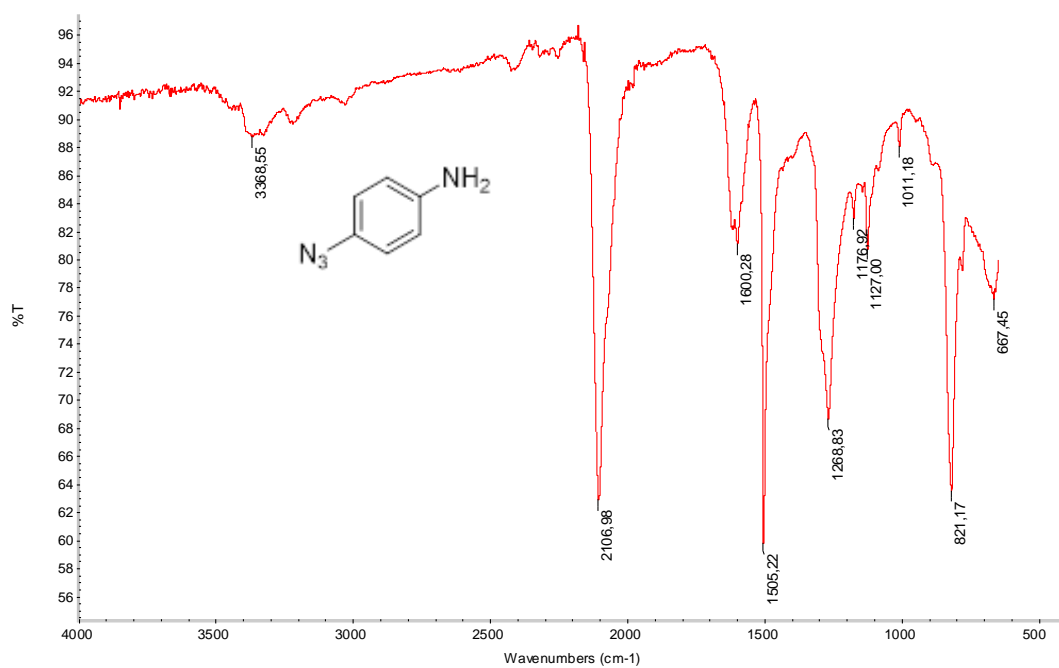
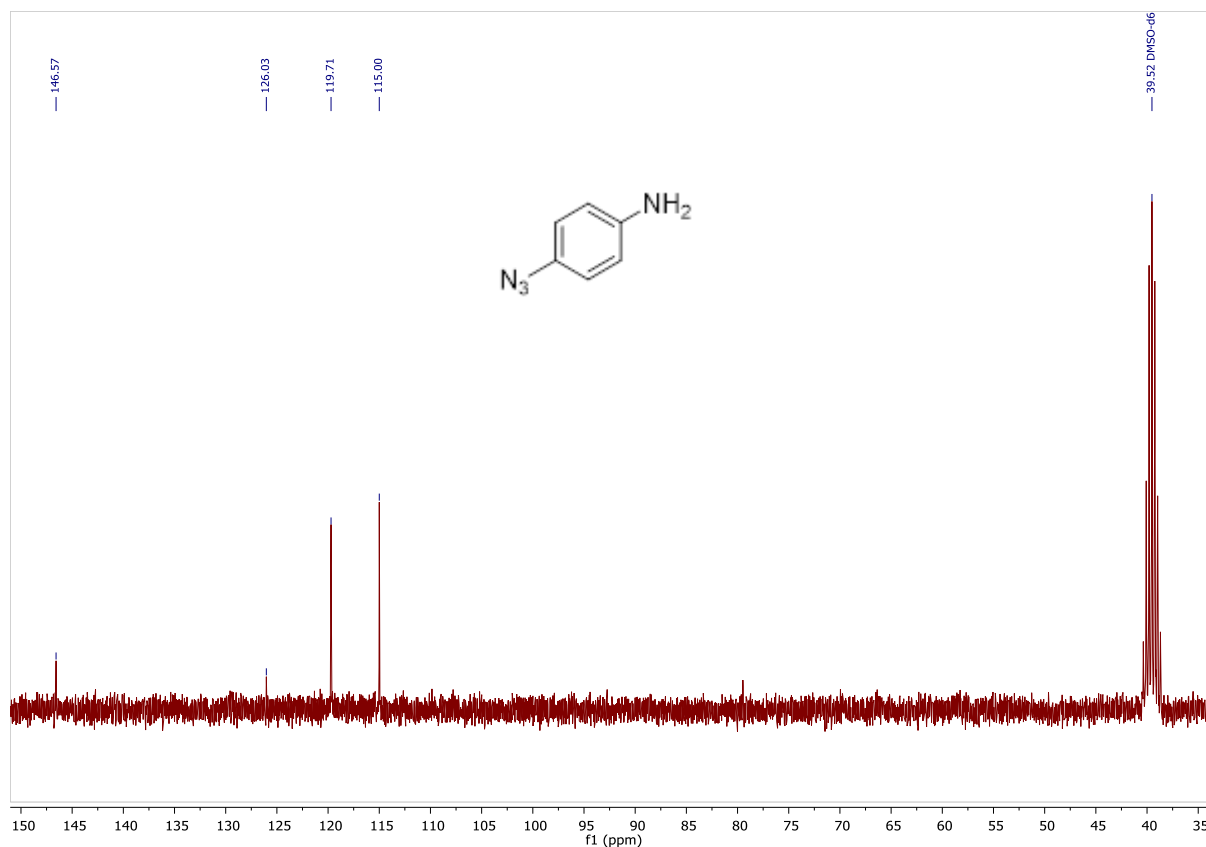




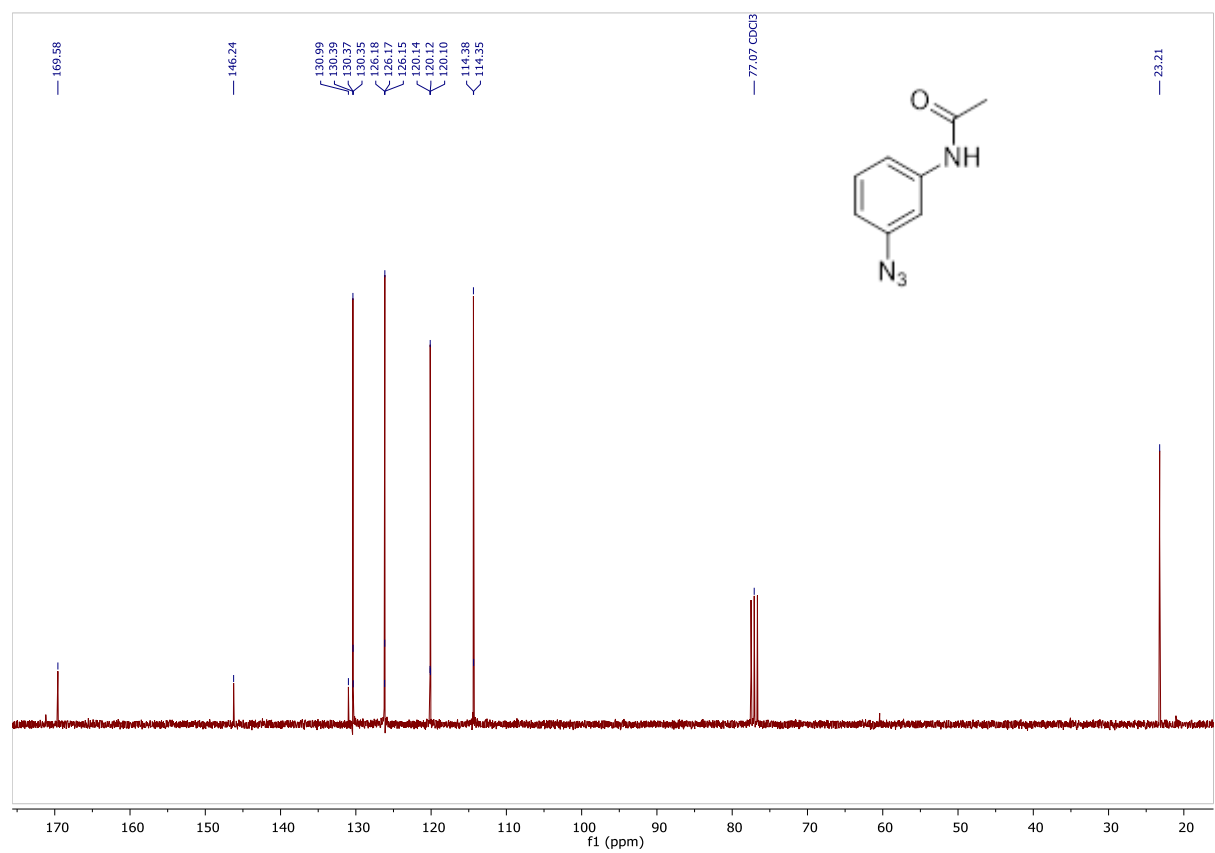
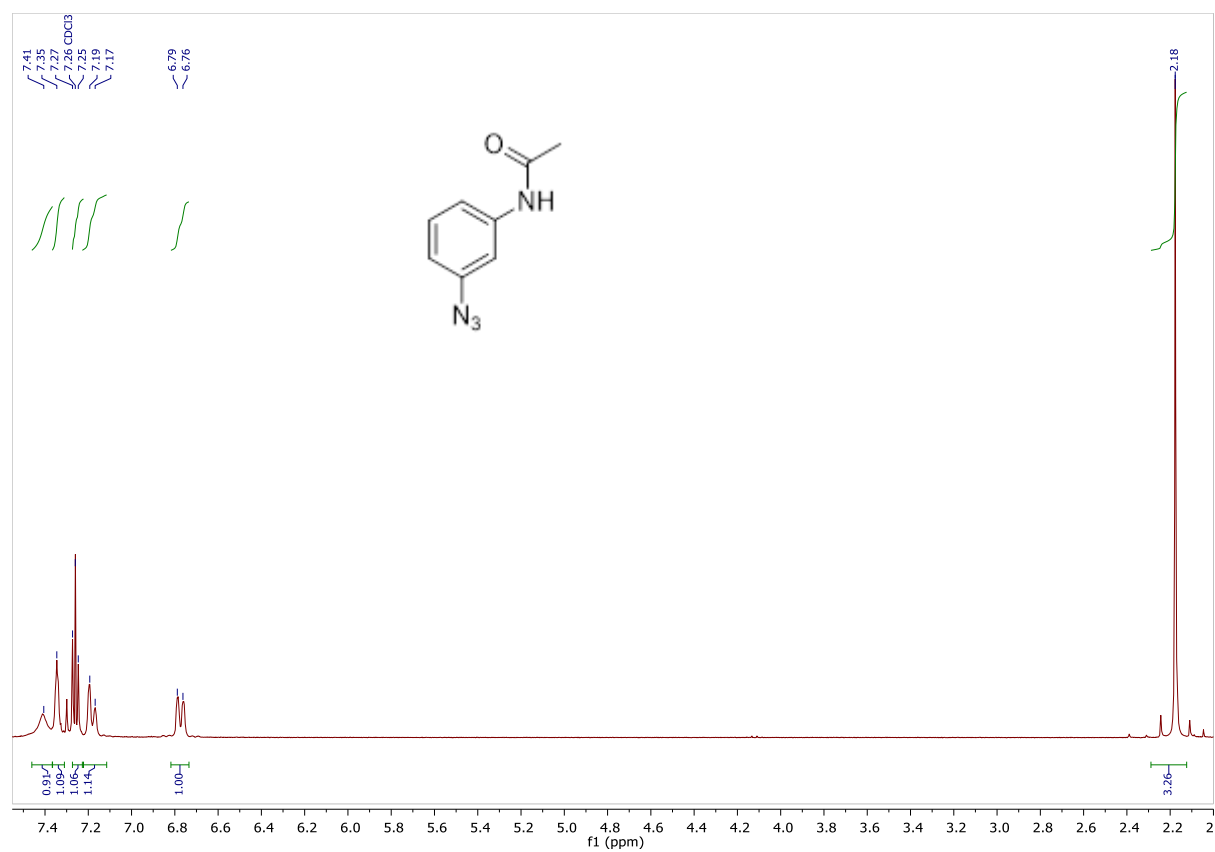
4-azidoaniline

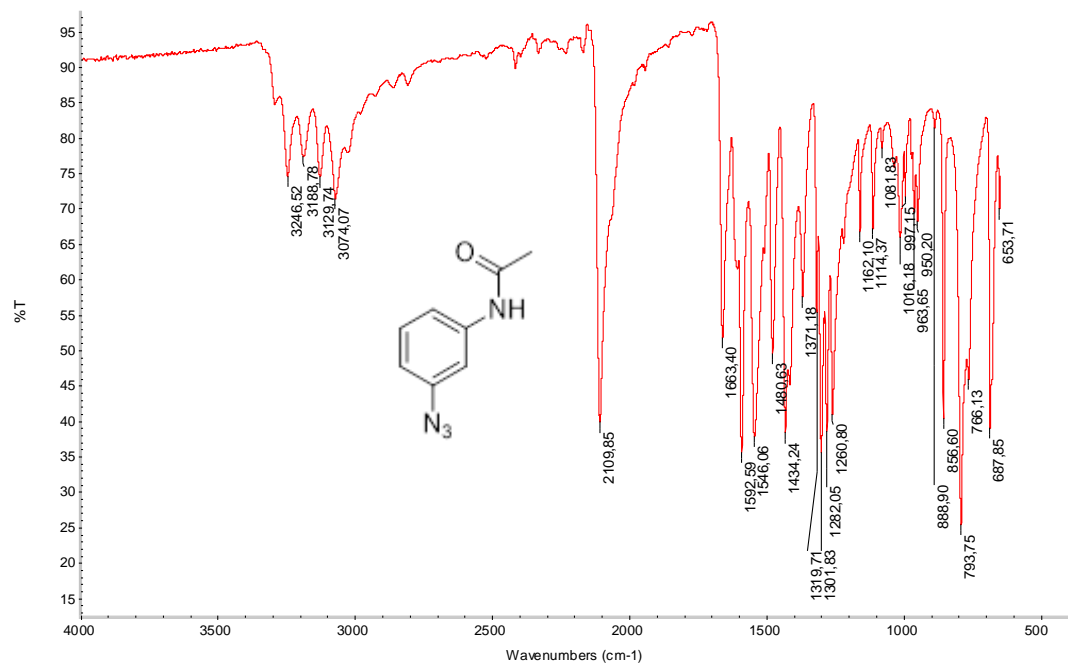
V



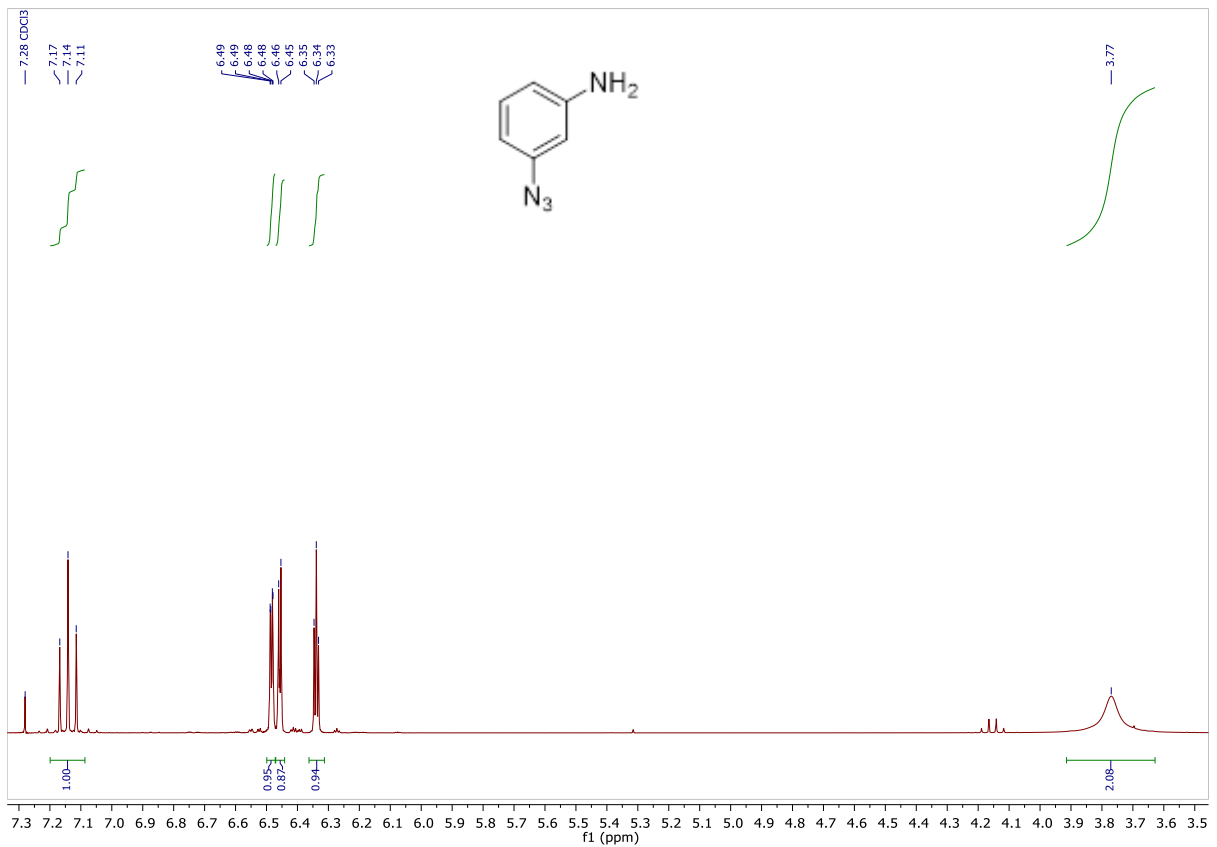


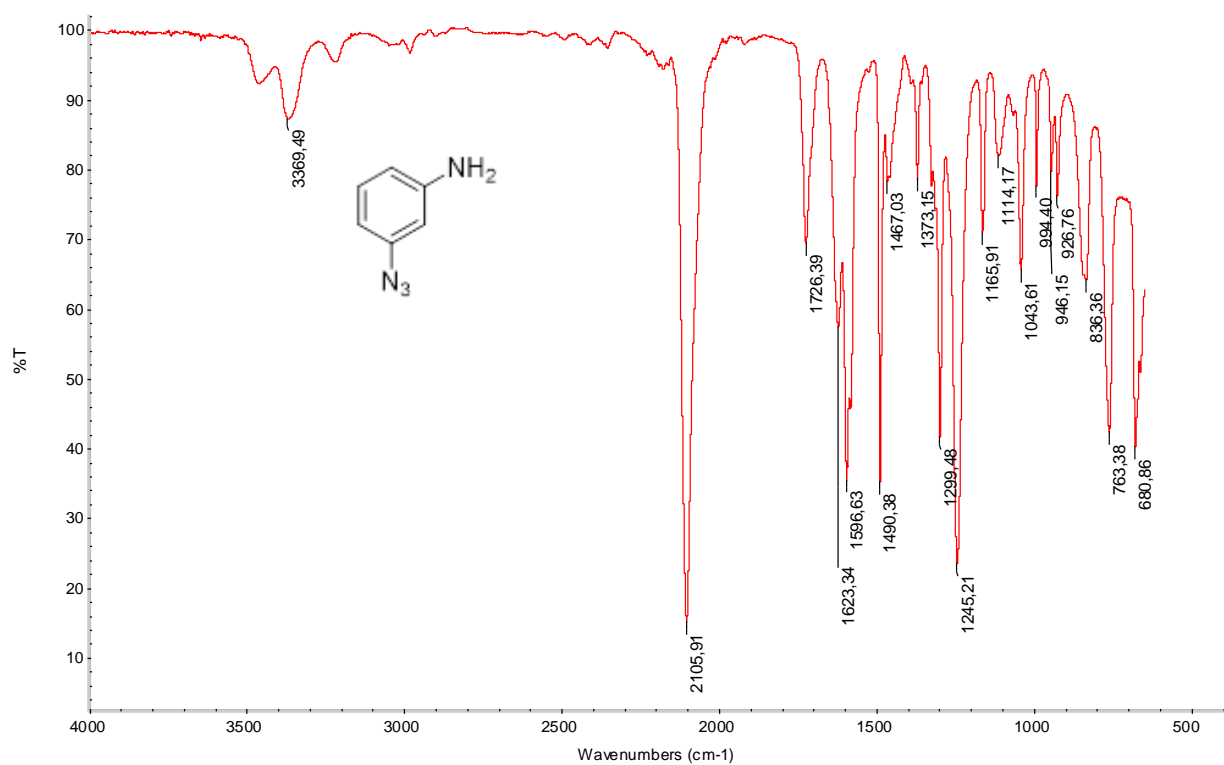
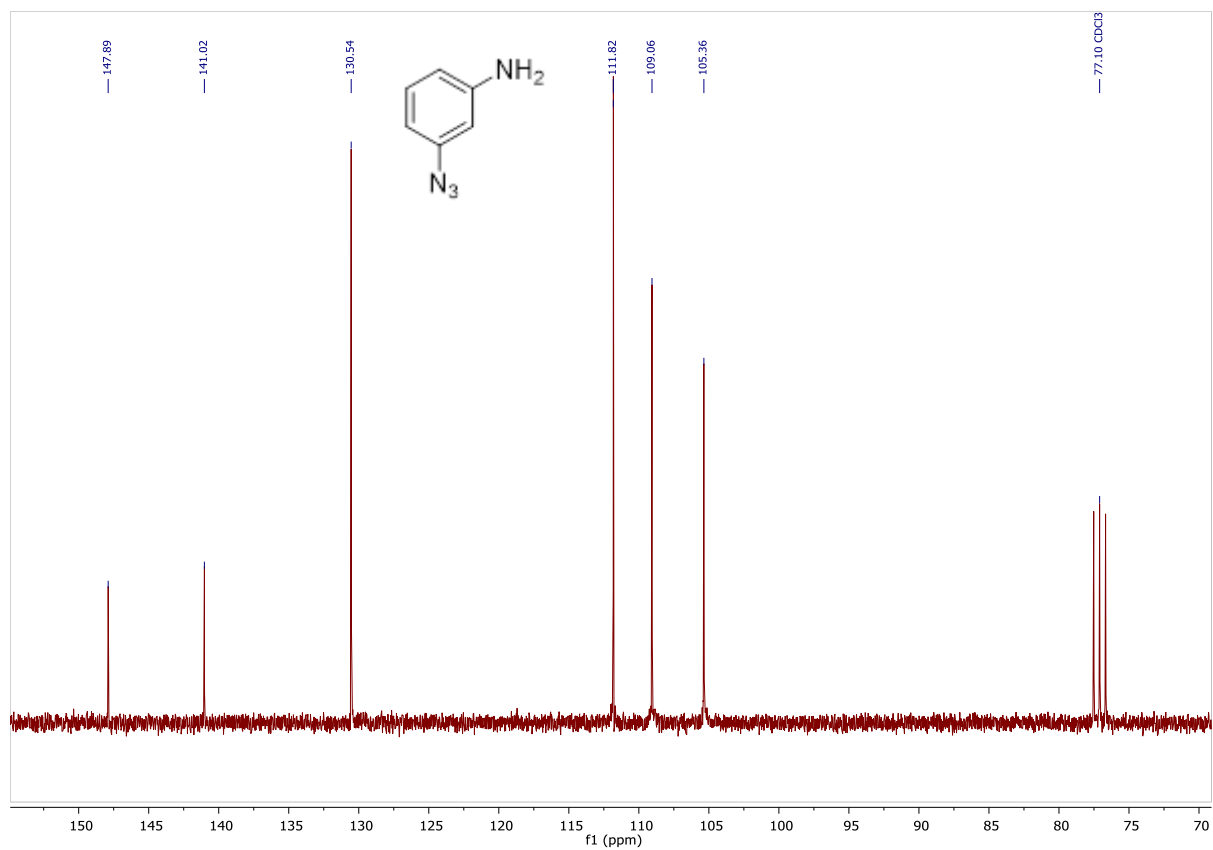
N-(3-azidophenyl)acetamide



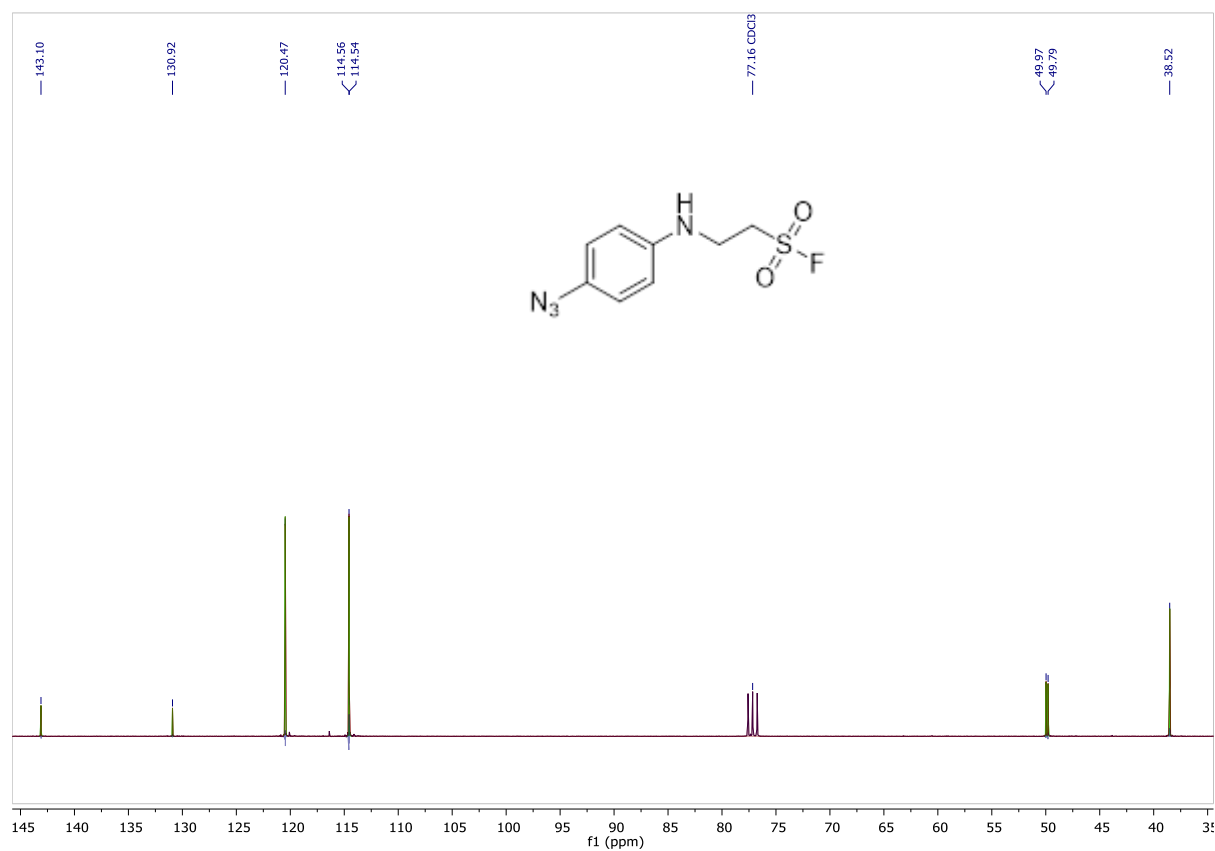
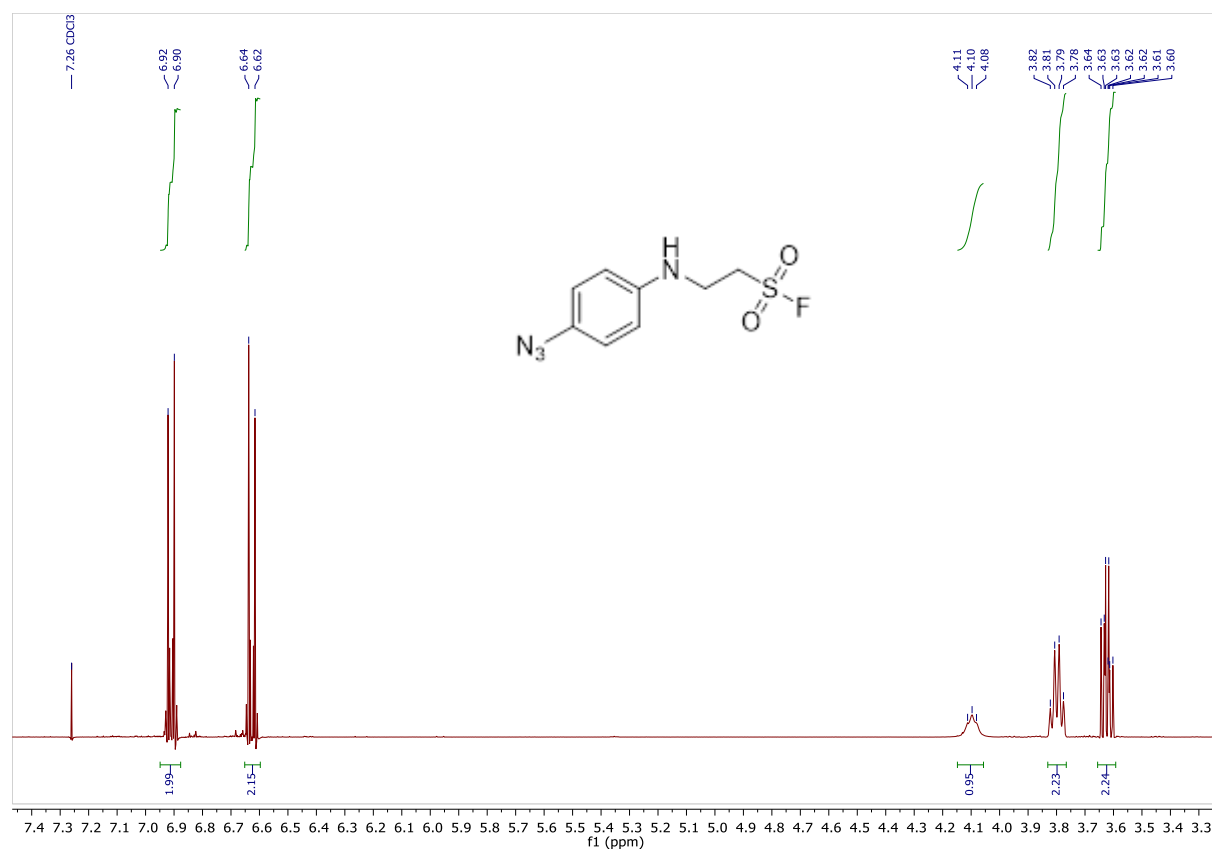


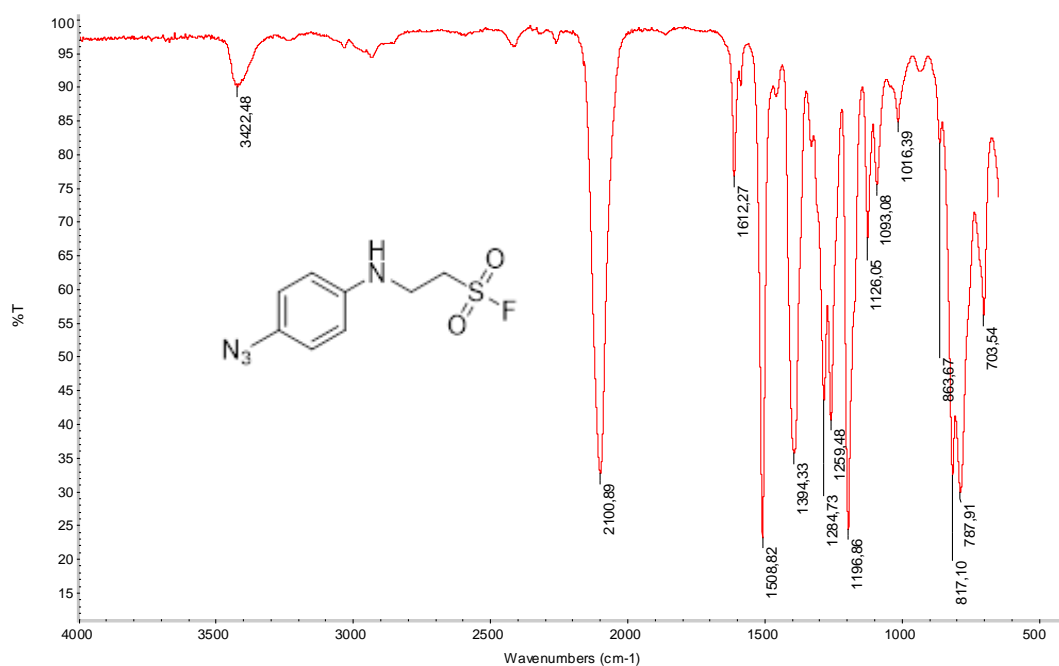
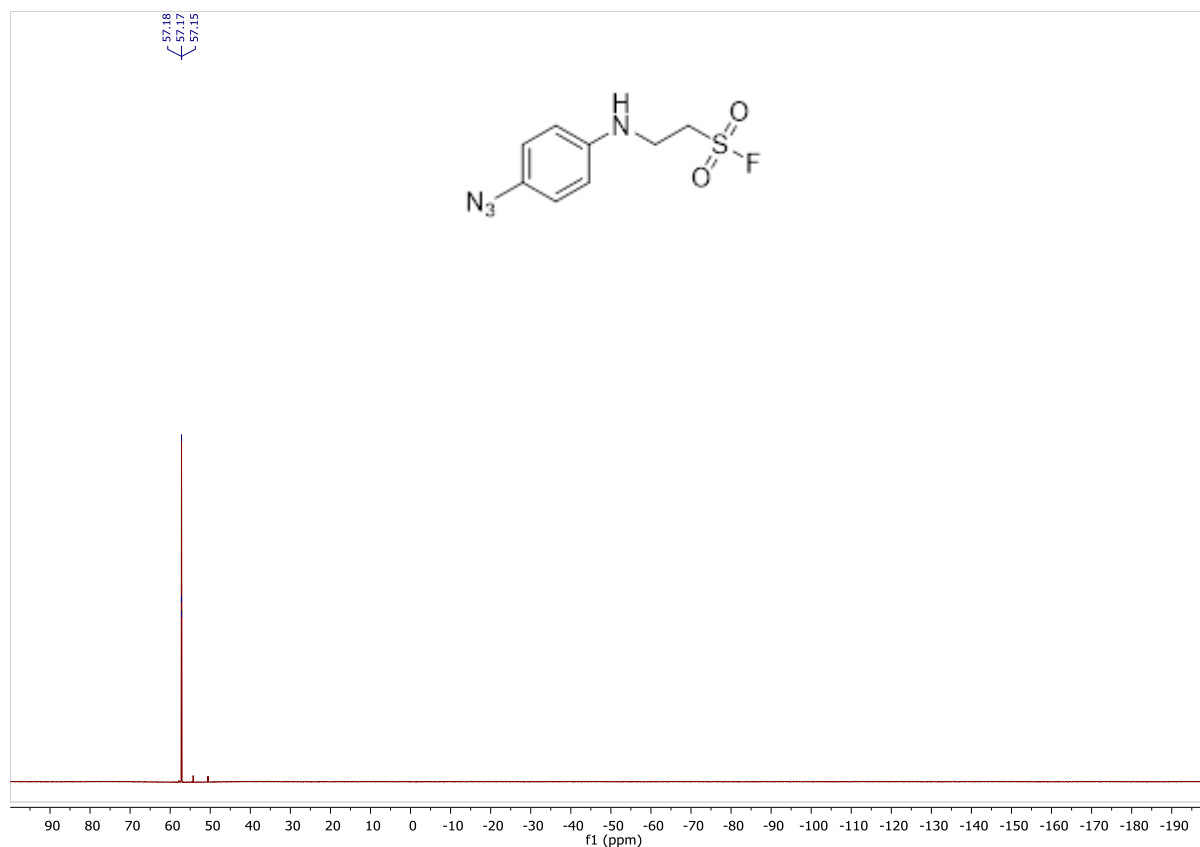
3-azidoaniline

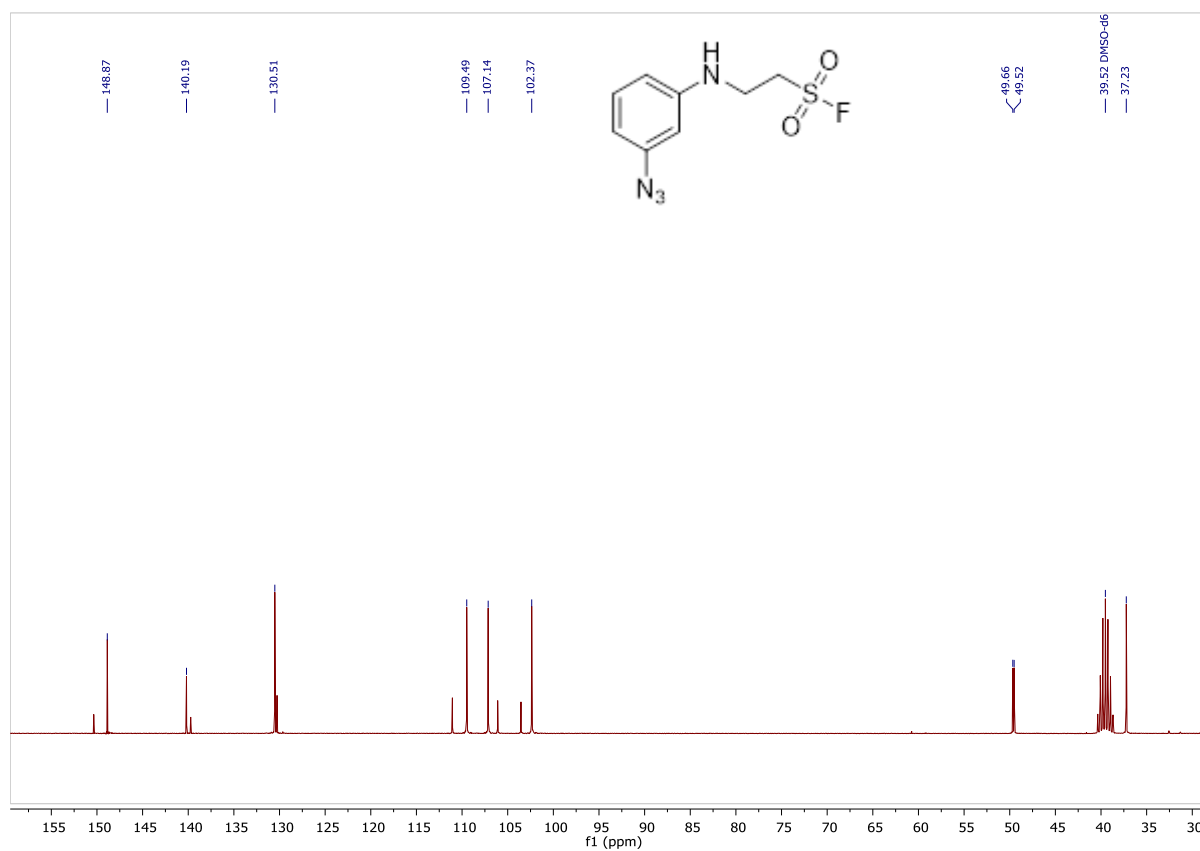
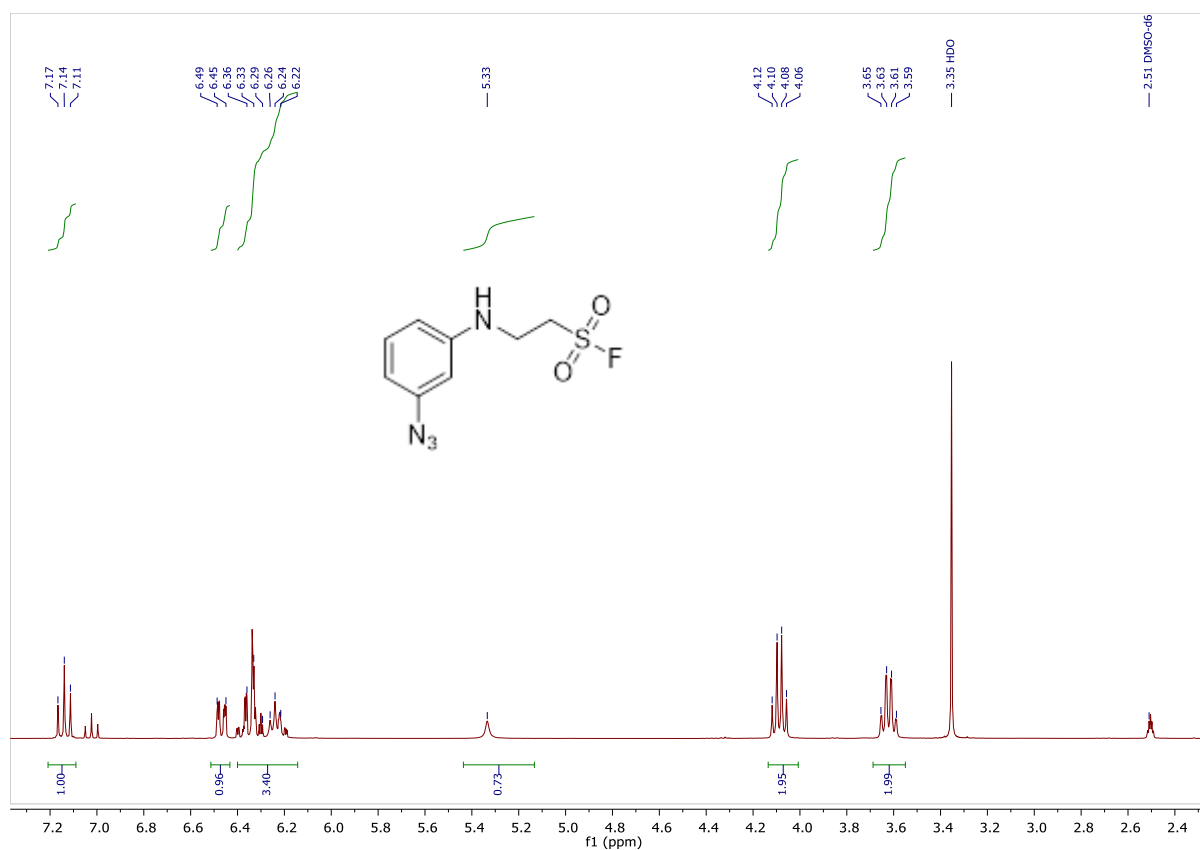


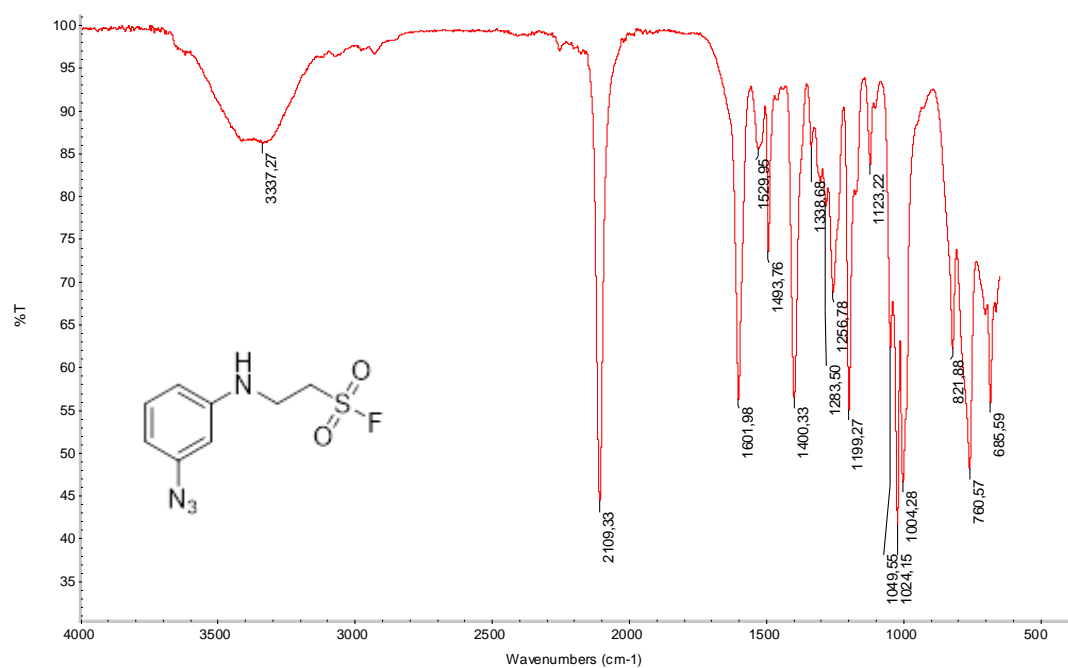
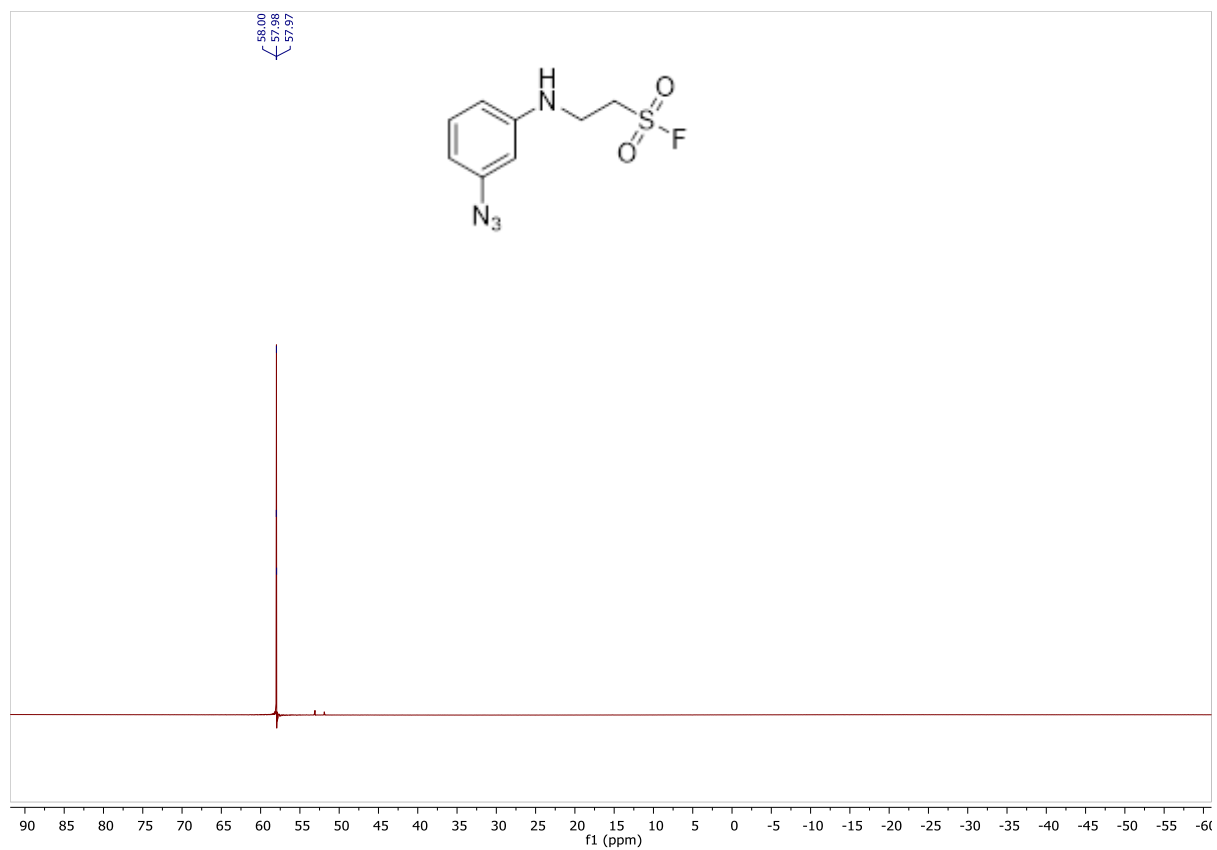


2-((4-azidophenyl)amino)ethane-1-sulfonyl fluoride





2-((3-azidophenyl)amino)ethane-1-sulfonyl fluoride



2-((3-(((2-chloropyrimidin-4-yl)amino)methyl)-1H-1,2,3-triazol-1-yl)phenyl)amino)ethane-1-sulfonyl fluoride

